NOVA SCHOOL OF SCIENCE & TECHNOLOGY

DEPARTAMENT OF EARTH SCIENCES

EVOLUTION OF POLACANTHID DINOSAURS AND DESCRIPTION OF A NEW SKELETON FROM THE UPPER JURASSIC OF PORTUGAL

JOÃO PAULO VASCONCELOS MENDES RUSSO

Master in Paleontology

DOCTORATE IN GEOLOGY

NOVA University Lisbon
November 2024

NOVA SCHOOL OF SCIENCE & TECHNOLOGY

DEPARTAMENT OF
EARTH SCIENCES

EVOLUTION OF POLACANTHID DINOSAURS AND DESCRIPTION OF A NEW SKELETON FROM THE UPPER JURASSIC OF PORTUGAL

JOÃO PAULO VASCONCELOS MENDES RUSSO

Master in Paleontology

Advisor: Octávio João Madeira Mateus
Associate Professor with Habilitation, NOVA School of Science and Technology

Examination Committee:

Chair: José Paulo Moreira dos Santos,
Full Professor, NOVA School of Science and Technology

Rapporteurs: Victoria Megan Arbour,
Curator of Paleontology, Royal British Columbia Museum, Canada

James Ian Kirkland,
State Paleontologist, Utah Geological Survey, USA

Advisor: Octávio João Madeira Mateus,
Associate Professor with Habilitation, NOVA School of Science and Technology

Members: Ausenda Cascalheira Assunção de Cáceres Balbino,
Full Professor, Évora University

José Carlos Ribeiro Kullberg,
Full Professor, NOVA School of Science and Technology

Vicente Daniel Crespo Roures,
Researcher, NOVA School of Science and Technology

DOCTORATE IN GEOLOGY

NOVA University Lisbon
November 2024

EVOLUTION OF POLACANTHID DINOSAURS AND DESCRIPTION OF A NEW SKELETON FROM THE UPPER JURASSIC OF PORTUGAL

Copyright © João Russo, NOVA School of Science and Technology, NOVA University Lisbon.

The NOVA School of Science and Technology and the NOVA University Lisbon have the right, perpetual and without geographical boundaries, to file and publish this dissertation through printed copies reproduced on paper or on digital form, or by any other means known or that may be invented, and to disseminate through scientific repositories and admit its copying and distribution for non-commercial, educational or research purposes, as long as credit is given to the author and editor.

ACKNOWLEDGMENTS

It seems a lifetime ago that I started my paleontological journey. Almost 14 years have passed since I first arrived in Lourinhã, fresh out of college and looking for my first opportunity. Since 2017, I have dedicated my life to this project, and I can honestly say that it has been the most challenging and transformative period of my life, but also the most rewarding professionally and personally. So many people have enriched this experience for the last seven years, and for that I am deeply thankful to all of them.

First and foremost, I would like to thank my supervisor Octávio Mateus, without whom I would not have been able to forge this path that started more than a decade ago. I deeply appreciate everything he taught me, the experiences we shared, and the opportunities he opened to me. He was kind (and brave) enough to believe in me and offer me the chance to study such a remarkable specimen and embark on this project. I have him to thank for the knowledge and expertise he imparted with me, as well as the patience to steer me in the right direction in so many occasions, while at the same time giving me the freedom to learn and work by myself, not just over the course of this PhD, but throughout these almost 14 years working together.

I want to thank also everyone at NOVA FCT that made this work possible and worked hard to make sure I would have the best possible experience to achieve my goals. A few deserve a special mention, starting with the head of the Doctoral Program at NOVA FCT, Prof. José Carlos Kullberg, for his continued support and tireless work on making sure I had all the conditions to achieve my objectives. I want to thank also my CAT (Comissão de Acompanhamento de Tese) members, my dear friends and colleagues Miguel Moreno Azanza (University of Zaragoza) and James I. Kirkland (Utah Geological Survey), for all their help, comments, and support for this

project. More specifically, I deeply appreciate the always insightful, helpful and positive discussions with Miguel, even when I was annoying him with basic questions. To Jim, I cannot appreciate enough everything he did for me. Without his mentorship, I could not have done this. I will be forever grateful for all his kindness, time, and patience to meet and share his unique experience and knowledge from thousands of kilometres away, for many long hours, at a time when we were locked down in our homes. The deepest appreciation also for his kindness to share with me his data from years of research on ankylosaurs and invite me to work with him and Mark Loewen (Natural History Museum of Utah, University of Utah) on their ankylosaur phylogeny. And I will forever be deeply grateful for his continued support and effort to make sure I would be able to go to the US and visit collections, look at specimens, and work alongside him, which, to my great regret and for a myriad of reasons, did not come to be.

My deepest thanks to Museu da Lourinhã, my paleontological home since 2010, and all the people with whom I have crossed paths there, from staff to volunteers to Direction board members. The warmest appreciation goes to Carla Tomás, the person who taught me everything I know about fossil preparation and whose guidance, support, and help were crucial in dealing with many of the challenges that this project presented me with. Without her, I am sure I would still be preparing the specimen. And of course, neither me nor her would have been able to accomplish the successful preparation of such a complex specimen without the aid of so many people, namely Micael Martinho, who dedicated many hours to make sure my unending requests to "just clean a little better, expose that surface a little more" were answered. Many thanks also to all the volunteers, students, and researchers that gave their contribution to make sure I had a specimen to study. Thanks also to all the help and support from everyone at Parque dos Dinossauros da Lourinhã, particularly my long-time companions, Simão Mateus and João Marinheiro, who have shared this journey with me from the very beginning, many years ago.

A project like this is highly dependent on many institutions and people that one way or another have allowed to improve this research, whether by granting access to comparative material or by reviewing and commenting on aspects of this research. Unfortunately, and due to a global pandemic, the list of institutions is shorter than I planned at the beginning of this PhD. Nonetheless, I am deeply grateful for the hospitality and help of the many people that made it possible for

me to access specimens. I want to thank Rúben Dias (LNEG) and Jorge Sequeira (MG) for granting me access to the holotype of *Dracopelta*, Kristen Spring and Scott Hocknull (QM) for their hospitality and assistance while visiting the collections of the Queensland Museum, Lucy Leahey (UQ) for providing photos of Australian material I could not examine myself, Matthew McCurry (AM) for the assistance during collection visiting, and Xabier Pereda-Suberbiola (EHU) and João Luís Cardoso (UAb) for reviewing and helpful comments on the publication of Chapter 3 of this thesis.

This study would not have been possible without the financial support of Fundação para a Ciência e Tecnologia, I. P., Portugal, through my doctoral grant (SFRH/BD/128717/2017) and COVID extension grant (COVID/BD/152142/2021). Travel assistance was kindly provided by the Jackson School of Geosciences Travel Grant for the attendance and poster presentation at the 79th Society of Vertebrate Paleontology meeting in Brisbane, 2019.

Many thanks to my friends and colleagues, especially my fellow doctoral colleagues at NOVA-FCT and everyone that throughout these years became part of our Lourinhã team and gave your contribution to this project. Thank you all for your support and sharing this rollercoaster ride with me!

To my family, who have been there for me throughout and whose unwavering support, love, and patience gave me the strength to carry on and pulled me up when I felt overwhelmed, my words are short to describe how thankful I am for everything you taught me, for all your support and for helping me reach this point. A special mention to my Lourinhã family, Isabel, Simão, and Octávio, who "adopted" this kid when he first arrived in Lourinhã 14 years ago and helped him pursue his childhood dream, while teaching him so much about life. Never have I imagined the impact you would have on me and how inextricably linked I would be to all of you. And for that I will always be thankful.

Finally, and most important of all, I want to thank and dedicate this work to three most important persons in my life: my children Rita and David, and my wife Marta. You are my Polaris star, my armour, and your love kept me going through it all. To Marta, there are no words to describe how much I love you and how thankful and humbled I am for your love, for your kindness, for your honesty, and for your unending patience. You have trailed this path with me since it began in 2017 and I could not have asked for a better partner in crime.

Abstract

Ankylosaurs are one of the most iconic groups of dinosaurs. Their most conspicuous characters are the widespread dermal ossification, heavily ornamented, hyperossified skull, coossification of posterior dorsal and anterior caudal vertebrae with the sacrum into a synsacrum, and in some, fusion of the posterior half of the tail, forming the recognizable tail club. Specimens have been identified worldwide, dating at least from the Middle Jurassic to the latest Cretaceous. The phylogenetic relationships within the group have always been a matter of debate, particularly of non-ankylosaurid ankylosaurs, and remain poorly understood, especially due to a poor pre-Cretaceous record. The best-preserved specimens come from the Late Jurassic Morrison Formation, USA, as well as the Lourinhã formation, Portugal. The Portuguese record has until recently been restricted to the poorly known *Dracopelta zbyszewskii* from the upper Tithonian, known from a partial, articulated ribcage and an autopodium.

This study reports and describes a second ankylosaur specimen, mostly complete and articulated, from the uppermost Tithonian of the Lourinhã formation, in the coastal cliffs one kilometre North from the beach of Porto da Calada, Mafra, about 40 km North of Lisbon, Portugal. It consists of axial, appendicular, and dermal armour skeletal elements: nearly complete skull, left mandible, complete articulated cervical, dorsal, and sacral vertebral series, as well as 13 anterior caudal vertebrae, ribs, pectoral and partial pelvic girdles, right humerus, both femora, and dermal armour, thus making it the most complete ankylosaur from the Jurassic. Furthermore, the holotype of *D. zbyszewskii* was redescribed, including hitherto unknown elements of the appendicular skeleton, such as a partial right hindlimb,

composed of the distal end of the femur, tibia, fibula, and articulated autopodium, which is herein reidentified as a right pes. Also, its type locality and discovery history were established. Comparisons of both specimens allowed to conclude that *D. zbyszewskii* is now known from two specimens, and is herein rediagnosed, based on a unique combination of characters, ten of which are autapomorphic. A Maximum Parsimony analysis was performed to assess the phylogenetic position of *D. zbyszewskii*, using a new dataset (330 characters, 95 taxa). The analysis recovered four major clades within Ankylosauria, Ankylosauridae, Nodosauridae, Struthiosauridae, and Polacanthidae, occurring together with a large polytomy formed of both traditionally considered earlier and later diverging taxa. Also, *Scelidosaurus harrisonii* is the earliest diverging ankylosaur, placing the origin of Ankylosauria in the Early Jurassic. Moreover, polacanthids are the earliest diverging group of ankylosaurs, appearing as early as the Late Jurassic. *D. zbyszewskii* is recovered as an early branching polacanthid, and is the sister taxon of *Gargoyleosaurus parkpinorum*, forming a sister group to *Mymoorapelta maysi*, both from the Morrison Formation, USA. The three are grouped together in an early diverging polacanthid clade, herein proposed as Jurapelta clade. nov. Jurapeltans suggest a Late Jurassic (Kimmeridgian) North American origin for polacanthids, immediately followed by an Iberian dispersion in the uppermost Tithonian and achieving a Laurasian distribution by the Early Cretaceous. These results not only highlight the paleobiogeographical connections and paleoecological relationships between North America and Iberia during the Late Jurassic, but also underline the need for improved specimen and character sampling to increase the resolution of problematic taxa.

Keywords: Ankylosauria; Upper Jurassic; *Dracopelta zbyszewskii*; phylogeny; Polacanthidae; Jurapelta.

RESUMO

Os anquilossauros são um dos mais icónicos grupos de dinossauros. As suas características mais evidentes são a abundante ossificação dérmica, um crânio densamente ornamentado e hiperossificado, coossificação de vértebras dorsais posteriores e caudais anteriores com o sacro, formando um sinsacro, e em alguns, fusão da metade posterior da cauda, formando a reconhecida maça. Foram identificados espécimes em todo o mundo, datando desde pelo menos o Jurássico Médio ao Cretácico mais tardio. As relações filogenéticas no grupo têm sido assunto de debate, particularmente em anquilossauros não-anquilossaurídeos, e continuam pouco compreendidas, especialmente devido a um pobre registo pré-Cretácico. Os melhores espécimes provêm da Formação de Morrison, EUA, mas também da Formação da Lourinhã, Portugal, ambas datadas do Jurássico Superior. O registo português estava até recentemente restrito ao pouco conhecido *Dracopelta zbyszewskii* do Titoniano superior, conhecido por uma caixa torácica parcial e articulada e um autopódio articulado.

Este trabalho reporta e descreve um segundo espécime de anquilossauro, maioritariamente completo e articulado, do topo da formação da Lourinhã, datado do Titoniano superior, recolhido nas arribas costeiras um quilómetro a Norte da Praia de Porto da Calada, Mafra, cerca de 40 quilómetros a Norte de Lisboa, Portugal. Consiste de elementos do esqueleto axial, apendicular, e da armadura dérmica: um crânio praticamente completo, mandibula esquerda, séries vertebrais cervicais, dorsais, sacro, e 13 vértebras caudais anteriores, costelas, cinturas peitoral e pélvica parciais, úmero direito, ambos os fémures, e armadura dérmica, tratando-se assim do mais completo anquilossauro do Jurássico. Além disso, o holótipo de *D. zbyszewskii* foi redescrito, incluindo elementos do esqueleto

apendicular desconhecidos até agora, como um membro posterior direito parcial, composto pela metade distal do fémur, tíbia, e fíbula, e o autopódio articulado, este último aqui reidentificado como um pé direito. Também a sua localidade tipo e história da descoberta foram estabelecidas. Comparações de ambos os espécimes permitiram concluir que o *D. zbyszewskii* é agora conhecido por dois espécimes, sendo aqui rediagnosticado, baseado numa combinação única de caracteres, dos quais dez são autapomórficos. Uma análise de máxima parcimónia foi realizada para avaliar a posição filogenética do *D. zbyszewskii*, utilizando um novo conjunto de dados (329 caracteres, 95 taxa). A análise recuperou quatro clados principais dentro dos Ankylosauria: Ankylosauridae, Nodosauridae, Struthiosauridae e Polacanthidae, ocorrendo juntamente com uma grande politomia formada por taxa tradicionalmente considerados precoce e tardiamente divergentes. Também, *Scelidosaurus harrisonii* é o anquilossauro mais precoce, colocando a origem dos Ankylosauria no Jurássico Inferior. Ademais, os polacantídeos são o grupo com divergência mais precoce, aparecendo no Jurássico Superior. *D. zbyszewskii* surge como um dos primeiros polacantídeos, e como táxone irmão de *Gargoyleosaurus parkpinorum*, formando um grupo irmão de *Mymoorapelta maysi*, ambos da Formação de Morrison, EUA. Os três agrupam-se num clado de polacantídeos precoces, aqui proposto como Jurapelta clade. nov. Os jurapeltanos sugerem uma origem norte-americana durante o Jurássico Superior (Kimmeridgiano) para os polacantídeos, imediatamente seguida por uma dispersão ibérica no Titoniano mais tardio e distribuindo-se pela Laurásia no Cretácico Inferior. Estes resultados não só realçam as conexões paleobiogeográficas e relações paleoecológicas entre a América do Norte e a Ibéria durante o Jurássico Superior, como também sublinham a necessidade de melhorar a amostragem quer de espécimes quer de caracteres por forma a melhorar a resolução de taxa problemáticos.

Palavras-chave: Ankylosauria; Jurassic Superior; *Dracopelta zbyszewskii*; filogenia; Polacanthidae; Jurapelta.

TABLE OF CONTENTS

LIST OF FIGURES

D, E) TV 10, F) TV 8, G) TV 7, H,) TV 13, I) TV 9. Antunes and Sigogneau-Russell (1991).

Figure 1.4.1. (previous page). Location of *D. zbyszewskii*. Simplified regional geological map (top), showing Late Jurassic units (light blue). Red rectangle highlights the area where *D. zbyszewskii* was found. Below are shown the localities of the studied specimens, and the coastal profile correlation (red stars: 1, holotype; 2, NOVA-FCT-DCT-5556). Map modified from Russo *et al.*, 2017. Satellite image modified from Google Earth Pro® (2024). Coastal profile photo by André Carvalho (2019) and geological profile by Lope Ezquerro (2021).

Figure 1.4.2 (previous page). Stratigraphy and localities of *D. zbyszewskii* specimens. Stratigraphic column and correlation of the sections where the specimens of *D. zbyszewskii* were found. Red stars with numbers mark the occurrence of *Dracopelta* in the sequence: 1) holotype, 2) NOVA-FCT-DCT-5556. Photographs show the type locality near Porto Barril (bottom), and the site of NOVA-FCT-DCT-5556 (above) at Praia da Escadinha, marked with a red star. Stratigraphic log and correlation by Lope Ezquerro (2021).

Figure 2.1.1.1. Goniopholidid osteoderm. Associated osteoderm (possibly ventral) attributed to an unidentified goniopholid, found with NOVA-FCT-DCT-5556.

Figure 3.1. Holotype material of *Dracopelta zbyszewskii*. (a) IGM 5787, ribcage and dermal armour; (b) IGM 3, autopodium; (c) best preserved elements from the postcranial material (stored at LNEG, no inventory number), from left to right: right tibia, anterior view; distal right femur, anterior view, with an osteoderm and ossified tendon below; rib segments (above); osteoderms (below). Scale bars in (a, c) and (b): 10 cm and 5 cm, respectively.

Figure 3.2. Regional simplified geological map (right), with location of Dracopelta zbyszewskii (red star). Gray coloured areas on the right represent Late Jurassic units. Satellite (top left) and coastal profile (bottom left) photographs of the Praia da Assenta Sul area. Green star indicates the site of the new ankylosaurian specimen NOVA-FCT-DCT-5556; white dashed line on bottom left represents approximate J-K boundary according to Mateus *et al.* (2017); red dashed line marks the coastal equivalent unit to the type locality. Satellite image modified from Google Earth® and panoramic photo of the coast by André Carvalho.

Figure 3.3. Historical record of the holotype of *Dracopelta zbyszewskii*. Top) sketch of the holotype in Georges Zbyszewski's 1964 fieldbook. "Dinosaure de Assenta" (dinosaur of Assenta) is noted on the left edge of the page. The content of the rest of the page is unrelated with this sketch (see text for further information on Georges Zbyszewski's field notes); Bottom) holotype in situ in 1964 (photograph by Leonel Trindade, kindly shared by Torres Vedras municipal archives).

Figure 3.4. Type locality of *Dracopelta zbyszewskii* (above) and local stratigraphic log showing the placement of the holotype in the section (below).

Figure 3.5. Main historic contributors. (a) Leonel Trindade (from Travanca, 1999); (b) Georges Zbyszewski (right) and Octávio da Veiga Ferreira (left) (kindly shared by João Luís Cardoso); (c) Peter M. Galton (photograph by Octávio Mateus).

Figure 4.1.1.1. Holotype (MG 5787) of *Dracopelta zbyszewskii*. Dorsal (top) and right anterolateral (bottom) views of the ribcage of *D. zbyszewskii*. Sections A-E in Figure 4.1.2. c8) cervical vertebrae 8, d1-d11) dorsal vertebrae 1-11, lp) lateral plate, r) rib. Scale bars: 15 cm.

Figure 4.1.1.2. Details of the holotype (MG 5787) of *Dracopelta zbyszewskii*. A, B) dorsal view of the cervicodorsal region, with the paired keeled dorsal scutes and underlying vertebrae c8 and d1-2, and ossified tendons; C) detail of dorsal row osteoderm; D) right lateral view of lateral plates. The dorsal keel is distinguished in the two scutes in the center of the image; E) anterior right lateral plates in cross-section. In E, note the dorsal keel in the two anteriormost plates. Abbreviations: ot - ossified tendon; poz – postzygaphysis; sc – scute; sp – spinous process; tp - transverse processes. Scale bars: 10 cm in A, E, 5 cm in B, D, and 1 cm in C.

Figure. 4.1.1.3. Ribs of *Dracopelta zbyszewskii*. Fragment of right dorsal ribs, in dorsal view (top) and proximal cross section (bottom). Notice the triangular cross section of the rib. Note: this material does not yet possess an inventory number. Scale bar: 2 cm.

Figure 4.1.1.4. Right femur of *Dracopelta zbyszewskii*. Posterior view (bottom) of the right femur of *D. zbyszewskii* and cross section in proximal view (top) of the femoral shaft. Note: this material does not yet possess an inventory number.

Abbreviations: do – dorsal ossicle; lec – lateral epicondyle; mdc – medullary cavity; ot – ossified tendon. Scale bar: 5 cm.

Figure 4.1.1.5. Right tibia and fibula of *Dracopelta zbyszewskii.* Anterior (A), posterior (B), medial (C), proximal (D), and distal (E) views of the right tibia. Note: this material does not yet have an inventory number. Abbreviations: f - fibula. Scale bar: 10 cm.

Figure 4.1.1.6. Autopodium (MG 3) of *Dracopelta zbyszewskii*. Right pes of *D. zbyszewskii* in ventral (palmar) view. Abbreviations: mt - metatarsal Scale bar: 5 cm.

Figure 4.1.1.7. Left thoracic distal osteoderms from the holotype of *Dracopelta zbyszewskii*. Dorsal (A) and posterior (B) views of two subtype I scutes of the holotype of *D. zbyszewskii*. The external keel is visible in A and in posterior profile in B. C shows a detail of the keel in anterodorsal view. Scale bars: 5 cm in A, B, 2 cm in C. Note: this material does not yet have an inventory number.

Figure 4.1.1.8. Osteoderms of the holotype of *Dracopelta zbyszewskii*. Isolated osteoderm fragments from *D. zbyszewskii*. A, B) lateral plate fragment. Dorsal view in A, with keel facing dorsally and covered by sediment; cross-section in B shows the dorsal keel rising from the base. C) cross-section of lateral plate, dorsal keel projecting from the curved base. D, E) fragments of osteoderms. Scale bar: 5 cm. Note: this material does not yet have an inventory number.

Figure 4.1.1.9. Assorted unidentified material. Smaller unprepared fragments that include some distal rib (top) and osteoderm (middle) fragments. This material does not yet have an inventory number.

Figure 4.1.1.10. Assorted unidentified material. Fragments (top and bottom) and unprepared blocks (middle). This material does not yet have an inventory number.

Figure 4.1.1.11. Assorted unidentified material. Unprepared fragments and block (bottom). In the middle right there is an osteoderm fragment covered by the adhesive used in the preliminary preparation done in the 1960's. This material does not yet have an inventory number.

Figure 4.1.1.12. Assorted unidentified material. Unprepared blocks and fragments. In the middle right, fragments of ribs are observable. This material does not yet have an inventory number.

Figure 4.2.1. Skeleton of *Dracopelta zbyszewskii* (NOVA-FCT-DCT-5556). Photo montage of specimen NOVA-FCT-DCT-5556 of *D. zbyszewskii* in ventral view, showing the articulation of the axial and appendicular elements. Because the specimen was collected in separate blocks, this montage was obtained by positioning and stitching the blocks which showed confirmed articulating elements. Scale bar: 50 cm.

Figure 4.2.2. Skeleton of *Dracopelta zbyszewskii* (NOVA-FCT-DCT-5556). Photo montage of specimen NOVA-FCT-DCT-5556 of *D. zbyszewskii* in dorsal view, showing the articulation of the axial and appendicular element, as well as the distribution of dorsal dermal armour. Because the specimen was collected in separate blocks, this montage was obtained by positioning and stitching the blocks which showed confirmed articulating elements. Scale bar: 50 cm.

Figure 4.2.3. Schematic dorsal view of *Dracopelta zbyszewskii* (NOVA-FCT-DCT-5556). Line drawing of Figure 4.2.2 with dermal armour colour coded by region. Scale bar: 50 cm.

Figure 4.2.1.1. Skull of *Dracopelta zbyszewskii* (NOVA-FCT-DCT-5556). A) dorsal, B) ventral, C) right lateral, and D) anterior views of the skull of *D. zbyszewskii* (NOVA-FCT-DCT-5556). In A, the asymmetrical pattern of caputegulae on the dorsal surface of the rostrum (also in D) as well as the transverse ridges on the parietal region are visible. E) detail of nuchal region. F) detail of anterior maxillary palate. Abbreviations: ar – alveolar ridge; be – buccal emargination; h – humerus; j – jugal; jh – jugal horn; mdb – mandible; mx – maxillary; mxtm – maxillary tomium; o – orbit; p – parietal; pal – palate; pop – paroccipital process; proa – proatlas; q – quadrate; qj – quadratojugal; sq – squamosal. Scale bars: 10 cm in A, B, C, 5 cm in D, E, F.

Figure 4.2.1.2. Teeth of *Dracopelta zbyszewskii* (NOVA-FCT-DCT-5556). A) right alveolar ridge in ventral view, B) detail of left anterior maxillary tooth row in buccal view, C) isolated dentary? tooth, D) left posterior maxillary teeth in buccal view, E) right maxillary erupting tooth in lingual view. In A, anterior is to the right. In D, the black arrowheads indicate preserved denticles. Abbreviations: sf – special foramina; t – teeth. Scale bars: 2 cm in A, 1 cm in B-D, 5 mm in E.

Figure 4.2.2.1 (previous page). Cervicothoracic section of *Dracopelta zbyszewskii* (NOVA-FCT-DCT-5556). Dorsal (above) and ventral (below) views of the

cervicothoracic section of NOVA-FCT-DCT-5556. Cranial is to the left. Inset is a cross section of d3, in posterior view, where the prezygapophyses of d4 are visible. Abbreviations: c5-7 – cervical vertebrae; crsc – cervical ring scute; d1-d3 – dorsal vertebrae; nc – neural canal; poz – postzygapophyses; prz – prezygapophyses; r – rib; scb – scapular blade; sp – spinous process (neural spine); tp – transverse process; vf – ventral fossa; vk – ventral keel. Scale bars: 10 cm in dorsal and ventral views, 2 cm in inset.

Figure 4.2.2.2. Posterior cervical vertebrae of *Dracopelta zbyszewskii* (NOVA-FCT-DCT-5556). Left lateral (above) and right lateral (below) views of vertebrae c5-8 of NOVA-FCT-DCT-5556. Right side of c5 and c6 was obliterated during collection of the specimen. Abbreviations: c5-8 – cervical vertebrae; dia - diapophysis; fo – foramen; para – parapophysis; prz – prezygapophyses; tp – transverse process; vf – ventral fossa; vk – ventral keel. Scale bar: 2 cm.

Figure 4.2.2.3. Dorsal section of *Dracopelta zbyszewskii* (NOVA-FCT-DCT-5556). Dorsal (above), and ventral (below) views of the dorsal section of NOVA-FCT-DCT-5556, from d4-14, with ribs and armour *in situ*. Cranial is to the left. D14 is the first dorsosacral (ds1, Table 4). Abbreviations: d4-d14 – dorsal vertebrae 4 to 14; do – dorsal osteoderms; ot – ossified tendons; r – ribs; sc – scute; sp – spinous process. Scale bar: 20 cm.

Figure 4.2.2.4. Dorsal vertebrae of *Dracopelta zbyszewskii* (NOVA-FCT-DCT-5556). Details of the dorsal vertebrae (d4-d10) of specimen NOVA-FCT-DCT-5556. A) left lateral, B) right lateral, C) detail of d6-d8 in left lateral view, D) close-up of d11, in posterolateral view, showing the coossification of the rib at the parapophysis, along the transverse process and diapophysis. Abbreviations: acpl – anterior centroparapophyseal lamina; d1-d10 – dorsal vertebrae; ot – ossified tendon; para – parapohysis; pcpl – posterior centroparapophyseal lamina; poz – postzygapyhysis; prz – prezygapophyses; tp – transverse process. Scale bars: 5 cm in A-C, 2 cm in D.

Figure 4.2.2.5. Sacrum of *Dracopelta zbyszewskii* (NOVA-FCT-DCT-5556). Dorsal (previous page) and ventral views of the sacral region of NOVA-FCT-DCT-5556. In dorsal view, the sacral shield covers most of the surface. In ventral view, in the lower right corner, the postacetabular process is obscured by sediment. Abbreviations: a – acetabulum; cd1-2 – caudal vertebrae 1-2; cr2 – caudal rib 2; d15-16 – dorsal vertebrae 15-16; dr – dorsal ribs; fh – femoral head; is – ischium; ns – neural spine;

ot – ossified tendons; pb – pubis; ppsc – peripheral pelvic scute; prap – preacetabular process; rf – right femur; s1-4 – sacral vertebrae 1-4; sr – sacral ribs (sr2, sacral rib 2). Scale bars: 20 cm.

Figure 4.2.2.6. Anterior caudal vertebral series of *Dracopelta zbyszewskii* (NOVA-FCT-DCT-5556). Dorsal (top) and ventral (bottom) views of the anterior portion of the tail of NOVA-FCT-DCT-5556. Abbreviations: cd1-11 – caudal vertebra 1-11; cdlp – caudal lateral plate; ch – chevron; chevron articulation facet; cr – caudal rib; dos – dorsal ossicle; ot – ossified tendon; sp – spinous process. Scale bar: 10 cm.

Figure 4.2.2.7. 12th caudal vertebra of *Dracopelta zbyszewskii* (NOVA-FCT-DCT-5556). Anterior (A), posterior (B), dorsal (C), ventral (D), left lateral (E), and right lateral (F) views. Abbreviations: chf – chevron facet; cr – caudal rib; nc – neural canal; np – neural pedicels; ntb – notochordal bump; poprl – postzygoprezygapophyseal lamina; poz – postzygapophysis; prz – prezygapophyses; sp – spinous process. Scale bar: 5 cm.

Figure 4.2.3.1. Scapulocoracoid of *Dracopelta zbyszewskii* (NOVA-FCT-DCT-5556). Left scapulocoracoid in ventral (A) and ventrolateral (B) views; right scapulocoracoid in ventral (C) and ventrolateral (D) views. In C and D, the ribs (r) are visible crossing the glenoid. Abbreviations: agn, anteglenoidal notch; ap, acromion process; co, coracoid; cof, coracoid foramen; gl, glenoid; r, rib; scb, scapular blade; spl, scapula. Scale bars: 5 cm.

Figure 4.2.3.2. Right humerus of *Dracopelta zbyszewskii* (NOVA-FCT-DCT-5556). Proximal (top) and posterior (bottom) views. Abbreviations: dpc, deltopectoral crest; in, intercondylary notch; lc, lateral condyle; lateral supracondylary ridge; mc, medial condyle; msr, medial supracondylary ridge; of, olecranon fossa; Scale bars: 5 cm (top), 10 cm (bottom).

Figure 4.2.3.3. Pubis-ischium of *Dracopelta zbyszewskii* (NOVA-FCT-DCT-5556). Left pubis and ischium in ventral view. Abbreviations: fh, femoral head; il, ischial lamina; ip, iliac peduncle; is, ischial shaft; of, obturator foramen; pp, pubic peduncle; ppp, postpubic process. Scale bar: 5 cm.

Figure 4.2.3.4 (next page). Femora of *Dracopelta zbyszewskii* (NOVA-FCT-DCT-5556). Left femur in lateral (A), posterior (B) views; right femur in posterior (C) view;

distal end of right femur in posterior (D), anterior (E), medial (F), lateral (G), proximal (H) and distal (I) views; complete distal end of right femur in posterior (J) and distal (K) views. Dashed red line in J and K indicate the breakage line of the two distal femur fragments. Abbreviations: at – anterior trochanter; fh – femoral head; ft – fourth trochanter; gt – greater trochanter; if – intercondylary fossa; in – intercondylary notch; itf – intertrochanteric fossa; lc – lateral condyle; lec – lateral epicondyle; lp – lateral plate; mc – medial condyle; mdc – medullary cavity; pf – popliteal fossa. Scale bars: 10 cm in A-C, 5 cm in D-K.

Figure 4.2.4.1 (previous page). Schematic drawing of NOVA-FCT-DCT-5556 in dorsal view illustrating dermal armour classification. Colours represent dermal armour regions, numbers together with letters represent transverse bands, and letters on the osteoderms indicate position along the band. Refer to sub-section 2.1.1 on Anatomical Nomenclature for further details. Scale bar: 50 cm.

Figure 4.2.4.2. Associated thoracic osteoderms of the holotype of *Dracopelta zbyszewskii* (NOVA-FCT-DCT-5556). Four thoracic subtype II ossicles from NOVA-FCT-DCT-5556 in dorsal (A, C, D), and lateral (B) views. Exact position unknown. Note the faint keel in A and C. Scale bar: 1 cm.

Figure 4.2.4.3. Lateral plates of *Dracopelta zbyszewskii* (NOVA-FCT-DCT-5556). Lateral plates in ventral (A, E), dorsal (B, D), proximal (F) and posterior (G) views; cross-section of plate in C, with dorsal keel prominent. Note in F the rugose margins of the basal groove. Abbreviations: bg – basal groove; pg – posterior groove. Scale bar: 10 cm in A, B, D, and E, 5 cm in F and G, 2 cm in C.

Figure 5.1.1. Strict consensus tree with equal weighting. Consensus tree from 50000 MPTs recovered from the NTS analysis followed by TBR. 1391 steps; CI = 0,289; RI = 0,755; RSI = 0,218. *Dracopelta zbyszewskii* highlighted in red.

Figure 5.1.2. Map of synapomorphies of equal weighting analysis. Strict consensus tree showing the synapomorphic characters and character states of Ankylosauria, including of Panoplosauridae (four synapomorphies) and Struthiosauridae (one synapomorphy), the lowermost branches of the tree.

Figure 5.1.3. Map of synapomorphies of equal weighting analysis. Strict consensus tree showing the synapomorphic characters and character states for the Polacanthidae.

Figure 5.1.4. Map of synapomorphies of equal weighting analysis. Strict consensus tree showing the synapomorphic characters and character states for the Ankylosauridae.

Figure 5.2.1. Strict consensus trees with implied weighting (left, k = 5; right, k = 10). Consensus trees from 5250 MPTs (left) and 11970 (right) recovered from the NTS analysis followed by TBR. Left: 1419 steps; CI = 0,283; RI = 0,748; RSI = 0,212. Right: 1406 steps; CI = 0, 286; RI = 0, 751; RSI = 0,215. *Dracopelta zbyszewskii* highlighted in red.

Figure 5.2.2. Strict consensus trees with implied weighting (left, k=12; right, k=15). Consensus trees from 8736 MPTs (left) and 624 (right) recovered from the NTS analysis followed by TBR. Left: 1401 steps; CI = 0,287; RI = 0,752; RSI = 0,216. Right: 1397 steps; CI = 0,288; RI = 0,753; RSI = 0,217. *Dracopelta zbyszewskii* highlighted in red.

Figure 5.2.3. Map of synapomorphies of implied weighting analysis (k = 15). Strict consensus tree showing the synapomorphic characters and character states of Ankylosauria, including Struthiosauridae, the lowermost branch of the tree shown.

Figure 5.2.4. Map of synapomorphies of implied weighting analysis (k = 15). Strict consensus tree showing the synapomorphic characters and character states for the Panoplosauridae (one synapomorphy).

Figure 5.2.5. Map of synapomorphies of implied weighting analysis (k = 15). Strict consensus tree showing the synapomorphic characters and character states for the Polacanthidae (four synapomorphies).

Figure 5.2.6. Map of synapomorphies of implied weighting analysis (k = 15). Strict consensus tree showing the synapomorphic characters and character states for the "Asian" group (one synapomorphy) of ankylosaurids.

Figure 5.2.7. Map of synapomorphies of implied weighting analysis (k = 15). Strict consensus tree showing the synapomorphic characters and character states for the "North American" group (six synapomorphies) of ankylosaurids.

Figure 6.2.1. Strict consensus tree of the parsimony analysis, with equal weighting. Phylogenetic relationships of Ankylosauria, with *Dracopelta zbyszewskii* highlighted in red. Numbers over branches indicate bootstrap values (only values above 50% are shown), while numbers below branches indicate Bremer support. 1) Ankylosauria; 2) Jurapelta.

Figure 6.2.2. Strict consensus tree of the parsimony analysis, with implied weighting (k = 15). Phylogenetic relationships of Ankylosauria, with *Dracopelta zbyszewskii* highlighted in red. Numbers over branches indicate bootstrap values (only values above 50% are shown), while numbers below branches indicate Bremer support. 1) Ankylosauria; 2) Jurapelta.

Figure 6.2.3. Distribution of taxa from the main clades of Ankylosauria over time. Phylogeny (EW, Fig. 6.2.1 of this dissertation) of Ankylosauria showing the time range of the taxa of the four main clades. Taxa falling outside the main ankylosaur clades were removed as to highlight the members of each group. Dashed lines represent uncertainty of lineage origin in time. Duration of taxa was taken from the literature.

Figure 7.1. Life reconstruction of *Dracopelta zbyszewskii*. Artistic rendering of *D. zbyszewskii* showing its distinct armour pattern and flat head. Colouring is based on *Borealopelta markmitchelli* (Brown *et al.*, 2017). Illustration by Pedro Andrade.

LIST OF TABLES

ABBREVIATONS

Institutional

CMN, Canadian Museum of Nature, Ottawa, Canada; **DMNH**, Denver Museum of Nature and Science, Denver, Colorado, USA; **FCT-UNL**, Faculdade de Ciências e Tecnologia da Universidade Nova de Lisboa (NOVA School of Science and Technology), Caparica, Portugal; **FWMSH**, Fort Worth Museum of Science and History, Fort Worth, Texas, USA; **LNEG**, Laboratório Nacional de Energia e Geologia, Alfragide, Portugal; **MG**, Museu Geológico, Lisboa, Portugal; **ML**, Museu da Lourinhã; **MPC**, Mongolian Paleontological Center, Mongolian Academy of Sciences, Ulaanbaatar, Mongolia; **MUHNAC** (formerly MNHN), Museu Nacional de História Natural e da Ciência, Lisboa, Portugal; **NHMUK**, Natural History Museum, London, UK; **QM**, Queensland Museum, Brisbane, Australia; **ROM**, Royal Ontario Museum, Toronto, Canada; **SMU**, Southern Methodist University, Dallas, Texas, USA; **USNM**, Smithsonian Museum of Natural History, Washington, D.C., USA; **ZPAL**, Zaklad Paleobiologii, Polish Academy of Sciences, Warsaw, Poland

Anatomical

Acpl, anterior centroparapophyseal lamina; **ap**, acromion process; **ar**, alveolar ridge; **at**, anterior trochanter**; be**, buccal emargination; **bg**, basal groove; **c1-c7**, cervical vertebrae (number indicates position of vertebra); **cd1-13**, caudal vertebrae (number indicates position of vertebra); **cds**, caudosacral vertebrae; **chf**, chevron articulation facet; **clp**, caudal lateral plate; **co**, coracoid; **cof**, coracoid foramen; **cr**, caudal rib; **16**, dorsal vertebrae (number indicates position of vertebra); **dia**, diapophysis; **do**, dorsal osteoderm; **ds**, dorsosacral vertebrae; **dsc**, dorsal scute; **dsr**, dorsosacral rib; **f**, fibula; **fh**, femoral head; **ft**, fourth trochanter; **gl**, glenoid; **gt**, greater trochanter; **h**, humerus;

hap, haemal arch pedicel; **hc**, haemal canal; **if**, intercondylary fossa; **il**, ischial lamina; **in**, intercondylary notch; **ip**, ischial peduncle; **is**, ischial shaft; **itf**, intertrocahnteric fossa; **j**, jugal; **jh**, jugal horn; **lc**, lateral condyle **lec**, lateral epicondyle; **lp**, lateral plate; **lpsc**, lateral pelvic scutes; **lsr**, lateral supracondylary ridge; **mc**, medial condyle; **mdb**, mandible; **mdc**, medullary cavity; **msr**, medial supracondylary ridge; **mt**, metatarsal; **mx**, maxillary; ; **mxtm**, maxillary tomium; **nc**, neural canal; **np**, neural pedicel; **o**, orbit; **of**, obturator forâmen; **ol**, olecranon fossa; **oss**, ossicle; **ot**, ossified tendon; **p**, parietal; **pal**, palate; **para**, parapohysis; **pcpl**, posterior centroparapophyseal lamina; **pf**, popliteal fossa; **pg**, posterior groove; **pop**, paroccipital process; **poz**, postzygapophysis; **pp**, pubic peduncle; **ppp**, postpubic process; **prap**, preacetabular process; **proa**, proatlas; **prpol**, postzygoprezygapophyseal lamina; **prz**, prezygapophysis; **q**, quadrate; **qj**, quadratojugal; **r**, rib; **rf**, right femur; **s**, sacral vertebrae; **sc**, scute; **scb**, scapular blade; **sf**, special foramina**; sp**, spinous process; **spl**, scapula; **sq**, squamosal; **sr**, sacral ribs; **ss**, sacral shield.

1

INTRODUCTION

The Ankylosauria Osborn 1923 is a group of armoured, quadrupedal, ornithischian dinosaurs that are mainly characterized by the massive ossification throughout the body, exemplified by the presence of parasagittal rows of osteoderms, a heavily ornamented skull, and the recognizable tail club, albeit the latter is considered synapomorphic for more derived forms (e.g. Maryańska, 1977; Coombs, 1995; Vickaryous and Russell, 2002; Vickaryous *et al.*, 2004; Thompson *et al.*, 2012; Arbour and Currie, 2016; Zheng *et al.*, 2018; Arbour and Zanno, 2019). Some of the most iconic dinosaurs, such as *Ankylosaurus* and *Polacanthus*, are ankylosaurs. Together with Stegosauria (Marsh, 1877), its sister group, they form the two major clades within Thyreophora Nopcsa 1915, the armoured or "shield bearing" dinosaurs (Nopcsa, 1915, 1929; Romer, 1927; Sereno, 1998; Thompson *et al.*, 2012; Arbour and Currie, 2016). As with stegosaurs, members of Ankylosauria can be dated back to at least the Middle Jurassic (Lydekker, 1893; Galton, 1980a, 1983a; Zhiming, 1993). However, as stegosaurs disappeared by the late Early Cretaceous, ankylosaurs diversified and dispersed all over the world during the Cretaceous, with many of the forms appearing by the Late Cretaceous (e.g. Maryańska, 1977; Coombs, 1978; Vickaryous *et al.*, 2004; Thompson *et al.*, 2012; Arbour and Currie, 2016). Nevertheless, ankylosaurs were remarkably conservative in their bauplan and general anatomy across their evolution. All forms were graviportal and obligate quadrupeds. They were exclusively herbivorous,

feeding on a wide range of lower lying plants, and became important components of Cretaceous ecosystems.

The classification of Ankylosauria and its close relationship with Stegosauria have been recognized by various authors even before the widespread use of phylogenetic analysis (Marsh, 1890a; Wieland, 1911; Nopcsa, 1915; Osborn, 1923; Romer, 1927; Nopcsa, 1929; Romer, 1956; Coombs Jr, 1971; Maryańska, 1977; Coombs Jr, 1978a). The landmark works of Walter Coombs (1971, 1978) revised the entire group and established the two major clades within Ankylosauria, Nodosauridae Marsh 1890 and Ankylosauridae Brown 1908, which is accepted to this day. However, internal relationships have proved to be much more chaotic and uncertain as shown by recent analyses (Thompson *et al.*, 2012; Arbour and Currie, 2016). The nature of the often-incomplete remains, in many cases consisting solely of osteoderms and/or fragmentary cranial bones, and a high degree of homoplasy, particularly closer to the base of the group, have hindered an accurate classification of many of its members. Additionally, the fact that some taxa (mostly from the Jurassic and Early Cretaceous) show a mix of early diverging and derived characters states contributed further to the uncertain affinities of several taxa. A third clade, the Polacanthidae (Jaekel, 1910), grouping these forms, and which the major unifying character is the presence of a fused sacral shield, has been proposed as early as 1910, and its validity, either at the same level of Ankylosauridae and Nodosauridae or as a subgroup (Polacanthinae, *sensu* Kirkland, 1998) within these clades, has been assessed by other researchers (Wieland, 1911; Lapparent and Lavocat, 1955; Kirkland, 1998; Carpenter, 2001; Vickaryous *et al.*, 2004; Thompson *et al.*, 2012; Arbour and Currie, 2016; Raven *et al.*, 2023). The more recent studies have shown a much more complex evolutionary history though, and the relationships between taxa are still blurry in many cases, due to the absence of more complete material or the lack of updated reviews of the existing material. Taxa like *Mymoorapelta maysi* Kirkland and Carpenter 1998, *Gargoyleosaurus parkpinorum* Carpenter *et al.* 1998 or *Dracopelta zbyszewskii* Galton 1980, the first two from the Late Jurassic of the USA, and the latter from the Late Jurassic of Portugal, are examples of ankylosaurs which have had an inconsistent phylogenetic positioning (see Thompson *et al*, 2012; Arbour and Currie, 2016; Raven *et al.*, 2023, and references therein for additional details on phylogenetic details; see also the Discussion subchapter 5.2 of this work). In fact, *Dracopelta* has systematically

been excluded from any phylogenetic analysis, until very recently (Raven *et al.*, 2023), and even then, it revealed too incomplete to be conclusive, therefore its exact position remains unclear. Moreover, the relationship between the Late Jurassic taxa is unknown, which becomes even more important when considering the close relation between the North American and Iberian faunas at that time (e.g., Mateus, 2006; Mateus *et al.*, 2006; Hendrickx and Mateus, 2014; Tschopp *et al.*, 2015; Costa and Mateus, 2019). On this regard, the discovery and description of additional material will prove invaluable to a better understanding of the early evolution of Ankylosauria and the clarification of the phylogenetic relationships of its early diverging forms and the paleobiogeographical implications for the whole group.

This study describes a new, mostly complete, articulated ankylosaur skeleton from the Upper Jurassic of Portugal, and reviews and redescribes the holotype of *Dracopelta zbyszewskii*, described by Galton in 1980, identifying also additional unpublished holotype material. The anatomical description is followed by a phylogenetic analysis to ascertain for the first time the systematic position of *Dracopelta* within Ankylosauria, and the implications for ankylosaur evolution and paleobiogeography.

1.1 Historical overview

The Ankylosauria are one of the most historically important group of dinosaurs. The first findings date back to the mid-19th century and some of the earliest dinosaurs named were ankylosaurs, like *Hylaeosaurus* and *Polacanthus*. On December 5th 1832, Gideon Mantell (1833a) reports on a new, armoured reptile from the Tilgate Forest, in Sussex, as follows:

> *"A still more extraordinary peculiarity of osteological structure was exhibited in a series of spinous bony apophyses, which, varying in size from 3 to 17 inches in length, and from 1 and 1/2 to 7 in width at the base, maintained a certain parallelism with the vertebral column, as if they had been placed in a line along the back. This circumstance […] induced the author to suggest that they might be the remains of a dermal fringe, with which, as in some recent species of Iguana, the back of the animal was armed. […] The author proposed forming a new genus for this animal, […] and he suggested the name of* Hylaeosaurus*, or Forest-Lizard…".*

Figure 1.1.1. Lithograph of *Hylaeosaurus armatus* holotype (NHMUK PV OR3775). Illustration of the holotype of *Hylaeosaurus armatus*, showing the pectoral girdle, vertebrae, ribs, and lateral spines. This is the first known representation of an ankylosaur skeleton. Mantell (1833b).

This is the first time an ankylosaur is ever reported, even though the Ankylosauria itself as a group was only named almost 100 years later by Osborn (1923). *Hylaeosaurus armatus* (Mantell, 1833a, 1833b) was thus the third dinosaur to be named, and was one of the three dinosaurs recognized by Sir Richard Owen (1842) to erect Dinosauria. In the following years, both Owen and Mantell wrote on *Hylaeosaurus* and its armour (Mantell, 1841, 1849; Owen, 1858). Osteoderms are also reported from the Isle of Wight at this time (Lee, 1843). At about the same time, Joseph Leidy (1856) reported on a single tooth from the Late Cretaceous of Montana, USA. This would be the first record of an ankylosaur in North America and the second genus of an ankylosaur to be named, *Palaeoscincus costatus* Leidy 1856, nowadays considered a *nomen dubium* (Coombs Jr, 1971; Carpenter, 2001; Vickaryous *et al.*, 2004). Nine years later, on September of 1865, at the 35th Meeting of the British Association For The Advancement Of Science, William Fox (1866) would report on "…a new reptile of the Saurian family."

> *"[…] This strange reptile was clothed with long armour-plates of bone, from 1/2 an inch to 4 inches in diameter, and about 1/2 an inch thick, that covered its body, with the exception of its back, which was protected by a great bony shield. Another remarkable characteristic of this animal was a process of spine-like bones which ran along the sides of the body and tail,*

> *some of which are 15 inches long, and in weight 7 lbs. […] with reference to the extraordinary nature of the spine-like bones, Professor Owen is of opinion that the most appropriate name for this new Saurian would be* Polacanthus*."*

This is the first mention of the name *Polacanthus*, although the formal description and the scientific name *Polacanthus foxii* only came in 1881 by Hulke, and the name itself had been mentioned previously in the description of yet another ankylosaur, *Acanthopholis horridus* (Huxley, 1867), which is nowadays considered *nomen dubium* (Pereda-Suberbiola and Barrett, 1999; Carpenter, 2001; Vickaryous *et al*., 2004). In 1869, Harry Seeley catalogued new material, which he ascribed to *Acanthopholis*, and also named *Cryptosaurus eumerus* (later synonymized with *Cryptodraco eumerus* Lydekker 1889 based on an incomplete right femur, today also widely regarded as *nomen dubium* (e.g. Galton, 1983; Vickaryous *et al*., 2004; Naish and Martill, 2008). The following years saw a period of great scientific production. Until the end of the nineteenth century, the number of discoveries and new taxa kept increasing. As it often happens, some of these taxa would be later considered *nomina dubia* or included into existing taxa. Such an example is *Struthiosaurus austriacus*, named by Emanuel Bunzel in 1871, which is considered a senior synonym of several genera erected during this time, such as *Danubiosaurus*, *Crataeomus*, *Pleuropeltis*, or *Hoplosaurus*, usually based on fragmentary or isolated material (e.g., Bunzel, 1871; Seeley, 1881; Vickaryous *et al*., 2004). Similarly, *Anoplosaurus curtonotus* Seeley 1879 would later include different taxa considered by Seeley as distinct (Pereda-Suberbiola and Barrett, 1999). Seeley added also to this roster of ankylosaurs *Priodontognathus philippsi* Seeley 1875, another dubious ankylosaurian taxon that is here singled out simply because it may be one of the oldest ankylosaurs, possibly from the Oxfordian, although the specimen lacks information on the locality (Galton, 1980a, 1983a; Carpenter, 2001; Vickaryous *et al*., 2004). The last quarter of the nineteenth century was marked by the Bone Wars, a period of bitter rivalry between two of the foremost paleontologists in history, Othniel Charles Marsh and Edward Drinker Cope, that greatly increased our knowledge of extinct organisms and produced a plethora of new taxa, namely dinosaurs (over 136 new species). Among these, *Nodosaurus textilis* Marsh 1889 is of particular relevance, being the second armoured dinosaur from North America, and served as the anchor for Marsh (1890) to coin the term Nodosauridae, which

he recognized as closely related to Stegosauria. A more detailed review of the systematics of Ankylosauria is presented in subchapter 1.2. Three years later, in 1893, Lydekker describes *Sarcolestes leedsi*, a partial left mandible, and possibly the oldest definitive specimen of an ankylosaur (Galton, 1980a, 1983a, 1983b; Vickaryous *et al.*, 2004; Arbour and Currie, 2016).

The twentieth century kept the trend of the last decades of the previous one of more discoveries and descriptions of new taxa, and a shift from Europe being the hub of ankylosaur discoveries to North America. The expansion towards the West of North America drove the discovery of new forms and the recognition of a higher diversity of ankylosaurs in Cretaceous rocks. The first decade alone saw the discovery and naming of *Hoplitosaurus marshi* Lucas 1902, *Euoplocephalus tutus* Lambe 1910 (= *Stereocephalus tutus* (Lambe, 1902), *Stegopelta landerensis* Williston 1905, and *Ankylosaurus magniventris* Brown 1908. The latter is of special relevance since it provided the basis for Barnum Brown (1908) coining and establishing the Ankylosauridae. The next two decades produced a significant number of new discoveries and studies (e.g, (Wieland, 1909, 1911; Moodie, 1910; Lambe, 1919; Parks, 1924; Romer, 1927; Sternberg, 1928, 1929). Of special relevance is the coining of Ankylosauria by Henry Fairfield Osborn (1923). *Panoplosaurus mirus* Lambe 1919, *Dyoplosaurus acutosquameus* Parks 1924, *Edmontonia longiceps* Sternberg 1928, and *Anodontosaurus lambei* Sternberg 1929 are named during this time.

During this period, one individual merits a special reference. Franz Nopcsa (1877-1933), a Hungarian aristocrat of Romanian origin who stepped into the spotlight and assumed a leading role, one that would make him one of the most prominent and visionary palaeontologists of his time and, in fact, in the history of Palaeontology. Ankylosaurs were a major part of the many different groups he studied. In 1905, for example, Nopcsa redescribes the holotype of *Polacanthus foxii* and illustrates for the first time a reconstruction of the skeleton and dermal armour. Ten years later, he erected a new species of *Struthiosaurus*, *Struthiosaurus transylvanicus* Nopcsa 1915, and proposed grouping the stegosaurs and ankylosaurs into the Thyreophora (see subchapter 1.2 for further details). He wrote extensively on the subject (Nopcsa, 1918, 1928, 1929), examining and describing specimens all over Europe, like *Scolosaurus cutleri* Nopcsa 1928, which was found

in Dinosaur Provincial Park, in Canada, in 1914, and is currently housed at the NHMUK.

The 30's and 40's are generally poorer, with fewer discoveries, compared to the first years of the twentieth century, but with a couple of works worth noting nonetheless: Gilmore (1930, 1933) and Mehl (1936). The first described *Palaeoscincus rugosidens* (= *Edmontonia rugosidens*) and *Pinacosaurus grangeri*, and the second *Hierosaurus coleii* (= *Niobrarasaurus coleii* Carpenter *et al*. 1995). During these years the Asian paleontological exploration began, on which ankylosaurs came to be front and centre. Two campaigns were undertaken in 1929-1931 and 1946-1949: the Sino-Swedish Expedition and the Joint Soviet-Mongolian Paleontological Expedition, respectively. These recovered a plethora of specimens that would provide, years later, important amounts of information on Late Cretaceous Asian ankylosaurs (e.g., Maleev, 1952, 1954, 1956; Bohlin, 1953), including new taxa such as *Talarurus plicatospineus* Maleev 1952 and *Sauroplites scutiger* Bohlin 1953. Even before, in the early 20's, Roy Chapman Andrews had led expeditions to Mongolia sponsored by the AMNH. Joint Polish-Mongolian Paleontological Expeditions returned to Mongolia between 1963-1972 (Maryańska, 1977; Tumanova, 1977, 1987), recovering abundant remains of ankylosaurs from the Late Cretaceous of Mongolia, including the holotypes of *Saichania chulsanensis* and *Tarchia kielanae* (Maryańska, 1977). The comprehensive work of Maryańska was one of the most important to that point, because it provided for the first time an in-depth look at Asian ankylosaurs.

At the same time, Walter Coombs Jr (1971) concluded his PhD at the University of Columbia, and his work would become a cornerstone on ankylosaur systematics. He recognized the lack of a thorough description and revision of ankylosaur taxonomy, and he went on to establish a classification that lasted to this day. More details on the systematics of Ankylosauria can be found in subchapter 1.2. He eventually published the results of his landmark research (Coombs Jr, 1978a, 1978b, 1979) and would continue to work on ankylosaurs and be a prolific author on the subject (Coombs Jr, 1972, 1986, 1990, 1995; Coombs, 1995; Coombs Jr and Deméré, 1996). His and Teresa Maryańska's ground-breaking works have influenced palaeontologists for decades and represented a shift in the way researchers defined Ankylosauria and its members.

Up to this point, the fossil record of ankylosaurs is limited to the Cretaceous of Laurasia, apart from a few poorly preserved remains from the Jurassic of England. In 1980, this changes, with the first ankylosaur from Gondwana, *Minmi paravertebra* Molnar 1980, from Australia, and the first articulated remains from the Late Jurassic, *Dracopelta zbyszewskii* Galton 1980. *Minmi* would not be last reported ankylosaur remains from the Southern hemisphere. In 1987, Gasparini *et al.* reports on ankylosaur (and the first dinosaur) remains from Antarctica. During the 80's, based on the contributions of Coombs and Maryańska just a couple of years before, there was a remarkable effort to readdress and review several specimens that hitherto were either too incomplete to properly classify, lacking enough diagnostic characters, or never described at all. Examples are the works of Peter Galton on the English fauna (1986) or the works on the Mongolian ankylosaurs (Tumanova, 1983, 1986, 1987), of which *Shamosaurus scutatus* Tumanova 1983 stands out. Bakker (1988) also describes the new genus *Denversaurus schlessmani* and proposes *Chassternbergia rugosidens*. The 90's began with the discovery of the best Gondwanan ankylosaur known thus far, an almost complete, articulated skeleton from the Early Cretaceous of Australia (Molnar, 1996; Molnar and Clifford, 2000). This was a very prolific research period (e.g., Carpenter, 1990199; Tumanova, 1993; Zhiming, 1993; Kirkland and Carpenter, 1994; Carpenter *et al.*, 1995, 1998, 1999; Coombs, 1995; Coombs Jr, 1995; Blows, 1996; Lee, 1996; Carpenter and Kirkland, 1998; Kirkland, 1998; Kirkland *et al.*, 1998; Godefroit *et al.*, 1999; Sullivan, 1999), with nine new taxa, such as *Gastonia burgei* Kirkland 1998, *Tsagantegia longicranialis* Tumanova 1993 or *Pawpawsaurus campbelli* Lee 1996. It is important to highlight that known Jurassic ankylosaurs more than double in this period, with three new taxa, *Tianchisaurus nedegoapeferima* Zhiming 1993, from the Middle Jurassic of China, *Mymoorapelta maysi* Kirkland and Carpenter 1994, and *Gargoyleosaurus parkpinorum* Carpenter *et al.* 1998, from the Late Jurassic of the USA.

The last 20 years witnessed the development of new techniques, methods, and approaches that, coupled with an increasing number of specimens, some exquisitely preserved, improve greatly the knowledge not just on ankylosaur systematics and evolution, but on the biology of the animals themselves. Studies on teeth wearing and feeding mechanisms, histology, biomechanics, or detailed cranial osteology become more common and provide crucial details on important aspects, such as

ontogeny and growth, armour development, and niche partitioning (e.g., (Molnar and Clifford, 2000; Vickaryous, 2001; Vickaryous and Russell, 2002; Scheyer and Sander, 2004; Arbour *et al.*, 2011; Miyashita *et al.*, 2011; Stein *et al.*, 2013; Burns and Currie, 2014; Mallon and Anderson, 2014; Ősi *et al.*, 2014; Leahey *et al.*, 2015; Brown, 2017; Brown *et al.*, 2017, 2020; Bourke *et al.*, 2018; Paulina-Carabajal *et al.*, 2018; Arbour and Zanno, 2019; Cerda *et al.*, 2019; Perales-Gogenola *et al.*, 2019; Botfalvai *et al.*, 2020; Kuzmin *et al.*, 2020; Park *et al.*, 2020; Kubo *et al.*, 2021; Soto-Acuña *et al.*, 2021). This holistic approach has also profited from a more thorough sampling of the fossil record, with a plethora of global occurrences, and an increased number of well-preserved specimens. More and better specimens resulted in better phylogenetical resolution and augmented diversity, i.e., almost half of the currently accepted taxa were named in 21st century (Ford, 2000; Carpenter, 2001; Carpenter *et al.*, 2001; Ford and Kirkland, 2001; Vickaryous *et al.*, 2001; Xu *et al.*, 2001; Averianov, 2002; Zhiming, 2002; Garcia and Pereda-Suberbiola, 2003; Ősi, 2005; Salgado and Gasparini, 2006; Lü *et al.*, 2007; Xu *et al.*, 2007; Carpenter *et al.*, 2008; Arbour *et al.*, 2009; Miles and Miles, 2009; Parsons and Parsons, 2009; Burns and Sullivan, 2011; Stanford *et al.*, 2011; Chen *et al.*, 2013; Kirkland *et al.*, 2013; Penkalski, 2013; Yang *et al.*, 2013; Arbour *et al.*, 2014c, 2014a; Arbour and Currie, 2016; Kinneer *et al.*, 2016; Arbour and Evans, 2017; Brown *et al.*, 2017; Penkalski and Tumanova, 2017; McDonald and Wolfe, 2018; Penkalski, 2018; Rivera-Sylva *et al.*, 2018; Wiersma and Irmis, 2018; Zheng *et al.*, 2018; Raven *et al.*, 2020; Maidment *et al.*, 2021; Soto-Acuña *et al.*, 2021; Riguetti *et al.*, 2022; Pond *et al.*, 2023). *Liaoningosaurus paradoxus* Xu *et al.* 2001, *Hungarosaurus tormai*, Ősi, 2005, *Antarctopelta oliveroi* Salgado and Gasparini 2006, *Europelta carbonensis* Kirkland *et al.* 2013, *Kunbarrasaurus ieversi* Leahey *et al.* 2015, *Zuul crurivastator*, Arbour and Evans 2017, *Borealopelta markmitchelli* Brown *et al.* 2017, *Jinyunpelta sinensis* Zheng *et al.* 2018, or *Stegouros elengassen* Soto-Acuña *et al.* 2021 are examples of taxa erected during this period. Future and ongoing work on existing and new material will update and improve the current knowledge on the paleobiology, paleobiogeography, and paleoecology, and help resolve the evolutionary relationships of Ankylosauria.

1.2 Systematics of Ankylosauria

The classification of Ankylosauria and its interrelationships have been a matter of debate since the XIX century. One of the major contributing factors for its convoluted and complex history is the unique anatomy of the group. During their evolutionary history, the most conspicuous trait of the Ankylosauria, the extensive dermal armour, reached extreme levels of ossification, particularly during the Late Cretaceous, as exemplified by the fusion of the bones of the posterior half of the tail, forming the tail club, hyperossification of the skull, or the large, lateral spines and heavily built armour, as observed for example in *Ankylosaurus*, *Euoplocephalus*, *Saichania*, *Edmontonia*, or *Panoplosaurus* (e.g. Lambe, 1919; Maryańska, 1977; Carpenter, 1990, 2004; Vickaryous and Russell, 2002; Vickaryous *et al.*, 2004; Arbour and Currie, 2016). The presence of dermal armour, external ossification of the skull, which often completely obliterates cranial sutures, or the conservative morphology of the postcranial skeleton have often made it difficult to produce accurate identifications and diagnosis. Coupled with the incompleteness of the record and/or often fragmentary nature of the finds, phylogenetic studies have been further complicated by either the, and thus potential important data gaps, and/or the high degree of homoplasy (Parsons and Parsons, 2009; Thompson *et al.*, 2012; Raven, 2021; Riguetti *et al.*, 2022). Furthermore, there has been a bias towards codification of cranial characters compared to the postcranial skeleton, possibly due to an apparent tendency for the preservation of the hyperossified skull in ankylosaurs, but also to an intrinsic complexity of cranial osteology and its interspecific variation potential (e.g., Godefroit *et al.*, 1999; Vickaryous, 2001; Vickaryous and Russell, 2003; Arbour and Mallon, 2017, and references therein; see also character list of Arbour and Currie, 2016), which can eventually lead to an eschewed phylogenetic signal.

Nonetheless, several authors have throughout the years observed and attempted to establish the classification of Ankylosauria, either focused on the group itself or within a broader analysis of Thyreophora. The first attempt to define a group of armoured dinosaurs was by Huxley (1869), identifying a diagnostic combination of five characters in his observations of English material (i.e., *Hylaeosaurus*, *Polacanthus* and *Acanthopholis*), which he named Scelidosauridae. The latter would be used again by Marsh (1895) as a subgroup of Stegosauria,

together with Nodosauridae. The same author (1890b) had defined Nodosauridae based on the "heavy dermal armour, solid bones, large forelimbs, and ungulate feet". However, in the same publication, Nodosauridae was included in Ceratopsia, solely because of the Cretaceous age of its single member, *Nodosaurus*, which had been ascribed to Stegosauria the year before (Marsh, 1889), thereby recognizing the close relationship between stegosaurs and ankylosaurs. The same conclusion was made by different authors, such as Nopcsa (1902), who grouped ankylosaurs under Stegosauria into the now invalid Acanthopholidae, Brown (1908), who erected the Ankylosauridae, based mostly on the anatomy of *A. magniventris* (AMNH 5895) and including also *E. tutus* within Stegosauria, or Wieland (1911), who considered only Nodosauridae as valid but notes the plausibility of more complex relationships between taxa based on the observations of the different dermal armour, mentioning Polacanthidae in passing. Further complicating the classification at the time, on this regard, Jaekel (1910) is the first author to coin Polacanthidae, considering it a subgroup of Ornithischia, without providing a diagnosis though. The year before, Huene (1909) had included *Polacanthus* and other ankylosaurs into the Omosauridae, separately from the exclusively North American "Ancylosauridae [*sic*]", and both at the same level taxonomically as Stegosauridae. Regardless, the affinities between stegosaurs and ankylosaurs prompted Nopcsa (1915) to erect the Thyreophora, which included the Acanthopholidae, the Stegosauridae, and the Ceratopsidae, pointing to the skull morphological similarity, quadrupedal posture, and herbivory. The same author (Nopcsa, 1923) coined Struthiosaurinae and Acanthopholinae without providing any comment. In the same year, Osborn (1923) coins the term Ankylosauria, although no argument was presented for its use. The close relationship between stegosaurs and ankylosaurs was also noted by Romer (1927), who concluded that, although closely related, there were substantial differences in pelvic structure and dermal armour between different armoured dinosaurs to support two distinct groups, the "*stegosaurs proper and the heavily armoured forms, such as* Polacanthus*,* Nodosaurus*,* Ankylosaurus*, and the like*". Similar criteria were used by Lapparent and Lavocat (1955) in their proposed classification, using the term "Polacanthinae" for the first time. However, they place it at the same level as Nodosaurinae and Panoplosaurinae, and in turn consider these as sub-families within the Nodosauridae. The same authors synonymize Nodosauridae with Ankylosauridae, including it in the Stegosauroidea, together with

Acanthopholidae, Stegosauridae and Syrmosauridae. The latter has since then been considered a junior synonym of Ankylosauridae (Arbour and Currie, 2016). Lapparent and Lavocat (1955) based this classification largely on cranial differences, but the Polacanthinae were diagnosed on the presence of a sacral shield and included *Polacanthus* and *Hoplitosaurus*. Other authors (e.g., Hennig, 1915; Nopcsa, 1918, 1923a, 1928; Gilmore, 1930) have proposed alternative systematic arrangements, generally following the same nomenclature for the groups, but always considering ankylosaurs as a subgroup of stegosaurs. Romer (1956) further elaborated on his assertions for the separation between Stegosauria and Ankylosauria defined by a distinct group of anatomical characters, such as the superficial dermal ossification covering the skull, closure of all or nearly all cranial fenestra, short neural spines, or the greatly reduced pubis. He further divides Ankylosauria in two groups, the Acanthopholidae, composed of *Hylaeosaurus*, '*Acanthopholis*', and *Struthiosaurus*, and the Nodosauridae, composed of all other ankylosaurs. However, he also recognized the difficulty in the systematics of the group due to the poor record.

The pre-cladistic benchmark work of Coombs (1971, 1978) provided the first comprehensive revision of all ankylosaurs and, based on detailed cranial and postcranial anatomical comparisons, classified and diagnosed the Ankylosauria, dividing it into two groups, as Romer (1956) had proposed, but considering Acanthopholidae invalid, thus definitively establishing the Ankylosauridae + Nodosauridae paradigm, which has been the taxonomical basis for subsequent works (e.g., Sereno, 1986, 1998; Tumanova, 1987; Coombs, 1990; Lee, 1996; Vickaryous *et al.*, 2004; Thompson *et al.*, 2012). While Coombs did not resolve the lower taxonomy of each group, he did recognize the possibility of subgroups or "lineages" of nodosaurids, whereas ankylosaurids were more anatomically conservative and therefore less distinctive between forms. He also observed the presence of a tail club was restricted to ankylosaurids. At the same time, he hypothesized that, since nodosaurids and ankylosaurids had each such distinct anatomical traits, the evolutionary divergence had to be pre-Cretaceous. Tumanova (1983) proposes a subgroup of early Cretaceous ankylosaurids, the Shamosaurines, which included *Shamosaurus* and *Saichania*, that exhibited features observed in nodosaurids and ankylosaurids, and that she postulated would be the ancestors to the Ankylosaurinae (Tumanova, 1987:14, Fig. 14). The first numerical approaches

to ornithischian relationships (Norman, 1984; Sereno, 1984, 1986) corroborated the Stegosauria and Ankylosauria as sister taxa within Thyreophora, as well as *Scutellosaurus* and *Scelidosaurus* as the earliest thyreophorans, with *Scelidosaurus* as sister taxon to stegosaurs and ankylosaurs. The improved resolution of Ankylosauria prompted Sereno (1998) to formally define Ankylosauridae as all ankylosaurs closer to *Ankylosaurus* than to *Panoplosaurus*, Ankylosaurinae as all ankylosaurids closer to Ankylosaurus than to either *Shamosaurus* or *Minmi*, Nodosauridae as all ankylosaurs closer to *Panoplosaurus* than to *Ankylosaurus*, and Nodosaurinae as all nodosaurids closer to *Panoplosaurus* than to either *Sarcolestes* or *Hylaeosaurus*. As more specimens became available (see subchapter 1.1 for further details), character sampling improved, which occurred concomitantly to the more widespread use of phylogenetic analytical techniques in studies. At the same time, however, more discoveries in the Early Cretaceous and Upper Jurassic increasingly casted doubts on the Ankylosauridae + Nodosauridae dichotomy, as more specimens showed characters present in both groups or as plesiomorphies of Ankylosauria. Kirkland (1998) recovered Polacanthinae as a monophyletic group to include these forms and considered it and Shamosaurinae to be successive sister groups of Ankylosaurinae within Ankylosauridae. Carpenter (2001) performed a phylogenetic analysis of all ankylosaurs and equalled Polacanthinae to Nodosauridae and Ankylosauridae, recovering the term Polacanthidae of Jaekel (1910), and defining it as "all ankylosaurs that are closer to *Gastonia* than to *Edmontonia* and *Euoplocephalus*". Moreover, the same author found *Scelidosaurus* as sister taxa to Ankylosauria, naming that grouping as Ankylosauromorpha. However, Carpenter compartmentalized the analysis, i.e., separate analyses were performed for each individual clade and merged into a broader analysis, with each group (Polacanthidae, Ankylosauridae, and Nodosauridae) having taxa attributed *a priori*, based on anatomical characters. Posterior analyses of Ankylosauria (e.g., Vickaryous *et al.*, 2004; Thompson *et al.*, 2012, Arbour and Currie, 2016) were unable to recover a similar topology, instead finding the Ankylosauridae + Nodosauridae result and placing most or all polacanthids as early diverging nodosaurids. Other studies, such as the works by Vickaryous (2001) and Hill *et al.* (2003), increased character and taxon sampling from previous ones, but focused on cranial characters, resulting in taxa known from fragmentary cranial material or postcranial material to be disregarded. Those studies found, for example,

Gargoyleosaurus, *Gastonia* and *Kunbarrasaurus* (at the time, assumed as *Minmi paravertebra*) as early diverging ankylosaurids, and *Cedarpelta* as an early diverging nodosaurid. Further iterations of these analyses were used in new taxa descriptions (e.g., Ősi, 2005; Lü *et al*., 2007; Parsons and Parsons, 2009), with slight modifications to the datasets. The datasets introduced by Thompson *et al*. (2012) and Arbour and Currie (2016), the former based on the unpublished dissertation of Parish (2005) and the latter resulting from the revision and modification of previous analyses (Thompson *et al*., 2012; Arbour and Currie, 2013a; Arbour *et al*., 2014a, 2014c), were the most comprehensive at the time, respectively including 56 taxa and 170 characters, and 44 taxa and177 characters. It is worth mentioning that Yang *et al*. (2013) performed an analysis using the dataset of Thompson *et al*. (2012) to test the position of *Taohelong jinchengensis* and recovered Polacanthinae within Nodosauridae, defining it "as the most inclusive clade containing *Polacanthus foxii* but not *Ankylosaurus magniventris* or *Panoplosaurus mirus*". The study by Arbour and Currie (2016) focused on Ankylosauridae and did not test non-ankylosaurid relationships in detail. It did increase the resolution of ankylosaurid relationships though, and considered not only the Shamosaurinae of Tumanova (1983) monophyletic but also that Stegopeltinae, proposed by Ford (2000), is not monophyletic and that the taxa included were nodosaurids (except *Aletopelta*, which came out as an ankylosaurid). This study became the basis for subsequent descriptions of new taxa, which kept the general Ankylosauridae + Nodosauridae Recent studies (e.g., Wiersma and Loewen, 2018; Soto-Acuña *et al*., 2021; Raven *et al*., 2023) have begun changing this paradigm, revealing a more complex phylogeny than previously thought. Wiersma and Loewen (2018) conducted, in their description of *Akainacephalus johnsoni*, a novel analysis using the dataset of Loewen and Kirkland (2013), which coded 293 characters across 35 taxa, even though only eleven were non-ankylosaurids, and two of those (*Gargoyleosaurus* and *Mymoorapelta*) were set as representatives of Polacanthidae. An expanded and revised version of this dataset (329 characters, 95 taxa) is used herein to resolve the position of *Dracopelta* and to analyse the phylogeny of Ankylosauria. The thorough study by Norman (2021) of *Scelidosaurus* again recovered an Ankylosauridae + Nodosauridae topology, finding *Jinyunpelta* (considered by Zheng *et al*. [2018] as the earliest ankylosaurine) and *Kunbarrasaurus* as successive earlier diverging ankylosaurs. The same analysis defined a stem-based Ankylosauria as "all

taxa more closely related to *Euoplocephalus* and *Edmontonia* than to *Stegosaurus*", which would include *Scelidosaurus* as a stem ankylosaur, a result that has been debated (Madzia *et al.*, 2021; Soto-Acuña *et al.*, 2021; Yao *et al.*, 2022; Raven *et al.*, 2023). Soto-Acuña *et al.* (2021) alternatively placed *Scelidosaurus* as the sister taxa of Eurypoda (Ankylosauria + Stegosauria) while proposing a different arrangement for Ankylosauria, based on their analysis of *Stegouros*. Using distinct modified previous datasets, those authors found an early diverging group of ankylosaurs, the Parankylosauria, composed exclusively of Gondwanan Late Cretaceous forms, as the sister group to Euankylosauria, composed of "*the first ancestor of* Ankylosaurus – *but not* Stegouros – *and all of its descendants*". The Euankylosauria in turn present the Ankylosauridae + Nodosauridae topology. In another study, Madzia *et al.* (2021), even though not conducting any phylogenetic analysis in their study, revised the nomenclature of known ornithischian clades following the International Code of Phylogenetic Nomenclature (PhyloCode), and provided definitions for Ankylosauria, Ankylosauridae, Ankylosaurinae, Ankylosaurini, Nodosauridae, Nodosaurinae, Panoplosaurini, Polacanthinae, Shamosaurinae, and Struthiosaurini. Although useful, these definitions were based on reference phylogenies and therefore may require redefining or readaptation to reflect the results of later studies, such as the one performed herein. In particular, the authors address the "polacanthid/polacanthine" problematic, considering Polacanthidae as a synonym of Polacanthinae and defining it as "the largest clade within Ankylosauridae or Nodosauridae containing *Polacanthus foxii* but not *Ankylosaurus magniventris* and *Panoplosauurus mirus*". This definition is based on the reference phylogeny of Yang *et al.* (2013) which placed Polacanthinae within Nodosauridae, in agreement with other authors (e.g., Thompson *et al.*, 2012; Rivera-Sylva *et al.*, 2018; Zheng *et al.*, 2018) but contrary to Kirkland (1998) who proposed Polacanthinae as an early diverging group of ankylosaurids. Still, Madzia *et al.* (2021) also admit that Polacanthidae should be preferred if the clade including *Polacanthus* is found to fall outside the Ankylosauridae + Nodosauridae, which is the case in this work. More recently, Raven *et al.* (2023) conducted a thorough analysis of Thyreophora (340 characters, 91 taxa) and recovered four distinct ankylosaur clades, defined as: Ankylosauridae, all ankylosaurs more closely related to *Ankylosaurus* than to *Panoplosaurus*, *Struthiosaurus austriacus*, or *Gastonia burgei*; Panoplosauridae, all ankylosaurs more closely related to *Panoplosaurus* than

to *Ankylosaurus*, *Struthiosaurus austriacus*, or *Gastonia burgei*; Polacanthidae, all ankylosaurs more closely related to *Gastonia burgei* than to *Ankylosaurus*, *Panoplosaurus*, or *Struthiosaurus austriacus*; Struthiosauridae, all ankylosaurs more closely related to *Struthiosaurus austriacus* than to *Ankylosaurus*, *Panoplosaurus*, or *Gastonia burgei*. This general topology is found herein, although with differences since the dataset is distinct, and the definitions of the four major clades are assessed for conformity and adapted when applicable. The results obtained in this work corroborate the hypothesis that ankylosaur phylogeny, namely of non-ankylosaurid ankylosaurs, is more complex than previously thought, and confirm the validity of Polacanthidae as an early branching clade of ankylosaurs.

1.3 Fossil record

1.3.1 Jurassic

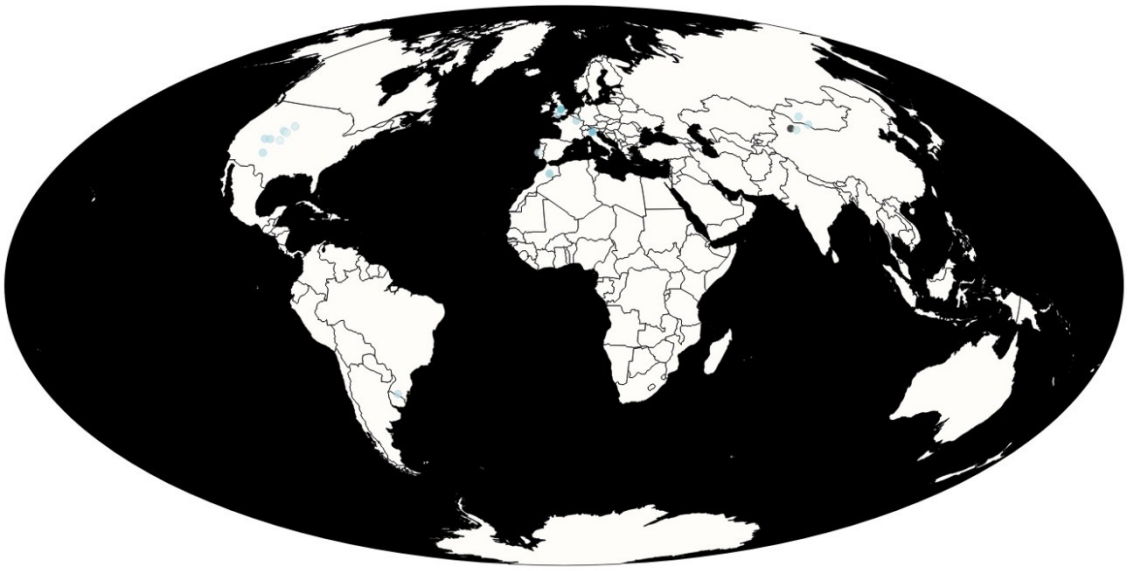

Figure 1.3.1.1. Map of Jurassic worldwide ankylosaur occurrences. Blue circles follow the International Commission on Stratigraphy colour coding for the Jurassic. Map from the Paleobiology Database (https://paleobiodb.org/navigator/).

The fossil record of Ankylosauria is extensive, dating at least as early as the Middle Jurassic up to the end of the Cretaceous (Figs. 1.3.1.1, 2.1; Table 1.3.1.1), and having been reported from every continent. Galton (2019) described dermal armour of putative ankylosaurian affinity from the Early Jurassic (Sinemurian-Pliensbachian) of India, thus potentially making it the oldest record of the group.

Fragmentary thyreophoran remains from the Middle Jurassic (Early Bajocian) have been identified as possibly belonging to ankylosaurs (Clark, 2001; Delsate *et al.*, 2018). Purported tracks from the Middle Jurassic (Aalenian-Bajocian) of the UK suggest a thyreophoran, possibly ankylosaurian, affinity (McCrea *et al.*, 2001), as well as tracks from the Middle Jurassic (Bajocian) of Mexico (Rodríguez-de la Rosa *et al.*, 2018). The oldest skeletal record definitively ascribed to an ankylosaur is a single rib fragment with coossified spines attributed to *Spicomellus afer* Maidment *et al.* 2021, from the Middle Jurassic of Morocco. From the Callovian of the UK, there is *Sarcolestes leedsi* (Lydekker, 1893; Galton, 1980a, 1983a, 1983b, 1994). Also from the UK, purportedly from the Oxfordian of Yorkshire and Cambridgeshire, there are, respectively, *Priodontognathus philipsii* and *Cryptosaurus eumerus* (Seeley, 1875; Lydekker, 1889; Galton, 1980b, 1983a). However, the first lacks locality information and although generally accepted to be Oxfordian in age, doubts remain if this specimen is indeed from the Upper Jurassic or rather from the Early Cretaceous. Both have been considered a *nomen dubium* due to the paucity and undiagnostic character of the remains, instead referred to Ankylosauria indet. (Vickaryous *et al.*, 2004). A partial skeleton, referred to *Tianchisaurus nedegoapeferima*, has been considered from the Middle Jurassic of China (Zhiming, 1993). However, recent stratigraphical work (Huang, 2019) places the occurrence in the early Upper Jurassic (Oxfordian-Kimmeridgian). Ankylosaur remains were also recently reported from the Qigu Formation (Kimmeridgian-Tithonian), China (Augustin *et al.*, 2020) The Upper Jurassic has a more abundant record, mainly from the Morrison Formation, USA, with most of the occurrences ascribed to either *Gargoyleosaurus parkpinorum* or *Mymoorapelta maysi* (Galton, 1980c; Kirkland and Carpenter, 1994; Carpenter *et al.*, 1998, 2013; Kirkland *et al.*, 1998, 2016; Kilbourne and Carpenter, 2005; Tremaine *et al.*, 2015; Russo and Mateus, 2019, 2021; Foster, 2020). Outside North America, the Upper Jurassic Lourinhã Formation (upper Kimmeridgian-uppermost Tithonian) of Portugal has the best record, specifically in the upper Tithonian, represented by the occurrence of *Dracopelta zbyszewskii* (Russo and Mateus, 2019, 2021, 2023; this work). From Gondwana, the only occurrence reported for the Jurassic are tracks from the Guará Formation, Brazil (Francischini *et al.*, 2018).

Table 1.3.1.1. Jurassic ankylosaur taxa and material ascribed to each taxon.

Taxa	Material	References
Dracopelta zbyszewskii	Partial articulated ribcage and dermal armour (MG 5787), partial right pes (MG 3), partial right femur, tibia, dermal armour and unidentified elements (uncatalogued), mostly complete articulated skeleton, including cranial, axial, appendicular, and dermal armour elements (NOVA-FCT-DCT-5556).	Galton (1980, 1983a), Pereda-Superbiola *et al.* (2005), Russo and Mateus (2019, 2021, 2023), this work.
Gargoyleosaurus parkpinorum	Partial disarticulated skeleton, including cranial, axial, appendicular and dermal elements (DMNS 27726), partial pelvis (DMNS 58831).	Carpenter *et al.* (1998, 2013), Kilbourne *et al.* (2005).
Mymoorapelta maysi	Disarticulated elements, including cranial, axial, appendicular, and dermal elements (MWC 939, 1800-1840, 1908, 2677, 2678, 2843, 3616, 5438, 5643, 6743, 6745), partial articulated skeleton (MWC 2610), partial sacrum (LACM 154873).	Kirkland and Carpenter (1994), Kirkland *et al.* (1998); Foster (2020)
Tianchisaurus nedegoapeferima	Associated fragmentary and partially articulated elements, including cranial, axial, appendicular, and dermal elements (IVPP V 10614).	Zhiming (1993)
Sarcolestes leedsi	Partial left mandible (NHMUK PV R2682), partial osteoderm (SMC J.46884), two partial osteoderms (OUM J.48052).	Lydekker (1883), Galton (1983b, 1994a).
Spicomellus afer	Partial rib with four co-ossified spines (NHMUK PV R37412).	Maidment *et al.* (2021)

1.3.2 Cretaceous

Gondwana

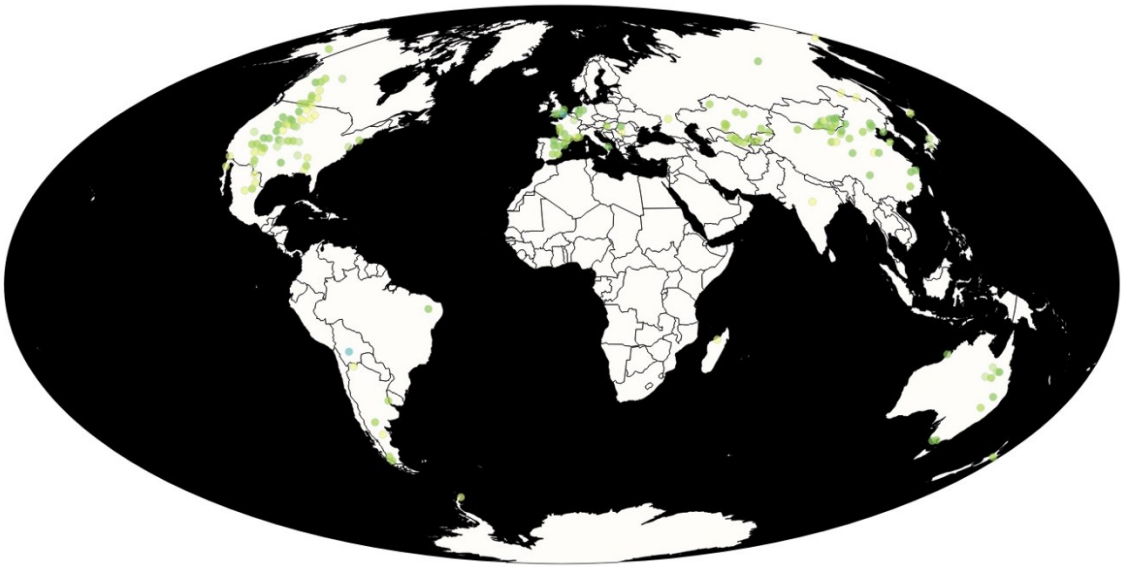

Figure 1.3.2.1. Map of Cretaceous worldwide ankylosaur occurrences. Green circles follow the International Commission on Stratigraphy colour coding for the Cretaceous. Map from the Paleobiology Database (https://paleobiodb.org/navigator/).

The Cretaceous is by far the richest in ankylosaur remains, mostly from Laurasia. In Gondwana, ankylosaurs are scarce and usually fragmentary. Australia has the most and the best-preserved occurrences, mostly from the Early Cretaceous. *Kunbarrasaurus ieversi*, from the Allaru Mudstone (Upper Albian-?lower Cenomanian) of Queensland, is the most complete ankylosaur from the Southern hemisphere. *Minmi paravertebra*, from the Bungil Formation (Aptian) of Queensland was the first ankylosaur reported from Gondwana. Additional material is known from Australia, ranging from the upper Hauterivian to the early Turonian (Barrett *et al.*, 2010; Leahey and Salisbury, 2013; Bell *et al.*, 2018; Leahey *et al.*, 2019). Albeit consisting of a few isolated elements, material has also been reported from the Campanian-Maastrichtian-aged Tahora Formation from New Zealand (Molnar and Wiffen, 1994; Agnolin *et al.*, 2010) and possibly from the Cenomanian-Turonian of Madagascar (Russell *et al.*, 1976; Maidment, 2010). From the uppermost Cretaceous (Maastrichtian) Lameta Formation of India, putative ankylosaur remains have been reported (Chatterjee and Rudra, 1996; Chatterjee, 2020). In South America, most of the reported occurrences are tracks and isolated skeletal remains (Salgado and Coria, 1996; Coria and Salgado, 2001; McCrea *et al.*, 2001; De Valais *et al.*, 2003; Apesteguía and Gallina, 2011; Murray *et al.*, 2019; Riguetti *et al.*, 2022). However, recent studies have revealed more diagnostic material, such as *Patagopelta cristata* Riguetti *et al.* 2022, from the Allen Formation (upper Campanian-lower Maastrichtian), or the partially complete, semi-articulated *Stegouros elengassen* Soto-Acuña *et al.* 2021, from the coeval Upper Cretaceous Dorotea Formation (upper Campanian-lower Maastrichtian). The latter is the most complete ankylosaur from South America and remarkable for its unique caudal armour morphology (Soto-Acuña *et al.*, 2021). From Antarctica comes *Antarctopelta oliveroi* Salgado and Gasparini 2006, from the upper Campanian Snow Hill Island Formation (Gasparini *et al.*, 1987, 1996; Olivero *et al.*, 1991; de Ricqlès *et al.*, 2001; Cerda *et al.*, 2019; Murray *et al.*, 2019; Soto-Acuña *et al.*, 2024).

North America

As pointed out above, the bulk of ankylosaur fossils come from the Cretaceous of Laurasia, i.e., North America, Europe, and Asia. Although the record is extensive throughout, it becomes progressively more abundant from the Early Cretaceous through the Late Cretaceous. In North America, the earliest Cretaceous record comes from the lower Cedar Mountain Formation (Berriasian-Hauterivian), *Gastonia burgei*,

and Lakota Formation, *Hoplitosaurus marshi*, of Utah and South Dakota respectively (Lucas, 1901; Gilmore, 1914; Carpenter and Kirkland, 1998). *Gastonia* may be the earliest record of an ankylosaurid in North America (Arbour and Currie, 2016). Considering that dating from Early Cretaceous formations in North America has been controversial and only recently have more accurate (predominantly older) ages been suggested, the fossil record is nonetheless generally richer towards the late Early Cretaceous. One of these fossils is the exceptionally preserved *Borealopelta markmitchelli*, from the Clearwater Formation (Aptian), Canada. Higher in the Cedar Mountain Formation, from the Aptian-Albian, the occurrences are abundant and widespread (Kirkland *et al.*, 2016), such as *Gastonia lorriemchinneyae* Kinneer *et al.* 2016, *Peloroplites cedrimontanus* Carpenter *et al.* 2008, *Cedarpelta bilbeyhallorum* Carpenter *et al.* 2001, *Animantarx ramaljonesi* Carpenter *et al.* 1999, and footprints have also been reported (McCrea *et al.*, 2001). Of the same age, ankylosaur remains are known from the Cloverly Formation, namely *Tatankacephalus cooneyorum* Parsons and Parsons 2009, and *Sauropelta edwardsorum* Ostrom 1970. Ankylosaurs are known from the Patuxent Formation (early Albian), Maryland, such as *Propanoplosaurus marylandicus* Stanford *et al.* 2011, and from the Arundel Formation, teeth attributed to *Priconodon crassus* Marsh 1888. The Paw Paw Formation (Albian) has also produced ankylosaur material, as *Texasetes pleurohalio* Coombs Jr 1995b and *Pawpawsaurus campbelli* Lee 1996. Occurrences are also known in the Dakota Formation (upper Albian-Cenomanian), namely *Silvisaurus condrayi* Eaton Jr 1960. Early Cretaceous tracks attributed to ankylosaurs have been reported all over North America, mostly from the Dakota Group of Colorado, but also from the Gething and Gates Formations (Aptian-Albian), British Columbia and Alberta respectively, Canada (Sternberg, 1932; McCrea *et al.*, 2001; Lockley, 2006; Lockley and Gierlinski, 2014). From the Frontier Formation (Cenomanian), remains are comparatively limited, but *Stegopelta landerensis* and *Nodosaurus textilis* were identified from these strata. Tracks of possible ankylosaurian origin have been reported in the Aptian-Cenomanian aged Chandler and Dunvegan Formations of northern North America, in Alaska and Canada respectively (see McCrea *et al.*, 2001). Recently, fragmentary remains were reported from the Dunvegan Formation, British Columbia, Canada (Arbour *et al.*, 2020). Few remains are known from the mid-Upper Cretaceous of North America: *Niobrarasaurus coleii* Mehl 1936, *Acantholipan gonzalezi* Rivera-Sylva *et al.* 2018, and *Invictarx zephyri* McDonald

and Wolfe, 2018, respectively from the Smoky Hill Chalk Member (Coniacian) of the Niobrara Chalk Formation, Kansas, the Pen Formation (Santonian) of Mexico, and the Menefee Formation (early Campanian), New Mexico, as well as fragmentary material and tracks from Mexico (Rivera-Sylva and Espinosa-Chávez, 2006; Kappus *et al.*, 2011; Rivera-Sylva *et al.*, 2011, 2018). Contrarily, the last ten million years of the Cretaceous have an extremely rich and diverse ankylosaur record, with continuous presence of ankylosaurs throughout the different formations (Brown, 1908; Coombs Jr, 1995a; Vickaryous *et al.*, 2004; Arbour and Currie, 2013a; Arbour *et al.*, 2014b; Burns and Lucas, 2015; Arbour and Currie, 2016). This abundance is represented by, for example, the approximately 25 % of consensually accepted taxa that were found in the Campanian-Maastrichtian of North America. From the Judith River Formation (Campanian), Montana, are notable the occurrences of *Zuul crurivastator* and the first ankylosaur remains from North America, teeth first attributed to *Palaeoscincus costatus*, now of indeterminate ankylosaurian affinity (Carpenter, 2001; Vickaryous *et al.*, 2004). Plentiful remains were found in the Two Medicine Formation, Campanian, of Montana and southern Alberta (Vickaryous *et al.*, 2001; Arbour and Currie, 2013a; Penkalski, 2013, 2018), attributed mostly to *Scolosaurus cutleri* Nopcsa 1928, *Scolosaurus thronus* Penkalski 2018, *Oohkotokia horneri* Penkalski 2013, and *Edmontonia rugosidens* Gilmore 1930. Some of these taxa occur also in the Dinosaur Park Formation (late Campanian), which produced the bulk of Late Cretaceous North American ankylosaur material (Vickaryous *et al.*, 2001; Arbour *et al.*, 2009; Arbour and Currie, 2013a; Penkalski, 2018), among which are *Platypelta coombsi* Penkalski 2018, *Panoplosaurus mirus*, *Euoplocephalus tutus*, *Anodontosaurus inceptus* Penkalski 2018, and *Dyoplosaurus acutosquameus*. In southern North America, the Kirtland Formation (late Campanian), in New Mexico and Colorado, stands out as the most productive, with three taxa known so far: *Ziapelta sanjuanensis* Arbour *et al.*, 2014b, *Nodocephalosaurus kirtlandensis* Sullivan 1999, and *Ashislepelta minor* Burns and Sullivan 2011. Coeval material is also known, albeit to a lesser extent, in the Point Loma and Kaiparowits Formations, from California and Utah respectively (Coombs Jr and Deméré, 1996; Ford and Kirkland, 2001; Loewen *et al.*, 2013; Wiersma, 2016; Wiersma and Irmis, 2018), notably *Aletopelta coombsi* Ford and Kirkland 2001, and *Akainacephalus johnsoni* Wiersma and Irmis 2018. In the slightly younger Horseshoe Canyon Formation (upper Campanian-lower Maastrichtian),

southwestern Alberta, the record for ankylosaurs is comparatively poorer to the rich Dinosaur Park Formation, but *Anodontosaurus lambei* Sternberg 1929 and *Edmontonia longiceps* Sternberg 1928 both were found in the formation. The record in the North American Maastrichtian is scarcer, but still significant, primarily by the almost ubiquitous presence of *Ankylosaurus magniventris* Brown 1908. Material ascribed to this taxon comes from the Scollard, Hell Creek, Frenchman, and Lance Formations (e.g., Carpenter, 2004; Arbour and Currie, 2016; Arbour and Mallon, 2017). The latter has also produced remains of, namely, *Denversaurus schlessmani* Bakker 1988, among unidentified material. More fragmentary, mostly unidentified, material hails from the Ojo Alamo Formation, New Mexico, (Ford, 2000). *Glyptodontopelta mimus* Ford 2000 was identified in this formation.

Asia

The Cretaceous of Asia represents one of the most relevant records of ankylosaurs, behind only North America, even though the occurrences in the Lower Cretaceous are rare (Maleev, 1952, 1954, 1956; Shuvalov, 1974; Maryańska, 1977; Tumanova, 1983, 1987; Nessov, 1995; Tang *et al.*, 2001; Averianov, 2002; Jia *et al.*, 2010; Arbour and Currie, 2013b, 2016; Arbour *et al.*, 2014a; Han *et al.*, 2014; Ji *et al.*, 2014). Indeed, the earliest occurrences are from the mid-Early Cretaceous, probably from the Barremian-Aptian, such as *Taohelong jinchengensis* Yang *et al.* 2013 and *Sauroplites scutiger* Bohlin 1953, from the Hekou Group and Zhidan Group, respectively. *S. scutiger* was very fragmentary and the specimen has since been lost (Arbour and Currie, 2016). More complete material was found in the Yixian and Jiufotang Formations (Aptian), Liaoning Province, China, which correspond to the rich fossil assemblage of the Jehol Biota, such as the early diverging ankylosaurs *Liaoningosaurus paradoxus* and *Chuanqilong chaoyangensis* Han *et al.* 2014, although these might represent two ontogenetic stages of the same taxon (Zheng, 2018). Although most occurrences are from Mongolia and China, fragmentary remains, mostly isolated teeth or osteoderms, have been reported from the Lower Cretaceous of Central Asia (Riabinin, 1939; Tumanova, 1986; Nessov, 1995; Averianov, 2002; Arbour and Currie, 2016). McCrea *et al.* (2001:433) considered trackways from the Albian of Tajikistan as putatively ankylosaurian (*Metatetrapous valdensis* Nopcsa 1923). In the Dzun Bayn Formation (Aptian-Albian), Mongolia, partially complete remains were found and attributed to *Shamosaurus scutatus*. Slightly younger, the Sunjiwan Formation (Albian), China, has

also produced material, namely *Crichtonpelta benxiensis* Lü *et al*. 2007. *Crichtonsaurus bohlini*, from the same formation, was considered a *nomen dubium* by Arbour and Currie (2016). From the Albian-Cenomanian of China, significant remains are known and represent the southernmost occurrence of ankylosaurs in Asia. Zheng *et al*. (2018) considered *Jinyunpelta sinensis*, from the Liangtougang Formation (Albian-Cenomanian), as the oldest and most early diverging ankylosaurine. From the similar aged Chaochuan Formation, recovered material was ascribed to *Dongyangopelta yangyanensis* Chen *et al*. 2013 and *Zhejiangosaurus lishuiensis* Lü *et al*. 2007. The validity of the latter has been questioned (Arbour and Currie, 2016) and both taxa may represent a single taxon. Putative ankylosaurian footprints have been reported from the Aptian-aged Atotsugawa Formation (Fujita *et al*., 2003) of Japan. Also from Japan, but from the Cenomanian, fragmentary material has been reported from the Hikagenosawa Formation (Hawakaya *et al*., 2005). In the Upper Cretaceous, occurrences are comparatively much more common, particularly in Mongolia. The Bayan Shireh Formation (Cenomanian-Santonian) has provided abundant remains (Maleev, 1952; Tumanova, 1993; Arbour and Currie, 2016; Park *et al*., 2020), of which the most complete and better preserved belong to *Talarurus plicatospineus* and *Tsagantegia longicranialis* (a single skull). From the younger Ulansuhai Formation (?Turonian), remains were recovered and attributed to *Gobisaurus domoculus* Vickaryous *et al*. 2001. Xu *et al*. (2007) ascribed additional material to *Zhongyuanosaurus luoyangensis* Xu *et al*. 2007, but Arbour and Currie (2016) regard it as a junior synonym of *G. domoculus*. Approximately coeval, in the fossil-rich Bissekty Formation (Turonian), Uzbekistan, material attributed to ankylosaurs is restricted to isolated elements, of which the more relevant is the braincase holotype of *Bissektipelta archibaldi* Averianov 2002 (Averianov, 2002; Parish and Barrett, 2004; Kuzmin *et al*., 2020). The richest and most diverse record for Asian ankylosaurs, including tracks, comes from the Campanian (Gilmore, 1933; Maleev, 1952, 1954, 1956; Maryańska, 1977; Barrett *et al*., 1998; Pang and Cheng, 1998; Godefroit *et al*., 1999; Ishigaki *et al*., 2009; Miles and Miles, 2009; Arbour and Currie, 2013b; Arbour *et al*., 2013, 2014a; Penkalski and Tumanova, 2017; Wang *et al*., 2020). Approximately 50% of all Asian Upper Cretaceous occurrences are Campanian-aged, particularly from the Baruungoyot Formation (upper Campanian-?lowest Maastrichtian), Mongolia (Maryańska, 1977; Barrett *et al*., 1998; Pang and Cheng, 1998; Arbour *et al*., 2013,

2014a; Arbour and Currie, 2016). Taxa like *Saichania chulsanensis* Maryańska 1977, *Tarchia kielanae* Maryańska 1977, and *Zaraapelta nomadis* Arbour *et al.* 2014 were found in the formation. Other latest Cretaceous Mongolian formations have a record of ankylosaurs, such as the Bayan Mandahu, Djadokhta, and the Nemegt Formations. Two species of *Pinacosaurus*, respectively *P. mephistocephalus* Godefroit *et al.* 1999 and *P. grangeri*, have been described from the first two (Gilmore, 1933; Young, 1935; Maleev, 1952, 1954, 1956; Godefroit *et al.*, 1999; Arbour and Currie, 2016). Remains from Djadohkta include material attributed to *Minotaurasaurus ramachandrani* Miles and Miles 2009, which the validity has been debated (Arbour *et al.*, 2014a; Penkalski and Tumanova, 2017). The Maastrichtian is remarkably poor in occurrences, with very few occurrences reported. Most fossils come from the Nemegt Formation (upper Campanian-Maastrichtian), the most relevant of which includes a possible second species of *Tarchia*, *T. teresae* Penkalski and Tumanova 2017 (Maleev, 1956; Maryańska, 1977; Tumanova, 1987; Arbour *et al.*, 2013, 2014a; Penkalski and Tumanova, 2017). The youngest record was reported by (Godefroit *et al.*, 2009) on ankylosaur teeth from a polar microfossil assemblage from the late Maastrichtian Kakanaut Formation in the Russian Northeast (Fig. 1.3.2.1).

Europe

The Cretaceous record of Europe contrasts with the North American and Asian in the abundance of ankylosaur remains in the Lower Cretaceous and the poorer Upper Cretaceous (Fig. 1.3.2.1). The Lower Cretaceous is marked by the occurrences of the Wealden facies (Berriasian-Aptian), which are by far the most abundant and well-documented (e.g.,(Mantell, 1833a, 1841, 1849; Lee, 1843; Fox, 1866; Seeley, 1879; Hulke, 1881; Lydekker, 1889; Nopcsa, 1905; Pereda-Suberbiola, 1993; Blows, 1996, 2015; Canudo *et al.*, 1997, 2004; Pereda-Suberbiola and Galton, 1999; Pereda-Suberbiola *et al.*, 1999, 2007, 2012; McCrea *et al.*, 2001; Pereda-Suberbiola and Ruiz-Omeñaca, 2005; Petti *et al.*, 2010; Gasulla *et al.*, 2011; Blows and Honeysett, 2013; Sachs and Hornung, 2013; Hornung and Reich, 2014; Ősi, 2015; Perales-Gogenola *et al.*, 2019; Raven *et al.*, 2020; Pond *et al.*, 2023). However, the earliest record in the European Cretaceous are fragmentary remains from the Berriasian of Romania (Jurcsák and Kessler, 1991; Grigorescu, 2003). Tracks from the Berriasian of Germany and Britain have been attributed to ankylosaurs (McCrea *et al.*, 2001; Hornung and Reich, 2014). Other purported

ankylosaur trackways are also known in the Early Cretaceous of Italy (Sacchi *et al.*, 2009; Petti *et al.*, 2010). The Lower Cretaceous of Britain has the richest record in Europe, namely from the Wealden Supergroup (latest Berriasian-Aptian). *Hylaeosaurus armatus*, found in the Grinstead Clay Formation and dated from the Valanginian, and *Polacanthus foxii*, from the younger Wessex and Lower Greensand Formations (Barremian and Aptian-Early Albian, respectively), are historically the most important and the best preserved (Mantell, 1833a, 1843, 1849; Fox, 1866; Nopcsa, 1905; Blows, 1987, 1996, 2015; Blows and Honeysett, 2014; Raven *et al.*, 2020). Fragmentary material from the Valanginian of Germany has been attributed to *Hylaeosaurus* sp. (Sachs and Hornung, 2013). More material ascribed to *Polacanthus* has been reported also from Spain, from the Valanginian to the Aptian, such as the uppermost Valanginian-lowermost Barremian of Golmayo Formation or the lower Aptian Arcillas de Morella (Pereda-Suberbiola and Galton, 1999; Pereda-Suberbiola *et al.*, 1999, 2007, 2012; Canudo *et al.*, 1997, 2004; Gasulla *et al.*, 2012; Perales-Gogenola *et al.*, 2019). Additional material from the Wessex Formation has recently been identified as *Vectipelta barretti* Pond *et al.* 2023. In the upper Lower Cretaceous, ankylosaur material is known from the Aptian-Albian (Seeley, 1879; Knoll *et al.*, 1998; Pereda-Suberbiola and Barrett, 1999; Kirkland *et al.*, 2013; Raven *et al.*, 2020). Some of this material includes the fragmentary remains ascribed to *Anoplosaurus curtonotus*, from the Albian-aged Gault Formation of England, and the more complete *Europelta carbonensis* from the Escucha Formation (lower Albian) of Spain (Seeley, 1879; Pereda-Suberbiola and Barrett, 1999; Kirkland *et al.*, 2013). The European Upper Cretaceous is, as aforementioned, comparatively poorer in ankylosaur occurrences. Few occurrences have been reported from the lower part of the Upper Cretaceous and is restricted to isolated fragmentary remains, namely from the Cenomanian of France (Vullo *et al.*, 2007). The Santonian-Maastrichtian (~86-66 Ma) interval produced the most abundant record from ankylosaurs of the Upper Cretaceous. From the Santonian of Hungary, abundant remains have been mostly ascribed to *Hungarosaurus tormai* (Ősi, 2005, 2015; Ősi and Makádi, 2009; Ősi and Prondvai, 2013). Also Santonian in age, tracks attributed to ankylosaurs have been reported from Italy (Sacchi *et al.*, 2009; Petti *et al.*, 2010). The youngest (Campanian-Maastrichtian) record of Europe is dominated by *Struthiosaurus*, known from both isolated fragmentary and articulated remains in Spain, France, Austria, and Transylvania (Bunzel, 1871;

Seeley, 1881; Nopcsa, 1918, 1929; Pereda-Suberbiola, 1999; Pereda-Suberbiola and Galton, 1999; Garcia and Pereda-Suberbiola, 2003; Ősi and Prondvai, 2013; Ősi, 2015). Isolated teeth tentatively identified as belonging to *Struthiosaurus* were found in the Maastrichtian of Portugal (Antunes and Sigogneau-Russell, 1991; see below for further details on the Portuguese record).

1.3.3 Ankylosauria in Portugal

The record of ankylosaurs in Portugal is scarce and until now poorly known. Besides *Dracopelta zbyszewskii* from the Late Jurassic, represented by the two specimens described herein, there are only three reported occurrences, all problematic. The oldest is dated to the Early Jurassic, possibly Sinemurian, and consisted of a partial maxilla with eight teeth (Fig. 1.3.3.1; MNHN), described by Lapparent and Zbyszewski in 1951 and again in 1957, when it was figured. Based on the original associated information, which consisted only of Liassic and *Scelidosaurus*, the authors considered the specimen as belonging to an early diverging thyreophoran closely related to the approximately coeval *Scelidosaurus harrisoni* Owen 1861 from the UK. However, the specimen differed from

Figure 1.3.3.1 (previous page). Holotype of *Lusitanosaurus liassicus*. Fragment of maxilla of *L. liassicus* in left lateral view. Anterior is to the left. Specimen uncatalogued. Scale bar: 2 cm. Specimen photo from Lapparent and Zbyszewski (1957).

Scelidosaurus in its larger size, absence of denticles, and narrower teeth. According to the authors, there were eight exposed, peg-like teeth, with a pronounced cingulum (Fig. 1.3.1), and four replacement teeth. The latter were visible anteriorly and posteriorly, two on each side. The largest exposed tooth measured 14 mm. The same authors also recognize the impressions of three mandibular teeth. Observations of the limestone matrix on the specimen led to the conclusion that its most likely provenance was from the marine beds that form the coastal outcrops of the S. Pedro de Moel region, in the Central Western coast of Portugal. Based on the differences relative to *Scelidosaurus* and provenance, Lapparent and Zbyszewski (1957) erected *Lusitanosaurus liasicus*. The incompleteness of the material and the fact that the specimen has since been lost precludes further classification and has led some authors to regard it as a *nomen dubium* (Pereda-Suberbiola and Galton, 1999; Norman *et al.*, 2004a).

In the Upper Jurassic of Lourinhã, Galton (1983a) ascribed an isolated dermal plate (FUB C) to a lateral plate of *D. zbyszewskii*. However, the same author (Galton, 1994b) reassigns it as a left dorsal plate from a stegosaur instead, putatively *Dacentrurus*, based on the occurrence of a right tail spine and partial dorsal rib from the same locality, between Porto das Barcas and Porto Dinheiro (Galton, 1983a, 1991, 1994b). This specimen has not been revisited or figured since then, and the

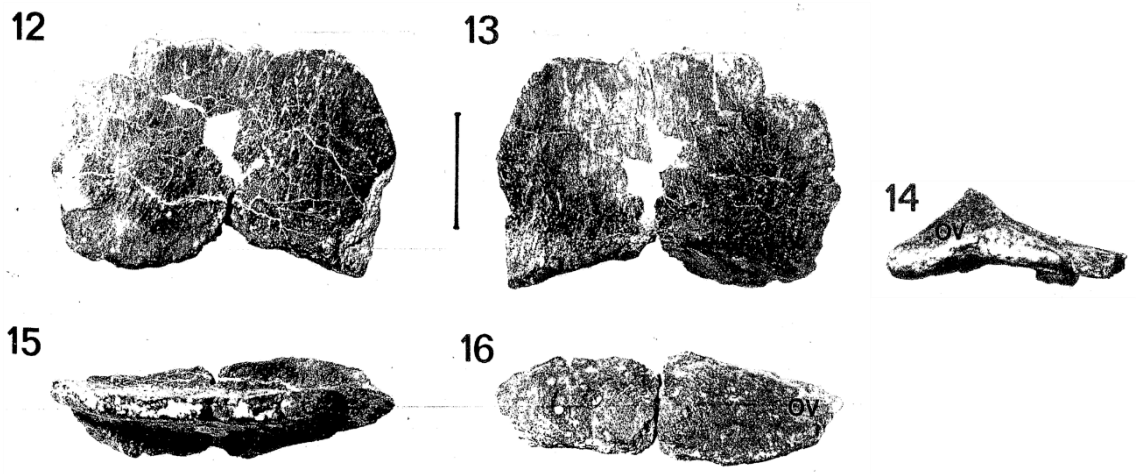

Figure 1.3.3.2 Isolated osteoderm from the upper Kimmeridgian of Lourinhã. Osteoderm FUB C assigned to *Dracopelta* (Galton, 1983a) or stegosaur (Galton, 1994b) from Porto das Barcas-Porto Dinheiro area, in Lourinhã, in dorsal (12), ventral (13), posterior (14), lateral (15) and medial (16) views. Scale bar: 5 cm. Galton (1983a).

original description and posterior works provide little detail to accurately ascribe the specimen to a specific taxon. In addition, the attributed age is problematic, with studies pointing between to the upper Kimmeridgian to the lower Berriasian (Galton, 1983a, 1991, 1994b, and references therein). More recent stratigraphical work (Hill, 1988, 1989; Schneider *et al.*, 2009, 2010; Martinius and Gowland, 2011; Taylor *et al.*, 2014; Mateus *et al.*, 2017; Gowland *et al.*, 2018) dates the section from where the specimen purportedly comes from as latest Kimmeridgian-earliest Tithonian. Based solely on the original figure (Fig. 1.3.2), the osteoderm seems more similar to dorsolateral osteoderms present in *Dracopelta*, and the presence of an apparent anteroposterior keel (Fig. 1.3.3.2: 14, 15) on what is assumed as the dorsal surface seemingly supports that hypothesis. This would represent the oldest occurrence of skeletal remains of an ankylosaur in the Lourinhã fm., and the only ankylosaur record in the entire Lourinhã formation besides the two specimens of *Dracopelta* referred above. However, cervical plates of *Miragaia longicollum* also exhibit an identifiable keel on the medial surface, which coupled with the occurrence of other stegosaur material from the same site, could also support a stegosaur affinity. As such, without an updated and improved observation of the specimen, the assignment to a specific taxon remains tentative.

From the Maastrichtian of Taveiro, Coimbra, ten teeth (TV 6, 7, 8, 10, 11, 13, 14, 15, 16) (Fig. 1.3.3.3) were identified by Antunes and Sigogneau-Russell

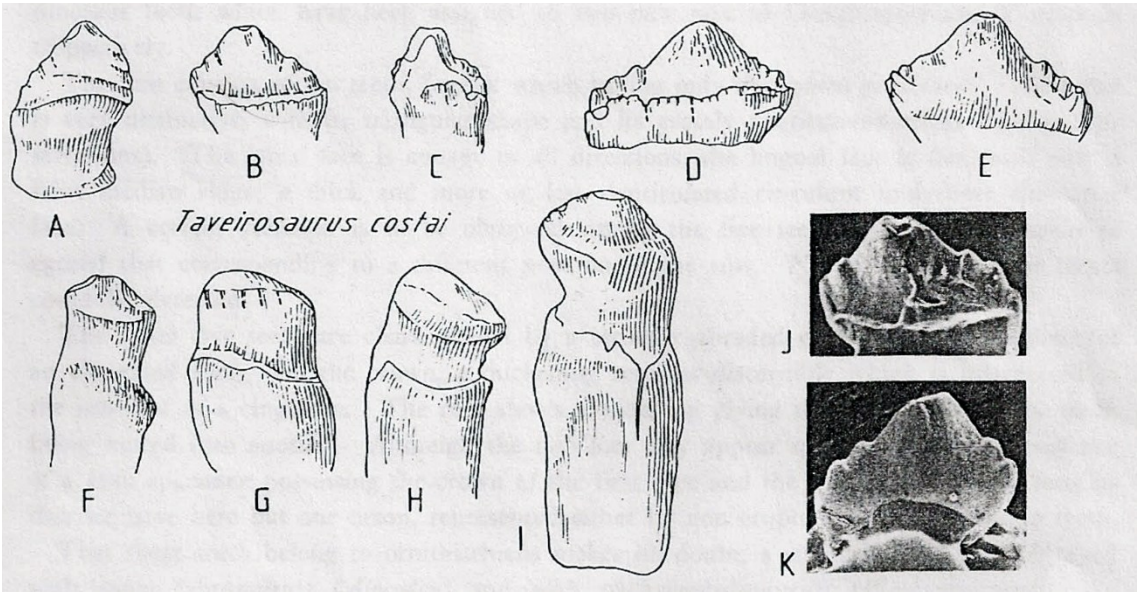

Figure 1.3.3.3. Holotype of *Taveirosaurus costai*. Teeth from the Maastrichtian of Taveiro, Coimbra, Portugal, assigned to *T. costai*. A) TV 16, B, J, K) TV 11, C) TV 14, D, E) TV 10, F) TV 8, G) TV 7, H,) TV 13, I) TV 9. Antunes and Sigogneau-Russell (1991).

(1991:119), assigning it to *Taveirosaurus costai*, in honor of the locality, and Carrington da Costa, a Portuguese paleontologist. This taxon is problematic due to the very fragmentary remains. Four of the teeth preserve the crown whilst the remaining are very eroded, with a discernible cingulum. The crown is low, triangular, and expanded anteroposteriorly (more pronounced in TV 10), with six low denticles. Based on this, the authors ascribed *T. costai* to Pachycephalosauria. However, in 1996, the same authors reassigned it to Nodosauridae. Galton (1996) recognized the similarity between the teeth of *T. costai* and ankylosaur teeth from Laño, Spain. Pereda-Superbiola and Galton (1999) remarked the same and compared them with similar material from other Maastrichtian sites in Spain. These authors regarded the taxon as a Nodosauridae indet., and considered that *T. costai* may be a junior synonym of *Struthiosaurus*. Norman *et al.* (2004a) considered it a *nomen dubium*.

Recent track finds in the Upper Jurassic may be tentatively ascribed to an ankylosaur track maker, but more studies are needed to confirm this assertion.

1.4. Geological and paleontological framework

The specimens studied herein were recovered from the top of the Lourinhã formation (Figs. 1.4.1-2), a thick, continental, siliciclastic sequence, dated from the late Kimmeridgian to the latest Tithonian-earliest Berriasian (Hill, 1988, 1989; Wilson, 1988; Leinfelder, 1993; Leinfelder and Wilson, 1999; Mateus, 2006; Kullberg *et al.*, 2013; Taylor *et al.*, 2014; Mateus *et al.*, 2017). Informally defined by Hill (1988), the Lourinhã formation represents an alternating succession of sandstone-mudstone, approximately 200 to 1000 meters in thickness, deposited in a fluvio-deltaic setting, with brief, shallow marine intercalations. The deposition was conditioned by the evolution of the Lusitanian Basin, a peri-atlantic sedimentary basin that formed in the early Late Triassic, at the onset of the opening of the North Atlantic, and was active until the earliest Late Cretaceous (Hill, 1988, 1989; Wilson, 1988; Leinfelder, 1993; Ravnås *et al.*, 1997; Alves *et al.*, 2003; Martinius and Gowland, 2011; Kullberg *et al.*, 2013; Taylor *et al.*, 2014; Mateus *et al.*, 2017). The distensive regime during this interval, and the successive rifting episodes, influenced the development of smaller sub-basins within the Western Lusitanian Basin: the Consolação, Bombarral, Arruda, and Turcifal, which were constrained by differential fault and diapir activity, resulting in distinct depositional settings (for further details,

see (Ravnås *et al.*, 1997; Rasmussen *et al.*, 1998; Leinfelder and Wilson, 1999; Alves *et al.*, 2003; Taylor *et al.*, 2014). This resulted in a complex lithostratigraphy of the Lourinhã formation, which, although extensively studied, has contributed to

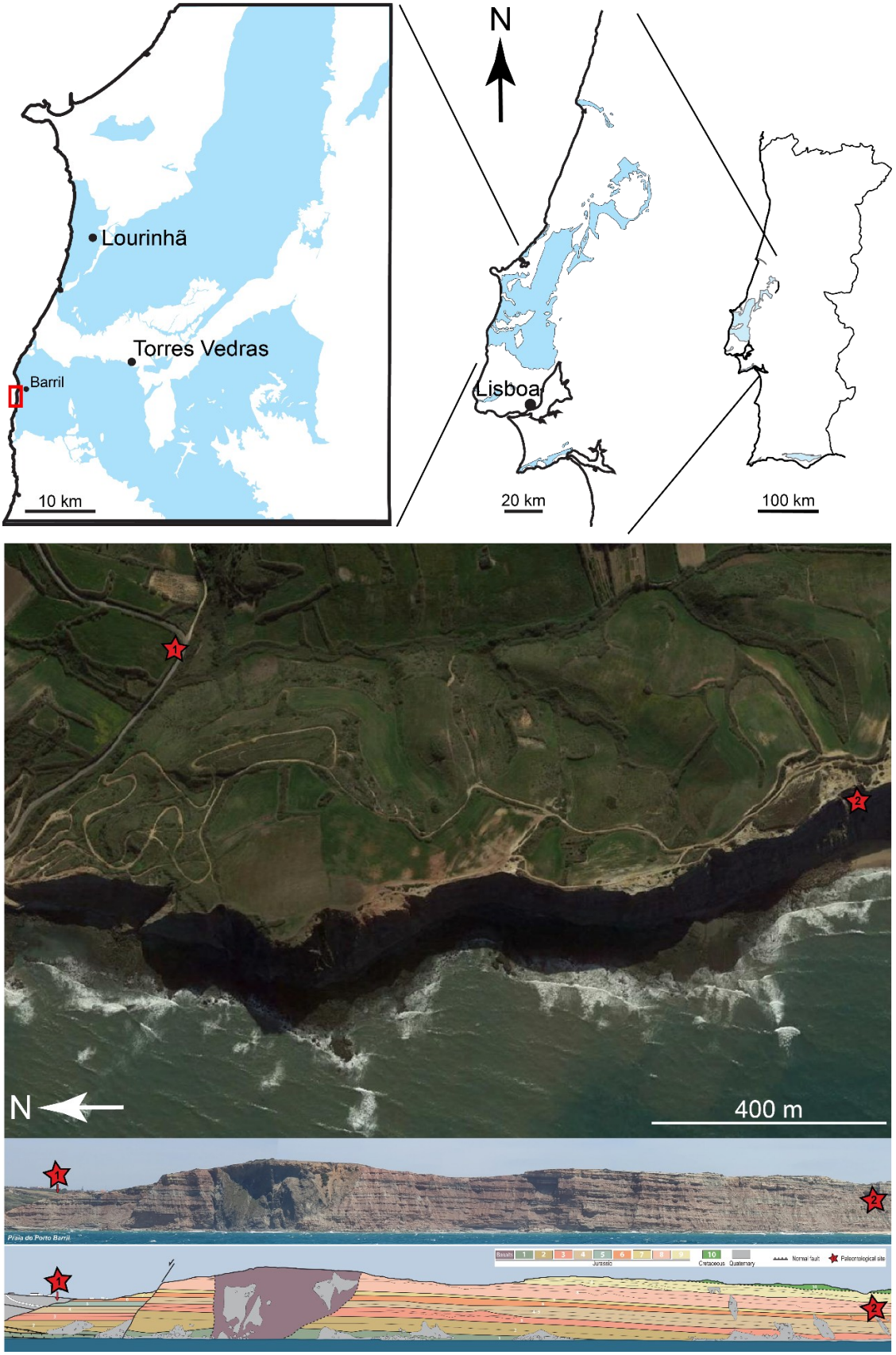

Figure 1.4.1. (previous page). Location of *D. zbyszewskii*. Simplified regional geological map (top), showing the Lourinhã formation distribution (light blue). Red rectangle highlights the area where *D. zbyszewskii* was found. Below are shown the localities of the studied specimens, and the coastal profile correlation at the bottom (red stars: 1, type locality; 2, NOVA-FCT-DCT-5556). Note that in the coastal profile locality 1 is represented as a horizontal projection of the inland type locality, and therefore appears higher than locality 2. Map modified from Russo *et al.*, 2017. Colors of units in the coastal profile correspond to the colors in Fig. 1.4.2. Satellite image modified from Google Earth® (2024). Coastal profile photo by André Carvalho (2019) and geological profile by Lope Ezquerro (2021).

the lack of consensual formally defined lithostratigraphic units (see (Mouterde *et al.*, 1972, 1979; Wilson, 1979, 1988; Hill, 1988; Leinfelder and Wilson, 1999; Manuppella *et al.*, 1999; Schneider *et al.*, 2009; Taylor *et al.*, 2014; Mateus *et al.*, 2017). Recently, Mateus *et al.*, (2017) have reviewed and correlated the different lithostratigraphical units proposed, recognizing four sub-units in the Lourinhã formation: the Praia da Amoreira-Porto Novo member, the Praia Azul member, the Santa Rita member, and the Assenta member. The latter is the southern equivalent to the coarser fluvial facies Santa Rita member of the Consolação sub-basin, identified by Hill (1989), and is largely restricted to the south of the NE-SW trending diapir and fault zone that defines the boundaries between the Consolação (North) and Turcifal (South) sub-basins (see Wilson, 1979, 1988; Hill, 1989; Ravnås *et al.*, 1997; Leinfelder and Wilson, 1998; Alves *et al.*, 2003, Taylor *et al.*, 2013, Mateus *et al.*, 2017, and references therein for further information on the tectonosedimentary framework). The Assenta member is the youngest stratigraphically, representing the late Tithonian to the earliest Berriasian, and is estimated to be approximately 300 meters thick (Wilson, 1979; Hill, 1988; Leinfelder and Wilson, 1998; Mateus *et al.*, 2017). This member is characterized by a sequence dominated by mudstones, intercalated with channelized cross-bedded sandstones, with abundant levels of nodular calcretes (Fig. 1.4.2), pedogenic carbonate concretions that evidence the existence of paleosols (Hill, 1989; Mateus *et al.*, 2017). The carbonate nodules usually appear as reworked material at the base of channels or forming high resistance levels. The reddish oxidized surfaces and the presence of rhizoliths and other bioturbation structures further indicate frequent subaerial exposure between lower and higher river flow discharge. Deformation structures, such as load-casts, are frequent, as is the presence of coalified plant remains. In the upper part of the unit, nodular carbonate

intercalations are more common, indicative of episodic shallow marine conditions.

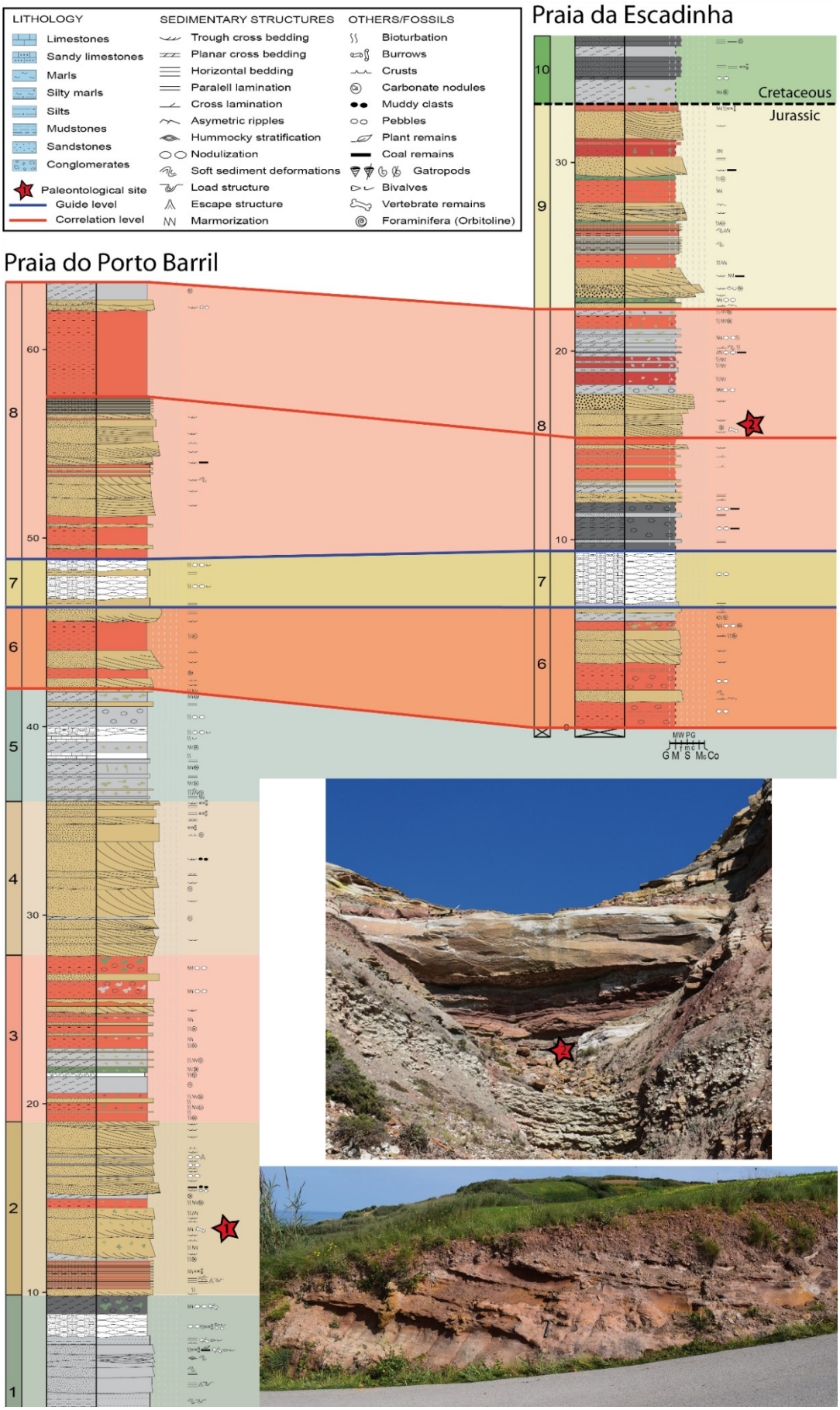

Figure 1.4.2 (previous page). Stratigraphy and localities of *D. zbyszewskii* specimens. Stratigraphic profiles and correlation of the sections where the specimens of *D. zbyszewskii* were found, in the top of the Assenta mb. (*sensu* Hill, 1988, 1989; Mateus *et al.*, 2017). Red stars with numbers mark the occurrence of *Dracopelta* in the sequence: 1) holotype, 2) NOVA-FCT-DCT-5556. Photographs show the type locality near Porto Barril (bottom), and the site of NOVA-FCT-DCT-5556 (above) at Praia da Escadinha, marked with a red star. Stratigraphy and correlation by Lope Ezquerro (2021).

The stratigraphy of the section (Fig. 1.4.2) indicates a braided fluvio-deltaic system, developed on a vegetated marshy coastal plain, with occasional, short lived transgressive events, also supported by the fossil invertebrate faunal changes and tidal modulation structures (Hill, 1988, 1989; Martinius and Gowland, 2010; Taylor *et al.*, 2013; Mateus *et al.*, 2017). *Dracopelta* specimens come from the top of this sub-unit (Fig.1.4.2). The holotype was found in a medium to fine-grained brownish light grey sandstone fining upwards and corresponding to a river channel, which thickens to the South into a multimetric thick erosive body. The sandstone bodies in this succession exhibit trough cross bedding and root bioturbation (Fig. 1.4.2), as well as carbonate and oxidized iron crusts near the top, indicative of subaerial exposure. Mudstones, grey marls and fine-grained sandstones generally alternate through the sequence, with coloured levels with rhizoliths and carbonated burrows in the mudstones indicating pedogenesis, and the presence of load casts and fluid escape structures indicating a water saturated depositional environment. The abundant rhizoliths and bioturbation, as well as the common occurrence of coal attests to a well-vegetated environment. The second specimen (NOVA-FCT-DCT-5556) was found approximately 45 meters higher in the sequence, and less than 20 meters from the Jurassic-Cretaceous transition (Figs. 1.4.1-2). The sequence here is dominated by tabular reddish mudstones and fine-grained sandstones ranging from decimetres to meters in thickness. Carbonate nodules and bioturbation tend to increase in abundance towards the top, as does the grain size, with the main channel body coarsening upwards, from fine to medium grained, and exhibiting cross and parallel lamination (Fig. 1.4.2). This is indicative of a higher energy depositional environment than for the holotype specimen, likely during an episodic higher river discharge event, further supported by the coarser sediment found with NOVA-FCT-DCT-5556.

The fossil vertebrate record of the Lourinhã formation is abundant and diverse, and is extensively documented, since at least the 19th century, and includes, besides dinosaurs, teleostean and elasmobranchian fish, amphibians, squamates, mammals,

chelonians, crocodylomorphs, and pterosaurs (Sauvage, 1898; Lapparent and Zbyszewski, 1957; Galton, 1980b, 1991; Mateus *et al.*, 1997, 2006, 2009, 2014; Mateus, 1998; Bonaparte and Mateus, 1999; Mateus and Antunes, 2001; Antunes and Mateus, 2003; Balbino, 2003; Pereda-Suberbiola *et al.*, 2005; Pérez-García and Ortega, 2011; Araújo *et al.*, 2013; Mannion *et al.*, 2013; Escaso *et al.*, 2014; Hendrickx and Mateus, 2014a, 2014b; Mocho *et al.*, 2014, 2017, 2019; Ribeiro *et al.*, 2014; Russo *et al.*, 2017; Costa and Mateus, 2019; Guillaume *et al.*, 2020; Malafaia *et al.*, 2020; Puértolas-Pascual and Mateus, 2020; Bertozzo *et al.*, 2021; Rotatori *et al.*, 2022; Fernandes *et al.*, 2023; López-Rojas *et al.*, 2024).

1.5. Objectives

This work aims to investigate the evolution and systematic relationships of Ankylosauria, a group of dinosaurs that has a comparatively understudied history. The fragmentary nature of the Jurassic fossil record casts doubts on the early evolution of the group and by proxy on the systematic relationships of the entire group. Therefore, to better understand the evolutionary history of Ankylosauria, a detailed dataset with as much information on early diverging forms is critical. A new, semi-complete and articulated ankylosaur skeleton from the Upper Jurassic of Portugal prompted a thorough look at its anatomy and *Dracopelta zbyszewskii*, a coeval Portuguese ankylosaur of uncertain affinities, using it as starting point to improve the phylogenetic resolution at the base of Ankylosauria and ultimately help clarify the taxonomy and evolution of Ankylosauria as a whole. As such, this thesis addresses the following questions:

1. Does the new specimen represent an additional, more complete skeleton of *D. zbyszewskii*?

The answer to this question is to be achieved by thoroughly describing the new specimen and compare it with the overlapping material of the *D. zbyszewskii* holotype. This will be complemented with field observations to confirm the geographical and stratigraphical proximity, since both specimens are dated from the upper Tithonian and were found one kilometre apart. While addressing this, and profiting from the completeness of the new skeleton, a secondary result is to establish a comprehensive, standardized anatomical nomenclatural system for the

ankylosaurian skeleton by compiling what is known in the literature and fill existing gaps with anatomical information, where applicable, used on other groups of dinosaurs.

2. Is *D. zbyszewskii* is a valid taxon?

The description of the new skeleton warrants a concomitant exhaustive review of the holotype of *D. zbyszewskii*, including unpublished material, as to compare both specimens and extract as much information as possible This approach is expected to result in the identification of clear potential autapomorphies that will help diagnose and establish *D. zbyszewskii* as a valid taxon. Additionally, other information, namely historical, is revisited, compiled, and cross-referenced to field observations to provide an improved background on the occurrence of the holotype specimen.

3. Is Polacanthidae a valid clade and is *Dracopelta* a polacanthid?

This question will be addressed through a comprehensive phylogenetic analysis, which, following the anatomical description of *Dracopelta* and confirmation of its validity, will include *Dracopelta* for the first time. Complemented with the comparison with other ankylosaurs, the aim is to recognize the presence of characters and character states that have often been either overlooked or merged together in past studies, and score them in a thorough character dataset to help identify previously hypothesized clades which have consistently been problematic, such as Polacanthidae, due to the combination of early and late-diverging character conditions. The completeness of *Dracopelta* and its age will add a new data point that will help resolve the early ankylosaur family tree and clarify a more complex evolutionary history than thought.

1.6. Structure of the thesis

This thesis is divided in six chapters, one of which, Chapter 3, is a published article. Citation is provided following the title of the chapter. Chapters 1 and 7 correspond to the introduction and conclusions, respectively. Chapter 2 is the material and methods section, which includes the character list for the phylogenetic analysis. Chapter 4 is the systematic palaeontology and anatomical description of the holotype of *Dracopelta zbyszewskii* and NOVA-FCT-DCT-5556. Chapter 5

presents the results from the phylogenetic analyses. Chapter 6 corresponds to the discussion, which includes comparative anatomical remarks, phylogenetic implications, and paleobiogeography and paleoecology considerations.

2

MATERIAL AND METHODS

2.1. Material

The holotype of *Dracopelta zbyszewskii* (Figs. 3.1.1, 4.1.1.1-3, 4.1.2.1-3, 4.1.3.1-2, 4.1.4.1-4) consists of MG 5787, MG 3, and unnumbered material. MG 5787 (Figs. 4.1.1.1-2) is a partial articulated rib cage, with dorsal and lateral osteoderms (Galton, 1980), and MG 3 (Fig. 4.1.6) is an incomplete articulated autopodium with three metapodials and digits II, III and IV (Pereda-Suberbiola *et al.*, 2005). Both are housed at Museu Geológico (MG) in Lisbon. The unnumbered material of the holotype (Figs. 4.1.3-5, 7-12) consists of 35 blocks (unprepared fragments larger than 10 cm) and over 70 fragments, totaling 102 pieces, varying in size approximately from 35 cm to 1 cm. This material is part of the collections of MG, stored at Laboratório Nacional de Energia e Geologia (LNEG), in Alfragide. It was found during road construction works, 400 meters East of the beach of Assenta Sul (Porto Barril), on the border between Torres Vedras and Mafra townships, in 1964, and collected later that year by Georges Zbyszewski and Octávio da Veiga Ferreira (Russo and Mateus, 2021). For further details on the discovery, see Chapter 3 of this dissertation. Most of the material is fragmented and requires preparation, particularly the unnumbered fragments, to remove the sediment. The matrix is a light gray, fine sandstone, with a few mud clasts, that covers most of the surface of the blocks. Therefore, identification of skeletal elements is, in most cases,

exceedingly difficult, either because the matrix obscures most of the specimen or/and of its fragmentary nature. Nevertheless, additional elements were identified from the ribcage, pelvic girdle, hindlimbs, and dermal armour, as follows: nine appressed partial rib shafts, possible unidentified pelvic elements, distal end of right femur and broken partial femoral shaft, incomplete right tibia and fibula, two phalanges, including an ungual, two dorsolateral overlapping osteoderms, and four possible lateral plates.

NOVA-FCT-DCT-5556 is an articulated skeleton, over 50% complete, composed of most of the axial skeleton, pectoral and pelvic girdles, proximal appendicular elements, and dermal armour (Figs. 4.2.1-16). The axial skeleton consists of the skull, missing the anterior narial region of the rostrum, left dentary, at least 38 maxillary teeth in situ and one isolated tooth, complete cervical, dorsal and sacral series, with seven cervical vertebrae, 16 dorsal vertebrae (the last three dorsal fuse to form the presacral rod) and four true sacral vertebrae, 13 anterior caudal vertebrae (first caudal vertebra fuses to the sacrum, and last two disarticulated from the series), at least 40 ossified tendons, and 19 semi-articulated partial ribs and at least 29 rib fragments. Both the pectoral and pelvic girdles are partially complete and include, respectively, both scapulocoracoids, and ilia and proximal ends of the ischia and pubes. The appendicular elements consist of the right humerus and both femora. The dermal armour is mostly preserved *in situ* and the osteoderms are the most abundant elements, which include the pelvic shield and over 190 osteoderms (at least 150 *in situ*). In addition, there are at least 100 unidentified bone fragments. In total, the specimen is composed of more than 400 elements. It was found in 2012 and excavated in 2013 and 2014 (Fig. 2.1). The harsh weather conditions and the inaccessibility of the site strongly conditioned the excavation and recovery, resulting in the separation of specimens in 19 main blocks. It was found in a fine, light gray sandstone corresponding to a fluvial channel (see subchapter 5.4 for further details on the taphonomy). The specimen is part of the collections of NOVA School of Sciences and Technology (FCT-NOVA) and is currently housed at Museu da Lourinhã (ML). The material was photographed using a Nikon D5300, with settings adjusted according to the ambient light, and specimen color and size, as to reduce image artifacts. Photograph processing was done in Adobe Photoshop CC© v20.0.6 and figures created in Adobe Illustrator© v23.0.6.

Measurements were taken using a caliper as much as the articulation of the specimen allowed.

The measurements of the skull and preserved vertebrae (Table 4.2.2), and an estimation of the missing section of the tail (>50%) were used to estimate the approximate length of the animal. Additionally, the approximate body mass was calculated by using R v4.2.2 with MASSESTIMATE package following the protocol of Campione and Evans (2012) and Arbour and Mallon (2017).

2.1.1. Taphonomy

Specimen NOVA-FCT-DCT-5556 was found articulated, with minimal remobilization of skeletal elements. The specimen is well preserved, without discernible signs of scavenging or other *post-mortem* alterations (Fig. 4.2.1, 4.2.2). The holotype of *D. zbyszewskii* on the other hand, albeit partially articulated, shows more signs of weathering as well as being more incomplete (see Figs. 4.1.1., 4.1.2.A, B, and Sub-chapter 4.1 of this dissertation). Both were found in fluvial facies corresponding to low sinuosity channels in a distal floodplain subjected to tidal and episodic marine influence (Hill, 1988, 1989; Martinius and Gowland, 2011; Taylor *et al.*, 2014; Mateus *et al.*, 2017; Gowland *et al.*, 2018; Ezquerro, pers. comm., 2021). Additionally, the specimens were found in distinct orientations: the holotype was found in the upright position (Figs. 3.3, 4.1.1), while NOVA-FCT-DCT-5556 was found lying on its back. The latter has been frequently reported, particularly in North American occurrences (e.g., Nopcsa, 1928; Sternberg, 1933, 1970; Carpenter, 1984, 1990; Coombs Jr and Deméré, 1996; Molnar, 1996; Arbour and Evans, 2017; Brown *et al.*, 2017; Mallon *et al.*, 2018). This contrasts with the upright position found more commonly in Asia (e.g., Lefeld, 1971; Jerzykiewicz *et al.*, 1993; Carpenter *et al.*, 2011; Currie *et al.*, 2011). These authors relate the different depositional settings, i.e., mostly sub-aerial, within aeolian sandstones in Asia, and mostly fluviodeltaic or marine facies elsewhere, to the preservation of the specimens in an upright or “belly up” position. Mallon and colleagues (2018) found statistical support for the occurrence of the latter in Late Cretaceous ankylosaurian occurrences and favoured a “bloat and float” model to explain the prevalence of inverted ankylosaurs within aquatic depositional settings. Sternberg (1933) had previously postulated a similar hypothesis, where the combination of bloating resulting from gas production during decomposition of the animal and the heavy

armour would cause the carcass to float upside down prior to deposition at the bottom, on a point bar, or similar depositional structure. Taking this into account, together with the stratigraphical, sedimentological, and preservation observations, the most plausible hypothesis is that the animals died in the vicinity, were transported over a short distance, and buried shortly after deposition. A second hypothesis would be a similar scenario to what has been proposed, namely, for *Borealopelta* (Brown *et al.*, 2017), but the stratigraphical and sedimentological evidence do not support this hypothesis.

The specimens of *Dracopelta* (MG 5787, NOVA-FCT-DCT-5556) show distinct levels of preservation and orientation, as mentioned above. The holotype MG 5787 was subjected to more intense erosive action, since it is more incomplete than NOVA-FCT-DCT-5556, but also various bones seem to have been abraded and totally or partially eroded away. The best examples are the vertebrae and ribs, which have only preserved the centra and distal shaft sections, respectively (Fig. 4.1.1.1). Considering the better preservation of other elements, such as the hindlimb, it suggests that the carcass was partially buried ventrally, with its back exposed. More preparation work on the holotype ribcage will help ascertain this. Its upright position also may be indicative of very little *post-mortem* reworking, possibly due to a lower energy depositional setting. The intercalation of finely grained levels (marls and mudstones) with the coarser, coal-rich channel body indicate an ephemeral fluvial channel. The presence of abundant plant bioturbation structures (e.g., rhizoliths), erosive, oxidized surfaces, and carbonate nodules are indicative of subaerial exposure and soil development, reinforcing the temporary character of the subaqueous depositional setting, and subsequent exposure of the carcass. The fact that most of the skeleton is missing seems to lend support to a more prolonged exposure of the holotype specimen comparatively to the NOVA-FCT-DCT-5556. In the latter, the level of completeness and articulation strongly suggest the animal was buried shortly after death, at least most of the carcass, exposed just enough time to be scavenged or partially disarticulated, which could account for the missing lower limbs and/or distal tail, but reworked enough so that it deposited in the upside-down position. The axial skeleton and hindlimbs are the least affected by bone remobilization, with the skull and vertebral column and femora articulated *in situ* (Figs. 4.2.1, 4.2.2). Comparatively, the forelimbs are all but gone, except for the right humerus, which has been moved posteriorly and is laying ventral to the

basicranium. As the right humerus, the right scapulocoracoid is dislocated anteriorly and medially from its position. Indeed, the anterior dorsal right side of the specimen has been more extensively affected by disarticulation and bone displacement. That is evidenced further by the ribs, rotated anteriorly, some almost parallel to the axis of the body, and the anterior dorsolateral armour, moved from its anatomical position and now located more medially (Figs. 4.2.4, 4.2.6). The lateralmost regions of the specimen are missing, likely due to erosion, particularly on the left side. This was exposed on the surface, which allowed its discovery. Some bones located on the edge of the specimen show irregularly cut surfaces and have been eroded away, such as the anteriormost rostral region of the skull (Figs. 4.2.1-3), or the lateral surface of the left femur (Fig. 4.2.14). The right side, even though buried deeper in the outcrop, seems to have been eroded away as well, giving further support to a partial subaerial exposure of the carcass for some time. Whether the missing elements (e.g., the limb bones) were subjected to scavenging, disarticulation and displacement caused by water currents, or diagenetic processes is unknown, but a combination of these processes is the most feasible hypothesis. Moreover, the surrounding matrix of the specimen shows a variation in grain size and cohesiveness. Matrix more peripheric to the fossil or with less overposition of bones is slightly more finely grained, with occasional multimilimetric clasts, and less coherent (e.g., distal ribs, lateral areas of the skull and cervical region) than matrix closer to the axial skeleton or in areas with higher bone compaction (e.g., intervertebral spaces, depressed bone structures, such as fossae or grooves, lateral plate surface). The latter matrix is harder, composed of larger feldspar and quartz clasts cemented by a siliceous cement, making the preparation of those areas increasingly difficult. The heterogeneity of the matrix suggests a complex interaction between the different decaying organic matter of the animal, depositional sediment, and water composition, which further investigation may help shed light on. As a further taphonomical note, there is a single occurrence of an associated osteoderm, likely a ventral osteoderm from a goniopholid (Fig. 2.1.1).

Figure 2.1.1.1. Goniopholidid osteoderm. Associated osteoderm (possibly ventral) attributed to an unidentified goniopholid, found with NOVA-FCT-DCT-5556.

2.1.1. Anatomical nomenclature

The anatomical terminology in this work is a result of the compilation of existing and widely used terms in the literature, mainly on ankylosaurs but also other dinosaurs (e.g., Romer, 1956; Coombs, 1971, 1978b, 1979; Maryańska, 1977; Vickaryous *et al.*, 2003, 2004; Carpenter, 2004; Wilson *et al.*, 2011; Kirkland *et al.*, 2013; Leahey *et al.*, 2015; Kinneer *et al.*, 2016; Pond *et al.*, 2023), and, taking advantage of the completeness of NOVA-FCT-DCT-5556, aims to provide a comprehensive glossary to ankylosaur anatomy, which is often inconsistent, lacking, or redundant. For direction for example, the terms used are straightforward and commonly used: anterior, when referring towards the front of the animal, posterior, when towards the back, lateral, when towards the sides, and medial, towards the middle; equivalents of these directional terms may appear in specific context and where stated, such as labial (= lateral), lingual (= medial), mesial (= anterior), and distal (= posterior) for teeth. Osteological structures follow previous works on ankylosaur anatomy, and, where needed, from other dinosaur groups (e.g., vertebral laminae and fossae in sauropods by Wilson *et al.*, 2011).

The *in-situ* preservation of the post-cranial armour of *Dracopelta* (holotype material and NOVA-FCT-DCT-5556) and its unique arrangement pattern allowed for a description of the osteoderms using a nomenclatural system which considers its morphological variation and position on the body, as to have an unambiguous, clear,

and consistent identification of osteoderms. Therefore, in this work, the nomenclatural system follows previous works on ankylosaur osteoderm terminology (Blows, 2001, 2015; Arbour *et al.*, 2011, 2014b; Kirkland *et al.*, 2013; Burns and Currie, 2014; Brown, 2017). Consequently, the dermal armour is firstly defined according to main regions of the body: cervical (C), transitional (TR), thoracic (T), pelvic, and caudal (Cd) (Arbour *et al.*, 2011; Burns and Currie, 2014; Brown, 2017). Because lateral armour is usually represented by plates, which may not correspond laterally to the dorsal transverse bands of osteoderms, and is the most incomplete in *Dracopelta*, is described separately herein, albeit following the system when applicable (e.g., relative position on the body). Burns and Currie (2014, Fig. 1) use medial, lateral, and distal to define the location of osteoderms relative to the sagittal plane, with distal the furthest away from the medial position, which is here also used to complement the description of the dermal armour. To define the placement of each individual osteoderm, it is adopted also the alphanumeric system proposed by Brown (2017), which attributes a number for the position of each transverse band of armour (starting anteriorly, 1-…) and each osteoderm (starting from the midline towards the sides, A-…), from the right (R) and left (L) sides. For example, the right second osteoderm from the third thoracic band is designated T3BR and is located lateral to the medial T3AR. The pelvic armour of *Dracopelta*, because of its specific morphology as a continuous fused sheet of bone, i.e., pelvic shield, will instead follow the classification of Arbour *et al.* (2011). Morphologically, the different types of osteoderms have lacked a consistent terminology (see Maryańska, 1969; Blows, 2001, 2015; Arbour *et al.*, 2013, 2014; Kirkland *et al.*, 2013), mostly because of the high morphological variability observed throughout Ankylosauria. In this dissertation, osteoderms are divided in major morphological types, as proposed by Blows (2015), which are then categorized in subtypes by using Roman numerals (I to …) to avoid confusion with the alphanumeric system for the position on the body.

Body mass was estimated using R v4.2.2 with MASSESTIMATE package following Campione and Evans (2012) and Arbour and Mallon (2017).

2.2. Methods

2.2.1. Fossil preparation

Preparation work focused on NOVA-FCT-DCT-5556 and was performed mostly at ML since 2013. Mechanical techniques, with both hand tools (e.g., dentistry tools) and pneumatic tools (e.g., air scribes), were applied to remove the sediment. The brittleness of the specimen, particularly of some of the osteoderms, its degree of articulation, and the heterogeneity of the matrix (soft, fine-grained sandstone vs hard, compact medium-grained sandstone) were major challenges during the preparation. Therefore, fossil consolidation and stabilization were done using different methods, such as the application of Paraloid® B72 of different concentrations (5% and 20% for general consolidation, and 50% as an adhesive for small, localized interventions) or gap filling using a mixture of loose sediment from the specimen itself and Paraloid® to provide support. Additionally, several iterations of reinforced plaster jackets ("clamshells") were done to better support each block during preparation and facilitate handling of the specimen. The holotype of *D. zbyszewskii* was prepared using air scribe and Paraloid® B72, although the work was limited to the tibia and femur.

2.2.2. Phylogenetic analysis

The phylogenetic position of *D. zbyszewskii* was assessed by performing a Maximum Parsimony (MP) analysis using a heavily modified version of the dataset (329 characters, 95 taxa) of Loewen and Kirkland (2013), where *Dracopelta* was included. The analysis was performed on TNT v1.5 (Goloboff and Catalano, 2016), following the protocol and script Vila *et al.* (2022). To test the degree of homoplasy, and therefore the reliability of the character coding and character stability across the tree space, five rounds were run, one employing equal weighting (EW), which assumes that for any given tree character state changes all have the same weight, and four with implied weighting (IW), which inversely accounts and downweighs characters that exhibit high degrees of homoplasy, and may introduce higher uncertainty in the phylogeny (Goloboff, 1993; Goloboff *et al.*, 2008). For the four IW analysis, concavity (k) values of 5, 10, 12, and 15 were used to compare how much highly homoplastic characters would affect the analysis when downweighted relatively to more stable characters (low k values = strongly downweighted homoplasy). No taxa were pruned. Characters were ordered when relevant (see

Character List below). New Technology Search (NTS) was applied with 100 cycles of Sectorial Search using RSS and CSS minimum size of 5, 100 cycles of Drift, and 100 cycles of Ratchet. Tree fusing was set at 10 rounds. Default settings were kept for the other parameters. To further explore tree space and attempt to find the most optimal set of trees, a second round of Tree-Bissection Reconnection (TBR), a branch swapping algorithm that regrafts each subtree of a tree onto a remaining branch after rerooting each subtree, was performed on the most parsimonious trees (MPTs) recovered. The EW round produced 50000 MPTs of 1391 steps, with a Consistency Index (CI) = 0,289, Retention Index (RI) = 0,755, and Rescaled Consistency Index (RSI) = 0,218. The IW rounds with k = 5, 10, and 12, produced, respectively, 5250 MPTs of 1419 steps, 11970 MPTs of 1406 steps, 8736 MPTs of 1401 steps. The round with k = 15 produced 624 MPTs of 1397 steps, with a CI = 0,288, RI = 0,753, and RSI = 0,217.

2.2.3. Character list

The 329 characters used in the phylogenetic analysis to determine the phylogenetic relationships of ankylosaurs within Thyreophora are listed below and are a heavily modified iteration of the dataset of Loewen and Kirkland (2013), which will be included in the publication of the description of the new specimen (NOVA-FCT-DCT-5556) and phylogenetic analysis (Russo *et al.*, in prep). A total of 297 characters (141 cranial, 47%, 105 postcranial, 35%, and 49 postcranial armour, 16%) were scored across Ankylosauria and 33 outgroup characters were introduced to resolve the outgroup Stegosauria. Recent previous use of characters is indicated by citations in parentheses. Characters presented in Thompson *et al.* (2012) were largely derived from the unpublished thesis of Parish (2005) and from Vickaryous *et al.* (2004). There are 107 new characters, which may have been identified by previous authors (cited where known) but not used with an Ankylosauria specific parsimony analysis prior to 1998: 2, 4, 7, 9, 13, 19, 22, 24, 25, 26, 29, 30, 33, 34, 41, 43, 44, 49, 51, 56, 58, 59, 65, 66, 71, 76, 80, 97, 101, 102, 103, 106, 107, 111, 113, 114, 115, 116, 117, 118, 119, 124, 125, 126, 127, 130, 134, 136, 137, 143, 150, 151, 152, 161, 163, 164, 166, 167, 168, 170, 174, 179, 181, 183, 186, 187, 189, 192, 194, 198, 201, 203, 204, 207, 211, 226, 230, 231, 234, 235, 244, 246, 247, 258, 263, 264, 265, 266, 268, 269, 270, 271, 273, 274, 275, 276, 278, 279, 280, 281, 284, 289, 290, 295, 296, 297, 301.

Ordered characters (a total of 50) are based on observed evolutionary directional trends, ontogenetic trajectory within a species, or on inclusion of a character state within another: 1, 2, 3, 7, 11, 14, 16, 18, 23, 25, 31, 38, 40, 52, 53, 59, 72, 96, 112, 114, 114, 116, 122, 124, 136, 137, 158, 159, 161, 163, 167, 168, 176, 182, 185, 194, 197, 216, 223, 227, 231, 239, 257, 259, 260, 264, 265, 266, 287, 295, and 306. Additional comments on the characters follow the citations. In the matrix, unapplicable characters were scored as "-" to differentiate from unknown character states ("?").

Skull

1. Skull, maximum width in dorsal view compared to length: < 65% of length (0); 70% to 90% of length (1); between 95% to 110% of length (2); >115% of length (3) (modified from Kirkland, 1998:2; Carpenter *et al.*, 1998:1; Sereno, 1999:94; Vickaryous *et al.*, 2004:1; Thompson *et al.*, 2012:4). Character reworded for clarity.

Coombs (1978) noted that all ankylosaurid skulls were wider than long as opposed to the elongated skulls in nodosaurids. Sereno (1986) used skull width equal to or wider than the length as present in Ankylosauridae and in *Kunbarrasaurus*, *Shamosaurus* and the Ankylosaurinae. Kirkland and Loewen (2023) modified the character to include more character states and define discrete percentage intervals which are then coded accordingly. Character states 2 and 3 were added to parse out the variation present in ankylosaurids. The character is ordered because it is a directional trend. Only *Scelidosaurus* scores (0). Outside Ankylosauridae, only *Chuanqilong* scores (2). All other non-ankylosaurid ankylosaurs score (1). In Ankylosauridae, early diverging ankylosaurids and *Ziapelta* score (1), North American ankylosaurids, excluding *Ziapelta* and *Nodocephalosaurus*, score (2), and Asian ankylosaurids as well as *Nodocephalosaurus* score (3).

2. Skull, maximum dorsoventral height in lateral view compared to skull length from premaxilla to occipital condyle: short, < 45% of length (0); between 48% to 58% of length (1); tall, > 60% of length (2) (new character). Character states reworded for clarity.

Sereno (1986) lists a dorsoventrally low skull as a derived nodosaurid character. All non-ankylosaurid ankylosaurs score (0). North American ankylosaurids (except for *Nodocephalosaurus*, UMNH VP 21000, and *Ziapelta*) and *P. mephistocephalus*

score (2). Asian ankylosaurids (except for *P. mephistocephalus*), *Nodocephalosaurus*, UMNH VP 21000, and *Ziapelta* score (1).

3. Skull, width at the center of the orbit in dorsal view compared to width at the posterior position of the squamosals: (0) – width of orbits less than < 100% width at the squamosal (0); width of orbits more than 105% to 125% width at the squamosal (1); width of orbits more than 130% to 145% width at the squamosal (2); width of orbits more than 150% width at the squamosal (3) (modified from Kirkland, 1998:1; Vickaryous *et al.*, 2004:10; Thompson *et al.*, 2012:5).

Coombs (1978) observed that ankylosaurid skulls were triangular in dorsal view while nodosaurid skulls were wider at the orbits than at the squamosals. Kirkland (1998:1) stated that polacanthid skulls were widest at the rear of the skull. Early diverging ankylosaurs, polacanthids, and ankylosaurids (excluding UMNH VP 21000, which scores (1)), score (0). Character state (2) is present in *Sauropelta*, *Texasetes*, *Tatankacephalus*, and most panoplosaurids (exceptions are *Propanoplosaurus* and *Denversaurus*). Character state (3) is only present in struthiosaurids and *Propanoplosaurus*.

4. Skull, posterior surface, width across paroccipital processes compared to the height from quadrate to the top of the paroccipital process: width less than 195% height from quadrate to top of paroccipital process (0); width greater than 200% height from quadrate to top of paroccipital process (1) (new character).

Sereno (1986) noted that ankylosaur skulls were rectangular in caudal view with long axis horizontal. In Ankylosauridae, this character is variable; most of North American ankylosaurids (except for *Nodocephalosaurus*, *Akainacephalus*, and UMNH VP 21000, which score 0) score (1), while most Asian forms score (0), with the exceptions of *P. grangeri*, *Saichania*, and *Minotaurasaurus*. In non-ankylosaurid ankylosaurs, only *Kunbarrasaurus*, *Tsagantegia*, *Gargoyleosaurus* score (1).

5. Skull, snout roof in lateral profile rostral to orbits: flat (0); domed (1) (Kirkland, 1998:3; Carpenter *et al.*, 1998:23; Vickaryous *et al.*, 2004:2; Thompson *et al.*, 2012:14). Character state (1) reworded for clarity.

Sereno (1999:79, 99) observed a low snout in ankylosaurs and characterized that it was levelled with or arching above the skull table in Ankylosaurinae. This character is restricted to the muzzle. Outside Ankylosauridae, only *G. burgei*,

Silvisaurus, *Tatankacephalus*, and *Animantarx* score (1). The ankylosaurids *T. teresae* and *Zuul* score (0).

6. Skull, cranial roof in lateral profile between and behind the orbits: flat or concave (0); domed (1) (modified from Vickaryous *et al.*, 2004:3; Thompson *et al.*, 2012:31). Character state (1) reworded for clarity.

Peloroplites, *Borealopelta*, *Silvisaurus*, *Niobrarasaurus*, *Sauropelta*, *Texasetes*, *Tatankacephalus*, *Animantarx*, struthiosaurids and panoplosaurids have a domed cranial roof. All other taxa score (0).

7. Skull, non-domed cranial roof in lateral profile between and behind the orbits: flat (0); slightly concave (1); strongly concave (2) (new character).

Kirkland (1998:29) identified a groove (depression between orbits and rear of skull) across the skull roof which was characteristic for some ankylosaurids. This character is ordered to parse out the differences within ankylosaurids. Character states (1) and (2) are present only in Ankylosauridae. *G. burgei* is the only non-ankylosaurid ankylosaur scoring (1). Character state (2) is present in *Tsagantegia*, *P. mephistocephalus*, *Tianzhenosaurus*, *Zuul*, *Platypelta*, *S. cutleri*, and *Euoplocephalus*.

8. Skull, mediolateral constriction in the lacrimal region anterior to the orbits: absent (0); present (1) (Arbour and Currie, 2015:34).

Arbour and Currie (2015:34) noted a lacrimal constriction in the skull roof of some ankylosaurids. Only *P. grangeri*, *Talarurus*, *Minotaurasaurus*, *Nodocephalosaurus*, and *Akainacephalus* score (1).

9. Skull roof in dorsal view, presence of a distinct postemporal notch between the postorbital and the squamosal only, regardless of the length of the postorbital and squamosal horns: absent (0); present (1) (new character). Character states reworded for clarity.

Carpenter *et al.* (1998:4) scores the presence of a lateral temporal fenestra notch in *Gargoyleosaurus* and nodosaurids. Polacanthids, *Animantarx*, *Tatankacephalus*, *Sauropelta*, and *Texasetes* score (1). *Animantarx, Tatankacephalus*, and *Sauropelta* have a lateral notch between the back of the orbit and the squamosal in dorsal view. *Texasetes* appears to have a notch between the postorbital and paroccipital processes, while the squamosals curve straight back without a notch.

10. Skull, nuchal shelf: does not obscure occiput in dorsal view (0); obscures occiput in dorsal view (1) (Kirkland, 1999:25; Carpenter *et al.*, 1998:12; Vickaryous *et al.*, 2004:12; Thompson *et al.*, 2012:89)

Coombs (1978) assumed that the nuchal extension of the skull roof obscured the paraoccipital processes in dorsal view in most genera. Kirkland (1999:25) specified that the paroccipital processes are hidden in Ankylosauridae. All ankylosaurids (except for *Minotaurasaurus*) score (1).

11. Skull, external nares orientation: lateral (0); anterolateral (1); anterior (2) (modified from Carpenter *et al.*, 1998:10; Thompson *et al.*, 2012:7). Character states reworded for clarity.

Kirkland (1998:11) stated that the narial openings were directed anteriorly in the Ankylosauridae. Almost all non-ankylosaurid ankylosaurs score (0). *Liaoningosaurus*, *Zhongyuansaurus*, *Shamosaurus*, *Jinyunpelta*, and *Tsagantegia* score (1). Character state (2) is present only in ankylosaurids. Ankylosaurids *Tianzhenosaurus*, *Nodocephalosaurus*, *Akainacephalus*, and *Ankylosaurus* score (0). *Ankylosaurus* is unique in having the external nares opening ventrolaterally. This character is ordered because the two derived states are inclusive.

12. Skull, external nares, visibility in dorsal view: most of the external naris is visible in dorsal view (0); almost completely hidden (1) (Thompson *et al.*, 2012:8).

Variable across Ankylosauria. All ankylosaurid taxa score (1), except for *Pinacosaurus* and *Tianzhenosaurus*.

13. Skull, external nares, position of anterior border in dorsal view: near the front of the premaxilla (0); posteriorly displaced (1) (new character).

Kirkland (1998:10) noted that the narial openings were displaced posteriorly in *Gastonia* and in Ankylosauridae. *Liaoningosaurus* also scores (1). All other ankylosaurs score (0).

14. Skull, presence of the antorbital fenestra: present (0); absent (1) (modified from Vickaryous *et al.*, 2004:42; Thompson *et al.*, 2012:1).

Sereno (1986) coded the closure of the antorbital and supratemporal fenestra as one character. However, it was ordered as present, small, and absent, recognizing that it was much smaller in *Scelidosaurus* relative to *Emausaurus*. The same author (1999:53) also retained it as a separate character, closed for all Ankylosauria. Only *Scelidosaurus* scores (0) by having a small but present antorbital fenestra.

15. Skull, supratemporal fenestra presence: present (0); absent (1) (Sereno, 1999:54; Vickaryous *et al.*, 2004:43; Thompson *et al.*, 2012:3).

Maryańska (1971) and Coombs (1978) recognized a closed supratemporal fenestra in all Ankylosauria. Sereno (1986) coded the closure of the antorbital and supratemporal fenestra together as one character. Kirkland and Loewen (2013) treat the two characters separately. All Ankylosauria (except for *Scelidosaurus*) score (1).

16. Skull, expression of laterotemporal fenestra in lateral view: completely visible (0); partially hidden as lateral expansion of the skull has the laterotemporal fenestra facing caudally (1); completely hidden (2) (modified from Kirkland, 1998:13; Carpenter *et al.*, 1998:6; Vickaryous *et al.*, 2004:4; Thompson *et al.*, 2012:2).

Both Coombs (1978) and Kirkland (1998:13) observed that the jugal-quadratojugal horn obscured the lateral temporal fenestra in ankylosaurids. Sereno (1986) noted that the quadratojugal and squamosal dermal ossifications hide the laterotemporal fenestra in lateral view and all but the tip of the quadrate. Sereno (1999:55) added that the jugal-postorbital bar was wider than the laterotemporal fenestra in Ankylosauria. Character state (2) occurs in ankylosaurids, *Kunbarrasaurus*, and *Cedarpelta*. *Europelta*, *Peloroplites*, *Silvisaurus*, and *Niobrarasaurus* score (1), all other ankylosaurs score (0).

Premaxilla

17. Premaxilla, maximum width of the premaxillary rostrum: nearly equal to or is less than the distance between the caudalmost maxillary teeth (0); greater than the distance between the caudalmost maxillary teeth (1) (Kirkland, 1998:4; Vickaryous *et al.*, 2004:14). Character states reworded.

Kunbarrasaurus, *G. burgei*, *Tsagantegia*, *Crichtonpelta*, and ankylosaurids score (1). All other ankylosaurs score (0).

18. Premaxilla, ventral margin in rostral view: flat or convex so that a wide premaxillary notch is absent (0); concave so that a wide premaxillary notch is present (1); very narrow premaxillary notch is present between premaxillae (2) (modified from Vickaryous *et al.*, 2004:15; Thompson *et al.*, 2011:20).

Kirkland (1998:5) recognized that a broad premaxillary notch was present in polacanthids. Sereno (1999:91) noted that a distinct interpremaxillary notch is present in all ankylosaurids, in which were included *Gastonia* and *Gargoyleosaurus*.

Scelidosaurus, *Gobisaurus*, *Zhongyuansaurus*, and *Shamosaurus* and panoplosaurids score (0). *Liaoningosaurus*, polacanthids, *Hungarosaurus*, *Peloroplites*, *Borealopelta*, *Silvisaurus*, and *Texasetes* score (1). Character state (2) is restricted to *Kunbarrasaurus*, *Crichtonpelta*, *Tsagantegia*, and ankylosaurids.

19. Premaxilla, cutting edge extends lateral to maxillary teeth: absent (0); present (1) (new character).

Sereno (1999:100) noted that the posterolateral cutting surface of the premaxilla obscures the anteriormost maxillary teeth in lateral view in nodosaurids. All non-ankylosaurid ankylosaurs score (0).

20. Premaxilla and maxilla, cutting edge of beak: contains teeth or the cutting edge is restricted to an extreme rostral position (0); extends caudally, so that the cutting surface is continuous with maxillary tooth row (1); extends caudally, lateral to maxillary tooth row so that maxillary teeth are medial to the cutting surface (2) (modified from Sereno, 1999:101; Kirkland, 1998:6; Carpenter *et al.*, 1998:14; Vickaryous *et al.*, 2004:16; Thompson *et al.*, 2012:21).

Coombs (1978) observed that the cutting edge of the beak is continuous with the maxillary tooth row in nodosaurids but not in ankylosaurids. Kirkland (1998:6) states that *Gastonia* shared this character with ankylosaurids. Sereno (1999:101) identified the edge of the premaxillary beak extending lateral to the maxillary teeth as a shared character for his Ankylosaurinae. A distinct cutting surface of the premaxilla lateral to the tooth row in *Gastonia* and ankylosaurids is recognized, while "panoplosaurines" have a cutting surface confluent with the tooth row.

21. Premaxilla, maximum anteroposterior length of premaxillary rostrum: equal to or greater than premaxillary palate width (0); less than premaxillary palate width (1) (modified from Vickaryous *et al.*, 2004:13; Thompson *et al.*, 2012:18).

The broad muzzle of ankylosaurids was noted by Coombs (1978) but not quantified. This character recognizes the width (wider than long) of the premaxillary rostrum in ankylosaurids. Character reworded.

22. Premaxilla, flat premaxillary shelf forming roof over extreme anterior end of palate: absent (0); present (1)

Coombs (1978) noted Ankylosauria is united by a flat premaxillary shelf forming a roof over the extreme anterior end of palate. Only *Scelidosaurus* and *Gargoyleosaurus* score (0).

23. Premaxilla, shape of the premaxillary palate: sub-triangular to elongated (0); sub-quadrangular (1); sub-oval (2) (modified from Sereno, 1999:80; Thompson *et al.*, 2012:19)

Coombs (1978) noted that premaxillary palates in nodosaurids were oval and commonly elongate. Character is ordered to conform to observed progression from elongated in *Scelidosaurus*, to quadrangular in polacanthids and ankylosaurids, to oval in panoplosaurids.

24. Premaxilla, fusion: unfused so that midline suture is visible (0); fused so that midline suture is completely obscured (1) (new character).

The premaxillae are completely fused in *Peloroplites*, *Borealopelta*, *Silvisaurus*, Texasetes, and panoplosaurids.

25. Premaxilla, overall shape in dorsal view: V-shape (0); U-shape (1); square or rectangular with flat rostral surface (2) (new character).

Kirkland and Loewen (2013) recognize a transition from a V-shaped premaxillae to U-shaped in polacanthids, ankylosaurids, *Cedarpelta*, and *Hungarosaurus* to square in *Peloroplites*, *Borealopelta*, *Silvisaurus*, *Texasetes*, and panoplosaurids.

26. Premaxilla, anterolateral corner forms lateral flange that projects laterally to become the widest point on the premaxilla so that anterior cutting surface on the ventral margin is bifurcated: absent (0); present (1) (new character).

Panoplosaurines have a bifurcated cutting surface caudally that continues to the tooth row medially and laterally to the cheek.

27. Premaxilla, presence of premaxillary sinuses: absent (0); present (1) (Arbour and Currie, 2015:9).

Some ankylosaurids have premaxillary sinuses.

Maxilla

28. Maxillary tooth row orientation relative to each other: linear rostrally, diverge caudally (0); curved into an hourglass shape, diverge rostrally and caudally, converge midway along the tooth row (1) (modified from Vickaryous *et al.*, 2004:16; Thompson *et al.*, 2012:24).

Coombs (1978) noted maxillary tooth rows diverged in ventral view in Ankylosauria, but that the palate was narrower in nodosaurids. Kirkland (1998:8) interpreted a wide palate as a shared character in *Gastonia* and Ankylosauridae and that an hourglass-shaped palate (Kirkland, 1998:9) was a derived feature of the Nodosauridae. Carpenter *et al.* (1998:25) scores an hourglass shape for nodosaurs. Panoplosaurids, *Texasetes*, *Scolosaurus*, and *Talarurus* are the only ankylosaurs scoring (1).

29. Maxilla, anterolateral corner forms lateral flange as continuation of cutting surface of snout: absent (0); present (1) (new character).

Sereno (1999:100) noted a premaxillary posteroventral rim which continues into this feature. This is a lateral extension of the cutting surface from the premaxilla forming a distinct flange lateral to the tooth row as present in all ankylosaurs, excluding *Scelidosaurus*, *Liaoningosaurus*, and *Kunbarrasaurus*.

30. Maxilla, anterolateral corner flange, orientation: lateral (0); vertical (1) (new character).

All ankylosaurids (except *Talarurus*) have a vertically oriented flange. All other ankylosaurs have a laterally oriented flange.

31. Maxilla, tooth row inset medially from lateral surface: absent (0); present, slightly inset (1); present, strongly inset (2) (modified from Carpenter *et al.*, 1998: 16; Vickaryous *et al.*, 2004:22; Maidment *et al.*, 2008:5; Thompson *et al.*, 2012:25).

Sereno (1986, 1999) noted an inset tooth row. The character was ordered to include a middle state. *Lesothosaurus* does not have an inset tooth row, but all stegosaurids, *Scutellosaurus*, *Emausaurus*, and *Scelidosaurus* have slightly inset tooth rows. Ankylosaurs (excluding *Scelidosaurus*) have a strongly inset tooth row, thus creating a lateral shelf and a cheek pocket.

32. Maxilla, paranasal sinus cavities: absent (0); present (1) (Vickaryous *et al.*, 2004:26; Thompson *et al.*, 2012:12).

Coombs (1978) noted complex nasal passages with sinuses in ankylosaurids and simple naris in nodosaurids (followed by Kirkland, 1998:12). Sereno (1986) lists paired sinuses in premaxilla, nasals, and maxilla as separate characters for ankylosaurids. Sereno (1999:95) lists snout with lateral sinus as a shared character for *Kunbarrasaurus*, *Shamosaurus*, and ankylosaurids. All ankylosaurids,

Tatankacephalus, '*Chassternbergia*', and *Panoplosaurus* are scored as having paranasal sinus cavities. It is absent in *Europelta*. Character reworded.

Nasal and palate

33. Nasal, length vs. width: nasals long, length more than 2 times width (0); nasals short, length less than 1.5 times width (1) (new character).

The nasal is longer than wide in most ornithischians, including stegosaurs. Short nasals are present in all ankylosaurs, including early diverging taxa such as *Scelidosaurus* and *Kunbarrasaurus*.

34. Nasal, internasal fusion in adults: unfused (0); fused (1) (new character).

There are visible unfused internarial sutures in stegosaurs and in the early diverging ankylosaurs *Scelidosaurus* and *Kunbarrasaurus.* All other ankylosaurs have a fused suture, often covered by ornamentations, such as caputegulae. The exceptions include *Europelta*, *Silvisaurus*, *Niobrarasaurus*, and *Sauropelta*.

35. Nasal, sagittal internasal septum: incomplete, does not separate nasal passages (0); complete (1) (Vickaryous *et al.*, 2004:20; Thompson *et al.*, 2012:10).

Sereno (1986, 1999:57) noted fusion of nasals forming a nasal septum separating the narial passages as an ankylosaur character. Carpenter *et al.* (1998:17, 18) scores a sagittal septum for nodosaurs and ankylosaurs. All ankylosaurs, with internal narial anatomy known score (1), except *Scelidosaurus*, *Gargoyleosaurus*, *G. burgei*, and *Europelta*. Character reworded.

36. Skull, shape of interior nasal passage: straight (0); with anterior and posterior loops (1) (Arbour and Currie, 2015:18).

Character reworded.

37. Palate, secondary palate complex between tooth rows: absent (0); secondary palate formed by palatine and vomers (1) (Vickaryous *et al.*, 2004:21; Thompson *et al.*, 2012:49; Arbour and Currie, 2015:31).

Coombs (1978) noted that in many ankylosaurs a complex secondary palate is present between the maxillary tooth rows, formed by various palatal elements and that some nodosaurids, like *Silvisaurus*, had no maxillary secondary palate. Kirkland (1998:7) resolved this character as one that was independently developed in later diverging nodosaurids and ankylosaurids. All ankylosaurids have a secondary palate, except *P. mephistocephalus*, *Talarurus*, and *Zuul*. All other ankylosaurs do not have a secondary palate.

Palpebral

38. Palpebral, shape of palpebral: rod shaped (0); plate shaped, possibly mobile, contacting only the prefrontal (1); plate shaped and totally fused into the orbit to become the anterior supraorbital (2) (modified from Sereno, 1999:5; Parish, 2005:23; Thompson *et al.*, 2012:27).

The palpebral in *Emausaurus* is plate shaped but possibly mobile (Haubold, 1990; Sereno, 1999; Norman, 2004). This character was ordered to include the plate-like condition of *Emausaurus* into the rest of thyreophorans.

39. Form of palpebral articulation: mobile contact with prefrontal (0); extensive sutural contact with prefrontal, frontal, and postorbital, palpebral forms anterodorsal rim of the orbit (1) (Sereno, 1986, 1999:9; Parish, 2005:24; Thompson *et al.*, 2012:28)

Sereno (1986) refers to the fused palpebral as supraorbital in Thyeophoroidea and notes that a single supraorbital separates the frontal from the orbital margin and separates the prefrontal and postorbital from each other. *Lesothosaurus* and *Emausaurus* are scored as having a mobile palpebral.

40. Supraorbitals, number of supraorbitals: one, large (the palpebral) (0); two supraorbitals (1); three supraorbitals (2) (new character).

Sereno (1986, 1999:13) notes that in Eurypoda (stegosaurs and ankylosaurs) two supraorbitals make up the dorsal rim of the orbit excluding the palpebral (first supraorbital). *Lesothosaurus* and *Emausaurus* are scored as having a single surpraorbital (the palpebral) and a prefrontal present. *Stegosaurus* and *Hesperosaurus* have an anterior supraorbital (palpebral), a medial supraorbital and a posterior supraorbital in addition to a prefrontal. *Scelidosaurus* and *Kunbarrasaurus* have two supraorbitals in addition to a prefrontal. All other ankylosaurs are scored as having three supraorbitals and a prefrontal. Character reworded for clarity.

Orbital Region

41. Orbits, angle of orbital axis: laterally oriented, angle of the surface of the orbit subparallel to sagittal plane (0); anterolaterally oriented (1) (Parish, 2005:11; Thompson *et al.*, 2011:13)

Gastonia and some ankylosaurids have distinct rostrally facing orbits. Character reworded.

42. Orbit, preocular wall present in anterior wall of internal orbit separating the orbit from the antorbital space: absent (0); present (1) (new character).

Sereno (1986, 1999:62) noted that an accessory antorbital ossification completely separated the orbit and antorbital space in Ankylosauria. All ankylosaurs were coded as (0), including *Scelidosaurus*, which has a medial flange on the lacrimal to exclude the orbit from the antorbital space.

43. Orbit, suborbital lip forming a thin, sharp flange on the lateral edge of the ventral surface of the orbit: absent (0); present (1) (new character).

Almost all ankylosaurids have a distinct lip or flange on the lateral edge of the ventral part of the orbit. The exceptions are *Zaraapelta*, *Nodocephalosaurus*, *Akainacephalus*, *Ziapelta*, and UMNH VP 21000.

44. Postorbital, postoccular wall in caudal wall of internal orbit: absent (0); present (1) (Vickaryous *et al.*, 2004:41; Thompson *et al.*, 2012:15).

Haas (1969) noted that a medial expansion of bone (postorbital division) separated the jaw muscles from the back of the orbit. Coombs (1978) considered this (postorbital shelf) a diagnostic feature of the Ankylosauria. Sereno (1986, 1999:104) noted that the postorbital and jugal formed a well-developed postocular shelf in ankylosaurids. All ankylosaurs have a postocular wall, including *Scelidosaurus*, which has a distinct medial flange on the medial surface of the jugal and postorbital.

45. Postorbital, supraorbital postorbital boss: absent or minimal (0); present (1) (modified from Vickaryous *et al.*, 2004:5).

This character is variable across Ankylosauria. It is scored as absent in *Scelidosaurus*, although there is some sculpturing present on the postorbital. A well-developed boss is present in *Kunbarrasaurus*, *Antarctopelta*, all polacanthids, and all ankylosaurids. Struthiosaurids have a minimal boss, while nodosaurs, except *Propanoplosaurus* and *Panoplosaurus*, have a distinct boss.

46. Postorbital, supraorbital boss form: rounded protuberance (0); longitudinal ridge or peak (1) (modified from Vickaryous *et al.*, 2004:5).

This character scores the shape of the boss and is variable across Ankylosauria. Absent in *Scelidosaurus*.

47. Postorbital, supraorbital boss, overall orientation of the boss in anterior view: laterally oriented (0); dorsolaterally oriented (1) (modified from Vickaryous *et al.*, 2004:5).

This character scores the orientation in lateral view of the apex or line of the boss. Dorsolateral orientation is present in all ankylosaurids.

48. Supraorbitals, shape of supraorbital complex: rounded (0); forming lateral rim (1) (modified from Arbour and Currie, 2015:38).

The shape of the supraorbital rim differs throughout ankylosaurs.

49. Postorbital, supraorbital boss, overall orientation of the boss in dorsal view: lateral (0); posterolateral (1) (new character).

Oriented posterolaterally in *Kunbarrasaurus, Antarctopelta*, and all polacanthids, and laterally in all other ankylosaurs. Absent in *Scelidosaurus*.

50. Postorbital, supraorbital boss, position of apex of boss compared to the dorsal margin of the orbit: positioned dorsally to the dorsal portion of the orbit (0); positioned ventrally to the dorsal portion of the orbit (1) (new character).

In *Silvisaurus*, *Texasetes* (=*Pawpawsaurus*), *Tatankacephalus* and *Animantarx* the apex of the boss is ventral to the dorsal portion of the orbit. All other ankylosaurs have a boss dorsal to the orbit margin.

51. Supraorbitals, shape of apices of supraorbital complex: rounded, no distinct apex (0); distinct apices present (1) (modified from Arbour and Currie, 2015:39).

The shape of the supraorbital rim differs throughout ankylosaurs.

52. Squamosal, squamosal boss: absent (0); present, rounded protuberance (1); present, low or equilateral pyramidal protuberance (2); present, elongated triangle longer than wide (3) (modified from Vickaryous *et al.*, 2004:6).

Coombs (1978) noted that the ornamentation on the squamosal in Ankylosauria ranged from blunt to large horns. Sereno (1986) notes a prominent wedge-shaped squamosal dermal ossification as present in ankylosaurids. Kirkland (1998:23) had three character states: absent, present (nodosaurids), and long (ankylosaurids). Sereno (1999:93) links it with quadratojugal dermal ossification as present in ankylosaurids. Transition was ordered from rounded to low pyramid to elongated triangle. States 1-3 are only present in ankylosaurids.

Jugal, Quadratojugal and Suborbital Region

53. Suborbital boss or cornice: absent (0); present, rounded protuberance (1); present, deltaic protuberance (2) (modified from Carpenter *et al.*, 1998:5; Vickaryous *et al.*, 2004:7).

Sereno (1986) refers to prominent, wedge-shaped quadratojugal dermal ossification. Kirkland (1998:23) had four states (absent, present, strong, or lost) since it was considered secondarily lost in *Panoplosaurus*. It is a deltaic protuberance in *Kunbarrasaurus*, *Antarctopelta*, polacanthids, most ankylosaurids (exceptions are *Platypelta*, S. *cutleri*, and *Anodontosaurus*), and *Texasetes*. All other ankylosaurs score (1), apart from *Scelidosaurus*, which scores (0).

54. Suborbital boss, distinct neck at base: absent (0); present (1) (Arbour and Currie, 2015:48).

Arbour and Currie (2015:48) noted a constriction of the jugal horn in some polacanthids and in some ankylosaurids. Character states reworded for simplification.

55. Suborbital boss composition: formed by jugal only (0); formed by jugal and quadratojugal (1) (new character).

Coombs (1978) noted that an armour plate was fused to jugal and quadratojugal posterior ventral to orbit in the Ankylosauridae. All ankylosaurs, except *Kunbarrasaurus* and polacanthids, have a boss covering both the jugal and quadratojugal.

56. Suborbital boss, size relative to the orbit: length of base of jugal/quadratojugal horn equal to or less than the length of the orbit (0); length of base of jugal/quadratojugal horn is 110% or greater length of orbit (1) (Arbour and Currie, 2015:49). Character reworded.

Arbour and Currie (2015:49) compared the size of the suborbital boss (jugal horn) to the orbits in some ankylosaurids.

57. Jugal, medial surface, large medially facing pocket: absent (0); present (1) (new character).

A medially facing pocket on the medial surface of the jugal is present only in *Gargoyleosaurus*, *Mymoorapelta*, and *Gastonia*.

58. Quadratojugal, visible in lateral view: visible posterior to jugal (0); not visible, quadratojugal is medial to jugal (1) (new character).

Sereno (1999:56) noted that the external surface of the quadratojugal was posteriorly oriented in Ankylosauria. It is not visible in polacanthids.

Quadrate

59. Quadrate, lateral profile: bowed, anteriorly convex, caudally concave (0); straight (1) (Vickaryous *et al.*, 2004:38; Thompson *et al.*, 2012:33). Character state 1 reworded.

A straight quadrate is present in *Gastonia* and all ankylosaurids.

60. Quadrate, inclination of quadrate in lateral view: near perpendicular to skull roof, 70-90° (0); anterolaterally, from 60° to 40° (1); nearly horizontal, less than 30° from skull roof (2) (modified from Lee, 1996:10; Kirkland, 1998:14; Carpenter *et al.*, 1998:20; Parish, 2005: 32; Thompson *et al.*, 2012:34; Arbour and Currie, 2015:60).

This character is variable across Ankylosauria. *Scelidosaurus*, *Gobisaurus*, *Shamosaurus*, *P. mephistocephalus* and *Cedarpelta* have vertically inclined quadrates, *Kunbarrasaurus*, *Gargoyleosaurus*, *Mymoorapelta*, *Hylaeosaurus*, *Gastonia*, *Europelta* and *S. transylvanicus* have almost horizontal, rostrally inclined quadrates, while every other ankylosaur has an inclination of 70° to 40°.

61. Quadrate, cross-sectional shape of the anterior surface of the shaft of the quadrate: transversely concave (0); flat (1) (Lee, 1996:12; Parish, 2005:33; Thompson *et al.*, 2012:35).

This character is variable across ankylosaurs, but *Scelidosaurus*, polacanthids, *Cedarpelta*, *Gobisaurus*, *Shamosaurus*, *Crichtonpelta*, *Tianzhenosaurus*, *Minotaurasaurus* and all North American ankylosaurids have a concave rostral surface of the shaft of the quadrate. *Sauropelta*, *Texasetes*, *Tatankacephalus*, *Animantarx*, *Tsagantegia*, *P. grangeri*, *Saichania*, *T. teresae*, struthiosaurids, and panoplosaurids have a flat rostral surface of the quadrate shaft.

62. Quadrate, fusion of the dorsal end of the quadrate to the paroccipital process: unfused (0); fused (1) (Vickaryous *et al.*, 2004:39; Thompson *et al.*, 2012:41)

Coombs (1978) noted that in most ankylosaurids the quadrate articulates with both the paroccipital processes and squamosal. Carpenter *et al.* (1998:13) notes fusion in *Gargoyleosaurus* and nodosaurs. *Gastonia*, *Gobisaurus*, *Shamosaurus*, *Tsagantegia*, *Saichania*, *Peloroplites*, *Silvisaurus*, *Sauropelta*, *Texasetes*, *Tatankacephalus*, *Animantarx*, and panoplosaurids score (1).

63. Quadrate, quadrate condyle visible in lateral view: visible (0); obscured by the suborbital boss (1) (Vickaryous *et al.*, 2004:40; Thompson *et al.*, 2012:36)

Coombs (1978) observed that the jugal-quadratojugal horn obscured the quadrate condyles in lateral view in ankylosaurids. All ankylosaurids and the struthiosaurid *Europelta* have the quadrate condyle obscured by the suborbital boss. Character reworded.

64. Quadrate, shape of condylar (articular) surface: sub-oval (0); condyles elongated laterally, width more than 3x that of anteroposterior length (1) (new character). Character states reworded.

Stegosaurs, ankylosaurids, *Cedarpelta*, and europeltines have mediolaterally elongated quadrate condyles.

65. Quadrate, condylar (articular) end, position of the anteroposterior thickest point in ventral view: medial condyle is larger so that the thickest point is located medially (0); middle of the condylar end (1) (new character). Character states reworded.

Stegosaurs, ankylosaurids, *Cedarpelta*, and europeltines have thickest point in the middle of the condyle.

66. Quadrate, lateral ramus: absent (0); present (1) (Arbour and Currie, 2015:61). Character reworded.

Outgroup character to stegosaurs and ankylosaurs.

67. Quadrate, depth of pterygoid process: deep (0); shallow (1) (Lee, 1996:7; Sereno, 1999:60; Thompson *et al.*, 2012:40; Arbour and Currie, 2015:62).

Outgroup character to stegosaurs and ankylosaurs.

Supraoccipital

68. Foramen magnum, orientation: directly posteriorly (0); posteroventrally (1) (Vickaryous *et al.*, 2004:37; Thompson *et al.*, 2011:62).

This character is variable across thyreophorans. Kirkland and Loewen (2013) code it based on the ventral surface of the foramen magnum.

69. Foramen magnum, posterior thickening of the dorsal margin of the foramen magnum relative to surrounding bone forming a dorsal shelf or collar above foramen magnum: no or incipient thickening (0); distinctly

thickened (1) (modified from Parish, 2005:49; Thompson *et al.*, 2012:53). Character state 0 reworded.

This character described a dorsal rim formed in the dorsal surface of the foramen magnum, expressed caudally. *Scelidosaurus*, *Niobrarasaurus*, *Gobisaurus*, *Zhongyuansaurus*, *Shamosaurus*, *Tsagantegia*, and all ankylosaurids (except Minotaurasaurus) score (0). A thickened dorsal rim on the foramen magnum is present in all other ankylosaurs.

Opisthotic

70. Paroccipital process, orientation of long axis in posterior view: directed ventrolaterally (0); directed laterally (1) (new character).

The paroccipital process is oriented laterally in *Kunbarrasaurus*, *Europelta*, and all ankylosaurids, except *Tianzhenosaurus* and *Saichania*. All other ankylosaurs have ventrally deflected paroccipital processes.

71. Paroccipital process, orientation of long axis in dorsal view: directed posterolaterally (0); directed laterally (1) (Vickaryous *et al.*, 2004:33; Thompson *et al.*, 2012:51).

Carpenter *et al.* (1998:18) noted that the paroccipital processes project posterolaterally in *Gargoyleosaurus* and nodosaurs. Variable throughout Ankylosauria. *Crichtonpelta*, *G. burgei*, *E. longiceps*, *Denversaurus*, and ankylosaurids (except *Talarurus*) score (1), all other ankylosaurs score (0).

72. Paroccipital process, dorsoventral expansion of distal paroccipital processes compared to the neck: expanded to more than 200% the dorsoventral height of the neck (0); expanded, but less than 150% the dorsoventral height of the neck (1); not expanded (2) (modified from Parish, 2005:48; Thompson *et al.*, 2012:52).

Scelidosaurus, *Kunbarrasaurus*, *Gargoyleosaurus*, *Hylaeosaurus*, *Gastonia*, *Gobisaurus*, *Crichtonpelta*, *Europelta*, and *S. transylvanicus* have bowtie shaped paroccipital processes. *Tianzhenosaurus*, *Shanxia*, *Minotaurasaurus*, *Oohkotokia*, and *Euoplocephalus* have completely unexpanded paroccipital processes.

Basioccipital

73. Basioccipital, form of the ventral surface of basioccipital-basisphenoid: transversely convex (0); distinct medial depression (1) (modified from Parish, 2005:51; Thompson *et al.*, 2012:55).

Polacanthus, *Texasetes* (=*Pawpawsaurus*), *Animantarx*, *Panoplosaurus*, *Chassternbergia*, *E. rugosidens*, *E. longiceps*, and *Denversaurus* have a medial depression on the ventral surface of the basioccipital.

74. Basioccipital, distinct medial longitudinal ridge on ventral surface: absent (0); present (1) (modified from Parish, 2005:51; Thompson *et al.*, 2012:55).

Kirkland and Loewen (2013) consider the longitudinal ridge variably present across Ankylosauria and score it present regardless of the state of the previous character.

75. Basioccipital, basioccipital foramen: absent (0); present (1) (new character).

A small foramen in the middle of the neck of the basioccipital is present in *Crichtonpelta*, *Saichania*, *Shanxia*, and *Minotaurasaurus*.

76. Occipital condyle, composition: multiple elements are evident by sutures in the occipital condyle (0); basioccipital is the only contributor to the occipital condyle excluding the suture (1) (Vickaryous *et al.*, 2004:34; Thompson *et al.*, 2012:54).

Sereno (1986, 1999:82) used a basioccipital-exclusive condyle as a nodosaurid character. Kirkland (1998:17) notes a spherical occipital condyle made up of only the basioccipital. Kirkland and Loewen (2013) recognize multiple contributing elements in all ankylosaurs, except in "panoplosaurines".

77. Occipital condyle, morphology in posterior view: reniform (0); ovoid/round (1) (Vickaryous *et al.*, 2004:35; Arbour and Currie, 2015:71). Character reworded.

Coombs (1978) noted a roughly spherical condyle in nodosaurids. Carpenter *et al.* (1998:26) scores a hemispherical ankylosaurid occipital condyle. Sereno (1999:81) linked hemisphericity and ventral deflection as one character for nodosaurs. *Peloroplites*, *Silvisaurus*, *Niobrarasaurus*, *Sauropelta*, *Texasetes*, *Animantarx*, and panoplosaurids score (1).

78. Occipital condyle, orientation of the neck of the occipital condyle: directly caudally (0); caudoventrally (1) (modified from Vickaryous *et al.*, 2004:36; Thompson *et al.*, 2012:61)

Coombs (1978) noted that the occipital condyle neck was directed ventrally in nodosaurids. Kirkland and Loewen (2013) find this character to be variable across

ankylosaurs and score it relative to the level of the maxillary tooth row and constrain it to the long axis of the neck of the condyle, not the articular surface which is scored in the next character.

79. Occipital condyle, orientation of the articular surface: directly caudally (0); caudoventrally (1) (new character).

This character deals strictly with the orientation of the articular surface of the occipital condyle. The occipital condyle is caudoventrally oriented in all thyreophorans, except *Scutellosaurus*, *Emausaurus*, *Scelidosaurus*, and *Cedarpelta*.

Basisphenoid

80. Basisphenoid, length between early diverging tubera and basipterygoids compared to length of basioccipital: long, greater than basioccipital length (0); short, less than basioccipital length (1) (Vickaryous *et al.*, 2004:31; Thompson *et al.*, 2012:56).

Character first noted by Sereno (1986, 1999:12) uniting his Thyreophoroidea (*Scelidosaurus*, stegosaurs and ankylosaurs).

81. Basisphenoid, early diverging tubera morphology: medially separated rounded rugose stubs (0); continuous transverse rugose ridge (1) (Vickaryous *et al.*, 2004:32; Thompson *et al.*, 2012:57).

All ankylosaurids, *Cedarpelta*, *Europelta*, *S. transylvanicus*, and *S. languedocensis* have a continuous transverse ridge crossing the early diverging tubera.

Basipterygoid

82. Basipterygoid, basipterygoid-pterygoid fusion: unfused (0); fused (1) (modified from Vickaryous *et al.*, 2004:30; Thompson *et al.*, 2011:44).

Coombs (1978) noted that in most ankylosaurids the basipterygoid and pterygoid are unfused and fused in all nodosaurids.

83. Basipterygoid, size of basipterygoid processes: long, twice or more as long as wide (0); short, less than twice as long as wide (1) (Parish, 2005:55; Thompson *et al.*, 2012:58).

Kirkland (1998:19) considered elongated basipterygoid processes to be a derived character in polacanthids. *Kunbarrasaurus*, *Gobisaurus*, and polacanthids are scored as having long basipterygoid processes while short basipterygoid processes are present in all other ankylosaurs.

Pterygoid

84. Pterygoid, extensive medial contact between pterygoids to form pterygoid shield: absent (0); present (1) (modified from Parish, 2005:40; Thompson *et al.*, 2012:42). Character state 1 reworded.

Coombs (1978) noted that nodosaurid pterygoids form a wide central plate. *Peloroplites*, *Silvisaurus*, *Texasetes*, and panoplosaurids score (1). All other ankylosaurs score (0).

85. Pterygoid, interpterygoid vacuity: pterygoids separate posteromedially, forming an interpterygoid vacuity (0); absent (1) (modified from Parish, 2005:40; Thompson *et al.*, 2012:42).

This character is probably linked to the presence of a pterygoid shield. *Lesothosaurus* and all thyreophorans have an interpterygoid vacuity.

86. Pterygoid, posterior margin of the pterygoid: anterior to the ventral margin of the pterygoid process of the quadrate (0); aligned with or posterior to the ventral margin of the pterygoid process of the quadrate (1) (modified from Sereno, 1999:83; Vickaryous *et al.*, 2004:28). Character state 1 reworded.

Sereno (1999:83) noted this as a nodosaurid character. This character is probably linked to the presence of a pterygoid shield. Only *Kunbarrasaurus*, *Texasetes*, and panoplosaurids have an aligned pterygoid caudal margin.

87. Pterygoid, pterygoid foramen: absent (0); present (1) (Hill, 2003:21; Thompson *et al.*, 2012:47).

This is a distinct small foramen on the ventral surface of the pterygoid. Only *Scelidosaurus*, *Peloroplites*, *Silvisaurus*, and panoplosaurids score (0).

88. Pterygoid, orientation of the pterygoid flange in anterior view: obliquely oriented (0); oriented vertically (parasagittally) (1); oriented nearly laterally (2) (modified from Vickaryous *et al.*, 2004:29; Thompson *et al.*, 2011:43). Character states reworded.

Coombs (1978) noted a thin anterolaterally directed pterygoid flange arising close to the mid-line in Ankylosauridae. Kirkland and Loewen (2013) observe a laterally oriented pterygoid flange in stegosaurs, an oblique flange in *Scelidosaurus* and all ankylosaurids. The flange is vertical in *G. burgei*, *Gobisaurus*, *Shamosaurus*, *Cedarpelta*, *Silvisaurus*, *Texasetes*, and panoplosaurids.

89. Pterygoid, orientation of surface between posterior margin and pterygoid flanges: nearly horizontal, forming posterior secondary palate (0); posteroventral (1) (modified from Vickaryous *et al.*, 2004:21; Thompson *et al.*, 2012:49).

Silvisaurus, *Texasetes*, and panoplosaurids have a posteroventrally angled caudal margin of the pterygoid flange.

90. Pterygoid, position of ventral margin of the pterygovomerine keel relative to alveolar ridge: dorsal (0); aligned (1) (Sereno, 1999:59; Thompson *et al.*, 2012:45, Arbour and Currie, 2015:67). Character states reworded for consistency.

Outgroup character.

Mandible

91. Predentary, size of predentary ventral process: distinct, prong shaped process (0); rudimentary eminence (1) (Sereno, 1986, 1999:66; Parish, 2005:72; Thompson *et al.*, 2012:76).

Coombs (1978) noted the reduced size of the predentary in Ankylosauria. All Ankylosauria, including *Scelidosaurus*, have a vestigial ventral predentary process.

92. Dentary, depth of the dentary symphysial ramus relative to the maximum depth of the dentary in lateral view: deep, symphysial ramus > 50% maximum dentary depth (0); shallow, < 45% maximum dentary depth (1) (Sereno, 1986, 1999:17; Parish, 2005:64; Thompson *et al.*, 2012:69).

Sereno (1986, 1999:17) noted a shallow symphysis as character of Eurypoda. A deep symphysis is scored in *Scutellosaurus*, *Emausaurus*, all stegosaurs (except *Chungkingosaurus*), *Scelidosaurus*, *Kunbarrasaurus*, *Liaoningosaurus*, *Gargoyleosaurus*, and struthiosaurids. "*Bienosaurus*", *Silvisaurus*, *Sauropelta*, *Animantarx*, ankylosaurids, and panolosaurids have a shallow symphysis.

93. Dentary, shape of dorsal margin of the dentary in lateral view: straight (0); sinuous or convex (1) (Sereno, 1999:4; Parish, 2005:65; Thompson *et al.*, 2012:70)

Sereno (1986, 1999:4) reports this as a late diverging condition present in *Scelidosaurus*, stegosaurs, and ankylosaurs. A sinuous or convex dorsal margin is present in *Emausaurus,* all stegosaurs, and all ankylosaurs.

94. Dentary, shape of ventral margin of the dentary in lateral view excluding the symphysis: straight (0); sigmoidal or concave (1) (modified from Parish, 2005:66; Thompson *et al.*, 2011:71).

Sereno (1986, 1999:85) uses this as a nodosaurid character. A sigmoidal ventral margin is present in *Emausaurus* and all ankylosaurs except *Scelidosaurus*. It is variable in stegosaurs.

95. Dentary, shape of the alveolar margin in dorsal view: straight (0); laterally concave (1); laterally convex or sigmoidal (2) (modified from Parish, 2005:67; Thompson *et al.*, 2012:72).

The tooth row is straight in early diverging thyreophorans, and *Scelidosaurus*. It is laterally convex or sigmoidal in *Gargoyleosaurus*, "europeltines", *Silvisaurus*, and *Sauropelta*. It is laterally concave in ankylosaurids, *Animantarx* and "panoplosaurines".

96. Dentary, presence of a horizontal shelf lateral to the tooth row: present as a rounded protuberance (0); present, as a distinct ridge, but with no lateral expansion to form a lateral shelf (1); present, as a distinct ridge with lateral expansion to form a lateral shelf (2) (new character).

There is a distinct ridge without a lateral shelf in *Lesothosaurus*, *Scutellosaurus*, *Emausaurus*, and *Scelidosaurus*. All stegosaurs, except *Chungkingosaurus* and *Tuojiangosaurus*, have a distinct ridge with a lateral shelf. *Chungkingosaurus*, *Tuojiangosaurus*, and ankylosaurines have a rounded protuberance lateral to the tooth row that does not form a ridge.

97. Dentary, size and projection of the dorsal surangular process: small, with no dorsal projection (0); well-developed, with a medially positioned dorsal projection (1) (Parish, 2005:71; Thompson *et al.*, 2012:75).

Coombs (1978) noted that there was only a small process in ankylosaurids. A well-developed process is present in *Scelidosaurus*, *Kunbarrasaurus*, *Gargoyleosaurus*, *Shamosaurus*, *Hungarosaurus*, *Peloroplites*, *Silvisaurus*, *Animantarx*, and "edmontoniines" nodosaurids. It is small in ankylosaurids.

98. Mandible, position of mandible articulation relative to mandibular adductor fossa: posterior (0); posteromedial (1) (Sereno, 1999:59; Thompson *et al.*, 2012:45, Arbour and Currie, 2015:78). Character states reworded.

Outgroup character.

99. Surangular, lateral ridge on dorsolateral surface of surangular: absent (0); present (1) (Butler *et al.*, 2018:106).

A distinct lateral ridge is present in *Lesothosaurus*, *Emausaurus*, *Scelidosaurus*, *Kunbarrasaurus*, *Tianchisaurus*, *Gargoyleosaurus*, *Shamosaurus*, *Cedarpelta*, and *Sauropelta*.

100. Surangular, coronoid process: absent (0); present (1) (new character).

Coombs (1978) identified the absence of a coronoid process in Ankylosauria. Kirkland and Loewen (2013) score a coronoid process as present in all ankylosaurs (*contra* Coombs, 1978).

101. Surangular, coronoid process height: low (0); higher than 30% length (1); high, almost as high as long (2) (new character). Character state 2 reworded.

Sereno (1999:108) reported that the coronoid process was typically of only moderate height in thyreophorans but was low in many ankylosaurines. Carpenter *et al.* (1998:24) has a low coronoid only present in ankylosaurids. It is variable across Ankylosauria. In *Saichania*, *Minotaurasaurus*, and *Euoplocephalus* the height is more than 30% of the length. *Peloroplites*, *Animantarx*, and "panoplosaurines" have an almost as high as long coronoid process. All other ankylosaurs have a low process.

102. Internal mandibular fossa, dorsal roof formed by coronoid process: absent (0); present across entire coronoid dorsal surface (1) (new character). Character reworded.

The medial surface of the surangular has a dorsal roof in *Scelidosaurus*, *Tianchisaurus*, *Liaoningosaurus*, *Gargoyleosaurus*, *Shamosaurus*, *Cedarpelta*, *Hungarosaurus*, and *Sauropelta.*

103. External mandibular fenestra: present (0); absent (1) (Vickaryous *et al.*, 2004:44; Thompson *et al.*, 2012:68).

The external mandibular fenestra is absent in all ankylosaurians including *Scelidosaurus*.

Dentition

104. Premaxilla, premaxillary teeth: present (0); absent (1) (Kirkland, 1998:20; Carpenter *et al.*, 1998:15; Vickaryous *et al.*, 2004:17; Thompson *et al.*, 2012:63).

Coombs (1978) noted the presence of premaxillary teeth in some nodosaurids, such as *Sauropelta* (AMNH 3035), *Silvisaurus*, and possibly *Struthiosaurus*. Nopsca (1928) used the anterior placement of teeth on the dentary of *S. austriacus* to infer premaxillary teeth. Sereno (1999:96) used the absence of premaxillary teeth as a character uniting *Kunbarrasaurus*, *Shamosaurus*, and the ankylosaurids. The presence of premaxillary teeth is scored in *Scelidosaurus*, *Liaoningosaurus*, *Gargoyleosaurus*, *Cedarpelta*, *Silvisaurus*, *Texasetes* (=*Pawpawsaurus*), and *Tatankacephalus*. The preserved portion of the premaxilla of *Peloroplites* does not have teeth, and a premaxilla for *Sauropelta* is unknown (*contra* Coombs, 1978).

105. Maxilla, tooth row extends to rostral end of maxilla: present or extends to within one alveolus length of the rostral end of the maxilla (0); absent, diastema at least two alveoli length is present (1) (new character). Character states reworded for clarity.

Most stegosaurs (except *Huayangosaurus*), all polacanthids, all ankylosaurids, and "panoplosaurines" have a distinct diastema. *Scelidosaurus*, *Liaoningosaurus*, *Silvisaurus*, *Texasetes* (=*Pawpawsaurus*), and *Tatankacephalus* have teeth that extend nearly to the rostral end of the maxilla.

106. Dentary, teeth extend nearly to the symphysis or predentary contact: present (0); absent, diastema between the symphysis and the rostralmost tooth (1) (new character).

The tooth row extends to the symphysis in all thyreophorans, except in ankylosaurids, *Animantarx*, and "panoplosaurines" in which there is a diastema.

107. Dentary or maxillary teeth, presence of cingulum: absent (0); present (1) (modified from Vickaryous *et al.*, 2004:19; Thompson *et al.*, 2012:64).

Kirkland (1998:21) noted the presence of cingula as a derived character. Carpenter *et al.* (1998:21) scores the absence of a cingulum in *Scelidosaurus* and *Gargoyleosaurus*. An incipient cingulum is observed and scored as present in *Lesothosaurus*, *Scutellosaurus*, *Emausaurus*, *Gargoyleosaurus*, *Dracopelta*, *Gastonia*, and *Gobisaurus*. Stegosaurs and all other ankylosaurs have distinct, well-developed cingula.

108. Dentary or maxillary teeth, tooth crown shape: pointed (0); rounded (1) (Thompson *et al.*, 2012:65, in part; Arbour and Currie, 2015:89).

The tooth shape differs amongst thyreophorans.

109. Dentary or maxillary teeth, number of tooth denticles: <13 denticles (0); ≥13 denticles (Thompson *et al.*, 2012:65, in part; Arbour and Currie, 2015:90). Character reworded.

The numbers of denticles per tooth differs amongst thyreophorans.

110. Dentary teeth, number of teeth: <25 teeth (0); ≥25 (1) (Thompson *et al.*, 2012:66; Arbour and Currie, 2015:91).

The number of dentary teeth differs amongst thyreophorans.

111. Maxillary and dentary teeth, relative size to skull: relatively large (0); relatively small (1); tiny (2) (new character).

Coombs (1978) noted that nodosaurids had relatively large teeth and ankylosaurids very small teeth. Relatively small teeth are recognized in *Liaoningosaurus*, *Chuanqilong*, polacanthids, and ankylosaurids. All other ankylosaus have relatively smaller teeth. All the tooth scorings for *Panoplosaurus* are derived from CT scan data.

Cranial Ornamentation

112. Cranial sutures on posterior skull roof: visible (0); obliterated (1) (modified from Sereno, 1986, 1999:63; Hill *et al.*, 2003:36; Thompson *et al.*, 2012:17).

Maryańska (1971) and Coombs (1978) first noted that extensive cranial ornamentation obscuring cranial sutures is characteristic of all but juvenile skulls in all Ankylosauria. Sereno (1986, 1999:63) notes dermal sculpturing of skull roof across Ankylosauria. Obliterated cranial sutures are recognized on the adult skull roof in all ankylosaurs, except *Scelidosaurus*, *Kunbarrasaurus*, and *Liaoningosaurus*. The cranial elements of *Antarctopelta* suggest obliteration.

113. Cranial sutures on lateral skull: visible (0); obliterated (1) (new character).

Obliterated cranial sutures on the lateral (circumorbital region) skull is recognized in all ankylosaurs, except *Scelidosaurus*. While *Kunbarrasaurus* has skull roof sutures present, the lateral sutures are obliterated by ornamentation.

114. Cranial ornamentation: absent (0); minimal (1); extensive with scale impressions (2) (new character).

This character was ordered to recognize the evolution of cranial ornamentation from early diverging thyreophorans to derived ankylosaurs. Minimal ornamentation

is present in *Scelidosaurus*, *Kunbarrasaurus*, *Liaoningosaurus*, and *Antarctopelta*. All other ankylosaurs have extensive scale impressions on the skull.

115. Cranial ornamentation, distinct pattern of scale polygons: polygons absent (0); present (1) (new character).

Distinct polygons are present in all ankylosaurs, except *Mymoorapelta*, *Gastonia*, *Gobisaurus*, *Shamosaurus*, *Zhongyuansaurus*, *Jinyunpelta*, *Europelta*, and *Cedarpelta.*

116. Cranial ornamentation, bone remodeling under the scale impressions: absent or minimal remodeling (0); bone remodeling perpendicular to scale but impression is still flat (1); extensive remodeling with rounded bulbous scale impressions (2); extensive remodeling with peaked bulbous scale impressions (3) (new character).

Coombs (1978) and Kirkland (1998:31) observed deeper grooves between armour elements on the skull roof in ankylosaurids. Polacanthids, *Texasetes*, North American ankylosaurids (except for *Nodocephalosaurus* and *Akainacephalus*), and the Asian ankylosaurids *Talarurus* and *Tianzhenosaurus* score (1). *Liaoningosaurus*, and the ankylosaurids *P. mephistocephalus*, *Saichania*, and *Zaraapelta* score (2). Character state (3) is observed only in the ankylosaurids *P. grangeri*, *Tarchia*, *Minotaurasaurus*, *Nodocephalosaurus*, and *Akainacephalus*. All other ankylosaurs score (0).

117. Cranial ornamentation, number of scale impressions on skull roof: ≤20 (0); ≥30 (1) (new character).

Ankylosaurids and *Texasetes* have 30 or more distinct scale impressions. All other ankylosaurs have 20 or less distinct scale impressions.

118. Cranial ornamentation, presence of a "beak line" separating nasal armour from premaxillary armour: absent, armour uniform across premaxillary nasal suture (0); transverse line separating relative smooth premaxilla from heavily rugose nasal (new character).

Kirkland and Loewen (2013) identify a distinct "beak line" differentiating the smooth area of the premaxilla that is presumably covered by a keratinous beak from the distinct ornamentation originating on the nasal. It is present in all ankylosaurs that have preserved premaxillae, except *Scelidosaurus*, *Kunbarrasaurus*, *Liaoningosaurus*, *Gargoyleosaurus*, *Gastonia*, *Gobisaurus*, and *Shamosaurus*.

119. Premaxilla, deep longitudinal furrow on middle portion of premaxilla: absent (0); present (1) (Arbour and Currie, 2015:7).

This is different from the beak line present in some ankylosaurids and is anterior and ventral to the beak line.

120. Cranial ornamentation, presence of ornamentation on the external surface of the premaxillae: absent, smooth (0); present as rugose ornamentation (1) (Vickaryous *et al.*, 2004:62; Arbour and Currie, 2015:8).

Kirkland (1998:22) noted armour on the premaxilla (remodelled bone) as a derived character.

121. Cranial ornamentation, midline osteoderm on premaxilla that forms cutting surface of snout: absent (0); present (1).

122. Cranial ornamentation, form of bulbous scale impressions on frontoparietal region of skull roof: flat (0); rounded (1); peaked (2) (new character).

Gargoyleosaurus, *Mymoorapelta*, *Dracopelta*, *Crichtonpelta, Pinacosaurus*, *Saichania*, and *Tarchia* have rounded impressions while *Tianzhenosaurus*, *Minotaurasaurus*, and *Nodocephalosaurus* are peaked.

123. Cranial ornamentation, nasal ornamentation compared to premaxillary ornamentation: similar to that of premaxilla (0); more pronounced than premaxillary ornamentation (1) (new character). Character states reworded.

Kirkland and Loewen (2013) recognize nasal ornamentation as more pronounced than premaxillary ornamentation in *P. mephistocephalus*, *P. grangeri*, *Tianzhenosaurus*, *Saichania*, *Tarchia*, *Minotaurasaurus*, *Nodocephalosaurus*, and *Euoplocephalus*.

124. Cranial ornamentation, form of scale impressions on nasal region of skull roof: absent (0); flat (1); rounded (2); peaked (3) (new character).

This character scores nasal scale impressions, which are rounded in *P. mephistocephalus* and distinctly peaked in *Tianzhenosaurus*, *P. grangeri*, *Saichania*, *Tarchia*, *Minotaurasaurus* and *Nodocephalosaurus*.

125. Cranial ornamentation, nasal region, raised ring of scales surrounding the dorsal and caudal rim of the external naris: absent (0); present (1) (new character).

Kirkland (1998:30) noted that the narial openings of ankylosaurids were often ringed by small scutes. Sereno (1999:92) scored accessory dermal ossifications

forming lateral margin of external nares in Ankylosauridae. This character is scored as a raised ring of scales and its present in *P. mephistocephalus*, *Tianzhenosaurus, P. grangeri*, *Saichania*, *Tarchia*, *Minotaurasaurus*, and *Nodocephalosaurus*.

126. Cranial ornamentation, nasal region, presence of a large midline ornamentation between the external nares: absent (0); multiple (more than 6) polygons between the nares (1); a large trapezoidal mid-nasal scale impression present (2); a single nasal scale covers most of the internarial region (3) (modified from Vickaryous *et al.*, 2004:9; Thompson *et al.*, 2012:81).

Coombs (1978) noted a large trapezoidal armour element between nares in nodosaurids. Kirkland (1998:26) also uses this as a late diverging nodosaurid character. A large mid-nasal scale impression is present in *Ankylosaurus*, *Oohkotokia*, and *Euoplocephalus*. A single nasal scale covering most of the internarial region is present in *Texasetes* (=*Pawpawsaurus*), *Tatankacephalus*, *Propanoplosaurus*, and panoplosaurines.

127. Cranial ornamentation, morphology of armour between naris and orbits, presence of two thin transverse plates between naris and parietal scale when scale impressions are present in the region: >3 scales on each side of midline between naris and parietal plate (0); two thin transverse plates dominate each side between naris and parietal plate (1) (modified from Arbour and Currie 2015:25). Character reworded.

Kirkland (1998) and Carpenter *et al.* (1998:2) used the presence of two pairs of plates on the nasal region as a derived nodosaurid character. Two thin transverse plates dominate each side between narial plate and parietal plate in *Tatankacephalus*, *Niobrarasaurus*, *Propanoplosaurus*, '*Chassternbergia*', *Panoplosaurus*, *E. rugosidens*, *E. longiceps*, and *Denversaurus*.

128. Cranial ornamentation, presence of a large midline frontal scale: absent (0); present (1) (new character).

A large midline frontal scale is only present in *Propanoplosaurus*, '*Chassternbergia*', and *E. rugosidens*.

129. Cranial ornamentation, presence of a large frontal-parietal scale: consists of three or more flat scales (0); one large scale present (1) (modified from Kirkland 1998:27; Carpenter *et al.*, 1998:9; Vickaryous *et al.*, 2004:8).

Kirkland (1998:27) and Carpenter *et al*. (1998:9) identified the presence of a large parietal plate in some non-ankylosaurid taxa. It is present in *Europelta*, *S. transylvanicus*, *S. austriacus*, *Silvisaurus*, *Sauropelta*, *Texasetes* (=*Pawpawsaurus*), *Tatankacephalus*, *Animantarx*, *Propanoplosaurus*, *Chassternbergia*, *Panoplosaurus*, *E. rugosidens*, *E. longiceps*, and *Denversaurus*.

130. Cranial ornamentation, distinct pattern of rostrolaterally trending lines radiating from the midline of the caudal region of the parietal: absent (0); present (1) (new character). Character states reworded to avoid redundancy.

This is present in *Gargoyleosaurus*, *Mymoorapelta*, *Dracopelta*, *Gastonia*, *Shamosaurus*, and *Zhongyuansaurus.*

131. Cranial ornamentation, shape of polygons covering prefrontal: flat (0); pointed and pyramidal (1) (modified from Vickaryous *et al*., 2001:5; Thompson *et al*., 2012:30; Arbour and Currie, 2015:36)

The shape of polygons differs within ankylosaurs.

132. Cranial ornamentation, presence of a distinct circumorbital ring scale complex: absent (0); distinct ring of scales around orbit (1) (new character).

A distinct scale complex that forms a raised circumorbital ring is variably present in later-diverging ankylosaurs.

133. Cranial ornamentation, small scale impressions between squamosal horn and quadratojugal horn: absent (0); present (1) (modified from Arbour and Currie, 2013:171).

This is the caputegulae of Arbour and Currie (2013:171). Present in *Minotaurasaurus*, *Anodontosaurus*, and *Oohkotokia*.

134. Cranial ornamentation, presence of a depressed sulcus or furrow between the postorbital and squamosal horns: absent (0); present (1) (new character).

Present in *Minotaurasaurus*, *Zarapelta*, and *Tarchia*.

135. Cranial ornamentation, extra horn in the depression between the postorbital and squamosal horns: absent (0); present (1) (new character). Character reworded to avoid redundancy.

Present in *Minotaurasaurus* and *Tarchia*.

136. Cranial ornamentation, nuchal sculpturing: absent (0); present as a rounded thickening at the parietosupraoccipital suture (1); present as a horizontal shelf overhanging the supraoccipital (2) (modified from

Vickaryous *et al.*, 2004:11; Thompson *et al.*, 2012:88). Character states reworded.

Kirkland (1998:28) noted a narrow plate was present along the back of skull in most ankylosaurs. Nuchal sculpturing is absent in *Scutellosaurus* and *Emausaurus*. A rounded thickening of the parietosupraoccipital suture is present in all stegosaurs and ankylosaurs, except in ankylosaurids, in which it forms a distinct shelf.

137. Cranial ornamentation, number of discrete nuchal caputegulae: none (0); two (1); more than two (2) (modified from Vickaryous *et al.*, 2001:5; Thompson *et al.*, 2012:30; Arbour and Currie, 2015:53).

This character assesses the presence and number of nuchal caputegulae on animals with a horizontal shelf overhanging the supraoccipital.

138. Cranial ornamentation, rim or shelf of armour from quadratojugal to squamosal to parietals forming an inverted "U"-shaped overhanging posterior cranial hood: absent (0); present (1).

139. Mandibular ornamentation, ornamentation on lateral surface of mandible: absent (0); present (1) (modified from Sereno, 1986, 1999:65; Vickaryous *et al.*, 2004:45; Thompson *et al.*, 2012:91).

Maryańska (1971) and Coombs (1978) first noted this defining character of Ankylosauria. It is present on all ankylosaurs including *Scelidosaurus*.

140. Mandibular ornamentation, anterior extent of distinct boss on lateral surface of mandible: does not approach anterior end of dentary tooth row (0); approaches anterior end of tooth row (1) (Carpenter *et al.*, 1999; Parish, 2005:83; Thompson *et al.*, 2012:60).

The mandibular ornamentation approaches the anterior end of the tooth row in *Minotaurasaurus*, *Ankylosaurus*, *Anodontosaurus*, and *Euoplocephalus*.

141. Mandibular ornamentation, ventral extent of distinct boss on lateral surface of mandible: does not extend below the ventral edge of the angular and dentary (0); extends well below the ventral edge of the angular and dentary (1) (new character).

Shamosaurus, *Gargoyleosaurus*, *Europelta*, *Hungarosaurus*, and ankylosaurids have ornamentation extending well below the ventral edge of the angular and dentary.

Atlas and Axis

142. Atlas, fusion to axis: separate (0); fused (1) (Vickaryous *et al.*, 2004:46); (Thompson *et al.*, 2012:94)

Coombs (1978) noted that fusion of atlas and axis was variable throughout Ankylosauria.

143. Atlantal neural arch, fusion to atlas: unfused, open (0); fused in adults (modified from Sereno, 1999:19; Parish, 2005:84; Thompson *et al.*, 2012:92).

Sereno (1986, 1999:19) identifies this character as derived in Eurypoda.

144. Atlantal neural arches, medial contact between both sides: no medial contact (0); two sides fused together medially into complete arch (1) (Sereno, 1986, 1999:68; Parish, 2005:85; Thompson *et al.*, 2012:93).

Fused in all ankylosaurs, except *Scelidosaurus*, *Polacanthus*, and *Europelta*.

Post-atlantal-axial Cervical Vertebrae

145. Cervical vertebrae, anteroposterior length of the centrum compared to dorsoventral centrum height: long, length greater than 110% centrum height (0); short, length less than height (1) (modified from Carpenter *et al.*, 1999; Parish, 2005:87; Thompson *et al.*, 2012:95).

Present in all ankylosaurs, except *Scelidosaurus* and *Stegopelta*.

146. Cervical vertebrae, mediolateral width compared to anteroposterior centrum length: longer than wide (0); wider than long (1) (modified from Kirkland *et al.*, 1998; Parish, 2005:87; Thompson *et al.*, 2012:95).

Present in all ankylosaurs, except *Scelidosaurus* and *Stegopelta*.

147. Cervical vertebrae, alignment of vertebral centrum faces of anterior cervical vertebrae: anterior and posterior faces are parallel and aligned (0); anterior face elevated dorsally compared to the posterior face (1); posterior face elevated dorsally compared to the anterior face (2) (Vickaryous *et al.*, 2004:47; modified from Thompson *et al.*, 2012:97).

Variable across Ankylosauria.

148. Cervical vertebrae, sagittal keel on ventral surface: absent (0); present (1) (new character)

Variable throughout Ankylosauria, but completely absent in struthiosaurids and panoplosaurids.

149. Cervical vertebrae, fossa on ventral surface: absent (0); present (1) (new character).

Present in *Scolosaurus*, *Europelta*, *Silvisaurus*, *Stegopelta*, *Sauropelta*, *Texasetes*, and *Animantarx*.

150. Cervical vertebrae, fossa on ventral surface, presence of the keel: absent (0); present (1) (new character).

Present in *Scolosaurus*, *Europelta*, and *Animantarx*.

Free dorsal vertebrae and ribs

151. Dorsal vertebrae, ratio of anteroposterior centrum length to posterior centrum height: long, length more than 110% centrum height (0); short, subequal to or shorter than tall (1) (Parish, 2005:89; Thompson *et al.*, 2012:98)

Variable in Eurypoda. In Ankylosauria, earlier diverging forms have long dorsal vertebrae, as well as *Jinyunpelta*, the Jurapeltans *Dracopelta* and *Mymoorapelta*, and the ankylosaurids *Akainacephalus*, *Shanxia*, and *Tianzhenosaurus*. All other ankylosaurs have short dorsal vertebrae.,

152. Dorsal vertebrae, longitudinal keel on ventral surface of centra: absent (0); present (1) (modified from Parish, 2005:90; Thompson *et al.*, 2012:99).

Variable across Eurypoda. In Ankylosauria, it is absent in all polacanthids and earlier diverging forms. Variable in all other ankylosaurs.

153. Posterior free dorsal vertebrae, cross-sectional shape of neural canal: circular (0); elliptical, with dorsoventral long axis (1) (Carpenter, 1990; Parish, 2005:91; Thompson *et al.*, 2012:100).

All ankylosaurs have a circular neural canal in cross section, except *Zhongyuansaurus*, *Shanxia*, *Akainacephalus*, *S. languedocensis*, *S. austriacus*, and *Peloroplites*.

154. Posterior free dorsal vertebrae, presence of ossified tendons along neural spine: absent (0); present (1) (Maidment *et al.*, 2010).

Absent in all ankylosaurs, except *Kunbarrasaurus*, *Minmi*, *Dracopelta*, *Mymoorapelta*, and *Hungarosaurus*.

155. Dorsal ribs, fusion with centra: absent (0); present (1) (Vickaryous *et al.*, 2004:48; Thompson *et al.*, 2012:102).

Coombs (1978) reported that dorsal ribs in all Ankylosauria commonly fuse to dorsal vertebrae. However, this does not occur along the whole dorsal series (e.g., in *Dracopelta*, dorsal ribs coossify with the centra from d9 on).

156. Dorsal ribs, cross-sectional shape of proximal end: triangular (0); L-shaped or T-shaped (1) (Parish, 2005:92; Thompson *et al.*, 2012:101).

Coombs (1978) reported that ankylosaur ribs are T-shaped in cross section.

Synsacrum

157. Sacrum, presence of a synsacrum of co-ossified dorsal, sacral, and caudal vertebrae: absent (0); present (1) (Vickaryous *et al.*, 2004:61; Parish, 2005:94; Thompson *et al.*, 2012:103).

Coombs (1978) reported that all ankylosaurs have co-ossified dorsal, sacral, and caudal vertebrae. Here all eurypodans are scored as having a synsacrum, except for *Liaoningosaurus*.

158. Sacrum, number of fused sacrodorsals in the presacral rod: three or less (0); four (1); five or more (2) (new character). Character states reworded.

Sereno (1986, 1999: 69) noted that all Ankylosauria have at least three sacrodorsals. *Mymoorapelta* is unique in only having one (Kirkland *et al.*, 1998).

159. Sacrum, number of true sacral vertebrae: five or more (0); four (1); three (2) (modified from Sereno, 1999:69; Parish, 2005:96; Thompson *et al.*, 2011:106). Character states reworded.

Variable throughout Ankylosauria.

160. Sacrum, number of fused vertebrae fused in the sacrum: three or less (0); four or more (1) (new character). Character states reworded.

Almost all ankylosaurs have four or more fused vertebrae in the sacrum, with the exceptions of *Scelidosaurus*, *Tianchisaurus*, *Liaoningosaurus*, *Mymoorapelta*, *Polacanthus*, *Zhejiangosaurus*, and *Saichania*.

161. Sacrum, forms a ventrally concave arch in lateral view: absent (0); present, slight arch (1); present, strong arch (2) (new character).

Most ankylosaurs do not have a ventrally arched sacrum. *Sauropelta*, *Silvisaurus*, and *Peloroplites* have a slightly arched sacrum. In ankylosaurids only *Akainacephalus* has a slightly arched sacrum. Struthiosaurids score either (1) or (2), although a strongly ventrally concave arch is observed only in *Europelta* and *Anoplosaurus*.

162. Sacrum, longitudinal groove in ventral surface of the sacrum: absent (0); present (1) (Parish, 2005:95; Thompson *et al.*, 2012:105).

Earlier diverging ankylosaurs score (0) on this character, as well as the Jurapeltans *Gargoyleosaurus* and *Dracopelta*. In Ankylosauridae, only *Zuul* and *S. thronus* have this groove.

Caudal Vertebrae and Chevrons

163. Proximal caudal (caudal 1) vertebrae, length: long, length more than 110% centrum height (0); short, length from 95% to 60% centrum height (1); very short, length less than 50% centrum height (2) (new character).

Most ankylosaurs score (1). *Scelidosaurus*, *Tianchisaurus*, *Liaoningosaurus*, ZLJ0143-145, BEXHM 2002 score (0). *Dyoplosaurus*, *Euoplocephalus*, *S. thronus*, *Oohkotokia*, *Anodontosaurus*, and *Ankylosaurus* score (2).

164. Proximal caudal (caudal 1) vertebrae, centra face with medial bump (notochordal projection): absent (0); present (1) (new character).

Coombs (1978) noted posterior dorsal vertebral central faces have medial bump (the notochordal projection of Gilmore, 1930) in both ankylosaurids and nodosaurids, albeit nodosaurids who have it usually only have this feature on proximal caudal centra.

165. Proximal caudal (caudal 1) vertebrae, alignment of vertebral centrum faces of vertebrae: anterior and posterior faces are aligned (0); anterior face elevated dorsally compared to the posterior face (1) (new character). Character state (0) reworded to avoid redundancy.

Peloroplites, *Niobrarasaurus*, *Sauropelta*, *Texasetes*, struthiosaurids, and panoplosaurids score (1), all other ankylosaurs score (0).

166. Anterior caudal vertebrae, neural spine distal mediolateral expansion of the dorsal end: not expanded (0); expanded so that the distal mediolateral width is more than 20% dorsoventral height of spine (1) (modified from Carpenter, 2001; Parish, 2005:97; Thompson *et al.*, 2011:107).

Variable throughout Ankylosauria. Present in all polacanthids.

167. Anterior caudal vertebrae, neural spine height: very short, length less than 50% centrum height (0); short, more than 90% but less than 200% centrum height (1); tall, more than 220% centrum height (2) (new character).

Most ankylosaurs have short neural spines. *Cedarpelta*, *Peloroplites*, *Niobrarasaurus*, *Sauropelta*, and *Texasetes*, and struthiosaurids are the only ankylosaurs scoring (2).

168. Proximal caudals, lateral length of transverse process compared to vertical neural spine height: < 80% neural spine length (0); sub-equal (1); approximately twice the length (2) (Sereno, 1999:70; Parish, 2005:99; Thompson *et al.*, 2012:109).

Sereno (1999:70) identified character states 1 and 2 for Ankylosauria.

169. Caudal vertebrae, transverse process, orientation in dorsal view: anteriorly projecting (0); caudally projecting (1); laterally projecting (2) (Carpenter, 2001; Parish, 2005:98; Thompson *et al.*, 2012:108).

Variable throughout Ankylosauria. Ankylosaurids score (0), except *Nodocephalosaurus* which scores (1).

170. Caudal vertebrae, transverse process, orientation in anterior view: laterally projecting (0); ventrally projecting (1); dorsally projecting (2) (modified after Maidment *et al.*, 2008:30).

Character states (0) and (1) are variable across Eurypoda. *Peloroplites* is the only that scores (2).

171. Caudal vertebrae, transverse process, curvature in anterior view: straight (0); dorsally concave (1); ventrally concave (2) (new character).

Variable throughout Ankylosauria.

172. Caudal series, persistence of transverse processes down the length of the caudal series: absent beyond the mid-length of the series (0); present beyond the mid-length of the series (1) (Parish, 2005:100; Thompson *et al.*, 2012:110).

Earlier diverging ankylosaurs and all polacanthids (except for *Zhejiangosaurus*) have transverse processes beyond the anterior half of the caudal series. All other ankylosaurs, except *Crichtonpelta*, *Cedarpelta*, *Europelta*, *Anoplosaurus*, and *Hungarosaurus* have the transverse processes restricted to the anterior half of the caudal series.

173. Distal caudal postzygapophysis shape: short with a sub-triangular end, wedge-shaped (0); long with a rounded end, tongue-shaped (1) (Sereno, 1999:110; Parish, 2005:102; Thompson *et al.*, 2012:112).

Ankylosaurids have long postzygapophyses with a rounded end.

174. Distal caudals, extent of pre- and postzygapophyses over their adjacent centra to form a "handle": extend over less than 45% the length of the adjacent centrum (0); extend over more than 45% the length of the adjacent centrum (1) (modified from Sereno, 1999:109; Parish, 2005:103; Thompson *et al.*, 2012:113).

Coombs (1978) argues that the extension of transverse processes helps stiffen the distal tail in ankylosaurids to support the club.

175. Distal caudals, shape of interlocking neural arches in dorsal view: little overlap and not interlocking (0); "V" shaped with an angle of divergence of more than 22° (1) (modified from Arbour and Currie, 2015:110).

V-shaped interlocking neural arches are present in all ankylosaurids.

176. Distal caudals, fusion of distal caudals: absent (0); present, between individual caudals (1); present, more than five distal caudals fused (2) (new character).

Liaoningosaurus, polacanthids, and *Europelta* fuse individual caudal vertebrae. All ankylosaurids, as well as *Jinyunpelta*, have more than five distal caudals fused. Other ankylosaurs do not fuse any caudals

177. Proximal caudal chevrons, fusion to caudal centra: absent, articulated (0); fused (1) (modified from Parish, 2005:101; Thompson *et al.*, 2012:111)

All ankylosaurids show fusion of proximal chevrons to the caudal centra.

178. Proximal caudal chevrons, expanded at distal tips: absent (0); present (1) (new character).

All ankylosaurids, *Liaoningosaurus*, and *Europelta* have distal expansion of the chevrons.

179. Distal caudal chevrons, shape: rod shaped (0); inverted T-shaped (1) (Sereno, 1986, 1999:71; Parish, 2005:104; Thompson *et al.*, 2012:114).

Sereno (1986, 1999) reported that the Ankylosauria had distal chevrons that were inverted T-shaped with the anterior and posterior ends in contact. *Scelidosaurus* and *S. languedocensis* have rod-shaped distal chevrons.

180. Distal caudal chevrons, fusion: absent (0); present (1) (new character).

Coombs (1978) recognizes the interlocking contact and fusion of distal chevrons to stiffen the tail in ankylosaurids.

181. Distal tail, presence of ossified tendons in distal region of tail: absent (0); present (1) (Sereno, 1999:97; Parish, 2005:105; Thompson *et al.*, 2012:115).

Sereno (1999:97) uses the presence of hypaxial ossified tendons as a shared character for '*Minmi*' (*Kunbarrasaurus*), *Shamosaurus* and Ankylosaurinae. It is present in all ankylosaurs, except in *Liaoningosaurus*, Sauropelta, Nodosaurus, struthiosaurids, Panoplosaurus, and *Akainacephalus*.

Shoulder Girdle

182. Scapula, acromion process, development of raised bone perpendicular to the blade of scapula to form tab: low ridge (0); "swollen" process (1); distinct raised flange (2) (modified from Vickaryous *et al.*, 2004:52; Thompson *et al.*, 2012:123).

Sereno (1999:73) noted that an everted acromion was observed across Ankylosauria. *Jinyunpelta* is the only ankylosaur scoring (0).

183. Scapula, acromion process, form of distinct raised flange: knob-like rounded flange (0); blade-like tab or flange (1) (new character).

Coombs (1978) identifies a knob-like acromion in all nodosaurids. *Chuanqilong*, polacanthids and ankylosaurids (except *S. thronus*) have a blade-like tab or flange. All other ankylosaurs have a knob-like rounded flange in the acromion process.

184. Scapula, acromion orientation in cross-sectional view of scapular shaft: perpendicular to lateral surface of the scapula (0); refolded laterally to almost parallel to the scapular surface (1) (new character).

Kirkland (1998:33) notes that a tall acromion bent toward the glenoid is a derived polacanthid character. All polacanthids (except *Mymoorapelta*) are scored as (1). All other ankylosaurs are scored (0).

185. Scapula, position of the base of the acromion process of scapula: positioned on the dorsal margin of the scapula (0); distinct space between the dorsal margin of the scapula and the acromion base (1); wide space present between the dorsal margin of the scapula and the acromion base, with acromion clearly directed towards the glenoid (2) (modified from Kirkland, 1998:32; Parish, 2005:115; Thompson *et al.*, 2012:124).

Coombs (1998) reports the acromion spine as a ridge along the extreme anterior edge of scapula, and that in nodosaurids, it is knob-like and extends over the coracoid either in the middle of the scapula or posteriorly near the glenoid. The

same author notes the differences in *Hylaeosaurus*, being positioned posteriorly and that it lacked a knob. All ankylosaurids score (0), as well as *Mymoorapelta*. Variable in other ankylosaurs.

186. Scapula, dorsal process of scapula distinct from scapular blade near suture with coracoid: dorsal expansion from dorsal edge of scapular blade ≤ 75% of the minimum dorsoventral dimension of the scapular blade (0); dorsal expansion from dorsal edge of scapular blade > 80% of the minimum dorsoventral dimension of the scapular blade but < 125% (1); dorsal expansion from dorsal edge of scapular blade > 150% of the minimum dorsoventral dimension of the scapular blade (2) (new character).

Scelidosaurus, *Kunbarrasaurus*, *Liaoningosaurus*, *Chuanqilong*, and ankylosaurids score (0). All other ankylosaur score (1).

187. Scapula, ventral process of scapula at the caudoventral margin of glenoid near suture with coracoid: absent (0); present (1) (modified from Parish, 2005:113; Thompson *et al.*, 2012:122).

Kunbarrasaurus, *Liaoningosaurus*, *Chuanqilong*, polacanthids (except *Dracopelta* and *Hylaeosaurus*, which score 1), *Panoplosaurus*, and '*Chassternbergia*' score (0). All other ankylosaurs score (1).

188. Scapula, orientation of glenoid: ventrolateral (0); ventral (1) (Sereno, 1999:87; Parish, 2005:112; Thompson *et al.*, 2012:121).

Sereno (1999) identifies this as a nodosaurid character. All polacanthids have the glenoid oriented ventrally. It is variable in other ankylosaurs.

189. Scapula, overall shape of scapular blade in lateral view: straight or concave dorsal surface (0); dorsally convex (1) (new character).

Variable across Ankylosauria. All polacanthids have a dorsally convex dorsal surface of the scapular blade.

190. Scapula, dorsoventral expansion of distal end of scapula shaft: distally expanded to >150% the minimum dorsoventral dimension of the scapular blade (0); expansion is absent or < 140% the minimum dorsoventral dimension of the scapular blade (1) (modified from Sereno, 1986, 1999:20; Parish, 2005:117: Thompson *et al.*, 2012:126).

Sereno (1986, 1999) noted that the scapula was parallel sided in Eurypoda. Most ankylosaurs score (1). *Scelidosaurus*, *Gargoyleosaurus*, *Hylaeosaurus*, *G.*

burgei, *Shamosaurus*, *P. mephistocephalus*, *Saichania*, and *Akainacephalus* score (0).

191. Scapula, extent of dorsoventral expansion (in expanded scapulae) of distal end of scapula along the long axis of the shaft: whole scapula is expanded to form paddle shape (0); expanded only along the distal 33% of shaft (1) (new character).

Only *Scelidosaurus* and *P. mephistocephalus* score (0).

192. Scapula and coracoid, fusion: articulated (0); fused (1) (Parish, 2005:110; Thompson *et al.*, 2012:120).

Coombs (1978) registered the fusion of the scapula and coracoid in all ankylosaurs, except *Struthiosaurus* and *Hylaeosaurus*. Sereno (1986) identified fusion as an ankylosaurian character, but not in 1999. According to Parish (2005:110), the scapula and coracoid are unfused in adult specimens of *Edmontonia*, *Hylaeosaurus*, *Kunbarrasaurus*, and *Scelidosaurus*. Scelidosaurus, *Kunbarrasaurus*, *Liaoningosaurus*, *Chuanqilong*, *Jinyunpelta*, and *Oohkotokia* score (0), all other ankylosaurs score (1).

193. Scapula, presence of scapulocoracoid buttress: absent (0); present (1) (Parish, 2005:116; Thompson *et al.*, 2012:125).

Reflected by the supraspinous fossa of Coombs (1978), present anteriorly to the acromion in all nodosaurids. Sereno (1999:86) notes the width of the scapula at the end of the scapular blade is at least 25% less than at the glenoid.

194. Coracoid, length: axis perpendicular to scapular suture is shorter than axis parallel to scapular suture (0); subequal to axis perpendicular to scapular suture is 105% to 110% longer than axis parallel to scapular suture (1); axis perpendicular to scapular suture is 120% of axis parallel to scapular suture but is < 70% scapula length (2); axis perpendicular to scapular suture is more than 120% of axis parallel to scapular suture and about 80% scapula length (3); axis perpendicular to scapular suture is more than 120% of axis parallel to scapular suture and almost as long as the scapula itself within 90% scapula length (4) (modified from Parish, 2005:106; Thompson *et al.*, 2012:116).

Coombs (1978) noted the coracoid was relatively small in ankylosaurids as compared to nodosaurids. Sereno (1986, 1999:88) and Kirkland (1998:34) noted

that an elongate coracoid was characteristic of nodosaurids. All polacanthids score (1).

195. Coracoid, shape of dorsal border of coracoid in profile: rounded, convex (0); pointed (1); straight (2) (new character).

The dorsal border of the coracoid in profile is convex in all polacanthids, variable across other ankylosaurs.

196. Coracoid, shape of ventral border of coracoid in lateral view: rounded, convex (0); rounded, concave (1); straight (2) (modified from Vickaryous *et al.*, 2004:53; Thompson *et al.*, 2012:117).

Only *Europelta*, *Anoplosaurus*, *Peloroplites*, and '*Chassternbergia*' have a convex ventral border of the coracoid in ventral view. All polacanthids score (1), except for *Dracopelta*, which scores (2). Variable in other ankylosaurs.

197. Coracoid, presence of anteroventral process: absent (0); present, short process with distinct notch between glenoid and process (1); present, long process with distinct notch between glenoid and process (2) (Parish, 2005:108; Thompson *et al.*, 2012:118)

All polacanthids have a short process, except for *Dracopelta* which scores (0). In struthiosaurids, only *Anoplosaurus* scores (1). Character state 2 is only present in some Asian ankylosaurs.

198. Coracoid, contribution to glenoid: contributes to less than half of the glenoid (0); contributes an equal share as the scapula to the glenoid (1) (new character).

All ankylosaurids (except *Ankylosaurus*), as well as *Shamosaurus*, *Crichtonpelta*, and *Jinyunpelta* have a glenoid with equal contributions of the scapula and coracoid. All other ankylosaurs, including *Ankylosaurus*, have a larger contribution of the scapula to the glenoid than the coracoid.

199. Sternum, fusion of bilateral sternal elements: not fused (0); fused (1) (Sereno 1986, 1999:112; Vickaryous *et al.*, 2004:60; Thompson *et al.*, 2012:127).

Coombs (1978) reports that ankylosaurid sternal plates are fused.

Forelimb

200. Forelimb, robustness: slender (0); robust (1) (new character). Character reworded for accuracy.

Coombs (1978) noted massive forelimbs that are 66% to 75% of the length of the hindlimbs in all ankylosaurs.

201. Forelimb, length of distal limb elements relative to the humerus: long lower limb, radius or ulna > 70% length of humerus (0); shortened lower limbs (1) (new character).

Cedarpelta, polacanthids, and ankylosaurids have shortened anterior lower limbs. All other ankylosaurs have long anterior lower limbs.

202. Humerus, separation of humeral head and deltopectoral crest in anterior view: continuous (0); separated by a distinct notch or peak (1) (Parish, 2005:119; Thompson *et al.*, 2012:128).

This character is variable across Ankylosauria. All polacanthids (except *G. lorriemchinneyi*) score (1), whereas all ankylosaurids, except *Akainacephalus* and *Ankylosaurus*, score (0).

203. Humerus, separation of humeral head and medial tubercle in anterior view: continuous (0); separated by a distinct notch or peak (1) (Parish, 2005:119; Thompson *et al.*, 2012:129).

This character is scored as (0) in *Kunbarrasaurus*, *Liaoningosaurus*, *Chuanqilong*, *Dracopelta*, *G. lorriemchinneyi*, all ankylosaurids (except *Crichtonpelta*), and *Niobrarasaurus*.

204. Humerus, position of proximal end of deltopectoral crest: proximal end of deltopectoral crest close to position of humeral head equal to or distal to medial tubercle (0); positioned distal to humeral head, equal to or distal to medial tubercle (1) (new character).

Variable throughout Ankylosauria, but all ankylosaurids score (0) and all polacanthids score (1).

205. Humerus, position of distal margin of deltopectoral crest relative to overall length of the humerus: short, < 50% (0); long, approximately ≥ 50% (1) (Kirkland, 1998:35; Vickaryous *et al.*, 2004:54; Thompson *et al.*, 2012:130).

Coombs (1978) notes a long deltopectoral crest in Ankylosauria, but it is variable throughout ankylosaurs. Except for *Hylaeosaurus*, all polacanthids have long deltopectoral crests.

206. Humerus, orientation of deltopectoral crest projection: lateral (0); anterolateral (1) (Sereno, 1999:113; Parish, 2005:121; Thompson *et al.*, 2012:131).

All polacanthids have an anterolaterally projected deltopectoral crest, as well as in *Chuanqilong*. It varies in non-polacanthid ankylosaurs.

207. Humerus, shape of the radial (medial) condyle of distal humerus in distal view (or the proximal end of radius): non-circular (0); circular (1) (Coombs, 1978; Parish, 2005:122; Thompson *et al.*, 2012:132).

Coombs (1978) identifies a rather flat radial capitulum with oval outline in ankylosaurids and subspherical knob raised well above humeral shaft that is almost circular in cross-section in nodosaurids. *Scelidosaurus*, *Kunbarrasaurus*, *Liaoningosaurus*, *Chuanqilong*, *Cedarpelta*, polacanthids, struthiosaurids, and ankylosaurids score (0).

208. Ulna, length of olecranon process (along the articular surface) to total ulnar length: short (0); long (1) (new character). Character states reworded.

Coombs (1971) suggested that the olecranon accounts for 25% to 33% of total ulna length in all ankylosaurs.

209. Metacarpals, ratio of the length of metacarpal (mc) V to metacarpal III: middle of manus long, mc V < 50% of mc III (0); middle of manus short, mc V > 55% of mc III (Sereno, 1999:6; Parish, 2005:123; Thompson *et al.*, 2012:133).

All eurypodans (except *Gigantspinosaurus*) score (1) for this character.

210. Manus, shape of manual unguals: claw shaped (0); hoof shaped (1) (Sereno, 1999:7; Parish, 2005:125; Thompson *et al.*, 2012:135)

All neoankylosaurs, excluding *Dyoplosaurus* and *Anodontosaurus*, have hoof shaped manual unguals. All early diverging ankylosaurs and polacanthids (except BEHXM 2002) have claw-shaped manual unguals.

Ilium

211. Ilium, length of the preacetabular process of ilium compared to the postacetabular process (measured from the pubic peduncle at the rostral end of the acetabulum): short, preacetabular process ≤ 50% ilium length (0); long, preacetabular process > 50 % ilium length (1) (modified from Sereno, 1999:21; Parish, 2005:126; Thompson *et al.*, 2012:136). Character states reworded for clarity.

Coombs (1978) noted the long preacetabular process in ankylosaurs, longer in the Ankylosauridae. Sereno identifies the same, but for all Eurypoda (1985, 1999). *Scelidosaurus*, *Kunbarrasaurus*, and *Polacanthus* are the only ankylosaurs with a short preacetabular process.

212. Ilium, lateral expansion: absent (0); present (1) (modified from Maidment *et al.*, 2018:52, 53)

Coombs (1978) considered that this character in ankylosaurs was developed by twisting the dorsal side of the ilium above the acetabulum laterally. All eurypodans score (1), excluding Jurapeltans, *Tianzhenosaurus*, and *Platypelta*,.

213. Ilium, angle of lateral deflection of the preacetabular process of the ilium in dorsal view: 0° to 20° (0); more than 30° (1) (Sereno, 1986, 1999:21; Parish, 2005:127; Thompson *et al.*, 2012:137).

Sereno (1986) defines 40 degrees and 45 degrees (Sereno, 1999) as approximate deflection for Eurypoda. However, this value is variable within Eurypoda. In Ankylosauria, *Kunbarrasaurus*, *Liaoningosaurus*, *Chuanqilong*, polacanthids (except Jurapeltans and *Polacanthus*), and ankylosaurids (except *Scolosaurus*) score (1). Almost all stegosaurs score (1), except for *Chungkingosaurus*, *Huayangosaurus*, and *S. stenops*.

214. Ilium, orientation of the preacetabular process: near vertical (0); lateral (1) (Kirkland, 1998:45; Thompson *et al.*, 2012:138). Character reworded for clarity.

A laterally oriented preacetabular process is synapomorphic for Ankylosauria.

215. Ilium, form of the preacetabular process: straight process (0); pronounced ventral curvature (1) (Parish, 2005:129; Thompson *et al.*, 2012:139). Character reworded for clarity.

All ankylosaurs, except for Jurapeltans, *Hylaeosaurus*, and *Zuul*, have a straight preacetabular process.

216. Ilium, form of supracetabular shelf: absent, or oriented vertically (0); forms a horizontal shelf dorsal to the acetabulum (1); partially encircles the acetabulum, obscuring it laterally (supracetabular flange) (2) (modified from Kirkland, 1998:45; Vickaryous *et al.*, 2004:55; Thompson *et al.*, 2012:138, 140).

Only in *Crichtonpelta* and some ankylosaurids (*Pinacosaurus*, *Talarurus*, *Saichania*, *Akainacephalus*, *Dyoplosaurus*, *Platypelta*, and *Euoplocephalus*) is the acetabulum laterally obscured (character state 2). All other eurypodans score (1).

217. Ilium, closure of acetabulum: open (0); closed (1) (Sereno, 1986; 1999:74; Vickaryous *et al.*, 2004:56; Thompson *et al.*, 2012:141).

Sereno (1986, 1999) noted that a closed acetabulum is found across Ankylosauria. *Scelidosaurus*, *Kunbarrasaurus*, Jurapeltans (unknown in *Dracopelta*), and *Hylaeosaurus* are the only exceptions.

218. Ilium, postacetabular length, relative to diameter of acetabulum: longer than acetabulum (0); shorter than acetabulum (1) (modified from Sereno, 1999:114; Parish, 2005:132; Thompson *et al.*, 2012:142). Character reworded for clarity.

Early diverging ankylosaurs, except for *Chuanqilong*, have a long postacetabular process. Most ankylosaurs have a short or even vestigial postacetabular process. The exceptions are *Dracopelta*, *Polacanthus*, *Taohelong*, *P. grangeri*, *Akainacephalus*, *Sauropelta*, *Animantarx*, *Nodosaurus*, and *E. rugosidens*.

Pubis

219. Pubis, contribution to the acetabulum: ≥ 20% (0); virtually excluded (1) (Sereno, 1999:117; Vickaryous *et al.*, 2004:59; Thompson *et al.*, 2012:146).

Scelidosaurus, *Kunbarrasaurus*, *Liaoningosaurus*, and polacanthids score (0), all other ankylosaurs have the pubis virtually excluded from contributing to the acetabulum.

220. Pubis, overall size compared to acetabulum: large (0); reduced (1) (Kirkland, 1998:46; Parish, 2005:133; Thompson *et al.*, 2012:143)

Coombs (1978) noted that a reduced pubis was diagnostic of the Ankylosauria. *Scelidosaurus*, *Kunbarrasaurus*, *Liaoningosaurus*, and polacanthids (except for *G. lorriemcwhinneyi*) have a large pubis compared to the acetabulum. All other ankylosaur score (1).

221. Pubis, robusticity of the body of the pubis: gracile (0); massive and robust (1) (modified from Carpenter, 2001; Parish, 2005:135; Thompson *et al.*, 2012:145).

A massive and robust body of the pubis is synapomorphic for Ankylosauria.

222. Pubis, rotation of the body of the pubis: unrotated (0); dorsolaterally rotated (1) (modified from Carpenter, 2001; Parish, 2005:135; Thompson *et al.*, 2012:145).

Synapomorphic for Ankylosauria.

223. Pubis, preacetabular pubic process: 3x longer than the body of the pubis (0); 1,2x to 1,8x longer than the length of the body of the pubis (1); absent or shorter than body of pubis (not the postpubic process) (2) (new character). Character states reworded for clarity.

Most ankylosaurs score (2). *Scelidosaurus*, *Kunbarrasaurus*, *Liaoningosaurus*, and polacanthids (except *G. lorriemcwhinneyi*) score (1), a condition shared with *Lesothosaurus* and *Scutellosaurus*.

224. Pubis, preacetabular pubic process, deflection from sagittal plane: sagittaly oriented (0); lateral deflection (1) (modified from Vickaryous *et al.*, 2004:56; Parish, 2005:134; Thompson *et al.*, 2012:144).

Variable across Ankylosauria. All ankylosaurids, except *P. grangeri* and *Tianzhenosaurus*, as well as struthiosaurids score (1). All other ankylosaurs score (0).

225. Pubis, preacetabular pubic process, dorsal deflection: anteriorly oriented (0); dorsally oriented (1) (modified from Vickaryous *et al.*, 2004:56; Parish, 2005:134; Thompson *et al.*, 2012:144).

P. grangeri, *Tianzhenosaurus*, and struthiosaurines have a dorsally oriented preacetabular pubic process. All other ankylosaurs score (0).

226. Pubis, preacetabular pubic process integration into acetabulum: free (0); integrated into acetabulum (1) (modified from Vickaryous *et al.*, 2004:56; Parish, 2005:134; Thompson *et al.*, 2012:144).

Struthiosaurids, the polacanthid *G. lorriemcwhinneyi*, and most ankylosaurids (with the exceptions of *P. grangeri* and *Tianzhenosaurus*) score (0). All other ankylosaurs score (1).

227. Pubis, opisthopubic posterior process: long, bladelike (0); long, rodlike (1); short, reduced (2) (new character).

Coombs (1978) recognized that all ankylosaurs had a highly reduced postpubic process. Sereno (1986, 1999:75) considered that all ankylosaurs had a pubis with a postpubic process < 50% the length of the ischium. The same author (1999:76) proposed that it was strap-shaped in all Ankylosauria as opposed to rod-shaped.

All ankylosaurs have a short postpubic process, except for early diverging ankylosaurs (character state 0) and *Mymoorapelta* (character state 1).

228. Pubis, postpubic process distal expansion: present (0); absent (1) (new character).

All ankylosaurs score (1). Synapomorphic for Ankylosauria.

Ischium

229. Ischium, shaft of ischium: little to no flexure (0); pronounced ventral flexure (1) (Kirkland, 1998:37; Vickaryous *et al.*, 2004:57; Thompson *et al.*, 2012:147). Character states reworded for clarity.

Coombs (1978) assumed that nodosaurids had a strong mid-shaft ventral flexion in the ischium that angled the distal end directly down. Sereno (1986, 1999) does not use this character. However, Sereno (1999:116) scores ischial shaft orientation: posteroventral (0); subvertical (1). Early diverging ankylosaurs, ankylosaurids, *Cedarpelta*, and struthiosaurines have a posteroventrally projected, straight ischial shaft. In polacanthids, *Sauropelta*, *Animantarx*, and *E. longiceps* the shaft is ventrally flexed.

230. Ischium, shape of the dorsal margin of ischium: straight (0); concave (1); convex (2) (modified from Sereno, 1999:115; Parish, 2005:137; Thompson *et al.*, 2012:148).

Sereno (1999) refers to the acetabular margin not the dorsal margin. Polacanthids, *Anodontosaurus*, *Sauropelta*, *Animantarx*, and *E. longiceps* score (2). All other ankylosaurs score (0). Character state (1) is observed only in *Lesothosaurus*.

231. Ischium, dorsal surface presence of distinct triangular process: absent (0); present as an incipient triangular process (1); present as a distinct triangular process (new character).

Early diverging ankylosaurs (except *Kunbarrasaurus*), ankylosaurids, *Jinyunpelta*, *Cedarpelta*, and struthiosaurids (except *Europelta*) score (0). *Kunbarrasaurus*, *G. lorriemcwhinneyi*, and *Europelta* score (1). Polacanthids (except *G. lorriemcwhinneyi*) score (2).

232. Ischium, distal expansion: distal end is distally expanded or blunt (0); absent, distal end is tapered (1) (new character).

Sereno (1999:23) identifies the ischial blade tapering distally as an Eurypoda character. All ankylosaurids (except *Ankylosaurus*), *Liaoningosaurus*, *Chuanqilong*,

and *Cedarpelta* have a distally expanded or blunt distal end of the ischium. In all other ankylosaurs the distal end tapers.

Femur

233. Femur, separation of the femoral head from greater trochanter: continuous (0); separated by a distinct notch or change in slope (1) (Parish, 2005:139; Thompson *et al.*, 2012:150).

Almost all ankylosaurids (*Dyoplosaurus* and *Ankylosaurus* are the exceptions) and early diverging ankylosaurs (except *Chuanqilong*) score (0). Polacanthids (except for *G. lorriemcwhinneyi*) have a separation of the femoral head from the greater trochanter. All other ankylosaurs, except for *Cedarpelta*, *Peloroplites*, *Niobrarasaurus*, and *Nodosaurus*, score (1).

234. Femur, angle between long axis of femoral head and long axis of shaft: < 100° (0); 100° to 120° (1); > 120° (2) (modified from Parish, 2005:138; Thompson *et al.*, 2012:149). Character states reworded.

Coombs (1978) reported that the femoral head was nearly terminal in the Ankylosauridae as opposed to its medial position in the Nodosauridae. Early diverging ankylosaurs and *Dracopelta* score (0). In polacanthids (except *Dracopelta*) and ankylosaurids, the condition is variable between character state (1) and (2). All other ankylosaurs score (1).

235. Femur, differentiation of the anterior trochanter of the femur: separated from femoral shaft by a deep groove laterally and dorsally (0); fused to femoral shaft (1) (Kirkland, 1998:36; Parish, 2005:140; Thompson *et al.*, 2012:151).

Sereno (1999) considered it fused in both stegosaurs and ankylosaurs. Early diverging ankylosaurs (except *Chuanqilong*), polacanthids (except for *Dongyangopelta* and *Zhejiangosaurus*), and *Texasetes* have the anterior trochanter separated from the femoral shaft. All other ankylosaurs have the anterior trocanther fused to the femoral shaft.

236. Femur, oblique ridge on lateral femoral shaft, distal to anterior trochanter: absent (0); present (1) (Parish, 2005:141; Thompson *et al.*, 2012:152)

Present in *Dongyangopelta*, *Zhejiangosaurus*, *Texasetes*, *Animantarx*, and *Nodosaurus*.

237. Femur, form of the fourth trochanter: pendant (0); ridge-like (1) (Sereno, 1999:24; Parish, 2005:142; Thompson *et al.*, 2012:153).

Sereno (1999:24) identifies this as an Eurypoda character. All ankylosaurs, excluding *Scelidosaurus*, *Tianchisaurus*, and *Liaoninogsaurus*, have a ridge-like fourth trochanter.

238. Femur, location of the fourth trochanter on the femoral shaft: proximal half of the femoral shaft (0); distal half of the femoral shaft (1) (Parish, 2005:143; Thompson *et al.*, 2011:154).

Coombs (1978) noted that the fourth trochanter was always on the proximal half of the femur in nodosaurids. Ankylosaurids score (1), while all other ankylosaurs score (0).

239. Femur, relation of lower limb, (tibia or fibula) to femoral length: extremely long, lower limb > 105% femoral length (0); relatively long, lower limb between 95% to 75% femoral length (1); short, lower limb < 70% femoral length (2) (new character).

Polacanthids (except for *Dracopelta*) and ankylosaurids (except for *Akainacephalus*) have a short lower limb. All other ankylosaurs score (1).

Tibia

240. Tibia, maximum distal width of the tibia, compared to the maximum proximal width: narrower or subequal (0); wider (1) (Sereno, 1999:188; Parish, 2005:144; Thompson *et al.*, 2012:155).

Variable across Ankylosauria. In early diverging ankylosaurs, only *Chuanqilong* scores (1). Both character states are evenly distributed among polacanthids. Ankylosaurids, excluding only *Akainacephalus*, score (1), as well as *Aletopelta*, *Stegopelta*, and *Niobrarasaurus*.

241. Tibia, 70° twist between distal and proximal ends: absent (0); present (1) (new character).

All ankylosaurs, except for "aletopeltines", have a rotation between the proximal and distal ends of the tibia.

242. Tibia, contact between tibia and astragalus: articulated (0); fused, with suture obliterated (1) (Parish, 2005:145; Thompson *et al.*, 2012:156).

Scelidosaurus, *Kunbarrasaurus*, *Liaoningosaurus*, and *Chuanqilong* score (0). In polacanthids, only *Mymoorapelta* and *Hylaeosaurus* have an unfused tibia-astragalus contact. All other ankylosaurs score (1).

243. Contact between fibula and calcaneum: articulated (0); fused, with suture obliterated (1) (new character).

Variable across Ankylosauria. Most ankylosaurs score (1), except for early diverging ankylosaurs, *Peloroplites*, *Niobrarasaurus*, the polacanthids *Mymoorapelta*, *Hylaeosaurus*, and BEXHM 2002, the struthiosaurids *Europelta*, and *Hungarosaurus* score (0).

244. Astragalus, contact between astragalus and calcaneum: articulated (0); fused, with suture obliterated (1) (new character).

Variable across Ankylosauria. All ankylosaurids and most non-ankylosaurid ankylosaurs score (1). Early diverging ankylosaurs, *Mymoorapelta*, *Hylaeosaurus*, *Europelta*, *Hungarosaurus*, and *Niobrarasaurus* score (0).

245. Pes, number of digits with claws: 4 (0); 3 (1) (Currie *et al.*, 2011).

Scelidosaurus, *Talarurus*, *Tianzhenosaurus*, *Europelta*, and *Sauropelta* score (0). *Liaoningosaurus*, *Chuanqilong*, *Zhejiangosaurus*, *P. grangeri*, *Saichania*, *Dyoplosaurus*, *S. cutleri*, and *Propanoplosaurus* score (1).

246. Pes, shape of pedal unguals: claw-shaped (0); hoof-shaped (1) (Sereno, 1999:7; Parish, 2005:125; Thompson *et al.*, 2012:135).

Early diverging ankylosaurs (except *Chuanqilong*), Jurapeltans, and *Dyoplosaurus* have claw-shaped pedal unguals. All other ankylosaurs have hoof-shaped unguals.

General postcranial armour

247. Armour, general distribution of osteoderms: multiple rows of osteoderms (0); two rows of osteoderms along midline (1) (modified from Sereno, 1999:7; Parish, 2005:125; Thompson *et al.*, 2012:135; Arbour and Currie, 2015:154).

Coombs (1986) recognized that a mosaic of postcranial armour arranged into transverse rows was a hallmark of the Ankylosauria. Sereno (1986, 1999:2, 3) used the presence of a parasagittal row of keeled scutes and multiple rows of low keeled scutes as two characters defining Thyreophora. Character state (1) is synapomorphic for Stegosauria.

248. Armour, dimensions of largest osteoderms: smaller than dorsal centrum (0); larger than dorsal centrum (1) (modified from Lee, 1997:125, Hill, 2005:309; Burns and Currie, 2014:68; Arbour and Currie, 2015:155).

All non-ankylosaurids (except for *Chuanqilong*) score (0). Varies within Ankylosauridae.

249. Armour, external cortical histology of skeletally mature osteoderms: lamellar bone (0); interwoven structural fiber bundles (ISFB) (1) (modified after Burns and Currie, 2014:80; Arbour and Currie, 2015:157)

All ankylosaurs (except *Scelidosaurus*) score (1).

250. Armour, haversian bone in osteoderms: absent in skeletally mature osteoderms (0); present in skeletally mature osteoderms (1) (modified after Burns and Currie, 2014:81; Arbour and Currie, 2015:158).

All ankylosaurs, excluding *Gargoyleosaurus* and *Ahshislepelta*, score (0).

251. Armour, early diverging cortex of skeletally mature osteoderms: present (0); absent or poorly developed (1) (modified after Burns and Currie, 2014:81; Arbour and Currie, 2015:159).

Only *Sauropelta* scores (1).

252. Armour, structural fiber arrangement in osteoderms: absent (0); reaches orthogonal arrangement near osteoderm surfaces (1); diffuse throughout (2); ordered sets of orthogonally arranged fibers in the superficial cortex (3) (modified after Burns and Currie, 2014:91; Arbour and Currie, 2015:160).

Scelidosaurus and *G. lorriemcwhinneyi* score (0), *Sauropelta* scores (2), and all other ankylosaurs score (1).

253. Dermal armour, presence of a solid based large armour element with a flat plate for a base and a thin spine emanating from the center (the "splate" of Blows, 1987): absent (0); present (1) (modified from Parish, 2005:158; Thompson *et al.*, 2012:169).

"Splates" are only observed in non-jurapeltine polacanthids, excluding *Hylaeosaurus*, BEXHM 2002, and *G. lorriemcwhinneyi*.

254. Dermal armour, marginal ornamentation on dorsal scutes rim or ridges around the periphery of the osteoderm: absent, or smooth (0); present, rim around plate (1) (new character).

The polacanthids *G. burgei*, *Hoplitosaurus*, *Polacanthus*, *Taohelong*, and *Dongyangopelta*, and the ankylosaurids *Zuul*, *Platypelta*, and *Scolosaurus* score (1). All other ankylosaurs score (0).

255. Dermal armour, surface texture: absent, or smooth (0); mildly to moderately rugose (1); extremely rugose (2) (Burns, 2008)

Early diverging ankylosaurs (except for *Liaoningosaurus*), polacanthids, struthiosaurids, *Borealopelta*, *Panoplosaurus*, and Chassternbergia score (1), while all other non-ankylosaurids score (0). In Ankylosauridae, Asian taxa have a mildly to moderately rugose osteoderm surface texture (character state 1), as well as *Ahshislepelta*, *Zuul*, *Euoplocephalus*, *Anodontosaurus*, and *Ankylosaurus*. All other ankylosaurids score (2).

256. Dermal armour, pitting: absent (0); present, sparse (1); present, extensive (2) (Burns, 2008)

Early diverging ankylosaurs (except for *Liaoningosaurus*), and polacanthids have sparse pitting of the dermal armour, as do most other non-ankylosaurids, with the exceptions of *Silvisaurus* (2), *Sauropelta* (0), *Panoplosaurus* (2), *Chassternbergia* (0), and *E. longiceps* (0). It is highly variable within Ankylosauridae.

Cervical Armour

257. Cervical armour, fusion of osteoderms on dorsal surface of neck region into neck bands or "rings": unfused (0); sutured together, into a quarter-ring but not into a half-ring (1); present, fused into a half-ring (2) (modified from Kirkland, 1998:38; Vickaryous *et al.*, 2004:49; Thompson *et al.*, 2012:163).

Synapomorphic for Ankylosauria. Coombs (1978) registered that the Ankylosauria had two fused cervical rings. Sereno (1986, 1999:77) further observed that all Ankylosauria had two bands of cervical armour as contiguous plates without intervening ossicles. Kirkland (1998) describes the two derived states as half rings and full rings. Sereno (1999:90) notes the presence of a pectoral collar of contiguous scutes in nodosaurids. Character state (2) is synapomorphic for Ankylosauridae.

258. Cervical armour, number of fused cervical armour bands even if one is moved back onto the shoulder: ≥ 3 (0); 2 (1) (modified from Thompson *et al.*, 2012:162).

Coombs (1978) observed that nodosaurids had three rings, with derived panoplosaurines extending the third ring up onto the back. *Scelidosaurus*, *Borealopelta*, *Silvisaurus*, *Sauropelta*, *Dracopelta*, and panoplosaurins score (0). All other ankylosaurs score (1).

259. Anteriormost cervical armour band, presence of raised perpendicular ornamentation on medial plate (shape in transverse cross-section of medial plate (plate 1)): present, large keel or spike (0); present, low keel (1); low raised bump or rounded swelling (2) (new character).

Scelidosaurus, *Pinacosaurus*, *Saichania*, *Euoplocephalus*, and *Ziapelta* score (0). Character state (2) is present only in ankylosaurids, *Dracopelta*, and *Gargoyleosaurus*. All other ankylosaurs score (1).

260. Anteriormost cervical armour band, presence of raised perpendicular ornamentation on plate lateral to the medial plate (shape in transverse cross-section of plate lateral to medial plate (plate 2)): present, large keel or spike (0); present, low keel (1); low raised bump or rounded swelling (2) (new character).

Variable throughout Ankylosauria. Character state (2) is only present in ankylosaurids.

261. Anteriormost cervical armour band, presence of raised perpendicular ornamentation on plate two positions lateral to the medial plate (shape in transverse cross-section of plate two positions away from medial plate (plate 3)): present, large keel or spine or spike (0); present, low keel or raised bump (1) (new character).

Early diverging ankylosaurs (except for *Liaoningosaurus*) and polacanthids score (0). Variable across the other ankylosaurs.

262. Anteriormost cervical armour band, presence of raised perpendicular ornamentation on plate three positions lateral to the medial plate (shape in transverse cross-section of plate two positions away from medial plate (plate 4)): plate 4 is absent (0); present, large keel or spine (1) (new character).

Character state (1) is present only in *Edmontonia* and *Chassternbergia*.

263. Cervical armour, osteoderms capping anteriormost cervical armour ring abut each other: absent (0); present (1) (modified from Arbour and Currie, 2013:172).

Arbour and Currie (2013) use this character generally. Kirkland and Loewen modified it to be specific to each cervical band of armour. Variable across Ankylosauria, although polacanthids all score (0).

264. Second cervical armour band, presence of raised perpendicular ornamentation on medial plate (shape in transverse cross-section of medial plate (plate 1)): present, large keel or spike (0); present, low keel (1); low raised bump or rounded swelling (2) (new character).

Variable across Ankylosauria. Character state (2) is present in ankylosaurids, *Liaoningosaurus*, and *Silvisaurus*. Jurapeltans score (1).

265. Second cervical armour band, presence of raised perpendicular ornamentation on plate lateral to the medial plate (shape in transverse cross-section of plate lateral to medial plate (plate 2)): present, large keel or spike (0); present, low keel (1); low raised bump or rounded swelling (2) (new character).

Variable across Ankylosauria. Character state (2) is present in ankylosaurids and *Liaoningosaurus*. *Kunbarrasaurus*, *Silvisaurus*, Jurapeltans, *S. transylvanicus*, the ankylosaurid *Platypelta*, and panoplosaurinins score (1).

266. Second cervical armour band, presence of raised perpendicular ornamentation on plate two positions lateral to the medial plate (shape in transverse cross-section of plate two positions away from medial plate (plate 3)): present, large keel or spike (0); present, low keel (1); low raised bump or rounded swelling (2) (new character).

Variable across Ankylosauria. *Liaoningosaurus*, the ankylosaurids Akainacephalus, and *Ziapelta* score (2). *Silvisaurus*, and panoplosaurinins (except *Denversaurus*), and the ankylosaurids *P. grangeri*, *Platypelta*, *Scolosaurus*, and *Oohkotokia* score (1). All other ankylosaurs score (0).

267. Second cervical armour band, presence of raised perpendicular ornamentation on plate three positions lateral to the medial plate (shape in transverse cross-section of plate two positions away from medial plate (plate 4)): plate 4 is absent (0); present, large keel or spine (1) (new character).

Only panoplosaurinins, excluding *Denversaurus*, score (1).

268. Cervical armour, osteoderms on second cervical armour ring abut each other: absent (0); present (1) (modified from Arbour and Currie, 2013:172).

Arbour and Currie (2013) use this character generally. Kirkland and Loewen modified it to be specific to each cervical band of armour. Variable across Ankylosauria. *Dracopelta* is the only polacanthid scoring (1).

269. Third cervical armour band, presence of raised perpendicular ornamentation on medial plate (shape in transverse cross-section of medial plate (plate 1)): present, large keel or spike (0); present, low keel (1) (new character).

Scelidosaurus scores (0). *Borealopelta*, *Silvisaurus*, *Sauropelta*, *Dracopelta* and panoplosaurids score (1).

270. Third cervical armour band, presence of raised perpendicular ornamentation on plate lateral to the medial plate (shape in transverse cross-section of plate lateral to medial plate (plate 2)): present, large keel or spike (0); present, low keel (1) (new character).

Scelidosaurus, *Borealopelta*, *Silvisaurus*, and *Sauropelta* score (0). *Dracopelta* and panoplosaurids score (1).

271. Third cervical armour band, presence of raised perpendicular ornamentation on plate two positions lateral to the medial plate (shape in transverse cross-section of plate two positions away from medial plate (plate 3)): present, large keel or spike (0); present, low keel (1) (new character).

All ankylosaurs which show this character score (0), except for *Silvisaurus* and *Chassternbergia*.

272. Third cervical armour band, presence of raised perpendicular ornamentation on plate three positions lateral to the medial plate (shape in transverse cross-section of plate two positions away from medial plate (plate 4)): plate 4 is absent (0); present, large keel or spine (1) (new character).

Only panoplosaurinins score (1). Synapomorphic for Panoplosaurini.

273. Cervical armour, osteoderms on third cervical armour ring abut each other: absent (0); present (1) (modified from Arbour and Currie 2013:172).

Arbour and Currie (2013) use this character generally. Kirkland and Loewen modify it to be specific to each cervical band of armour. *Borealopelta*, *Silvisaurus*, *Niobrarasaurus*, and the polacanthid *Dracopelta* score (1), all other ankylosaurs for which this character is valid score (0).

274. Third cervical armour band, moved onto shoulder: absent (0); present (1) (new character).

This character specifies the position of the bifurcated lateral spine on this band. Only panoplosaurinins score (1). Synapomorphic for Panoplosaurini.

275. Cervical armour, presence of true cervical spines on the cervical armour bands: absent (0); present (1) (new character). *Liaoningosaurus*, ankylosaurids, *Silvisaurus*, *Panoplosaurus*, and *E. longiceps* score (0).

276. Cervical armour, cervical spines, bifurcation: absent (0); present (1) (new character).

All ankylosaurs score (0), except for *Chassternbergia* and *Denversaurus*.

277. Cervical armour, orientation of lateral spines: laterally or caudolaterally (0); anterolaterally (1) (new character).

Only panoplosaurinins score (1). Synapomorphic for Panoplosaurini.

278. Cervical armour, small secondary ossicles fused to cervical armour bands between primary cervical plates 1-3: absent (0); present (1) (modified from Arbour and Currie, 2013:173)

Scelidosaurus, *Kunbarrasaurus*, *Borealopelta*, Jurapeltans, struthiosaurids *S. transylvanicus*, and *S. austriacus*, and the ankylosaurids *Saichania*, Anodontosaurus, and *Ziapelta* score (1). All other ankylosaurs score (0).

Thoracic armour

279. Thoracic armour, form of base: thin and/or hollow (0); solid or with only small excavation (1) (modified after Kirkland, 1998:41).

Coombs (1978) noted that ankylosaurids had deeply excavated oval keeled plates, whereas in nodosaurids they are flat or only slightly excavated. Early diverging ankylosaurs (except for Scelidosaurus) and polacanthids, excluding *G. lorriemcwhinneyi*, *Polacanthus*, *Dongyangopelta*, and *Zhejiangosaurus*, have a solid or slightly excavated thoracic osteoderm base. This is variable in non-ankylosaurids, whereas all ankylosaurids score (0).

280. Thoracic armour, lateral parascapular shoulder spines: absent (0); present without base (1); present with broad flattened base (2) (new character).

Kunbarrasaurus, ankylosaurids, and the panoplosaurinins *Panoplosaurus* and *E. longiceps* score (0). All other ankylosaurs score (1). Character state (2) is restricted to the stegosaurs *Huayangosaurus*, *Gigantspinosaurus*, *Loricatosaurus*, and *Kentrosaurus*.

281. Thoracic armour, presence of bifurcated lateral shoulder spines: absent (0); present (1) (Carpenter, 1990).

This character concerns the shoulder spines that form the lateralmost extent of the third cervical band, which had moved onto the shoulder (character 278). The presence of shoulder spines is synapomorphic for Panoplosaurini. *E. rugosidens* scores (0), while *Chassternbergia* and *Denversaurus* score (1).

282. Thoracic armour, lateral shoulder spines, presence of a posterior groove: absent, lateral shoulder spine conical with a sub-circular cross-section (0); present (1) (modified from Thompson *et al.*, 2012:165). Character states reworded for clarity.

Kirkland (1998:39) noted four character states for lateral shoulder spines: absent (0), present (1), present with posterior groove (2), and secondarily lost (3) as in *Panoplosaurus*. Only polacanthids (except *Hylaeosaurus*) have a posterior groove in the lateral shoulder spines.

283. Thoracic armour, vertical dorsal spines: absent (0); present (1) (Kirkland, 1998:40).

Coombs (1978) noted that, while the keels on ankylosaurids armour could be relatively tall, their height never exceeds the width of the armour element. Kirkland (1998) erected this character for large vertical spines documented in *Polacanthus* and *Gastonia*. Only the polacanthids *Gastonia*, *Hoplitosaurus*, *Polacanthus*, and *Horshamosaurus* exhibit vertical dorsal spines.

Sacral Armour

284. Sacral spikes on a base, in animals with multiple parasagittal rows of armour: absent (0); present (1) (new character).

Present only in *Europelta*, *Hungarosaurus*, and *S. transylvanicus*. Synapomorphic for Struthiosaurinae.

285. Sacral spikes on a base, in animals with multiple parasagittal rows of armour, length: short (0); longer than wide (1) (new character).

Only *Hungarosaurus* and *Struthiosaurus* score (1).

286. Sacral armour, spacing of true sacral osteoderms excluding skin impressions: adjacent (0); abutting each other with true osteoderms abutting (1) (modified from Arbour *et al.*, 2011).

Polacanthids, *Europelta*, *Hungarosaurus*, *Borealopelta*, *Aletopelta*, *Stegopelta*, *Sauropelta*, and *Nodosaurus* score (1).

287. Sacral armour, true sacral shield of osteoderm fusion: unfused (0); patches of multiple osteoderms fused but not the complete shield (1); remodeled into true, fused continuous sacral shield (2) (modified from Kirkland, 1998:42; Parish, 2005:155; Thompson *et al.*, 2012:166).

Kirkland (1998) observed that a true fused sacral shield of composed of ossicles remodeled into one continuous sheet of dermal bone from an initial mosaic of large and small ossicles was only documented in the polacanthids. Polacanthids (except for BEXHM 2002, which scores 1, and *G. lorriemcwhinneyi*, which scores 0) score (2). *Europelta*, *Hungarosaurus*, *Aletopelta*, *Stegopelta*, and *Nodosaurus* score (1). All other ankylosaurs score (0).

288. Sacral armour, form of ossicles in sacral armour: irregular ossicles (0); sub-hexagonal ossicles of similar sizes (1) (Parish, 2005:156; Thompson *et al.*, 2012:167).

Only *Stegopelta* and *Nodosaurus* score (1).

Caudal Armour

289. Lateral triangular caudal armour with hollow bases on tail excluding the distal region: absent (0); present (1) (Kirkland, 1998:43).

Kirkland (1998) noted that extensive caudal armour of this morphology was only known in the polacanthines. Early diverging ankylosaurs and polacanthids score (1). In ankylosaurids, *Akainacephalus*, *S. cutleri*, *Oohkotokia*, and *A. lambei* score (0). *Niobrarasaurus* and panoplosaurinins score (0).

290. Lateral armour, presence and persistence of large lateral caudal plates: present, extend well down the tail (0); present, but only proximal most two or three are large while the rest are small (1) (new character).

Europelta, *S. austriacus* and *Sauropelta* score (1), all other ankylosaurs score (0).

291. Lateral caudal plate, spacing: closely spaced (0); widely spaced (1) (new character).

Ankylosaurids score (1), all other ankylosaurs score (0). Synapomorphy of Ankylosauridae.

292. Lateral caudal plate, symmetry: asymmetrical, recurved (0); symmetrical (1) (new character).

Asymmetrical lateral caudal plates are synapomorphic for Ankylosauridae.

293. Distal tail club, presence: absent (0); present (1) (Sereno, 1986; 1999:98; Kirkland, 1998:44; Vickaryous *et al.*, 2004:51; Thompson *et al.*, 2012:170, 88).

Coombs (1978) was the first to demonstrate that the tail club is a synapomorphy of ankylosaurids. All ankylosaurids score (1).

294. Distal tail club, symmetry of lateral plates in dorsal view: semicircular (0); triangular (1) (Arbour and Currie, 2013:175).

Sereno (1999:98) uses the presence of a tail club composed of two pairs of dermal ossifications as a shared character for *Kunbarrasaurus*, *Shamosaurus* and the Ankylosaurinae. *Kunbarrasaurus* only preserves the proximal tail. *A. lambei* is the only ankylosaurid that scores (1).

295. Distal tail club, proportions of lateral plates in dorsal view: anteroposterior length >120% mediolateral width (0); subequal (1); wider than long (2) (modified from Arbour and Currie, 2013:176).

A. lambei is the only ankylosaurid that scores (2). Character states (0) and (1) vary throughout Ankylosauridae.

296. Distal tail club, proportions of caudal plate in dorsal view: longer than wide or subequal (0); wider than long (1) (new character).

Crichtonpelta, *Zuul*, and *Dyoplosaurus* score (0), all other ankylosaurs score (1).

Outgroup Characters for Stegosauria

297. Dentary, shape of rostroventral margin of the dentary, development of a pronounced chin: absent (0); present (1) (new character).

Huayangosaurus, *Gigantspinosaurus*, *Kentrosaurus*, and *Stegosaurus* score (1).

298. Dentary, posterior tooth row visible in lateral view: visible (0); teeth obscured by thin lateral lamina (1) (modified from Maidment *et al.*, 2008:14).

Tuojiangosaurus, *Kentrosaurus*, *Hesperosaurus*, and *Stegosaurus* score (1).

299. Dentary, orientation of alveoli: alveoli face dorsally (0); alveoli face dorsomedially (1) (Maidment *et al.*, 2008:15).

Tuojiangosaurus, *Gigantspinosaurus*, *Hesperosaurus*, and *Stegosaurus* score (1).

300. Quadrate, fossa on pterygoid flange: absent (0); present (1) (Sereno, 1986, 1999:29; Maidment *et al.*, 2008:8). Character reworded for redundancy.

Huayangosaurus, *Hesperosaurus*, and *Stegosaurus* score (1).

301. Posterior cervical vertebrae, elongation of the postzygapophyses: absent (0); elongated to project caudal to the centrum face (1) (Maidment *et al.*, 2008:22).

Tuojiangosaurus, *Miragaia*, *Hesperosaurus*, and *Stegosaurus* score (1).

302. Posterior free dorsal vertebrae, expansion of pedicels in anterior view: unexpanded (0); expanded (1) (Sereno, 1986, 1999:31).

Lesothosaurus, *Scutellosaurus*, *Huayangosaurus*, and *Gigantspinosaurus* score (0).

303. Posterior free dorsal vertebrae, expansion of pedicels between neural canal and transverse processes compared to the dorsoventral height of the neural canal in anterior view: area between neural canal and transverse processes is shorter than neural canal (0); area between neural canal and transverse processes is at least as tall as the neural canal (1) (new character).

Variable throughout Stegosauria. *Huayangosaurus*, *Gigantospinosaurus*, *Dacentrurus*, and *Miragaia* score (0), all other stegosaurs score (1).

304. Posterior free dorsal vertebrae, neural spine distal mediolateral expansion of the dorsal end: absent (0); present (1) (new character).

Present in *Wuerhosaurus*, *Hesperosaurus*, and *Stegosaurus*.

305. Anterior midcaudal (caudal 5-7) vertebrae, alignment of vertebral centrum faces of anterior cervical vertebrae: anterior and posterior faces are parallel and aligned (0); anterior face elevated dorsally compared to the posterior face (1) (new character).

Tuojiangosaurus, *Chungkingosaurus*, *Huayangosaurus*, and *Wuerhosaurus* score (0).

306. Caudal vertebrae, transverse process, presence of dorsal flange in anterior view: absent (0); present, insipient (1); present, pronounced (2) (new character).

Tuojiangosaurus and *Gigantspinosaurus* score (0), *Hesperosaurus* and *Stegosaurus* score (2), all other stegosaurs score (1).

307. Caudal vertebrae, extend well beyond the last substantial armour: extend well beyond last substantial armour (0); distal vertebrae fused into terminal armour (1) (new character).

308. Scapula, orientation of overall acromion process in lateral view: subparallel to scapular blade (0); perpendicular to scapular blade covering dorsal process and continuing to the glenoid (1) (new character).

All stegosaurs score (1). Character state (1) is synapomorphic for Stegosauria.

309. Scapula, dorsal process, anteroposterior extent along dorsal surface of scapula: extends less than the length of the coracoid (0); greater to or equal to the length of the coracoid (1) (new character).

All stegosaurs score (1). Character state (1) is synapomorphic for Stegosauria.

310. Scapula, dorsal process, forms peak away from the suture with the coracoid: absent, dorsal surface of dorsal process confluent with the dorsal surface of the coracoid (0); present, dorsal process forms a peak distal to the coracoid suture (1) (new character).

Tuojiangosaurus and *M. longicollum* score (1).

311. Scapula, change in angle between scapular blade and dorsal coracoid suture: sweeping curve (0); 70° to 90° forming "step" (1) (new character).

Kentrosaurus, *M. longicollum*, and *Stegosaurus* score (1).

312. Ilium, supracetabular shelf form: straight lateral edge (0); semicircular in dorsal view to form semicircular flange (1) (modified from Maidment *et al.*, 2008:54)

All stegosaurs score (1). Character state (1) is synapomorphic for Stegosauria.

313. Ilium, semicircular supracetabular flange orientation: flange projects laterally (0); flange folded over (1) (modified from Maidment *et al.*, 2008:55).

Wuerhosaurus, *Hesperosaurus*, and *Stegosaurus* score (1).

314. Ilium, postacetabular ilium form of caudal end: tapered (0); blunt (1) (modified from Maidment *et al.*, 2008:57).

Tuojiangosaurus, *Huayangosaurus*, *Chungkingosaurus*, *Kentrosaurus*, and *M. longispinus* score (0), all other eurypodans score (1).

315. Ilium, ventromedial flange backing the acetabulum: absent (0); present (1) (modified from Maidment *et al.*, 2008:58).

Wuerhosaurus, *Hesperosaurus*, and *Stegosaurus* score (1).

316. Dermal armour, dominated by a single pair of parasagittal rows of armour: present, a single row on each side of the midline (0); multiple rows of armour on each side of the body (1) (new character).

All stegosaurs score (0). Character state (0) is synapomorphic for Stegosauria.

317. Thoracic armour, type of single row of parasagittal armour: spines (0); plates (1) (new character). Character reworded for clarity.

Tuojiangosaurus, *Chungkingosaurus*, *Huayangosaurus*, *Gigantspinosaurus*, and *Loricatosaurus* present both spines and plates along the dorsum, therefore scoring (0&1). Kentrosaurus and Dacentrurus score (0). All other stegosaurs score (1).

318. Thoracic armour, form of single row of parasagittal plates: taller than long and pointed (0); longer than tall to subequal with rounded tops (1) (new character).

Wuerhosaurus, *Hesperosaurus*, and *Stegosaurus* score (1).

319. Thoracic plates, shape of base: flattened to slightly concave base (0); rooted base (1) (new character).

Only *Hesperosaurus* and *Stegosaurus* score (1).

320. Parascapular spine with broad flat base and spine pointing posteriorly along flank of animal: absent (0); present (1) (new character).

321. Sacral armour, shape of single row of parasagittal armour: spines (0); plates (1) (new character).

Chungkingosaurus and *Kentrosaurus* score (0), *Huayangosaurus* and *Gigantspinosaurus* score (0&1), *Hesperosaurus* and *Stegosaurus* score 1.

322. Caudal armour, shape of single row of parasagittal armour, excluding the distal caudal portion: spines (0); plates (1) (new character).

Gigantspinosaurus, and *M. longicollum* score (1).

323. Caudal armour, presence of distal spines with cupped base: absent (0); present, likely conforming to the curvature of the mid to distal tail cross-section (1) (new character).

Only *Dacentrurus* and *Miragaia* score (1).

324. Caudal armour, penultimate caudal tail spines: absent (0); present (1) (new character).

All stegosaurs score (1). Character state (1) is synapomorphic for Stegosauria.

325. Caudal armour, penultimate caudal tail spines, cross-sectional shape: round (0); lenticular (1) (new character).

Dacentrurines score (1), all other stegosaurs score (0). Synapomorphic for Dacentrurinae.

326. Caudal armour, terminal caudal tail spines: absent (0); present (1) (new character).

All stegosaurs score (1). Character state (1) is synapomorphic for Stegosauria.

327. Caudal armour, terminal caudal tail spines, fusion: absent (0); present (1) (new character).

Kentrosaurus, *Dacentrurus*, and *M. longicollum* score (1).

328. Caudal armour, terminal caudal tail spines, angle of fused spines in dorsal view: divergent (0); sub-parallel (1) (new character).

Only *Kentrosaurus* and *M. longicollum* score (1).

329. Caudal armour, terminal tail spines, cross-section shape: round (0); lenticular, bladed, or sword shaped (1) (new character).

Dacentrurines score (1). Synapomorphic for Dacentrurinae.

3

HISTORY OF THE DISCOVERY OF THE ANKYLOSAUR *DRACOPELTA ZBYSZEWSKII* (UPPER JURASSIC), WITH NEW DATA ABOUT THE TYPE SPECIMEN AND ITS LOCALITY

Published in Comunicações Geológicas:

Russo, J., and Mateus, O. 2021. History of the discovery of the ankylosaur *Dracopelta zbyszewskii* (Upper Jurassic), with new data about the type specimen and its locality. Comunicações Geológicas, 108(1): 27-34. DOI: https://doi.org/10.34637/dmdm-5w12

Abstract

Dracopelta zbyszewskii is a poorly known ankylosaur dinosaur from the Upper Jurassic of Portugal. Even its early history has hitherto remained problematic, mostly due to scarce recorded information. By reviewing published literature, unpublished photos and notes, and field observations, we identify the type locality as a roadcut 400 meters Southeast of Praia da Assenta Sul, approximately 1 km West of Barril, Mafra. Western Portugal, and date the discovery to early 1964 and the excavation to December 1964. This improves the existing records and allows to trace the early history of the holotype, providing important historical context on one of the most complete ankylosaurs from Europe. Furthermore, we preliminarily identify additional holotype material, i.e., putative pelvic elements, right hindlimb elements (distal

femur, tibia, and fibula), one ungual, ribs, and osteoderms, which will help ascertain its position within Ankylosauria. We also propose that a single repository number be used for the specimen.
Keywords: *Dracopelta zbyszewskii*; ankylosaur; Upper Jurassic; historical record.

Resumo

Dracopelta zbyszewskii é um dinossauro anquilossauro pouco conhecido do Jurássico Superior de Portugal. Mesmo a história da sua descoberta tem permanecido problemática até aqui, em grande parte devido à escassa informação registada. Revendo literatura publicada, fotografias e notas inéditas, e observações de campo, identificamos aqui a localidade tipo como um corte de estrada, cerca de 400 metros a Sudeste da Praia da Assenta Sul, aproximadamente 1 km a Oeste de Barril, Mafra, Costa Oeste de Portugal, e datamos a descoberta ao início de 1964 e a escavação a Dezembro de 1964. Esta informação melhora os registos existentes e permite clarificar a história inicial do holótipo, fornecendo contexto histórico importante para um dos mais completos anquilossauros da Europa. Além disso, identificamos preliminarmente material adicional pertencente ao holótipo, i.e., putativos elementos pélvicos, elementos do membro posterior direito (fémur distal, tíbia e fíbula), uma ungual, costelas e osteodermes, o que ajudará a determinar a sua posição dentro dos Ankylosauria. Propomos também que um único número de inventário seja utilizado para o espécime.
Palavras-chave: *Dracopelta zbyszewskii*; anquilossauro; Jurássico Superior; registo histórico.

Introduction

Dracopelta zbyszewskii Galton 1980 is an ankylosaurian dinosaur from the Upper Jurassic of Portugal. Ankylosaurs are dinosaurs mainly characterized by the extensive cranial and postcranial dermal ossification, and are known as far back as the Middle Jurassic (?Bathonian-Callovian) from fragmentary remains, becoming highly diverse during the Cretaceous, when occurrences are known worldwide, with the exception of Africa (e.g. Vickaryous *et al.*, 2004, Arbour and Currie, 2016). The holotype of *D. zbyszewskii* was the first articulated ankylosaur remains from the Jurassic and is one of the most complete Jurassic ankylosaurs from Europe (Galton, 1980, 1983; Pereda-Suberbiola *et al.*, 2005; Ösi, 2015). Therefore, it represents an important taxon to understand the evolution of the whole group Ankylosauria.

However, it remains poorly understood and its affinities are uncertain, with Galton (1980) tentatively ascribing it to the Nodosauridae. Since its description, it has consistently either been disregarded altogether in most studies or been deemed too incomplete and undiagnostic to allow a more accurate classification other than either as *incertae sedis* or as a *nomen dubium* (e.g., Carpenter, 2001; Vickaryous *et al.*, 2004). More recently, other occurrences of Late Jurassic ankylosaurs have been reported, especially from North America (Kirkland and Carpenter, 1994; Carpenter *et al.*, 1998). The close affinities between North American and Iberian Late Jurassic faunas are well documented (e.g., Mateus, 2006; Hendrickx and Mateus, 2014; Tschopp *et al.*, 2015) so *D. zbyszewskii* is an important element to further clarify the paleobiogeographical implications between Iberia and North America during the Late Jurassic and evolutionary relationships within Ankylosauria. Thus, having as much information as possible on this taxon is crucial, starting with its exact type locality and age, and including its historical context. These have been a matter of debate since the records on the discovery of the holotype of *D. zbyszewski* are sparse or almost nonexistent. When it was first described (Galton, 1980), the holotype, a partial articulated ribcage and osteoderms, and associated material (Figure 3.1), had been laying at the Serviços Geológicos de Portugal (SGP; presently Laboratório Nacional de Energia e Geologia, LNEG) storage for years (Galton, pers. comm., 2009, 2015). The little available information at the time allowed only to attribute the type locality and horizon as Ribamar on the Western coast of Portugal and Kimmeridgian. Herein we address this problem by tracing the holotype's history and providing a full account of its discovery and the main contributors, while identifying the type locality (Figures 3.2-3.4). We cross reference previously unknown archival records, i.e., field notes, photographs, reports, such as an original photograph from the holotype *in situ* as well as the original specimen sketch by Georges Zbyszewski (Figure 3.3), with field work and observations of the area (Figure 3.4), to review and establish the chronology of the discovery. We also report on additional material from the holotype (Figure 3.1c), which will be invaluable for a detailed, updated description of *D. zbyszewskii*. Studies are currently ongoing to redescribe in detail the specimen and address its phylogenetic relationships. This work provides significant historical background and a new geographical and stratigraphical framework to better understand one of the most complete yet lesser-known ankylosaurs in Europe, and one of the few known from the Jurassic.

Figure 3.1. Holotype material of *Dracopelta zbyszewskii*. (a) IGM 5787, ribcage and dermal armour; (b) IGM 3, autopodium; (c) best preserved elements from the postcranial material (stored at LNEG, no inventory number), from left to right: right tibia, anterior view; distal right femur, anterior view, with an osteoderm and ossified tendon below; rib segments (above); osteoderms (below). Scale bars in (a, c) and (b): 10 cm and 5 cm, respectively.

Institutional abbreviations: IGM, Instituto Geológico e Mineiro; IPFUB, Institute of Palaeontology of the Free University of Berlin; LNEG, Laboratório Nacional de Energia e Geologia; MG, Museu Geológico; SGP, Serviços Geológicos de Portugal.

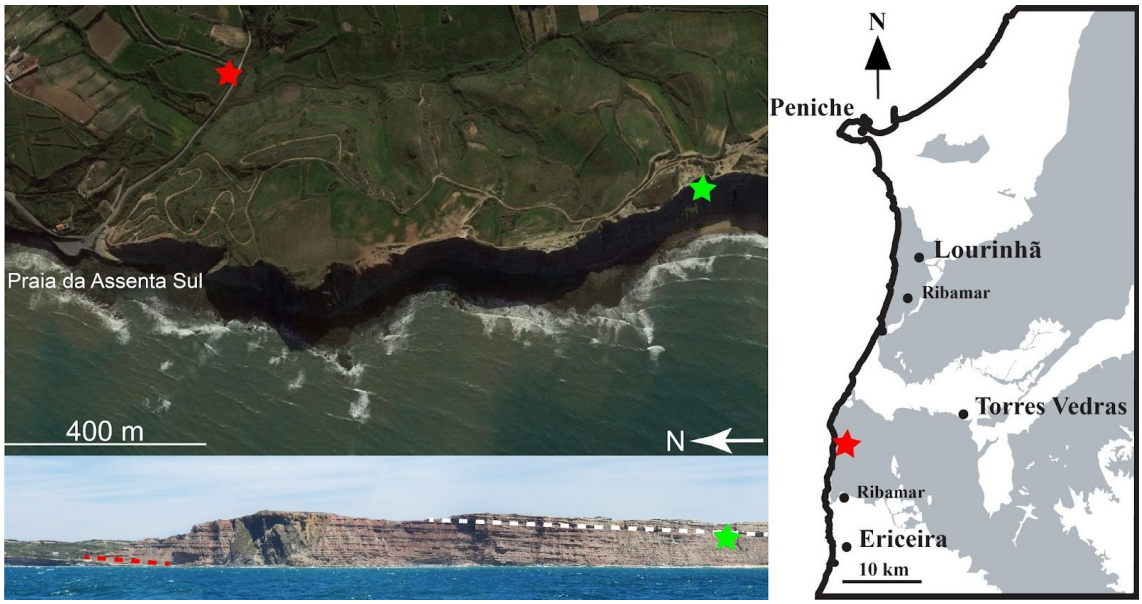

Figure 3.2. Regional simplified geological map (right), with location of *Dracopelta zbyszewskii* (red star). Gray coloured areas on the right represent Late Jurassic units. Satellite (top left) and coastal profile (bottom left) photographs of the Praia da Assenta Sul area. Green star indicates the site of the new ankylosaurian specimen NOVA-FCT-DCT-5556; white dashed line on bottom left represents approximate J-K boundary according to Mateus *et al.* (2017); red dashed line marks the coastal equivalent unit to the type locality. Satellite image modified from Google Earth® and panoramic photo of the coast by André Carvalho.

History of the discovery and study of *Dracopelta* type specimen

Very little is known about the discovery of *D. zbyszewskii*. The early records are virtually nonexistent, with the only official information available being a short, handwritten "Ribamar" label associated with the specimen, and previous descriptions of the holotype material (Galton, 1980; Pereda-Suberbiola *et al.*, 2005). According to Pereda-Suberbiola and colleagues (2005), improving on what was known until then, the holotype was found during road construction works in the Assenta region "*sometime between the end of 1963 and the beginning of 1964*". In fact, in early 1964, during the construction of a road between Barril and the beach of Assenta Sul, fossil bones were exposed. The local newspaper Badaladas no. 472, on January 9th, 1965, published a short article here titled "*140-million-year-old fossil found at Praia da Assenta"*, in which it reported the occurrence, as translated: "*When about one year ago a road was being opened between the village of Barril and Praia da Assenta, part of a fossil of a very old animal was discovered. [...] A local friend of ours was made aware of the finding and after going to the site to verify its existence, informed the Geological Services of Portugal about the*

appearance of the fossil. Thus, immediately went, on the last [December] *22nd, to Praia da Assenta, our friends, Dr. Georges Zbyszewski and Eng. Veiga Ferreira, senior officials of those services, accompanied by specialized personnel, who proceeded to survey the interesting fossil. As those friends informed us, it must be a dinosaur that is 140 million years old, but only after properly studied in the laboratory of those services, can it be classified scientifically to which genus it belongs."* This news report confirms 1964 as the discovery of fossil dinosaur bones in the area as well as the presence of Georges Zbyszewskii and Octávio da Veiga Ferreira. The aforementioned "local friend" that first confirmed the presence of the fossil was found to be Leonel Trindade and photographed the specimen *in situ* (Figure 3.3). In the back of the photograph, part of the personal files of Trindade at the Torres Vedras Museum archives, is written "Assenta", thus confirming that the dinosaur bones reported are indeed from *D. zbysewskii*. Leonel de Freitas Sampaio Trindade (Figure 3.5a) (Torres Vedras, July 16th, 1903 - January 4th, 1992) was an archaeologist in Torres Vedras, responsible for numerous studies mainly in the Neolithic from the Western Region, among which Castro do Zambujal and Tholos de Paimogo (e.g., Trindade and Veiga Ferreira, 1956; Gallay *et al.*, 1973; Sangmeister *et al.*, 1974). The Torres Vedras Museum bears his name in recognition of his work, as does the Associação Leonel Trindade, now Sociedade de História Natural, in Torres Vedras. Being an archaeologist with a peripheral interest in palaeontology, he forwarded relevant fossils in the area to his contacts in the SGP in Lisbon, namely Georges Zbyszewski. Georges Zbyszewski (Fig. 3.5b) (Gatchina, Russia, October 22nd, 1909 - Lisbon, March 1st, 1999) was one of the most prominent geologists and paleontologists in Portugal who, after his first visit in 1935, and over the course of more than 40 years working at the SGP, authored and/or co-authored over 200 publications, including the geological mapping of the country, studies on the Quaternary encompassing geology, archaeology and palaeontology, and paleontological works on invertebrates and vertebrates of the Cenozoic and Mesozoic of Portugal (e.g. Zbyszewski and Almeida, 1950; Lapparent and Zbyszewski, 1957; Zbyszewski and Ferreira, 1990) . As reported, together with Octávio da Veiga Ferreira, his colleague and protégé, he visited Porto do Barril beach on December 22nd, 1964, and organized the excavation and extraction of the specimen. Georges Zbyszewski drew a pencil sketch of the *D. zbyszewskii* rib cage in his fieldbook (Figure 3.3), with the dimensions of the specimen block "*0,80*"

for "*0,80*", "*route*" indicating the road, and "*Dinosaure de Assenta*" noted down on the side. To be noted that this information is mixed with the author's notes on unrelated work in the previous and following pages. The two adjacent sentences to the sketch are part of the geological description of the section of Ruivos, Palmela, 75 km to the Southwest, later published in the corresponding geological map explanation booklet (Zbyszewski *et al.*, 1965: pages 16 and 17). Georges Zbyszewski's field books are usually not dated or possess other references that could allow cross referencing field information or exactly date his field notes and visits. Nevertheless, by putting together these pieces of information, it was possible then to confirm that Zbyszewski and Veiga Ferreira visited the site in Assenta on December 22nd, 1964, and that the sketch was probably drawn on that day, which consequently also allows to date that portion of Zbyszewski's field notes and observations. Furthermore, by comparing the surrounding lithology on the photograph and performing field observations of the area, while cross-referencing it with information of the site in Pereda-Suberbiola *et al.* (2005), the outcrop on the side of the road was identified (Figure 3.4), thus confirming that *D. zbyszewskii* was indeed the occurrence reported and that the roadcut section is the type locality. The specimen was then collected by Zbyszewski and Veiga Ferreira and housed at LNEG (former Serviços Geológicos de Portugal), where it was briefly prepared by Manuel de Matos (Mateus, 2006).

Georges Zbyszewski co-authored the seminal work "Les Dinosauriens du Portugal" in 1957, with Albert de Lapparent, which would make him a natural candidate for the study of this new dinosaur specimen. Surprisingly, he did not study or seemed interested in co-authorship of the description of this dinosaur and rather focused on non-paleontological geology. In August 1978, Peter M. Galton visited the Geological Museum in Lisbon to observe stegosaur material during a one-week trip, before a scientific meeting in Paris. Peter Malcolm Galton (Figure 3.5c) (London, England, March 14th, 1942) is a prolific vertebrate paleontologist, Professor Emeritus at University of Bridgeport CT, who published extensively on dinosaurs, particularly ornithischians and early diverging sauropodomorphs, which mainly resulted from visiting unstudied collections in museums. During his time in Lisbon, new unstudied specimens caught his attention. His host, Zbyszewski, invited him to study it since "the Geological Survey encouraged Zbyszewski to concentrate on geology, not dinosaurs" (Peter M. Galton, pers. comm., 2009, 2015). As a result, in

June 1980, Galton described the specimen and erected the new taxon, *Dracopelta zbyszewskii* Galton, 1980, in honor of the collector and his host in Portugal, as a nodosaurid ankylosaur, based on the similarities of the armour to ankylosaurs known at the time. He was an author of additional work featuring *D. zbyszewskii* (Galton, 1983; Pereda-Suberbiola *et al.*, 2005) and other ornithischians from Portugal (Galton, 1981, 1991, 1994, 1996).

Figure 3.3. Historical record of the holotype of *Dracopelta zbyszewskii*. Top) sketch of the holotype in Georges Zbyszewski's 1964 fieldbook. "Dinosaure de Assenta" (dinosaur of Assenta) is noted on the left edge of the page. The content of the rest of the page is unrelated with this sketch (see text for further information on Georges Zbyszewski's field notes); Bottom) holotype in situ in 1964 (photograph by Leonel Trindade, kindly shared by Torres Vedras municipal archives).

Type locality and horizon

Galton (1980) wrongly pointed the type specimen to be from the Upper Jurassic (Kimmeridgian) of Ribamar, after the indications of Georges Zbyszewski. As aforementioned, Zbyszewski had knowledge of both the exact location of the finding and the age of the specimen. However, the toponym of Ribamar created obvious confusion on the location and age, since there are two localities with the same name, Ribamar, 25 km apart (Figure 3.2): 1) in Mafra municipality, to the South, and 2) in Lourinhã municipality, to the North. Antunes and Mateus (2003) reasoned that the type locality may have been Ribamar from Lourinhã because of the extensive

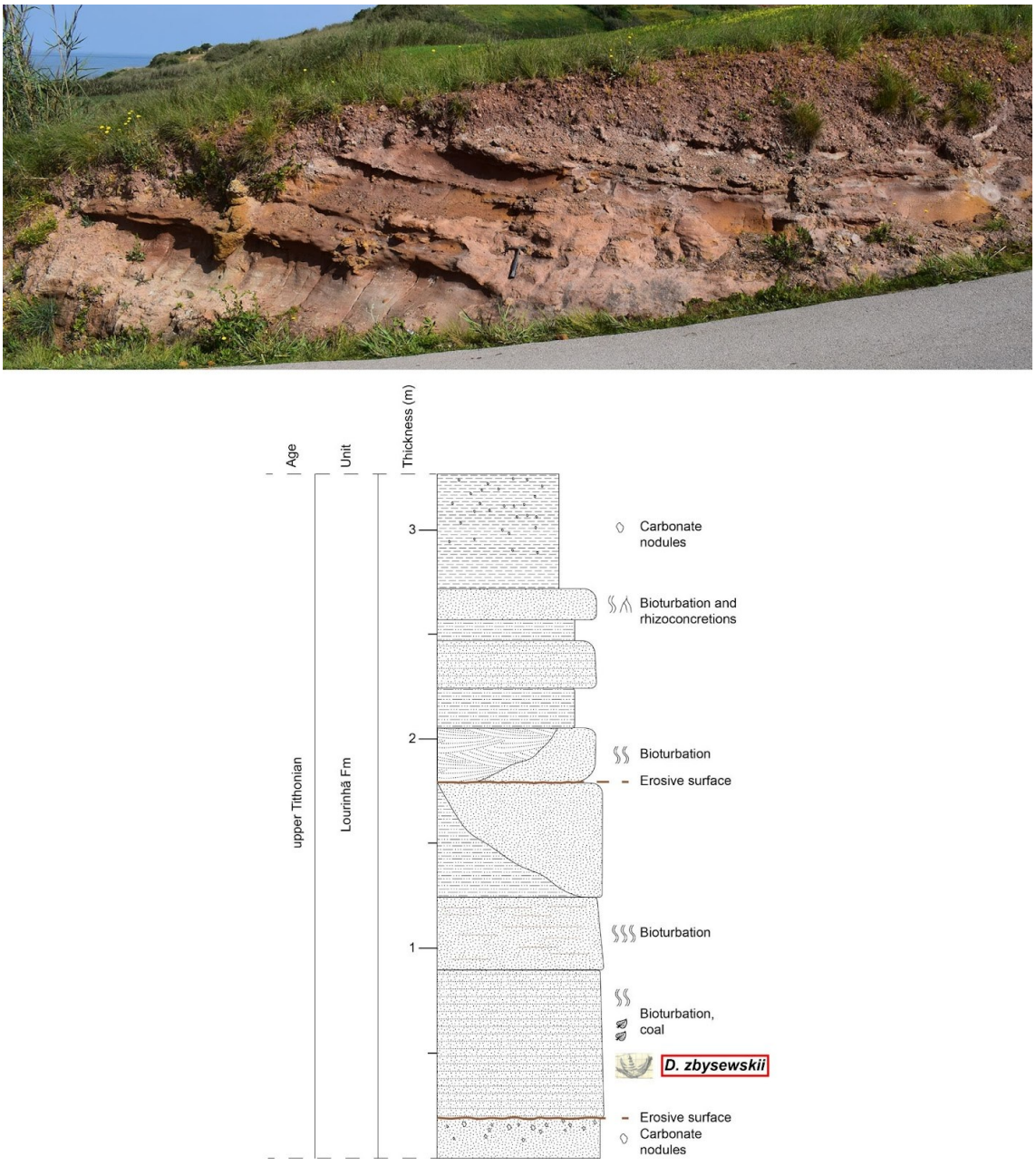

Figure 3.4. Type locality of *Dracopelta zbyszewskii* (above) and local stratigraphic log showing the placement of the holotype in the section (below).

Kimmeridgian-Tithonian outcrops and dinosaur record in the area. Ribamar from Mafra and its immediate surrounding area sit on Early Cretaceous igneous and sedimentary rocks that overlie the Upper Jurassic found further to the North. Therefore, those authors deemed as highly unlikely that *D. zbyszewskii* came from this locality: either the age or the location had been wrongly placed. At that time, samples of the the rock matrix of the type specimen were tested for palynology to try to attest on the age, but the results were inconclusive. New data from Pereda-Suberbiola *et al.* (2005) provided new inputs on the type locality and age, and date of discovery, while describing additional holotype material, a putative right manus (Figure 3.1b). Those authors propose a date of discovery between the end of 1963 and the beginning of 1964, and corrected the previous location and narrowed down the type locality to 400 meters East of Praia do Sul, near Assenta, Torres Vedras, but without figuring the location or providing coordinates. The same authors constrained the age to the uppermost lower Tithonian-upper Tithonian.

Through field observations, it was possible to confirm the exact type locality at 39°03'07.8" N 9°24'43.2" W, a roadcut between Barril and Praia da Assenta Sul, in the municipality of Mafra (Figures 2-4), 5 km North of Ribamar, Mafra. The specimen comes from a medium to fine-grained gray sandstone, stratigraphically low in the local sequence (Figure 3.4), representing a fluvial channel, with small coalified plant fragments. The 3 m type section is characterized by a succession of fluvial sandstones (some showing parallel lamination) intercalated by oxidized erosive surfaces showing moderate bioturbation and fossilized roots, which indicates periodic subaerial exposure, further confirmed by the presence of carbonated nodules. This is consistent with what is recognized in the uppermost part of the Lourinhã Formation, the Assenta Member (Mateus *et al.*, 2017). Therefore, we agree with the uppermost lower Tithonian-upper Tithonian age of *D. zbyszewskii*. This specimen is much higher than the Kimmeridgian/Tithonian boundary seen in the outcrops to the North and about 75-85 meters stratigraphically below the Jurassic Cretaceous boundary (Mateus *et al.*, 2017). Recently, a new ankylosaur specimen was reported about 1 km South, but stratigraphically higher, about 5 to 6 m below the JK boundary (Figure 3.2) (Russo and Mateus, 2019). Studies on this specimen are currently ongoing to clarify if it represents an additional, more complete specimen, of *D. zbyszewskii*, or a different taxon altogether.

Figure 3.5. Main historic contributors. (a) Leonel Trindade (from Travanca, 1999); (b) Georges Zbyszewski (right) and Octávio da Veiga Ferreira (left) (kindly shared by João Luís Cardoso); (c) Peter M. Galton (photograph by Octávio Mateus).

New unpublished material from the type specimen

The holotype of *D. zbyszewskii* is composed of MG 5787 (former IGM 5787), a partial rib cage with 12 dorsal vertebrae and articulated proximal ribs, and five different types of dermal armour (Galton, 1980), and MG 3 (IGM 3), an incomplete autopodium with three metapodials and digits II, III and IV (Pereda-Suberbiola *et al.*, 2005), and unpublished material. Galton (1980) described only the ribcage and osteoderms, because the remaining material was not located or available during his visit. The autopodium, described by Pereda-Suberbiola *et al.* (2005), was found and retrieved from storage, across the street of Museu Geológico, in 1979 by João Luís Cardoso (Cardoso, pers. comm., 2021), while inventorying the collections of the then-SGP as an undergraduate student, and who notified Georges Zbyszewski on the finding.

Additional material (uncatalogued) was recently identified at the LNEG storage and is here accounted for while a more detailed study is ongoing. It was not initially described by Galton (1980) nor Pereda-Suberbiola *et al.* (2005) because it was unprepared and misplaced, mixed in with a stegosaurian specimen from Atouguia da Baleia (also collected by Georges Zbyszewski) that was later described as another specimen of *Miragaia longicollum* by Costa and Mateus (2019). The rock matrix was a medium-grained, gray sandstone, similar in colour and grain size to the latter. Costa *et al.* (2017) sorted both specimens using anatomy and the chemical signature obtained by X-ray fluorescence (XRF). The geochemical signature on the sediment from the holotype of *D. zbyszewskii* showed an enrichment in K and Fe. To corroborate this result, an XRF analysis was performed using a Thermo Scientific

NitonXL3t Goldd+ on a sample collected from the specimen layer from the type locality. The geochemical profiles in both samplings were very similar, specifically registering peak amounts of K, Fe, and Rb. Also, the highest peak registered was of Si, which was expected and can be attributable to the high content of potassium feldspar in the matrix, namely orthoclase, a major component of the sandstones in the Lourinhã Formation.

The new holotype material presented herein is composed of 35 blocks (defined as any fragment larger than 10 cm) and over 70 fragments. Although most elements are unidentified fragments, a few can be identified. Most are osteoderms, of which four possible lateral plates based on its size and curved shape, but there are also nine partial ribs and appendicular bones. The latter are the best preserved and in a more advanced state of preparation and consist of the distal end of the right femur, right tibia, broken at the distal end, and right fibula, broken in three smaller fragments, two phalanges (one of them is an ungual), most likely from the autopodium. Either more poorly preserved or in need of further preparation, there is also a partial femoral shaft and possible pelvic elements. This new material is currently being described.

Numbering the type specimen

The catalogue specimen numbering of *D. zbyszewskii* is also somewhat problematic. As aforementioned, both the ribcage and the autopodium have different specimen numbers, IGM 5787 and IGM 3 respectively, whilst the remaining material does not have an inventory number. The institutional catalogue acronym of the type specimen has changed over the years, reflecting the various changes of the institutional name and in the institution itself that houses the specimen. Even though the museum remained relatively unaltered throughout, the only change being in 1993 when Museu dos Serviços Geológicos de Portugal was renamed as Museu Geológico, its institutional frame changed. It originated in 1859 with the purpose to store specimens from the surveys and works of the Comissão Geológica do Reino, created two years before, in 1857, by royal decree. The parent institution went through successive name changes in the next 60 years: Comissão Geológica de Portugal (1857-1869), Secção dos Trabalhos Geológicos de Portugal (1869-1886), Comissão dos Trabalhos Geológicos de Portugal (1886-1892), Direcção dos Trabalhos Geológicos de Portugal (1899-1901); Comissão do Serviço Geológico de Portugal (1901-1918). In 1918, it changed again, to Serviços Geológicos de

Portugal, until 1993 when it became Instituto Geológico e Mineiro. In 2003, IGM was decommisioned, and in 2006 its services came under the jurisdiction of Laboratório Nacional de Energia e Geologia, as it remains to this day. All SGP specimens were automatically converted to MG in 1993 without changing the number itself. Concerning the history of museum cataloguing record, it is important to note that the specimens initially collected by the Institute of Palaeontology of the Free University of Berlin (IPFUB) in Portugal also received a different acronym and number system, IPFUB, and not SGP or MG. That material, that include mostly Jurassic vertebrate from Guimarota, Pedrógão, Porto das Barcas, and Porto Dinheiro, were transferred to the Museu Geológico in 2007 and 2008, eventually receiving the final MG acronym and new catalogue number without preserving the original IPFUB numbers. At the beginning, the numbering system of the museum was largely according to the position of the fossil cabinets in the rooms rather than uniting the various anatomical elements of each vertebrate skeleton under the same number. As a result, the three portions of the type specimen of *D. zbyszewskii* are thus numbered differently despite belonging to the same individual: MG 5787, MG 3 and the new elements here reported presently unnumbered. A similar situation happened with other dinosaur holotypes, such as the types of *Lusotitan atalaiensis* Lapparent & Zbyszewski 1957 and *Lourinhasaurus alenquerensis* Lapparent & Zbyszewski 1957, in which the same individuals hold multiple specimen numbers (Antunes & Mateus, 2003). Therefore, considering that all material reported herein pertains to the holotype, and to avoid confusion in the future, we recommend that a single specimen, i.e., one skeleton, be kept under one single repository number. In this case, because there is no numbering in the original article, we recommend the lowest number (MG 3) for the entire holotype specimen. Regardless, MG holds collections that date back to the 1800s, and, despite these cases, the historical records are preserved with a remarkable level of detail, which allowed most findings to be traceable and reconstructed. The documentation available at LNEG and the records of the collections allow for an incomparable reconstruction of the history of Science in Portugal.

Conclusions

The history of the discovery of the holotype of the ankylosaur *D. zbyszewskii* is here reviewed and accounted for, as it remained obscure until now. New data (photographs, field notes, newspapers, and field observations) allowed to confirm

that it was found in early 1964 during road works between the locality of Barril and Praia da Assenta Sul, Mafra, Western Portugal, in a light gray sandstone, corresponding to a fluvial channel. This is thus defined as the type locality and is late Tithonian in age, located in the uppermost part (Assenta Member) of the Lourinhã Formation. It was first reported by Leonel Trindade to Georges Zbyszewski, and Octávio da Veiga Ferreira, who recovered the specimen on December 22nd, 1964. Additionally, new unpublished postcranial bones of the type specimen are also reported, namely right hindlimb elements and dermal armour. It is also proposed that a single repository number is used for the whole specimen to avoid confusion and facilitate future reference and access.

4

SYSTEMATIC PALEONTOLOGY

DINOSAURIA **Owen 1842**

ORNITHISCHIA **Seeley 1888**

THYREOPHORA **Nopcsa 1915**

EURYPODA **Sereno 1986**

ANKYLOSAURIA **Osborn 1923**

POLACANTHIDAE **Jaeckel 1910**

JURAPELTA clade. nov.

Definition: The minimum clade containing *Dracopelta zbyszewskii*, *Gargoyleosaurus parkpinorum*, and *Mymoorapelta maysi*, but not *Polacanthus foxii*.
Etymology: "*Jura*" as a reference to the Late Jurassic occurrence of the members of this group; "*pelta*" from the Ancient Greek for a small shield.
Reference phylogeny: Figure 6.2.1 (this work), from maximum parsimony analysis.
Composition: under the primary reference phylogeny, Jurapelta comprises *Dracopelta*, *Mymoorapelta* and *Gargoyleosaurus*.
Synonyms. No other taxon names are currently in use for the same or approximate clade.

Diagnosis. Jurapelta is supported by the following unambiguous synapomorphies, as per the reference phylogeny: flat scale impressions on nasal region of skull roof; dorsal centrum length > 110% of dorsal centrum height; laterally unexpanded ilium; lateral deflection of preacetabular process of the ilium between 0°-20°; claw-shaped pedal unguals.

Dracopelta zbyszewskii Galton 1980

Etymology. "*Draco*" from the Latin, meaning dragon; "*pelta*" from the Greek, meaning small shield, referring to the small dermal scutes, "*zbyszewskii*" named for Georges Zbyszewski, in recognition of all his geological and paleontological work in Portugal.

Holotype. MG 5787 (previously IGM 5787; Figs. 4.1.1.1-2; Tables 4.1.1.1), partial articulated ribcage, with one cervical vertebra and ten dorsal vertebrae, 22 partial ribs and 35 osteoderms, MG 3 (previously IGM 3; Figs 4.1.1.6; Table 4.1.2.1), an incomplete right pes with three metapodials and digits II, III and IV (Pereda-Suberbiola *et al.*, 2005), and uncatalogued material (Figs. 4.1.1.3-5, 4.1.1.7-12).

Type locality. 39° 03' 07.8" N, 9° 24' 43.2" W, a roadcut 400 meters East of Praia da Assenta Sul (Porto Barril), Mafra, Portugal (see Russo and Mateus, 2021, or Chapter 3 of this dissertation, for further details).

Horizon and age. Fluvial channel, light grey, reddish sandstone, ~60 meters from the top of the Assenta Mb, Lourinhã Fm; ~145 Ma, upper Tithonian, Upper Jurassic.

Referred specimen. NOVA-FCT-DCT-5556 (formerly FCT-UNL 702; Figs. 4.2.1-3, 4.2.1.1-2, 4.2.2.1-7, 4.2.3.1-4, 4.2.4.1-3; Tables 4.2.2.1-2), mostly complete, articulated skeleton, composed of skull, left mandible, most of the axial skeleton, pectoral and pelvic girdles, proximal appendicular elements (femora and left humerus), and dermal armour; 39° 2' 38.77" N, 9° 24' 54.33" W, coastal cliffs of Praia da Escadinha, ~1,5 km WSW of Barril, Mafra, Portugal; ~15 meters from the top of Assenta Mb, Lourinhã Fm; ~145 Ma, uppermost Tithonian, Upper Jurassic.

Revised diagnosis. *Dracopelta zbyszewskii* is defined by four autapomorphies: lateral processes of the cervical and dorsal vertebrae located anteriorly, at the edge of the anterior articulation facet of the centrum (Figs. 4.1.1.1, 2A, B, 4.2.2.2, 4); low position of the dorsal prezygapophyses relative to the neural arch, in alignment with the parapophyses (Figs. 4.1.1.2A, B, 4.2.2.4); two pairs of transitional cervicothoracic, medial, suboval, keeled ossicles, with thickened rims (Figs. 4.1.1.1-

2A, B, 4.2.2-3, 4.2.2.1, 4.2.4.1); dermal armour arrangement of eleven bands of four thoracic parasagittal subcircular ossicles, dorsolateral elongated keeled scutes, and a row of lateral plates (Figs. 4.1.1.1, 2, 4.2.2-3, 4.2.4.1).

Remarks. *Dracopelta zbyszewskii* has been diagnosed previously by Galton (1980) by "dermal armour of the thoracic region consists of very small isolated flat scutes, small medial paired circular plates with raised centre and rims, very long anterolateral plates, narrow nonprojecting overlapping dorsolateral plates and overlapping laterally projecting lateral plates". The same author (1983a) writes "dermal armour of the thoracic region consists of very small isolated flat scutes, small medial paired circular plates with raised centres and rims, very long anterolateral plates, narrow nonprojecting overlapping dorsolateral plates and overlapping laterally projecting and dorsoventrally compressed lateral plates with a sinusoidal proximal surface and a circular outline laterally". Pereda-Suberbiola *et al.* (2005) adds the following: "*Dracopelta* is diagnosed by the presence of proximal phalanges II and III as long as wide in the autopodium and distinctive thoracic armour." Observation of the specimen NOVA-FCT-DCT-5556 described herein recognizes the autapomorphies observed in the type specimen (MG 5878), as well as a unique combination of characters, including six additional autapomorphies (marked with an asterisk), as follows: maxillary tomial crest medially deflected at the premaxilla/maxilla contact, completely separating the buccal emargination from the premaxillary palate* (Fig. 4.2.1.1F); anteriorly narrow tooth rows relative to the posteriormost width of the tooth row (strongly concave)* (Fig. 4.2.1.1B, F); lateral processes of the cervical and dorsal vertebrae located anteriorly, at the edge of the anterior articulation facet of the centrum* (Figs. 4.2.2.2, 4); low position of the dorsal prezygapophyses relative to the neural arch, in alignment with the parapophyses* (Fig. 4.2.2.4); two dorsolaterally positioned bilateral bundles of overlapping ossified tendons* (Figs. 4.2.2, 4.2.2.3); deeply excavated intertrochanteric and popliteal fossae of the femur* (Fig. 4.2.3.4B-D, J); medial condyle of the femur twice the size of the lateral condyle* (Fig. 4.2.3.4C, D, H-K); hyperdeveloped lateral epicondyle of the femur (shared with *Gargoyleosaurus*); three cervical bands of armour made up by one pair of keeled scutes, each forming a quarter ring* (Figs. 4.2.2-3, 4.2.4.1); ellipsoidal osteoderm as central element in first cervical band (shared with *Gargoyleosaurus*); two pairs of cervicothoracic, medial, suboval, keeled ossicles, with thickened rims* (Figs. 4.1.1.1-2A, B, 4.2.2-3,

4.2.2.1, 4.2.4.1); dermal armour arrangement of eleven bands of four thoracic parasagittal subcircular ossicles, dorsolateral elongated keeled scutes, and a row of lateral plates* (Figs. 4.2.2-3, 4.2.4.1).

4.1. Description of the holotype

The holotype (MG 5787) of *Dracopelta zbyszewskii* (Figs. 4.1.1.1-2) is a partial articulated ribcage, composed of the last cervical (c8) and first eleven dorsal vertebrae (d1-d11), articulated, 22 partial ribs, ossified tendons, and dermal armour. Associated with the ribcage, there is also a partial autopodium (MG 3, Fig. 4.1.2.3, Table 4.1.2.1), and additional uncatalogued material (Figs. 4.1.4.1-4), namely distal rib fragments (Figs. 4.1.1.3, 4.1.4.1, 4), partial right hindlimb elements (Figs. 4.1.2.1-2), and osteoderms (Figs. 4.1.3.1-2, 4.1.4.1, 3). The skeleton is heavily eroded dorsally and laterally, preserving the centra of the vertebra, distal rib segments, and lateral plates. Additionally, cross sections of plates below the ribcage are visible, and other unidentified elements indicate more material is *in situ*. Despite the articulation and the dorsal exposure of the specimen, more preparation would be needed to remove the sediment, and access possibly better-preserved material. The anatomical information on the holotype was further complemented and/or confirmed by specimen NOVA-FCT-DCT-5556, e.g., the distinction between cervical and dorsal vertebrae, or the dermal armour arrangement.

4.1.1. Axial skeleton

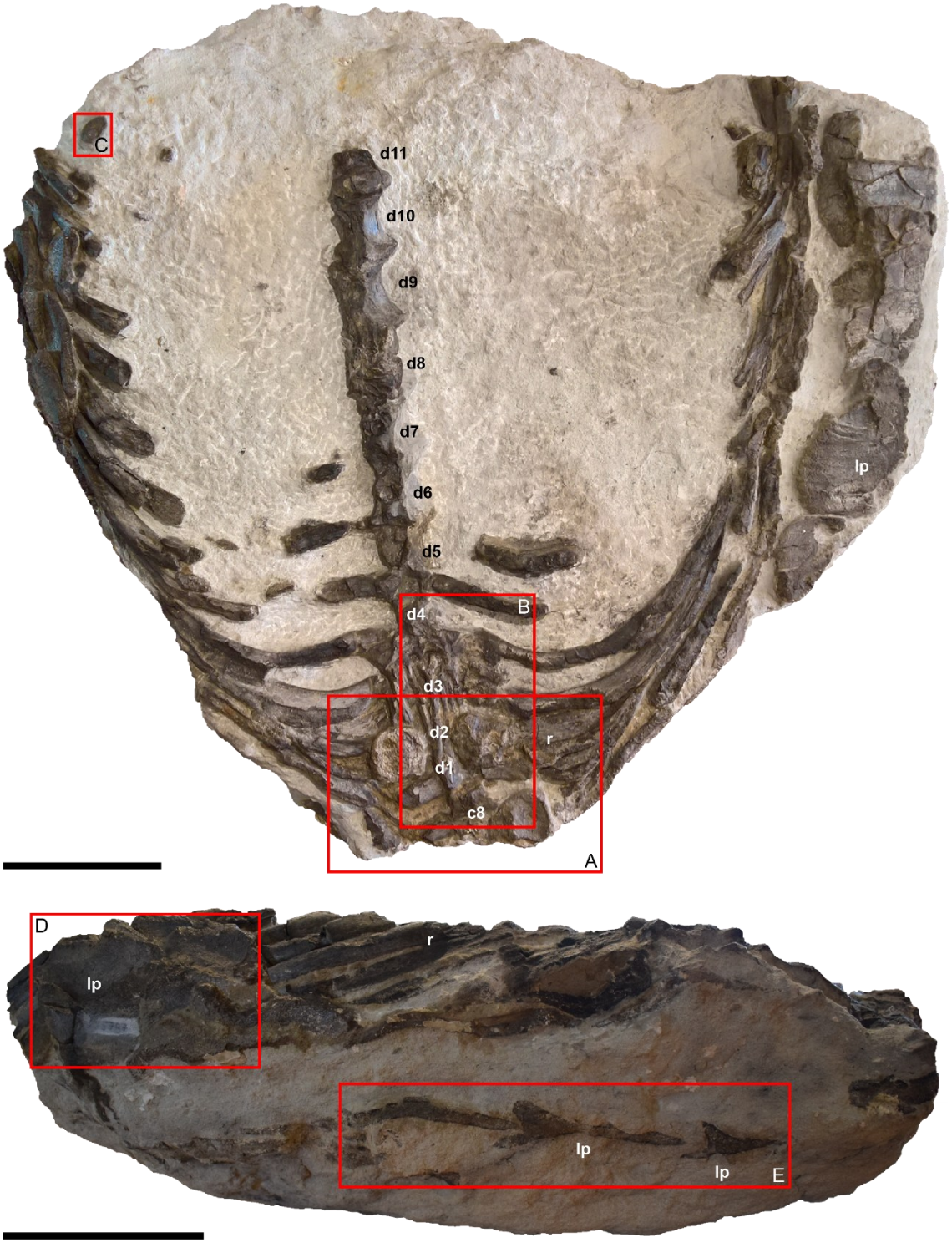

Figure 4.1.1.1. Holotype (MG 5787) of *Dracopelta zbyszewskii*. Dorsal (top) and right anterolateral (bottom) views of the ribcage of *D. zbyszewskii*. Sections A-E in Figure 4.1.1.2. c8) cervical vertebrae 8, d1-d11) dorsal vertebrae 1-11, lp) lateral plate, r) rib. Scale bars: 15 cm.

Cervical vertebrae (Fig. 4.1.1.2). The last cervical, c8, is mostly preserved, the anterior articulation facet heavily eroded and broken off. It is only observable in dorsal view, located ventrally and immediately posterior to the first pair of keeled cervicodorsal osteoderms (Fig. 4.1.1.2.A). The approximate anteroposterior length is 42 mm. Its state of preservation makes it impossible to measure the exact width and height, but the vertebra is at least as wide as long. In dorsal view, it is comparable to c8 in NOVA-FCT-DCT-5556 (Figs. 4.2.2.1). This is typical for cervical vertebrae of ankylosaurs, the narrower centrum at its mid-point relative to the expanded articulation facets, making for an anteroposterior short, spool-shaped

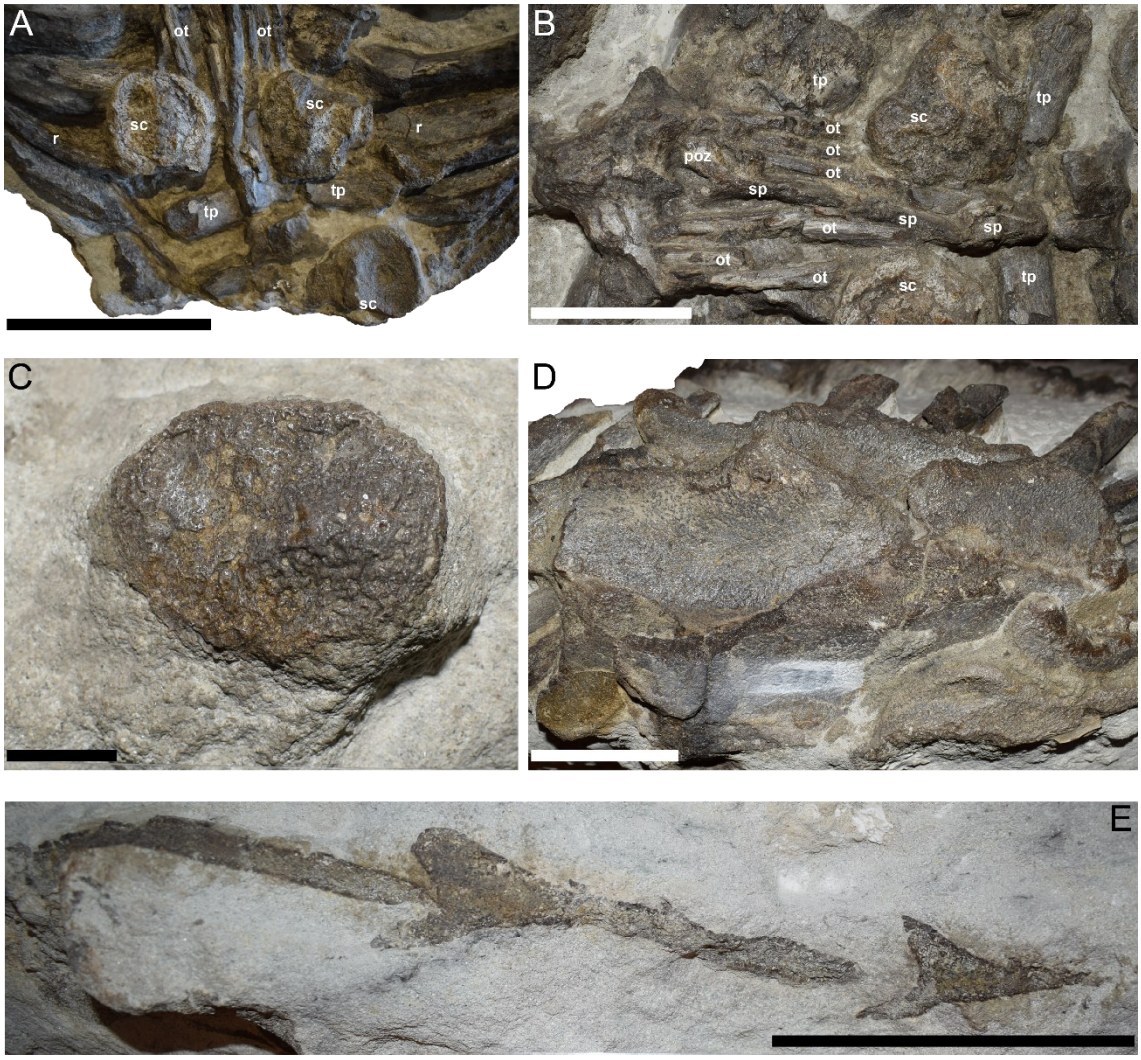

Figure 4.1.1.2. Details of the holotype (MG 5787) of *Dracopelta zbyszewskii*. A, B) dorsal view of the cervicothoracic region, with the paired keeled dorsal scutes (TR1AL, TR2AR-L) and underlying vertebrae c8 and d1-2, and ossified tendons; C) detail of thoracic distal osteoderm (T11…R?); D) right lateral view of lateral scutes. The dorsal keel is distinguished in the two scutes in the center of the image; E) anterior right lateral plates in cross-section. In E, note the dorsal keel in the two anteriormost plates. Abbreviations: ot - ossified tendon; poz – postzygaphysis; sc – scute; sp – spinous process; tp - transverse processes. Scale bars: 10 cm in A, E, 5 cm in B, D, and 1 cm in C.

vertebral body. The transverse processes (only the right process is visible) project laterally from the anterior articulation edge of the centrum, being autapomorphic for *Dracopelta*. The spinous process is broken at the base. The postzygapohyses are short, albeit only the right is clearly distinguishable. For a more detailed description of the cervical anatomy of *D. zbyszewskii*, see sub-chapter 4.2.1 of this dissertation.

Table 4.1.1.1. Measurements (in mm) of the vertebrae of *Dracopelta zbyszewskii* holotype (MG 5787). N/O) not observable; c) cervical; d) dorsal vertebrae. Numbers after vertebrae indicate position of vertebrae in the series (e.g., c8 = cervical vertebra 8).

Vertebra	Length	Width	Height
c8	42	N/O	N/O
d1	63	N/O	N/O
d2	70	N/O	N/O
d3	70	N/O	N/O
d4	70	N/O	N/O
d5	65	N/O	N/O
d6	70	N/O	N/O
d7	70	N/O	> 40
d8	70	N/O	> 30
d9	70	N/O	> 30
d10	65	40	> 30

Dorsal vertebrae (Figs. 4.1.1.1-2). The first eleven dorsal vertebrae (d1-11) are partially complete (Fig. 4.1.1.1). Apart from vertebrae d1-4, the vertebral centra are the only remaining elements preserved. In all vertebrae, the neural spines have been eroded away. In vertebra d10, the neural canal is still visible (Fig. 4.1.1.1). The centra are spool-shaped, i.e., wider at the articulation facets and narrower mid-centra, and generally increase in anteroposterior length along the anterior dorsal series (Fig. 4.1.1.1; see Tables 4.1.1.1 and 4.2.2.2 for comparison with NOVA-FCT-DCT-5556). The first four dorsal vertebrae are the best preserved, with the wing-like, laterally projecting transverse processes preserved (Figs. 4.1.1.1-2A, B). However, they are clearly visible only in d2, showing a slight anterior and dorsal orientation. As observed throughout Ankylosauria, the dorsal orientation is not as

pronounced as in more distal dorsal vertebrae, where the transverse processes project more pronouncedly dorsally, and the parapohysis migrate towards a more dorsal position, fusing with the transverse processes. Vertebra d3 shows the postzygapophyseal facets facing ventrolaterally, and the transverse processes are overlain by a pair of semicircular keeled ossicles (Figs. 4.1.1.2A, B). In vertebra d4, only the left transverse process is preserved. The breaking and anteriorly slanted position of the ribs suggests that they were not fused (at least not entirely) to the centra (Figs. 4.1.1.1-2A). Fusion of the rib to the centrum is known to variably occur along the dorsal series, more anteriorly in *Euoplocephalus* and *Ankylosaurus* (Coombs Jr, 1986; Vickaryous *et al.*, 2004). Comparing with NOVA-FCT-DCT-5556 (see subchapter 4.2.2 for further details), where completely fused ribs occur from vertebra d11 and posterior, it is plausible to infer that anterior dorsal vertebrae in *Dracopelta* were separated from the corresponding ribs. Six ossified tendons are present between vertebrae d1 and d4, lateral to the neural spines and dorsal to the centra and transverse processes, in bundles of three on each side. The presence of these overlapping ossified tendons, and a second, more laterally located bundle of overlapping three tendons on each side (present in NOVA-FCT-DCT-5556) is autapomorphic for *Dracopelta*.

Dorsal ribs (Figs. 4.1.1.1-3). Most of the ribs are fragmented and only preserve distally (Fig. 4.1.1.1). In total, there are nine left ribs and twelve right ribs, arching posteriorly. Taphonomic deformation has pressed the ribs together, and in most, they have been eroded away proximally (Fig. 4.1.1.1). The ribs are broadly arched and the more posterior ones, like rib 4, seem to have projected dorsolaterally from the lateral processes to form the typical, wide barrel-shaped ankylosaur trunk. Ribs 1-4 are the most complete, semi-articulated, having been rotated anteriorly from their original position (Figs. 4.1.1.1-2A). This anterior slanting, with only one side presently visible, paired with the heavily eroded exposed surfaces, makes a conclusive observation of the proximal cross-section difficult. However, the presence of posteriorly directed horizontal dorsal flanges of the shaft confers a typical L to T-shaped proximal cross-section to the ribs. Across Ankylosauria, this proximal cross section shows slight morphological variations, depending on the position of the rib on the dorsal series and location on the shaft (e.g., (Eaton Jr, 1960; Blows, 1987, 2015; Kirkland and Carpenter, 1994; Carpenter, 2004; Vickaryous *et al.*, 2004; Kilbourne and Carpenter, 2005; Kirkland *et al.*, 2013; Yang *et al.*, 2013; Kinneer *et*

al., 2016; Maidment *et al.*, 2021). In *D. zbyszewskii* the first dorsal rib is dorsoventrally taller than the rest (Fig. 4.1.1.2A), with a posterior dorsal flange, conferring an L-shaped in proximal cross-section (see also rib description of NOVA-FCT-DCT-5556 in subchapter 4.2.2). Distally, the flanges taper to make a more triangular cross-section, which becomes elliptical distally (Fig. 4.1.1.3).

Figure. 4.1.1.3. Dorsal ribs of the holotype of *Dracopelta zbyszewskii*. Fragment of right dorsal ribs, in dorsal view (top) and proximal cross section (bottom). The triangular cross section of the rib is visible. Note: this material does not yet have an inventory number, but is under the institutional abbreviation MG, associated and as part of the holotype. Scale bar: 2 cm.

4.1.2. Appendicular skeleton

Hind limbs

Femur (Fig. 4.1.2.1). Only the right distal end is preserved. The anterior surface is covered by sediment. The posterior surface is observable. However, anatomical structures are difficult to distinguish, either because they have been eroded away, such as both condyles, or obscured by sediment. It is greatly expanded mediolaterally, measuring approximately 15 cm. Although the exact position of the condyles is hard to define, a comparison with the right femur of NOVA-FCT-DCT-5556 (Fig. 4.2.3.4) makes it clear that the lateral epicondyle in this specimen is similarly well-developed. It tapers out proximally, likely functioning as a lateral buttress for the collateral ligament attachment surface. The shaft is broken, and its cross-section is oval (Fig. 4.1.2.1). The medullary cavity is filled with sediment and occupies approximately 80% of the section area. The cortical bone layer is thicker on the medial edge of the shaft than on the lateral edge, where it is approximately 50% thinner.

Figure 4.1.2.1 (previous page). Right femur of the holotype of *Dracopelta zbyszewskii*. Posterior view (bottom) of the right femur of *D. zbyszewskii* and cross section in proximal view (top) of the femoral shaft. Note: this material does not yet have an inventory number, but is under the institutional abbreviation MG, associated and as part of the holotype. Abbreviations: lec – lateral epicondyle; mdc – medullary cavity; oss – ossicle; ot – ossified tendon. Scale bar: 5 cm.

Tibia and fibula (Fig. 4.1.2.2). The tibia and the proximal and distal ends of the fibula are articulated. The latter is fused distally to the tibia, while the proximal end and the fibular shaft are broken and separated into smaller fragments. The tibia is broken at both ends (Fig. 4.1.2.2A-C), measuring 29 cm. The proximal end is comparatively more complete than the distal end, which is missing its medial corner, and is conspicuously broadened mediolaterally (Fig. 4.1.2.2A, B), while proximally it expands anteroposteriorly, slightly twisting the tibial shaft (Fig. 4.1.2.2A, D). There are two fibular shaft fragments broken, with a subcircular cross section.

Figure 4.1.2.2 (previous page). Right tibia and fibula of the holotype of Dracopelta zbyszewskii. Anterior (A), posterior (B), medial (C), proximal (D), and distal (E) views of the right tibia. Note: this material does not yet have an inventory number, but is under the institutional abbreviation MG, associated and as part of the holotype. Abbreviations: f - fibula. Scale bar: 10 cm.

Autopodium (Fig. 4.1.2.3, Table 4.1.2.1). The articulated autopodium, described by Pereda-Superbiola *et al.* (2005) as putatively a right manus, is here reinterpreted as a right pes, based on comparable material, known manual and pedal phalangeal formulas (Table 4.1.1.2), and the presence of other right hindlimb elements, namely a partial femur (Fig. 4.1.2.1), and tibia and fibula (Fig. 4.1.2.2).

Figure 4.1.2.3. Autopodium (MG 3) of *Dracopelta zbyszewskii*. Right pes of *D. zbyszewskii* in ventral (palmar) view. Abbreviations: mt – metatarsal. Scale bar: 5 cm.

The specimen is visible only in ventral (palmar or flexor) view (Fig. 4.1.2.3). It consists of twelve autopodial elements, identified as the distal ends of metatarsals II-IV, and nine phalanges, including two unguals broken distally. All the elements show a varying degree of surface damage (Fig. 4.1.2.3). The metatarsals are incomplete, broken proximally. Digits II and III are complete, while digit IV is missing at least one phalanx. The impressions on the sediment of missing pieces of metatarsals II and III are indicative that at least these were more complete when found (Fig. 4.1.2.3). The metatarsals are heavily damaged on the ventral surface. The distal trochlear surfaces of metatarsals II and III are covered by the first phalanges. Digit II is composed of the distal end of metatarsal II and phalanges 1-3 (Fig. 4.1.2.3). Metatarsal II is slightly more proximal to the other two and is eroded medially. It is wider at the distal end, and it has a sub-rectangular/reniform cross section, where it is also visible the slight concavity of the ventral surface. Metatarsal II is more robust than metatarsals III and IV. Phalanx II-1 is damaged proximally as well as at both condyles (Fig. 4.1.2.3). It is slightly longer than wide. The ventral surface is rugose proximally and pronouncedly concave, as the well-developed distal articulation expands dorsoventrally. Phalanx II-2 is disc-shaped, and slightly

dislocated medially relative to the long axis of phalanx 1, exhibiting a rugose edge (Fig. 4.1.2.3). Phalanx II-3 is the ungual and is dorsoventrally flat. It is longer than wide (>50 x 35 mm), and it is broken distally. A faint proximal lip is discernible, and immediately distal to it, there is a depressed area with a raised centre (the "eye-shaped ventral rugosity" of Pereda-Suberbiola *et al.*, 2005). The ventral surface of the ungual shows small longitudinal grooves and pits, which may represent anchorage structures for the keratinous claw (Norman, 2020a). It narrows distally to a likely blunt, rounded end (Fig. 4.1.2.3). Digit III consists of the distal end of metatarsal III and phalanges 1-4, a formula identified in most other ankylosaurs (Table 4.1.2.1). In cross-section, metatarsal III is sub-pyriform and thinner dorsoventrally than metatarsal II. Similar to the latter, the ventral surface is slightly concave, and the distal end is wider than the shaft. Distally, phalanx III-1 covers the articulation facet of metatarsal III. Phalanx III-1 is as long as wide, showing a deep concavity on the ventral surface (Fig. 4.1.2.3), limited proximally by a conspicuous rugose articular surface, and distally by a smooth articular surface with pronounced ventrally projecting distal condyles. Medially dislocated relative to III-1, phalanx III-2 is proximodistally flat (disc-shaped) and has a rugose margin. Phalanx III-3 is barely visible, mostly obscured by III-2 and the ungual (Fig. 4.1.2.3), but, as phalanx III-2, is disc-shaped. The ungual, phalanx III-4, is dorsoventrally flat and longer than wide (> 35 x 30 mm) but is broken distally. Therefore, the unguals of *Dracopelta* are the longest phalanges of the pes, which agrees with previous observations of ankylosaur pedes (e.g., Maleev, 1956; Ostrom, 1970; Coombs, 1986; Xu *et al.*, 2001; Carpenter *et al.*, 1995, 2011; Kirkland *et al.*, 2013). It is wider proximally and gradually narrows distally to a probable rounded end. Ventrally, at the proximal edge of the palmar surface, there is also an elliptical depression with a mediolaterally elongated raised bump, as in II-3 (Fig. 4.1.2.3). More distally, approximately halfway between the proximal ventral depression and the broken distal edge, two shallow ventral grooves, located medially to the lateral and medial margins of the ungual, are discernible (Fig. 4.1.2.3). Digit IV is the smallest of the three digits, with two phalanges as well as the distal end of metatarsal IV. The sub-pyriform cross-section of the metatarsal is overall similar to metatarsal III, dorsoventrally thicker laterally and thinning medially, where it is more eroded. On the ventral surface, the lateral thickening is visible and corresponds to the lateral condyle and its proximal prolongment. Albeit the medial counterpart has been

eroded, both would define the ventral surface concavity, as observed also in metatarsals II and III. In metatarsal IV, the medial and lateral edges are the most asymmetrical, as in the laterodistal corner there is small, protruding spur (Fig. 4.1.2.3). This is different than the lateral spur of *Saichania chulsanensis* figured by Carpenter *et al.* (2011:61, Fig. 15), which is medially oriented. The articulation surface of metatarsal IV is also oriented distally and laterally, and located slightly more proximally relative to the other metatarsals, differently than the distally facing articulation of the metatarsals II-III. The outwards orientation of the articular surface of metatarsal IV is similar to what is observed in metatarsals IV of other ankylosaurs, such as *Stegouros elengassen*, *S. chulsanensis*, *Dyoplosaurus acutosquameus*, or *Sauropelta edwardsorum* (Ostrom, 1970; Arbour *et al.*, 2009; Carpenter *et al.*, 2011; Soto-Acuña *et al.*, 2021), whereas metacarpals usually exhibit distally oriented, aligned articulation facets. The first phalanx, IV-1, is the shortest phalanx I in the pes, almost twice as wide as long, consistent with observations in other ankylosaurs (Coombs, 1986; Arbour *et al.*, 2009; Carpenter *et al.*, 2011; Currie *et al.*, 2011; Soto-Acuña *et al.*, 2021). Proximally, a distinct lip defines the edges of the articular facet. Immediately distal to it, the palmar surface is slightly concave, limited distally by a lip of the distal articular surface. This surface exhibits a pronounced medial depression, giving phalanx 1 an overall butterfly outline in ventral view (Fig. 4.1.2.3). Phalanx 2 is disc-shaped, with a proximal articular surface showing a medial rise that matches exactly with the distal articular medial depression of phalanx 1. There is a rugose outer rim like in phalanges II-2 and III-2. It is unknown if the phalangeal formula for digit IV would be 3 or 4. Based on the fact that most other known ankylosaur pedes have at least four phalanges in digit IV (Table 4.1.2.1), it is probable there would be a second disc-shaped phalanx (phalange 3) followed by an ungual, therefore resulting in a pedal formula of ?:3:4:4:?. Anatomically, the autopodium of *Dracopelta* is consistent to what is observed in the pedes (rather than the manus) of other ankylosaur taxa, such as *S. edwardsorum*, *S. elengassen*, *S. chulsanensis*, *P. grangeri*, *D. acutosquameus*, *Z. lishuiensis*, or *E. carbonensis* (Ostrom, 1970; Carpenter, 1984; Lü *et al.*, 2007; Arbour *et al.*, 2009; Carpenter *et al.*, 2011; Currie *et al.*, 2011; Kirkland *et al.*, 2013; Soto-Acuña *et al.*, 2021). The existence of digits I and IV is unknown, but the plesiomorphic phalangeal count is two phalanges in digit I and none in digit IV

Table 4.1.2.1. Manual and pedal phalangeal formulas of Ankylosauria. Comparative non-ankylosaur taxa are represented by the early diverging ornithischian *Lesothosaurus diagnosticus*, the early-diverging thyreophoran *Scutellosaurus lawleri*, and the early diverging stegosaurian *Huayangosaurus taibaii*. Numbers in parenthesis are minimum estimates of phalangeal count. (?) is unknown phalangeal count. (-) is unknown autopodial for the taxa.

Taxa	Manus	Pes	References
Lesothosaurus diagnosticus	2:3:4?:3?:0	2:3:4:5:0	Baron *et al.*, 2017
Scutellosaurus lawleri	-	(2:3:4:5:0)	Colbert, 1981; Breeden and Rowe, 2020; Breeden *et al.*, 2021
Huayangosaurus taibaii	-	0:2:2:2:0	Pereda-Superbiola *et al.*, 2005; Maidment *et al.*, 2010; Currie *et al.*, 2011
Scelidosaurus harrisonii	2:3:4:3:2	2:3:4:5:0	Norman *et al.*, 2004; Norman, 2019
Stegouros elengassen	2:2:?:?:?	2:3:4:5:0	Soto-Acuña *et al.*, 2021
Dracopelta zbyszewskii	-	?:3:4:(3):?	Pereda-Superbiola *et al.*, 2005; Currie *et al.*, 2011; this study
Euoplocephalus tutus	-	0:3:4:4:0	Currie *et al.*, 2011; Carpenter *et al.*, 2013
Liaoningosaurus paradoxus	2:3:3:2:2	-	Xu *et al.*, 2001; Zheng, 2018; Xiaobo and Reisz, 2019; Zheng and Xu, 2019
Niobrarasaurus coleii	-	2:3:4:4/5:0	Mehl, 1936; Carpenter *et al.*, 1995
Nodosaurus textilis	-	2:3:4:4:0	Lull, 1921; Carpenter and Kirkland, 1998
Pinacosaurus grangeri	2:3:3:3:2	0:3:3/4:3/4:0	Currie *et al.*, 2011
Ankylosauridae indet. MPC-D 100/1359	-	0:3:3:3:0	Park *et al.*, 2021
Saichania chulsanensis	Pentadactyl?	0:3:3:3?:0	Carpenter *et al.*, 2011; Currie *et al.* (2011); Arbour *et al.*, 2014; Arbour and Currie, 2016
Anodontosaurus lambei	-	0:3:4:5:0	Coombs, 1986
Talarurus plicatospineus	2:3:3:3:2	2:3:4:5:0	Maleev, 1956
Zhejiangosaurus lishuiensis	-	?:3:4?:5?:?	Lü *et al.*, 2007; Currie *et al.*, 2011; Arbour and Currie, 2016
Dyoplosaurus acutosquameus	-	0:3:4:4:0	Parks, 1924; Arbour *et al.*, 2009;
Jinyunpelta sinensis	(1):(1):(1):?:?	-	Zheng *et al.*, 2018
Scolosaurus cutleri	-	0?:?:3:?:0?	Nopcsa (1928); Penkalski and Blows (2013)
Shamosaurus scutatus	Pentadactyl?	-	Vickaryous *et al.*, 2004
Panoplosaurus mirus	2:3:3:0?:0?	-	Carpenter, 1990; Lambe, 1919; Sternberg, 1921
Sauropelta edwardsorum	2:3:4:3:2/3	2:3:4:5:0	Ostrom, 1970; Carpenter, 1984

(Table 4.1.2.1), and considering the age and preservation of *Dracopelta*, the most parsimonious hypothesis is that digit I had been present and it was lost.

4.1.3. Dermal armour

The holotype of *D. zbyszewskii* (MG 5787) is heavily eroded dorsally and therefore its thoracic armour has been lost, apart from a few sparse, preserved osteoderms (Figs. 4.1.1.1-2). The lateral and distal elements (*sensu* Burns and Currie, 2014), i.e. scutes and plates, are better preserved and more abundant (Figs. 4.1.1.1-2D, 4.1.3.1-2). Nonetheless, at least three osteoderm major morphotypes can be recognized, based on their size, shape, and location. The first morphotype corresponds to the smallest elements, the ossicles, up to 7 cm, subcircular or ellipsoidal, and can be divided into two subtypes: subtype I, consisting of large-sized (≈ 6 cm), sub oval paired cervicothoracic ossicles, and subtype II, smaller (≈ 3 cm), thoracic subcircular ossicles, covering the dorsum in parasagittal rows (see also description of dermal armour of NOVA-FCT-DCT-5556 in subchapter 4.2.2, Figs. 4.2.2-3, 4.2.2.1, 3, 4.2.4.1-3). Subtype I ossicles are the largest and in *Dracopelta* are restricted to the medial cervicothoracic region (Fig. 4.1.1.2A, B). Three elements are preserved but there were two pairs of osteoderms, confirmed in NOVA-FCT-DCT-5556 (Figs. 4.2.2, 4.2.2.1) and corresponding to TR1AR-L and TR2AR-L (see sub-section 2.1.1 Material and Methods, for details on the dermal armour nomenclature system used in this work). The ossicles are located medially, dorsal to the transverse processes of cervical vertebra 8 (c8) and dorsal vertebra 2 (d2). In dorsal view, the transverse processes of the first dorsal vertebrae (d1) are visible between the pairs (Fig. 4.1.1.2A). The anterior osteoderm is a left ossicle, of which approximately the posterior half is preserved, and is 6 cm in width. It is asymmetric, with the posterolateral corner extending further posteriorly. There is a pronounced anteroposterior median keel, and the rim is thickened (Fig. 4.1.1.2A). The osteoderms of the second row are ossicles 5 cm in diameter, with an eroded, external surface. The left ossicle is broken on its posterior rim, while the right is missing its anterior rim. There is a median keel and slightly thickened rims, although not as pronounced as in the anterior pair (Fig. 4.1.1.2A). These two pairs of transitional osteoderms are autapomorphic for *Dracopelta*. Subtype II ossicles consist of three elements, one *in situ*, a right posterior thoracic osteoderm preserved in the holotype specimen MG 5787 (Fig. 4.1.1.2C). It is ellipsoidal in shape,

measuring 3 by 2 cm, with a slightly raised centre. The external surface is rugose, with small, millimetric pits. This osteoderm possibly is the lateralmost ossicle in band eleven, the posteriormost of the series. Its exact position along the row is uncertain though, as in NOVA-FCT-DCT-5556 this part is lost, so the exact number of osteoderms is unknown, although in NOVA-FCT-DCT-5556 the thoracic rows seem to have at least four subtype II ossicles each (Figs. 4.2.2-3, 4.2.2.3, 4.2.4.1). Therefore, according to the nomenclatural scheme used herein, this would be T11(D-E?)R. Two other ossicles are preserved with the distal end of the right femur. One is only partially complete, the other is a complete semicircular ossicle, 3 cm in diameter, lodged between the femur and an ossified tendon (Fig. 4.1.2.1). It is dorsoventrally flat, with a faint central raised bump. Based on its morphology, and by comparing with specimen NOVA-FCT-DCT-5556 (Figs. 4.2.2, 4.2.2.3), these were from a more medial position than the element observed in Figure 4.1.1.2E, but their exact location is unknown.

A second morphotype is represented by larger, subelliptical or subrectangular, keeled osteoderms (Figs. 4.1.1.1-2D, 4.1.3.1), the scutes of Blows (2015). These are from a more distal position than the smaller ossicles, showing that the osteoderms increased in size distally along each parasagittal band of armour, which can also be observed in specimen NOVA-FCT-DCT-5556 (Fig. 4.2.2; see also description in sub-chapter 4.2.4). Two subtypes of scutes can be distinguished: subtype I, smaller (≈ 10 cm in length), dorsoventrally flat, with a medially offset low keel (Fig. 4.1.3.1), and subtype II, large-sized scutes (>10 cm), exhibiting a well-developed midline keel (Fig. 4.1.1.1-2D). Subtype I is represented by two, isolated, slightly overlapping subrectangular osteoderms (Fig. 4.1.3.1). These measure 10 cm in length and 7 cm in width. There is a well-developed external keel, which crosses obliquely the surface of the osteoderm, from the anteromedial corner to the middle of the posterior rim, dividing the external surface asymmetrically (Fig. 4.1.3.1A, C). As in the cervicothoracic transitional medial ossicles, the rim is thickened, so that the external surface lateral to the keel has a shallow depression. The external surface (Fig. 4.1.3.1A) exhibits a reticular pattern of neurovascular grooves (*sensu* Hieronymus *et al.*, 2009). The second osteoderm is partially overlapped by the first, and is broken posteriorly and medially, at the keel, which can only be identified by the rising surface (Fig. 4.1.3.1B). A comparison with NOVA-FCT-DCT-5556 allows to identify these osteoderms as left lateral scutes, and as a

transitional morphotype between the smaller, more medial ossicles, and the larger, more distal scutes which transition laterally to the lateral plates. Subtype II is represented by six left scutes and at least four right scutes (Figs. 4.1.1.1-2D). The latter overlap laterally and anteriorly the immediately adjacent lateral and posterior scutes, although, based on their relative position to each other and the ribcage, and by comparison with NOVA-FCT-DCT-5556, this arrangement is likely taphonomical. The osteoderms are heavily eroded and broken laterally, and at the same time have been imbricated and compressed together, making harder the identification of most individual elements and its exact boundaries. The midline dorsal keel is well developed but is eroded and broken, although distinguishable on only three elements. The largest element measures 14 cm anteroposteriorly and exhibits a pitted concave dorsal surface with anastomosing neurovascular grooves (Fig.

Figure 4.1.3.1. Left thoracic distal osteoderms from the holotype of *Dracopelta zbyszewskii*. Dorsal (A) and posterior (B) views of two subtype I scutes of the holotype of *D. zbyszewskii*. The external keel is visible in A and in posterior profile in B. C shows a detail of the keel in anterodorsal view. Scale bars: 5 cm in A, B, 2 cm in C. Note: this material does not yet have an inventory number, but is under the institutional abbreviation MG, associated and as part of the holotype.

4.1.1.2D) (*sensu* Hieronymus *et al.*, 2009). The six scutes on the left side are more individualized (Fig. 4.1.1.1), although still showing some posterior overlap. These are the largest dermal elements preserved, with the largest measuring 20 cm anteroposteriorly. However, the osteoderms are eroded and broken at the edges, and therefore incomplete and slightly shorter than they would be. The smooth external surface is heavily fractured, but an anastomosing neurovascular groove network is visible (Hieronymus *et al.*, 2009). The two most anterior scutes have the external surface facing anterolaterally, while the other four are closer to their original position, with the external surface facing dorsolaterally. This is likely due to taphonomy. In the two most posterior scutes, more visible in the posterior one, there is a well-developed keel, medially dislocated. The position of these scutes relative to the ribcage and comparison to the right side seem to indicate they would be in an immediately more distal position relatively to the scutes from the right, although this is hard to confirm due to the incompleteness and taphonomical remobilization of the elements.

A third morphotype consists of dorsoventrally flat, lateral plates, (Fig. 4.1.1.2E). Five are identifiable in cross section in articulation, on the right side of the holotype, but only the three most anterior ones are well visible. Isolated plate fragments are also identifiable (Fig. 4.1.3.2A-C). The cross-section is comparable to the cross-section of the largest dermal elements of NOVA-FCT-DCT-5556 (Fig. 4.2.4.3), with a pronounced posterior dorsal keel, and thinning out towards the anterior and posterior edges (Fig. 4.1.1.2E). The largest plate measures 14 cm anteroposteriorly, while the smallest, the most anterior, is 8 cm. The latter has a flat ventral surface and well-developed dorsal keel, slightly dislocated posteriorly relative to the middle, which is more vertical and sharper edge than the following plate (Fig. 4.1.1.2E). The immediately following plate has a slightly concave ventral surface and a prominent dorsoposteriorly projecting dorsal keel, with a round dorsal edge, located on the posterior half of plate. The third plate shows a similar ventral concavity to the second plate. However, the posterior half of the dorsal surface is broken, precluding the identification of a dorsal keel. In the first and second lateral plates, the cross section allows to observe an alignment of the sharp anterior edge with a posterior groove, suggesting an interlocking fit between adjacent plates. Similar morphology for lateral cervical and cervicothoracic armour is observed in ankylosaurs like *Gastonia*

burgei, *Gargoyleosaurus*, *Mymoorapelta*, or *Polacanthus* (Kirkland and Carpenter, 1994; Kirkland *et al.*, 1998; Kilbourne, 2005; Blows, 2015; Kinneer *et al.*, 2016).

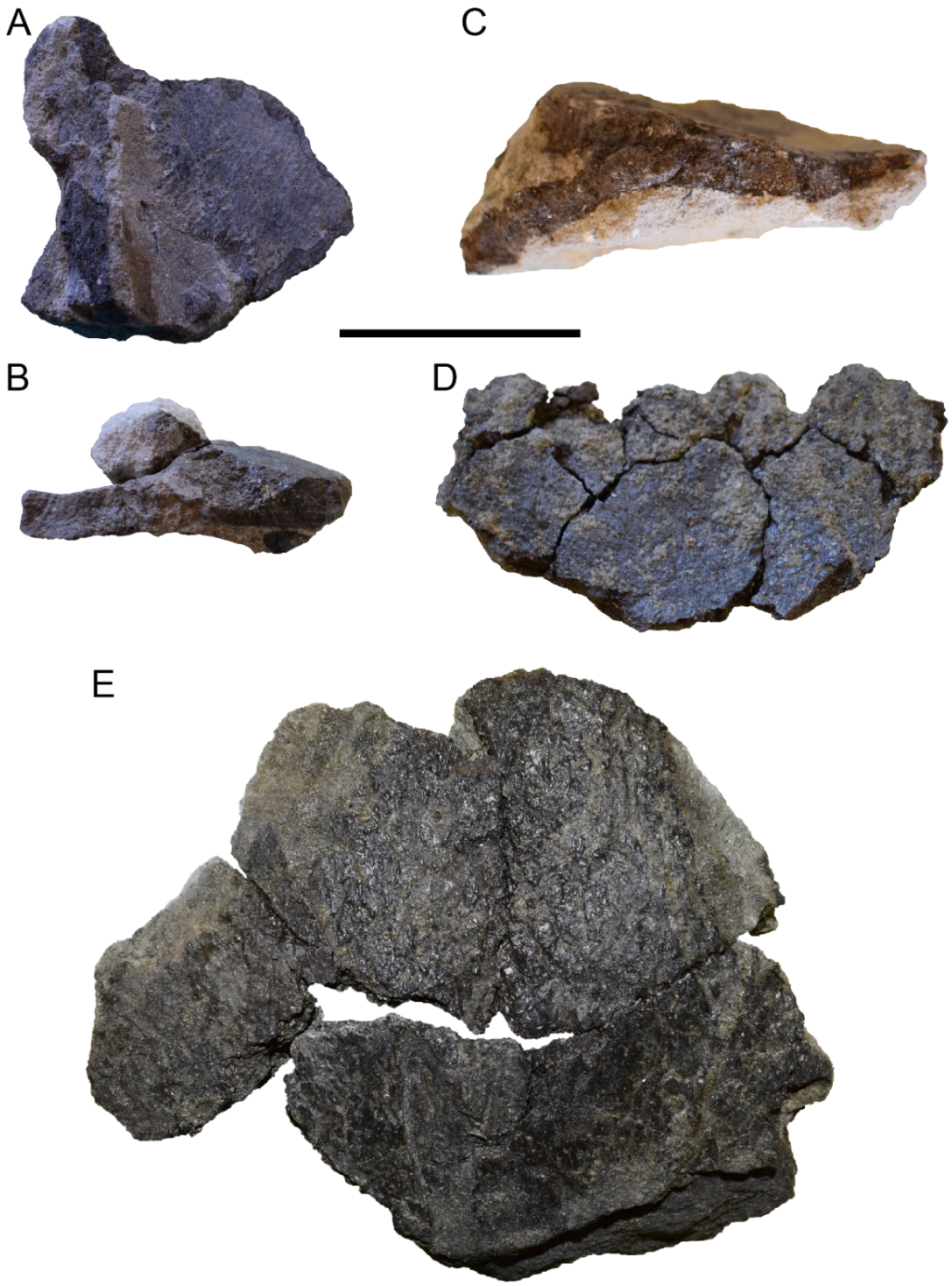

Figure 4.1.3.2. Osteoderms of the holotype of Dracopelta zbyszewskii. Isolated osteoderm fragments from D. zbyszewskii. A, B) lateral plate fragment. Dorsal view in A, with keel facing dorsally and covered by sediment; cross-section in B shows the dorsal keel rising from the base. C) cross-section of lateral plate, dorsal keel projecting from the curved base. D, E) fragments of osteoderms (possibly subtype II scutes). Scale bar: 5 cm. Note: this material does not yet have an inventory number, but is under the institutional abbreviation MG, associated and as part of the holotype.

4.1.4. Unidentified material

The unidentified material of the holotype (Figs. 4.1.4.1-4) varies in size from approximately 35 cm to <1 cm. There are over 100 elements, between unprepared blocks (>10 cm) and smaller fragments. The state of preservation of this material hinders the identification of most elements beyond some small rib and osteoderm fragments.

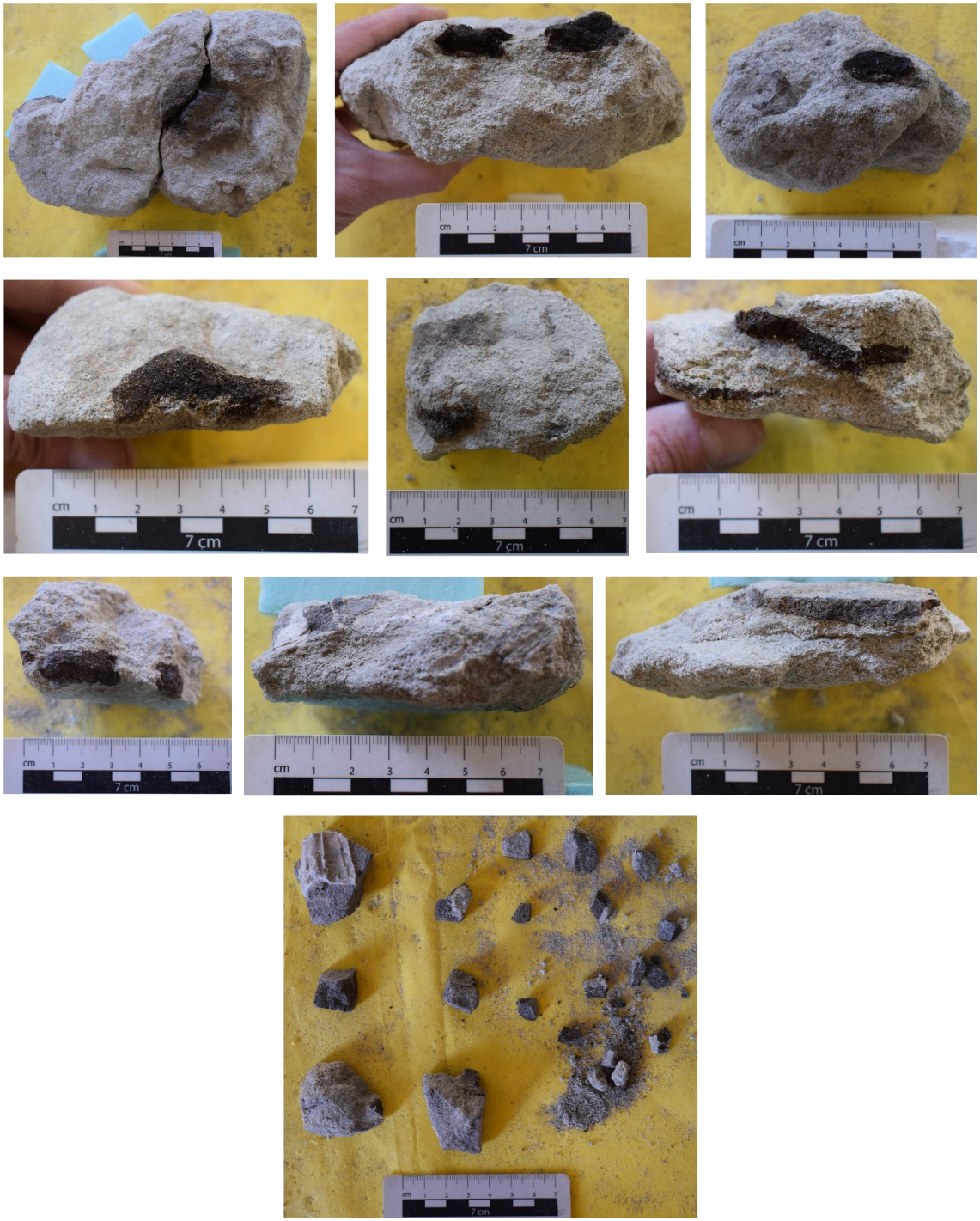

Figure 4.1.4.1. Assorted unidentified material. Smaller unprepared fragments that include some distal rib (top) and osteoderm (middle) fragments. This material does not yet have an inventory number, but is under the institutional abbreviation MG, associated and as part of the holotype.

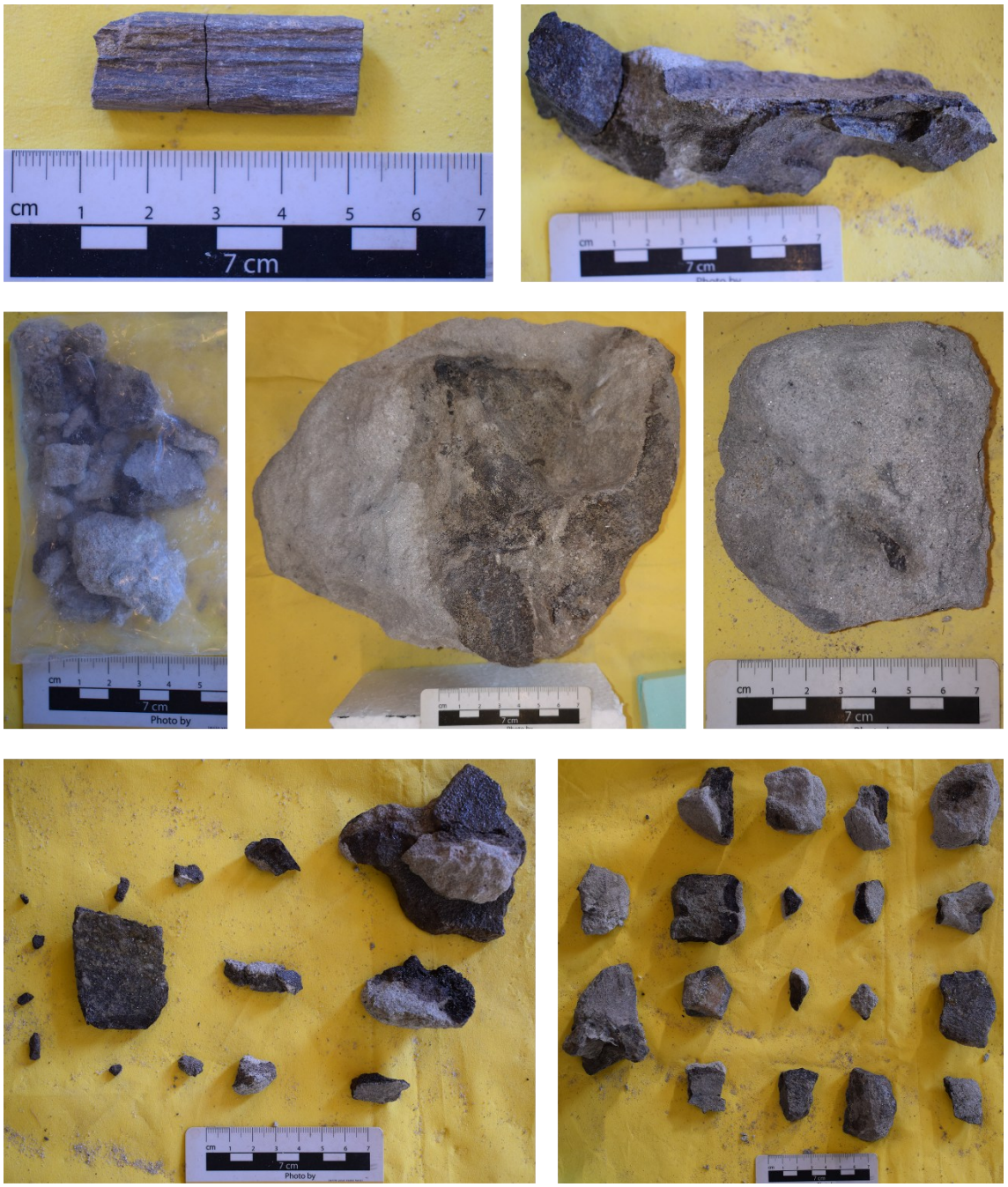

Figure 4.1.4.2. Assorted unidentified material. Fragments (top and bottom) and unprepared blocks (middle). this material does not yet have an inventory number, but is under the institutional abbreviation MG, associated and as part of the holotype.

Figure 4.1.4.3. Assorted unidentified material. Unprepared fragments and block (bottom). In the middle right there is an osteoderm fragment covered by the adhesive used in the preliminary preparation done in the 1960's. This material does not yet have an inventory number, but is under the institutional abbreviation MG, associated and as part of the holotype.

Figure 4.1.4.4. Assorted unidentified material. Unprepared blocks and fragments. In the middle right, fragments of ribs are observable. This material does not yet have an inventory number, but is under the institutional abbreviation MG, associated and as part of the holotype.

4.2. Description of NOVA-FCT-DCT-5556

NOVA-FCT-DCT-5556 is an articulated skeleton, over 50% complete, composed of most of the axial skeleton, pectoral and pelvic girdles, proximal appendicular elements, and dermal armour (Figs. 4.2.1-3, 4.2.1.1-2, 4.2.2.1-7, 4.2.3.1-4, 4.2.4.1-3, Tables 4.2.2.1-2). The axial skeleton consists of the skull, missing the anterior narial region of the rostrum, left dentary, at least 38 maxillary teeth in situ and one isolated tooth, complete cervical, dorsal and sacral series, with seven cervical vertebrae, 16 dorsal vertebrae (the last three dorsal fuse to form the presacral rod) and four true sacral vertebrae, 13 anterior caudal vertebrae (first caudal vertebra fuses to the sacrum, and last two disarticulated from the series), at least 40 ossified tendons, and 19 semi-articulated partial ribs and at least 29 rib fragments. Both the pectoral and pelvic girdles are partially complete and include, respectively, both scapulocoracoids, and ilia and proximal ends of the ischia and pubes. The appendicular elements consist of the right humerus and both femora. The dermal armour is mostly preserved in articulation and the osteoderms are the most abundant elements, which include the pelvic shield and over 190 osteoderms (at least 150 articulated). In addition, there are at least 100 unidentified bone fragments. In total, the specimen is composed of more than 400 elements.

Figure 4.2.1. Skeleton of *Dracopelta zbyszewskii* (NOVA-FCT-DCT-5556). Photo montage of specimen NOVA-FCT-DCT-5556 of *D. zbyszewskii* in ventral view, showing the articulation of the axial and appendicular elements. Cranial is to the left. Because the specimen was collected in separate blocks, this montage was obtained by positioning and stitching the blocks with articulating elements. Scale bar: 50 cm.

Figure 4.2.2. Skeleton of *Dracopelta zbyszewskii* (NOVA-FCT-DCT-5556). Photo montage of specimen NOVA-FCT-DCT-5556 of *D. zbyszewskii* in dorsal view, showing the articulation of the axial and appendicular element, as well as the distribution of dorsal dermal armour. Cranial to the left. Because the specimen was collected in separate blocks, this montage was obtained by positioning and stitching the blocks with articulating elements. Scale bar: 50 cm.

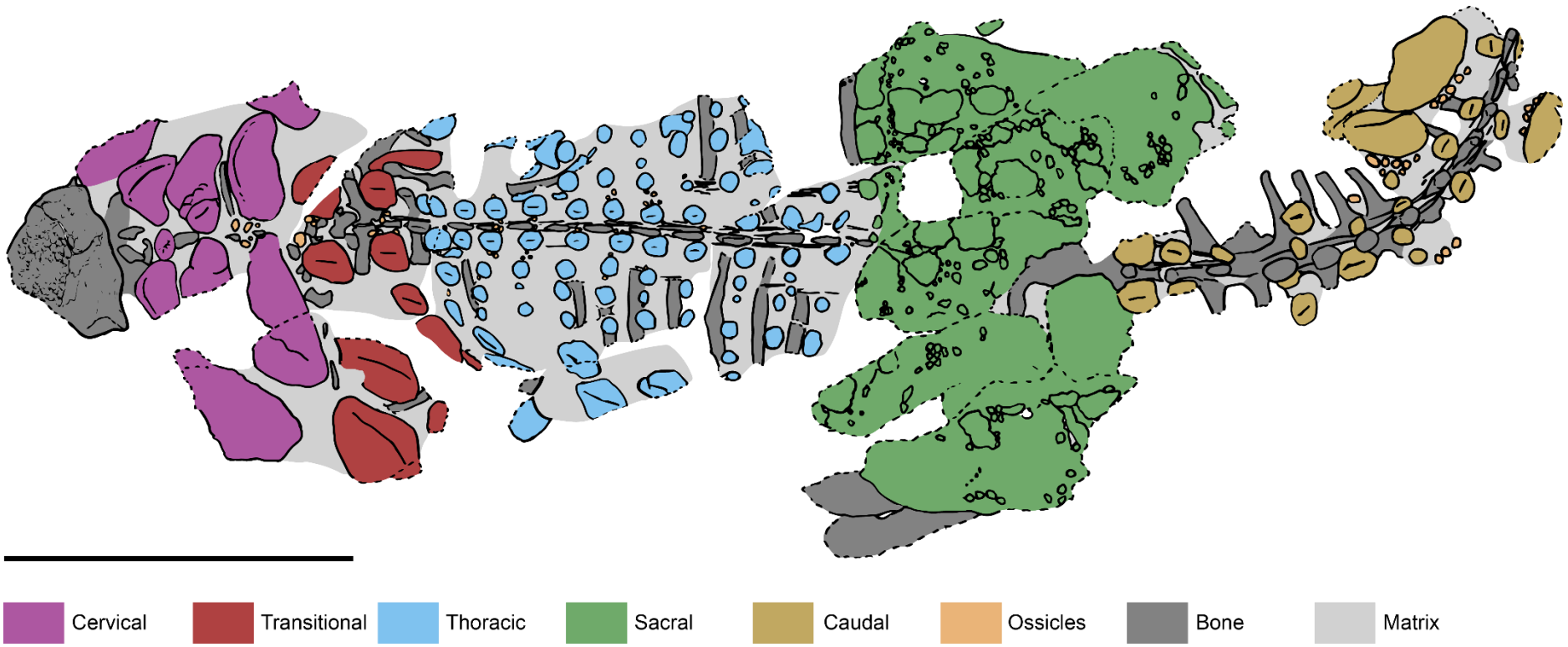

Figure 4.2.3. Schematic dorsal view of *Dracopelta zbyszewskii* (NOVA-FCT-DCT-5556). Line drawing of Figure 4.2.2 with dermal armour colour coded by region. Scale bar: 50 cm.

4.2.1. Skull

Skull (Fig. 4.2.1.1). This description will follow the division proposed by Vickaryous and Russell (2002) on topographic regions of the ankylosaur skull: rostral, temporal, palatal, occipital/basicranial, and mandibular. The skull is nearly complete, missing the anterior portion of the rostrum (i.e., the external nares and premaxilla) and the left lateral preorbital/rostral margin (Fig. 4.2.1.1A-D). In dorsal view (Fig. 4.2.1.1A), it is trapezoidal in shape, with an anteroposterior length of 24 cm, albeit total length of the skull would probably be about 20% longer (~29-30 cm), by comparison with the premaxillary region of *Gargoyleosaurus*. Anteriorly, the width of the rostral edge is 9 cm. However, because the left lateral surface of the rostral region is broken and comparing the right and left sides of the rostrum, the rostral edge approximately 10% wider (11-12 cm). Posterior to the rostral region, the skull is 24 cm in width, measured from the lateral edges of the orbits. Across the nuchal edge (Fig. 4.2.1.1E), the width is 23 cm. Since both lateral edges of the squamosals are broken (the left more complete than the right), and the presence of an osteodermal lateral projection, the squamosal horns, is highly likely, the posterior margin of the skull would be wider than at the orbits, resulting in the overall trapezoidal shape of the skull in dorsal view. The height of the skull, measured immediately anteriorly to the orbit, is 5 cm. The skull roof is flat and anteriorly sloped (Fig. 4.2.1.1C, D) and the dorsal surface is rugose and ornamented, with a combination of furrows, ridges, and a mosaic of small osteodermal bumps (Fig. 4.2.1.1A). The sutural contacts are indistinguishable, therefore precluding a thorough anatomical description of most of the bones. The obliteration of the sutures is due to a combination of i) bone remodeling, ii) cranial ornamentation, iii) ontogenetic stage, and iv) preservation of the specimen, with fracturing and sediment further masking the sutures.

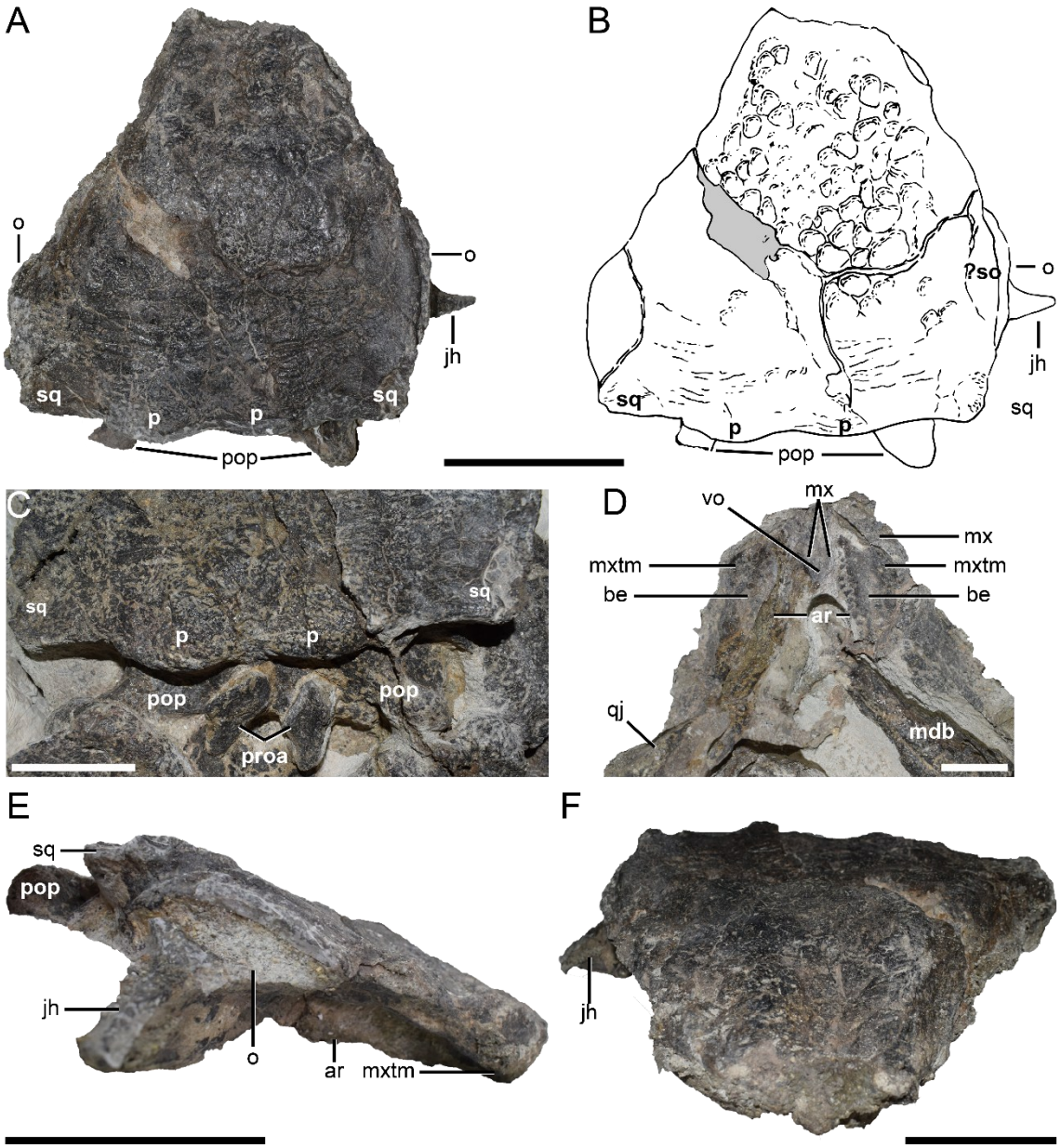

Figure 4.2.1.1. Skull of *Dracopelta zbyszewskii* (NOVA-FCT-DCT-5556). A) dorsal view and B) drawing of dorsal view of the skull of *D. zbyszewskii* (NOVA-FCT-DCT-5556). C) detail of the nuchal region and D) detail of anterior maxillary palate. E) right lateral and F) anterior views of the skull. In A, the asymmetrical pattern of caputegulae on the dorsal surface of the rostrum (also in F) as well as the transverse ridges on the parietal region are visible. Abbreviations: ar – alveolar ridge; be – buccal emargination; h – humerus; j – jugal; jh – jugal horn; mdb – mandible; mx – maxillary; mxtm – maxillary tomium; o – orbit; p – parietal; pop – paroccipital process; proa – proatlas; qj – quadratojugal; so – supraorbital; sq – squamosal; vo - vomer. Scale bars: 10 cm in A, B, and E, 5 cm in C, D, and F.

The rostral region is made up of maxillae, nasals, lacrimals, prefrontals (Vickaryous and Russell, 2002). The ornamentation is made up of slightly raised

centimetric polygonal caputegulae (Fig. 4.2.1.1A, D). In lateral view, the medially ins*et al*veolar ridge is visible (Fig. 4.2.1.1C). The maxillaries bend ventrally to form the maxillary tomial crests, which are restricted to the anterior portion, and taper posteriorly into the maxillary shelf. Anterior to the orbit, there is a horizontal shelf that extends posterolaterally from the maxillary rostrum which most likely represents the dorsolateral projection of the lacrimal, although the sutures are not observable, apart from a possible small segment of the contact between the posterior edge of the lacrimal and the anterior edge of the supraorbital, immediately anterodorsal to the orbit. The position of the lacrimal in NOVA-FCT-DCT-5556 is comparable to *Gargoyleosaurus*, where the lacrimal bends dorsolaterally to form a lateral ridge with the surface of the skull roof, albeit not nearly as shelf like as in NOVA-FCT-DCT-5556 (Kilbourne *et al.*, 2005; see also Carpenter *et al.*, 2001, on the skull of *Cedarpelta*, or Leahey *et al.*, 2015, on the skull of *Kunbarrasaurus*, where the lacrimal surfaces as a slender, vertical wedge-like element). Ventral to the rostral region, the palatal region (Figs. 4.2.1.1B, F) is composed of four bones: vomer, palatine, pterygoid, ectopterygoid (Vickaryous and Russell, 2002). Due to the position of the mandible and left humerus, which cover the posterior palate and most of the basicranium in ventral view, the vomer is the only observable element. The description of these elements is further hindered by the sediment covering it. Preparation is still ongoing, but the vaulted palate is discernible, with the choanae located in a slightly more posterior position. Relative to the tooth rows, the choanal recess is located medially and along the posterior half of tooth rows. Comparatively, in *Gargoyleosaurus*, this extends more anteriorly so that the anterior rim is almost parallel to the anteriormost maxillary tooth. Therefore, in NOVA-FCT-DCT-5556 the anterior secondary osseous palatal shelf, made up of the vomer, maxillaries, and premaxillaries (absent) continues slightly more posteriorly than in *Gargoyleosaurus*. It separates the buccal opening from the nasal chambers. Although difficult to individualize here, in ankylosaurs the anterior secondary palate is made up of the medial (or palatal) processes of the premaxillaries and maxillaries, and the vomer, which fuse together. In ventral view (Fig. 4.2.1.1F), a faint suture is visible where the maxillaries meet with the vomer along the sagittal plane. The vomer itself is a thin slither of bone in ventral view, although it is plausible to assume its projection dorsally, partitioning the internal nares. Its contribution to the nasal septum is

currently unknown. The vomerine keel is absent anteriorly, which could be due to erosion of the palatal surface since recent preparation has revealed an eroded surface of the vomerine keel protruding from the vaulted palate. Immediately lateral to the palate, the tooth rows are markedly inset medially, curving lateroposteriorly. At its narrowest, on the anterior end, the mediolateral distance between both rows is 33,84 mm, resulting in a very narrow anterior palate, while the distance between the lateralmost teeth, at the posterior end of the tooth rows, is 111 mm. Lateral to the tooth rows, on each side, there is a concave buccal emargination (*sensu* Vickaryous and Russell, 2002) that separates the tooth row from the maxillary tomium, which in turn separates the inner palate from the lateral margin of the maxilla. The buccal emargination is vaulted anteriorly (more pronounced than in *Gargoyleosaurus*) and it flattens gradually posteriorly into the maxillary shelf. The tomial crest bends slightly medially posteriorly, giving the buccal emargination a lanceolated shape, and arches medially at the anterior end, closing off the buccal emargination from the premaxillary palate (Fig. 4.2.1.1F). This condition is autapomorphic for *Dracopelta*, since in all other ankylosaurs the maxillary tomial crest conjoins with the premaxillary tomium. The absence of premaxilla in NOVA-FCT-DCT-5556 precludes the identification of the premaxillary tomium and it would join with maxillary tomium.

In the temporal region (*sensu* Vickaryous and Russell, 2003), the mosaic of caputegulae is cut by transverse furrows, arched slightly posteriorly, and extending nearly to the lateral edges (Fig. 4.2.4.A). It is the most fractured region of the skull, with a major fracture cutting diagonally across the frontoparietal surface to the left lacrimal/maxillary (Fig. 4.2.4.A). Coupled with the cranial dermal ornamentation and sediment cover, identification of most of the bones and distinction of possible suture lines from cranial ornamentation sulci is currently impossible. The orbits are elliptical, more so than in *Gargoyleosaurus*, measuring 59,46 mm anteroposteriorly, and 12,42 mm dorsoventrally, and are oriented laterally (Fig. 4.2.1.1C). The dorsal margins of the orbit are defined, in ankylosaurs, as in most other ornitischians, by the supraorbital complex, usually composed of three elements (presupraorbital, mesosupraorbital, and postsupraorbital), with the exception of *Kunbarrasaurus* (QM F18101) and possibly *Cedarpelta* (CEUM 12360), where only one element is present, seemingly fused together (Carpenter *et al.*, 2001; Vickaryous and Russell,

2002; Maidment and Porro, 2010; Leahey *et al.*, 2015). In NOVA-FCT-DCT-5556, this complex is hard to identify and whether it is composed of three articulated elements or a single fused element. Nonetheless, there is a conspicuous, laterally protruding dorsal supraorbital shelf, more visible over the right orbit (Fig. 4.2.1.1A, C), which likely represents the lateral exposure of the supraorbital, and delineates the dorsal rim of the orbital cavity. Immediately dorsal to the supraorbital shelf, there is an anteroposteriorly oriented supraorbital ridge that parallels the convex perimeter of the supraorbital shelf for approximately the anterior two-thirds of the orbit length. In the posterior one-third, this ridge straightens and extends into a crest posteriorly as the posterodorsolateral rim of the skull, seemingly into the lateralmost expression of the squamosal, and eventually merging with the squamosal horn. The postorbital is not identifiable. The squamosals are partially broken laterally but make up the posterodorsolateral corners of the skull. The right squamosal is seemingly broken medially along a potential suture line, as on the left side, a similar line is barely traceable. Because of this, and considering its presence in most ankylosaurs (e.g., Lee, 1996; Carpenter *et al.*, 1998; Vickaryous and Russell, 2002; Carpenter, 2004; Vickaryous *et al.*, 2004; Kirkland *et al.*, 2013; Arbour and Mallon, 2017; Penkalski and Tumanova, 2017; Park *et al.*, 2020), the expected squamosal horn is not present, and therefore its morphology cannot be assessed, although, inferring from the postorbital dorsolateral crest, it would be crested. Medial to the squamosals, and posterior to the frontal, the parietals are obscured, hindering the description. Considering the adult age of the specimen, the parietal would be a single, fused element, as found in most ornitischians (Romer, 1956; Sereno, 1991; Vickaryous and Russell, 2002), but it is not possible to confirm this. Paired parietals in ankylosaurs are known only in sub-adult specimens of *Pinacosaurus grangeri* (Maryanska, 1971; Maryańska, 1977). Posteriorly, and immediately dorsal to the occiput, the edge of the parietal forms the nuchal shelf. Two short, rounded protuberances protrude slightly from the shelf, conferring an undulating outline in dorsal view (Fig. 4.2.1.1A, E). Comparatively, it is similar to what is observed in *Gargoyleosaurus* (Carpenter *et al.*, 1998; Kilbourne and Carpenter, 2005), and differs from the convex edge in *Gastonia*, *Pawpawsaurus*, *Panoplosaurus*, *Edmontonia*, or *Texasetes* (Lambe, 1919; Sternberg, 1928; Russell, 1940; Bakker, 1988; Coombs Jr, 1995; Lee, 1996; Kirkland, 1998; Kinneer *et al.*,

2016), the almost straight outline in *Kunbarrasaurus* and ankylosaurids (Maryańska, 1977; Tumanova, 1986; Carpenter, 2004; Vickaryous *et al.*, 2004; Arbour and Currie, 2013a; Arbour *et al.*, 2014a; Leahey *et al.*, 2015; Penkalski and Tumanova, 2017; Paulina-Carabajal *et al.*, 2018; Park *et al.*, 2020). The rugose texture is indicative of osteoderm cover. The nuchal shelf does not cover the occipital region dorsally, which is similar to what is observed in most non-ankylosaurid forms, whereas the contrary is synapomorphic for Ankylosaurinae (Vickaryous and Russell, 2002; Vickaryous *et al.*, 2004; Thompson *et al.*, 2012; Arbour and Currie, 2016). Opposed to the dorsal skull roof bones, as the ventral counterpart of the supraorbital, the jugal limits the ventral rim of the orbit. Here, only the posterior half of the right jugal is present, forming the slightly curved surface of the orbital cavity floor. Its most evident feature is the ventrolaterally projecting horn, a narrow, cone-shaped structure. It should be noted though that, because sutural contacts are obliterated and the posterior position of this process, it is not totally clear at this time if it is strictly limited to the jugal, as in *Gargoyleosaurus*, *Gastonia*, *Pawpawsaurus* or BEXHM 1999.34.1-2011.23.1 (Lee, 1996; Carpenter *et al.*, 1998; Kirkland, 1998; Kilbourne and Carpenter, 2005; Blows and Honeysett, 2014; Kinneer *et al.*, 2016), or if it receives any contribution from the quadratojugal, as it happens in most ankylosaurs who exhibit this ornamentation (Vickaryous and Russell, 2002; Carpenter, 2004; Vickaryous *et al.*, 2004; Carpenter *et al.*, 2011; Arbour and Currie, 2013a; Arbour *et al.*, 2014a; Arbour and Evans, 2017; Penkalski and Tumanova, 2017; Park *et al.*, 2020). Considering the narrow base of the horn, the first case seems the most likely. Ventrally, very little information can be added, mostly due to the current state of preparation of the specimen, but also because of the position of the mandible and humerus which cover most of posterior ventral half of the skull (Fig. 4.2.1.1B). The rounded surface of the mandibular condyle of the right quadrate is visible, bounded lateroanteriorly by what seems to be the dorsally higher attached quadrate process of the quadratojugal (Fig. 4.2.1.1B). The ventral disposition of the quadratojugal and jugal, and the presence or extent of the infratemporal fenestra are not assessable at this stage. The same occurs with the lateral temporal fenestra.

The occipital and basicranial regions are the least visible, whether because of the articulation of the specimen (mainly for the occipital region) or the sediment and

disarticulated elements covering the posterior half of the ventral aspect of the skull (i.e., basicranium) (Figs. 4.2.1.1B, E). Therefore, little information can be extracted at this time, apart from the robust paroccipital processes which are visible in dorsal view (Fig. 4.2.1.1E). These project pronouncedly posterolaterally, forming a lateral notch posterior to the squamosal, and, although impossible to confirm at this stage, seemingly do not fuse with the squamosal head of the quadrate or the squamosal, as in *Kunbarrasaurus* for example, in contrast to what often happens in ankylosaurs (e.g., Tumanova, 1987; Carpenter, 2004; Arbour and Currie, 2013b; Arbour *et al.*, 2014a; Leahey *et al.*, 2015; Kinneer *et al.*, 2016; Penkalski and Tumanova, 2017; Paulina-Carabajal *et al.*, 2018; Park *et al.*, 2020, 2021). There is a clear neck of the paroccipital processes, proximally in relation to the thicker terminal capitulum (Fig. 4.2.1.1E). The composition of the paroccipital processes, i.e., the individual contribution of the exoccipitals and opistothic elements, is impossible to assess.

Mandible. Only the left mandibular ramus is preserved, wedged between the skull and the left humerus, slightly dislocated posteriorly relative to the articulation with the quadrate and rotated medially (Fig. 4.2.1.1C). Because of its position, many of the features are obscured. The anterior end has seemingly been broken off, so that the symphysis is missing. Overall, it is a long slender element, that thins anteriorly. It measures 22 cm rostrocaudally. Only the ventral and lateral surfaces are the clearly visible. Sediment covers most of the medial surface. The lateral surface is rugose, which is an indication of a lateral mandibular ornamentation, as observed in other ankylosaurs, such as *Sarcolestes* or *Gargoyleosaurus* (Galton, 1983b; Kilbourne and Carpenter, 2005).

Teeth (Fig. 4.2.1.2). Maxillary (and possibly mandibular) teeth are preserved in the alveoli, except for one isolated complete tooth (Fig. 4.2.1.2A-E). There at least 38 maxillary teeth in the alveoli, 18 in the left and 19 in the right. Most of the teeth are heavily worn. The more posterior left teeth (Fig. 4.2.1.2B, D) and one unerupted right tooth (Fig. 4.2.1.2E) are better preserved, showing an approximate lanceolate shape, and denticles are discernible. The tooth crowns are heavily worn, but the circular cross sections of the root can be observed in some better exposed teeth (Fig. 4.2.1.2A). Most of left alveoli, special foramina, and space between teeth are filled with sediment, which obscures most of the details of the alveolar ridge, but in the right those are more visible. As is typical in ankylosaurs, and other ornitischians,

teeth are small, relative to head size, and labiolingually flattened. The unerupted tooth exhibits a simple, unornamented morphology, with at least seven mesial denticles (Fig. 4.2.1.2E). The isolated tooth (Fig. 4.2.1.2C) was wedged between the first cervical ring and the nuchal region of the skull, on top of the left paroccipital process. The tooth is set in the sediment, therefore only visible on one side. It

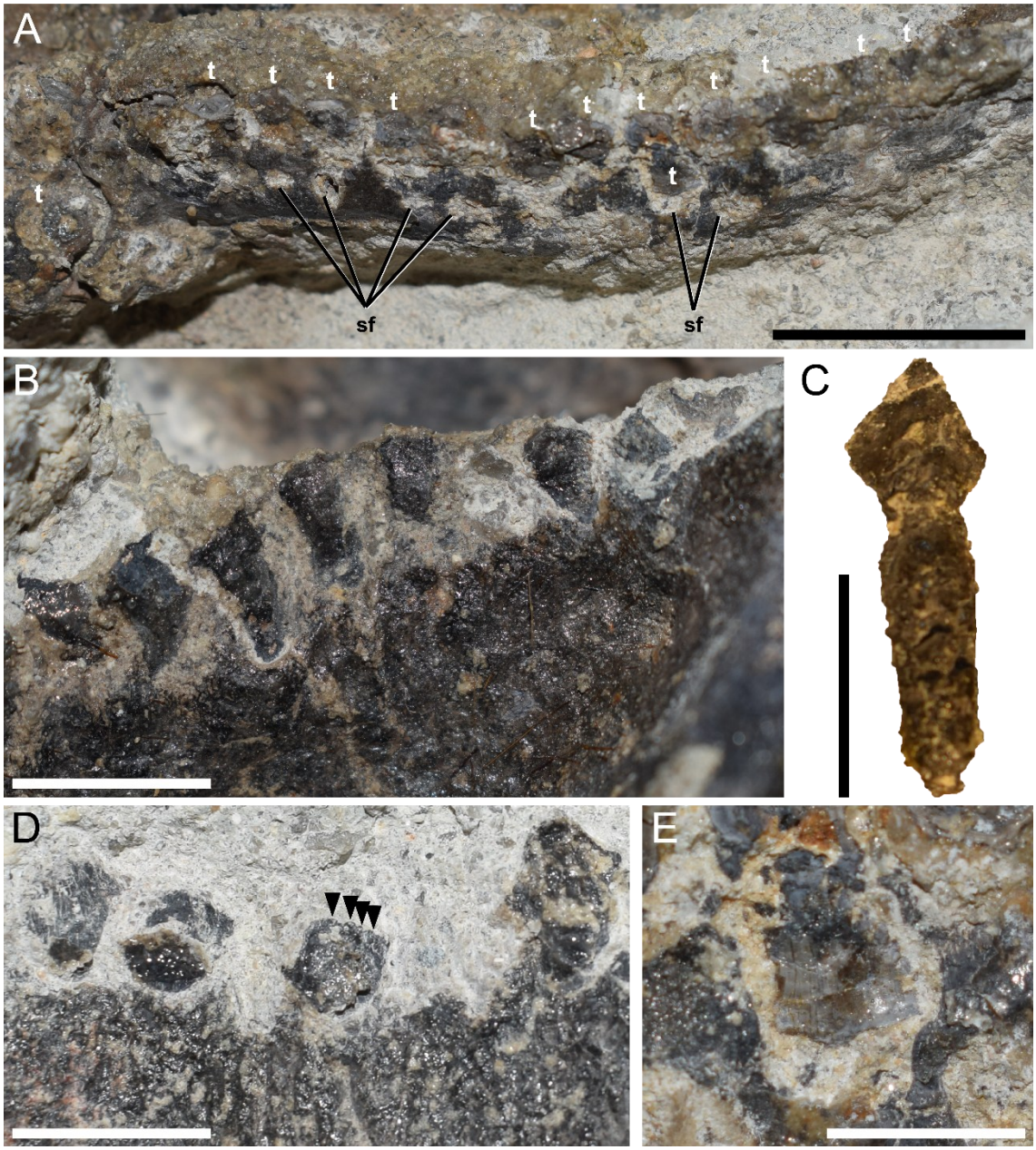

Figure 4.2.1.2. Teeth of *Dracopelta zbyszewskii* (NOVA-FCT-DCT-5556). A) right alveolar ridge in ventral view, B) detail of left anterior maxillary tooth row in buccal view, C) isolated dentary? tooth, D) left posterior maxillary teeth in buccal view, E) right maxillary erupting tooth in lingual view. In A, anterior is to the right. In D, the black arrowheads indicate preserved denticles. Abbreviations: sf – special foramina; t – teeth. Scale bars: 2 cm in A, 1 cm in B-D, 5 mm in E.

measures 20 mm dorsoventrally. More than half of the length is the root which measures approximately 13 mm. The root is round in cross-section and semi cylindrical in shape, widening slightly apically. There is no distinct cingulum between the root and the crown, rather a slight narrowing of the root, creating a neck just below the crown. The crown measures approximately 7 mm dorsoventrally and is lanceolate in shape, flattened labiolingually. The visible surface is smooth, with no discernible ornamentation. The mesial and distal margins show small denticles, restricted to the carinae, present up to the apex. The exact number of denticles is unknown since parts of the tooth are obscured by sediment, but approximately 7-10 denticles on each carinae are present. This morphology and the absence of fluting, grooves or ridges is similar to equivalent teeth of *Gargoyleosaurus* (Kilbourne and Carpenter, 2005). Teeth morphology in ankylosaurs is generally conservative and, among ornitischians, plesiomorphic (Galton, 1983b; Coombs Jr, 1990; Norman *et al.*, 2004a, 2004b; Norman, 2020b). The development of coronal ridges, grooving, or flutes, and a thickened cingulum is widespread among more derived ankylosaurs, such as *Edmontonia*, *Euoplocephalus*, or *Ankylosaurus* (Coombs Jr and Deméré, 19961; Vickaryous and Russell, 2002; Carpenter, 2004; Vickaryous *et al.*, 2004; Ősi *et al.*, 2014; Kubo *et al.*, 2021), have shallow, but well-marked coronal grooves, while teeth in stegosaurs have characteristic well-developed multiple vertical striations, and very pronounced cingula. The tooth was moved from its original position, which would make it difficult to determine to ascertain if it is a maxillary, dentary or eventually premaxillary tooth. However, premaxillary teeth are rare in ankylosaurs, and a plesiomorphy for Ankylosauria, and when present, such as in *Gargoyleosaurus*, *Pawpawsaurus*, *Silvisaurus*, the crown is slightly recurved posteriorly (Eaton Jr, 1960; Lee, 1996; Carpenter *et al.*, 1998; Vickaryous *et al.*, 2004; Kilbourne and Carpenter, 2005). The same is observed in *Scelidosaurus* and *Emausaurus* (Haubold, 1990; Norman *et al.*, 2004a; Norman, 2020b). Therefore, the isolated tooth (Fig. 4.2.1.2C) could only be either from the maxillary or dentary. Since all the maxillary teeth are varyingly eroded and *in situ*, the tooth is most likely a dentary tooth, unknown though if a left or right tooth.

4.2.2. Axial skeleton

Cervical vertebrae (Figs. 4.1.2, 2.2.1-2, Table 4.2.2.2). The cervical series is complete, with eight vertebrae, albeit the series was broken during collection of the specimen, and therefore cervical vertebrae 4-6 (c4-c6) were heavily damaged (Figs.

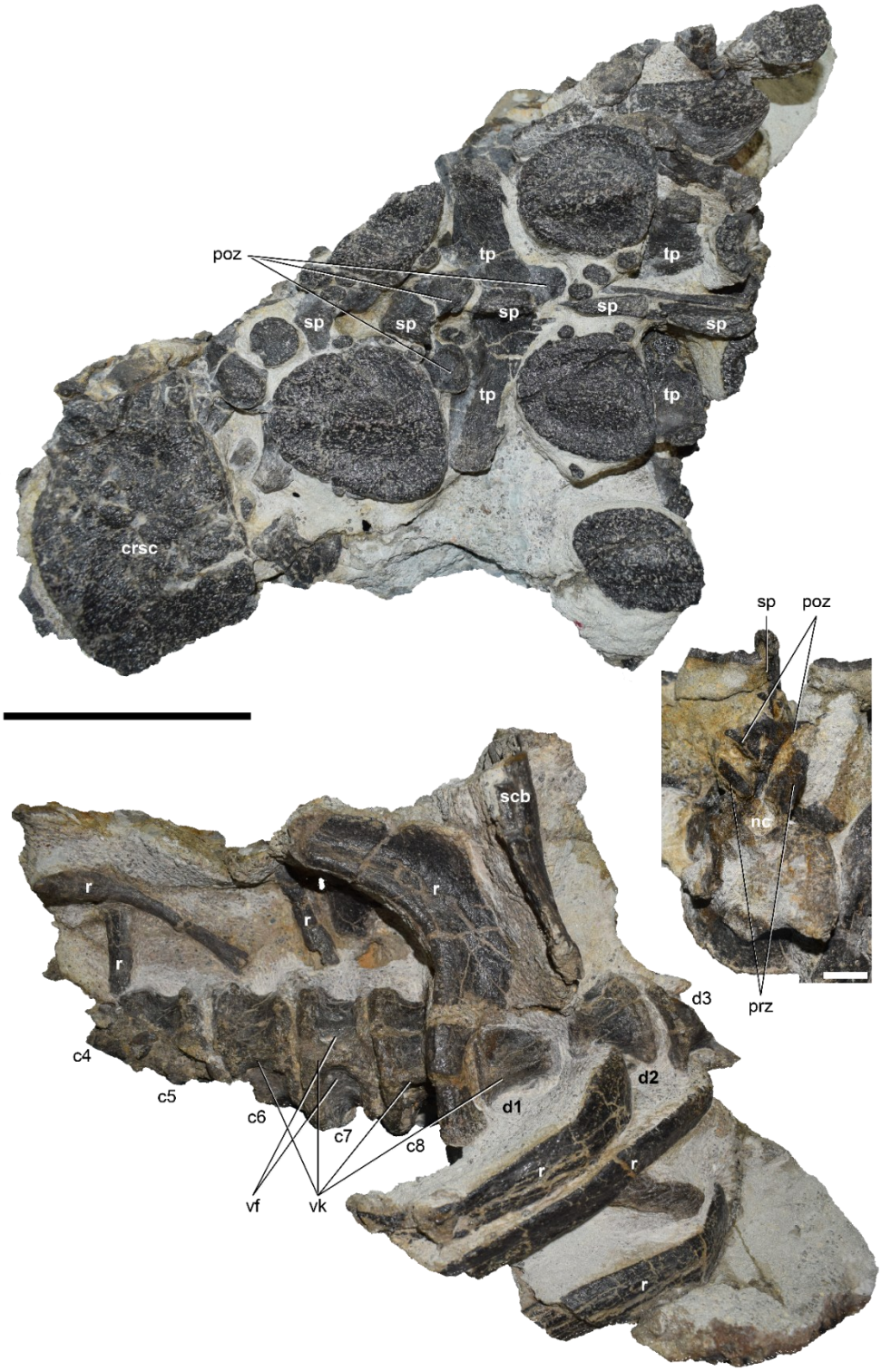

Figure 4.2.2.1 (previous page). Cervicothoracic section of *Dracopelta zbyszewskii* (NOVA-FCT-DCT-5556). Dorsal (above) and ventral (below) views of the cervicothoracic section of NOVA-FCT-DCT-5556. Cranial is to the left. Inset is a cross section of d3, in posterior view, where the prezygapophyses of d4 are visible. Abbreviations: c5-7 – cervical vertebrae; crsc – cervical ring scute; d1-d3 – dorsal vertebrae; nc – neural canal; poz – postzygapophyses; prz – prezygapophyses; r – rib; scb – scapular blade; sp – spinous process (neural spine); tp – transverse process; vf – ventral fossa; vk – ventral keel. Scale bars: 10 cm in dorsal and ventral views, 2 cm in inset.

4.2.2.1-2). The few preserved and observable small cervical ribs are disarticulated and are similar to cervical ribs of other ankylosaurs. The atlas is mostly obscured from direct observation because of the articulation of the specimen, apart from a small gap between the dorsal ornamentation, which allows to confirm its presence. Dorsal and between the atlas and the occipital complex, there are two, small, paired elements (Fig. 4.2.1.1E). The anterior half is wider than the posterior half, which narrows to a rounded end. The location, shape and relative position to the adjacent bones lead to the identification of these elements as the proatlas. Kilbourne and Carpenter (2005: Fig. 6) identify the same element in *Gargoyleosaurus*. Comparatively, the slight raised ridge on the right element is indicative of the ventral surface, implying that it was rotated 180° from its original position. This is further supported by the lateral concave edges facing the same direction (Fig. 4.2.1.1E; Kilbourne and Carpenter, 2005:128). Also, the dorsal displacement relative to the paroccipital processes is indicative of a slight remobilization from a more occipital-axial aligned position. As with the atlas, the axis is barely observable, although in this case, a robust spinous process is visible in dorsal view, nestled between the neck ornamentation, while ventrally the ventral surface of the narrow and elongated centrum is also visible. There is a faint mid-ventral raised expansion, representing an incipient, sagittal, midline ventral keel (or hypapophysis, *sensu* Vickaryous *et al.*, 2004:380), a structure which becomes pronouncedly more developed along the cervical series. The atlas and axis are seemingly unfused. Cervical vertebra 3 (c3) is visible only ventrally. It has a spool-shaped centrum, wider than long, with a noticeable ventral keel. The subcircular parapophyses are located on the lateral edge of the anterior articulation facet, extending posteriorly to mid-length of the centrum. Vertebra c4 was almost entirely lost, except for the anterior articulation facet of the centrum and a fragment of the posterior articulation facet, still articulated with c5

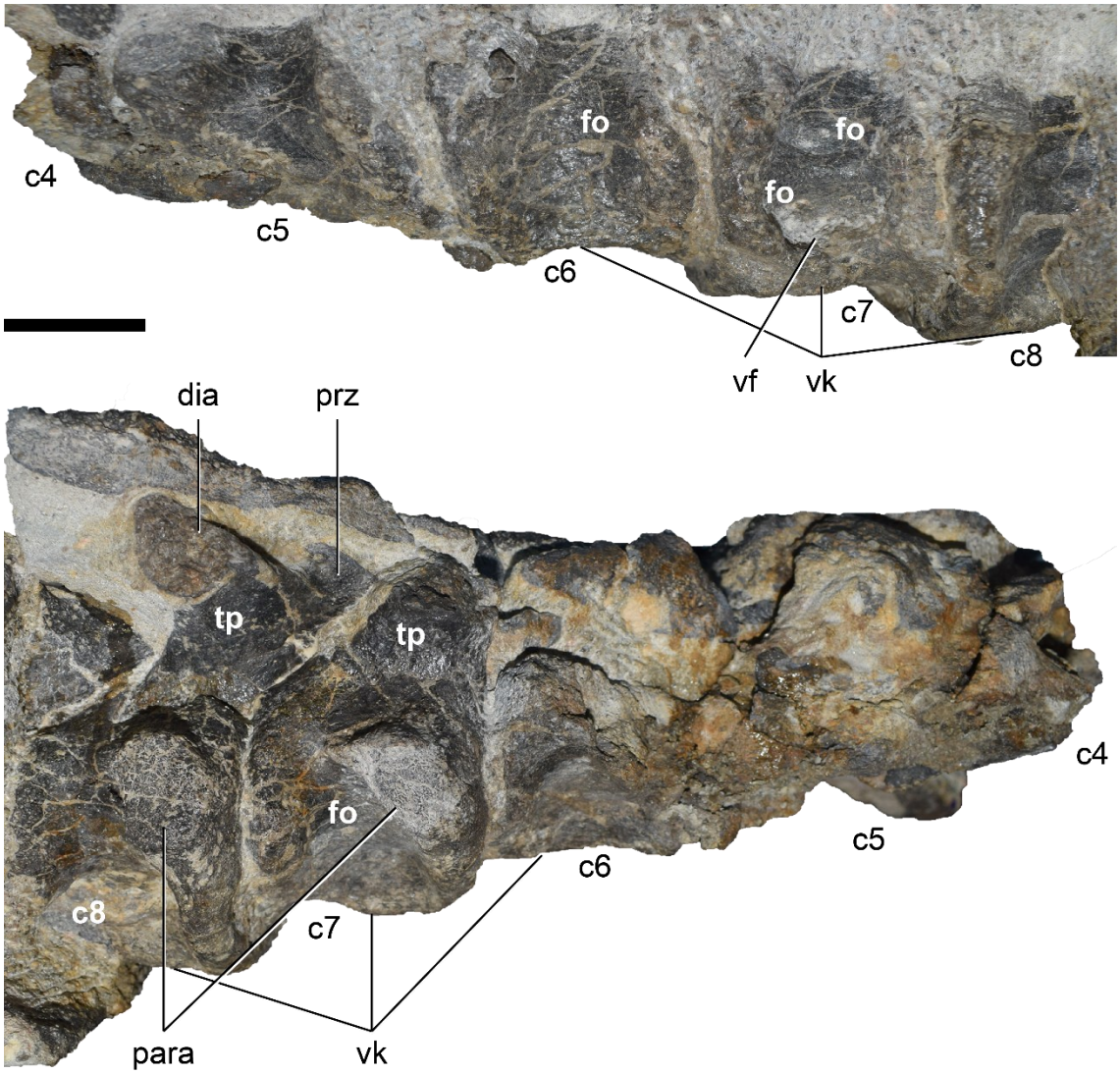

Figure 4.2.2.2. Posterior cervical vertebrae of *Dracopelta zbyszewskii* (NOVA-FCT-DCT-5556). Left lateral (above) and right lateral (below) views of vertebrae c5-8 of NOVA-FCT-DCT-5556. Right side of c5 and c6 was obliterated during collection of the specimen. Abbreviations: c5-8 – cervical vertebrae; dia - diapophysis; fo – foramen; para – parapophysis; prz – prezygapophyses; tp – transverse process; vf – ventral fossa; vk – ventral keel. Scale bar: 2 cm.

(Fig. 4.2.2.2). The right and dorsal sides of c5 are heavily damaged as well, with only the left damaged postzygapophysis identifiable in dorsal view. Vertebrae c6-8 are anatomically similar (Figs. 4.2.2.1-2), spool-shaped, successively increasing slightly in size (Table 4.2.2.2). The small shortening of c7 seems to be due to a slight compression between c7 and c8 (Fig. 4.2.2.1). As in c4 and c5, the right side of the centrum of c6 is damaged (Figs. 4.2.2.1-2). The right parapophysis was lost as was most of the neural spine. In dorsal view (Fig. 4.2.2.1), the left postzygapophysis is visible *in situ*. The articulation facet faces ventrally, and, as c7

and c8, the postzygapohyses join proximally to form a wide U in dorsal view. Ventrally and laterally, immediately dorsal to the ventral keel and ventral to the parapophyses, the centrum is slightly laterally constricted, forming two shallow ventral fossa which have an anteriorly placed foramen (Figs. 4.2.2.1-2). In c7-8, this is more pronounced, and the ventral keel in c7 is the widest of the series. Dorsally, the spinous process of c7 is broken just dorsal to its base. It is narrow and anteroposteriorly short (Fig. 4.2.2.1). The left postzygapophysis is hidden from view by the dermal armour, but the right is partially visible and faces ventrally (Fig. 4.2.2.1). The last cervical vertebra, c8, differs from c7 in the narrower but slightly more ventrally expanded midline ventral keel, the larger spinous process, and the narrower joining of the postzygapophyses (Fig. 4.2.2.1). The articular surfaces of c5-8 are offset from each other (Fig. 4.2.2.2), with the cranial surface slightly dorsal to the caudal surface. Both this condition and the caudal articular surface dorsal to the cranial articular surface are observable throughout Ankylosauria (Vickaryous *et al.*, 2004).

Dorsal vertebrae (Figs. 4.2.1-2, 2.2.3-5, Table 4.2.2.2). The dorsal vertebral series is composed of 16 vertebrae (d1-16). The three posteriormost vertebrae (d14-16) fuse together to form the presacral rod of the synsacrum (Figs. 4.2.1, 2.2.5, Table 4.2.2.1), a structure which is ubiquitous throughout Ankylosauria, albeit with varying vertebral contributions (Table 4.2.2.2). The anteroposterior length increases from d1 to d14, after which it starts decreasing (Table 4.2.2.2). The vertebrae are spool-shaped and slightly amphicoelous, even though all the articular surfaces are obscured due to the articulation of the specimen and the sediment filling the intervertebral spaces, except the anterior facet of the centrum of d3, which is broken transversely and exhibits a gently concave articular surface (Fig. 4.2.2.1). D1 exhibits wing-like transverse processes, projecting dorsolaterally (Fig. 4.2.2.1). At the proximal base of the processes, immediately ventral and anterior to the spinous process, there is an anteriorly facing depression, which seems to serve as an extended articulating surface for the postzygapohyses of c8 (Fig. 4.2.2.1). This structure is only visible in d1, since all dorsal vertebrae are obscured in dorsal view, except for the neurapophyses, which are rugose and comparatively robust. The right postzygapophysis is visible in dorsal view (Fig. 4.2.2.1). Ventrally, d1 is distinguished by the presence of a ventral keel, less pronounced than in the cervical

vertebrae (Fig. 4.2.2.1). Vertebra d2 does not have a ventral keel. As in the cervicals, the rugose rim of the articulation facets of the centra are well-defined, but this disappears after d14 due to the fusion of the last three dorsals to the sacrum. The

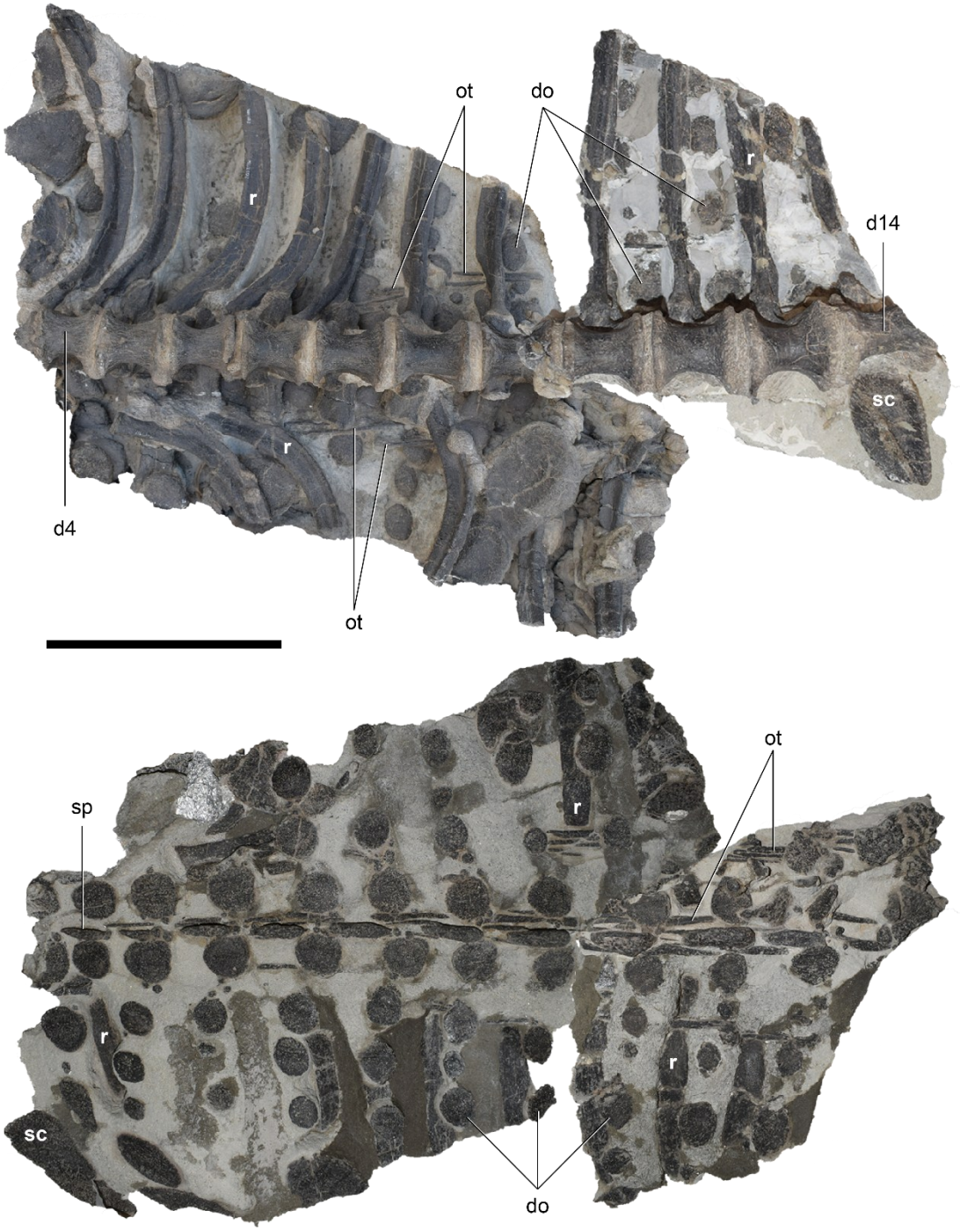

Figure 4.2.2.3. Dorsal section of *Dracopelta zbyszewskii* (NOVA-FCT-DCT-5556). Dorsal (above), and ventral (below) views of the dorsal section of NOVA-FCT-DCT-5556, from d4-14, with ribs and armour *in situ*. Cranial is to the left. D14 is the first dorsosacral (ds1, Table 4.2.2.1). Abbreviations: d4-d14 – dorsal vertebrae 4 to 14; do – dorsal osteoderms; ot – ossified tendons; r – ribs; sc – scute; sp – spinous process. Scale bar: 20 cm.

third dorsal vertebra (d3) is broken in half, allowing to observe its cross section (Fig. 4.2.2.1). The transverse processes are more dorsally projected than in d1. The cross section shows a circular neural canal. The spinous process is thin and terminates distally in a mediolaterally expanded neurapophysis. Between vertebrae d4 and d13 (Fig. 4.2.2.3), there is little change in morphology. The articulation facets of the spool-shaped centra have well-defined, rugose edges. As observed throughout Ankylosauria, the paraphophyses migrate dorsally towards the transverse processes, comparatively to the cervical vertebrae (Fig. 4.2.2.4). In d6, both are already cossified, suggesting this process may start happening at least in d4, albeit in the latter it is obscured by sediment and impossible to confirm (Fig. 4.2.2.4C). The subcircular parapophyses contrast with the dorsoventrally flattened diapophyses. The placement of the parapophyses and transverse processes at the anterior edge of the centra is autapomorphic for *Dracopelta zbyszewskii*. Immediately ventral to the parapophyses, there is a small, shallow depression, the centroparapophyseal fossa, bounded posteriorly and anteriorly by the posterior and anterior centroparapophyseal laminae, respectively (Fig. 4.2.2.4A-C). The first runs posteroventrally from the parapophysis to the posterior edge of the centrum, while the second extends ventrally from the ventral surface of the parapophysis to the anterior edge of the centrum. The prezygapophyses are barely exposed but its lateral surface is more visible on right side (Fig. 4.2.2.4B). They are oriented parallel to the pcpl of the consecutively anterior dorsal vertebra, with the pedicles originating immediately dorsal to the centrum, at the base of the neural arch, resulting in a low position of the prezygapophyses, in an alignment with the parapophyses (Fig. 4.2.2.4A-C). This is autapomorphic for *Dracopelta zbyszewskii*. Towards the posterior dorsal series, it is observable a gradual coossification of the ribs with vertebrae (see rib description below). The process starts in d9 and the ribs fully coossify in vertebra d11 (Figs. 4.2.2.3, 4). Anterior to d9, the ribs are disarticulated and slightly displaced, but the articular surfaces do not show signs of breakage, indicating the separation of the ribs occurred along articulation surfaces (Fig. 4.2.2.3). The last three vertebrae (d14-d16) of the dorsal series are morphologically simpler, specially d15 and d16, because of their fusion with the sacrum. They are longer and narrower than other dorsal vertebrae (Figs. 4.2.2.3, 5, Table 4.2.2.2), and solidly coossified into a presacral rod. For this reason, some

authors also refer to these vertebrae as dorsosacral vertebrae (e.g., Vickaryous *et al.*, 2004; Kirkland *et al.*, 2013; Arbour and Currie, 2013; Wiersma and Irmis, 2018;

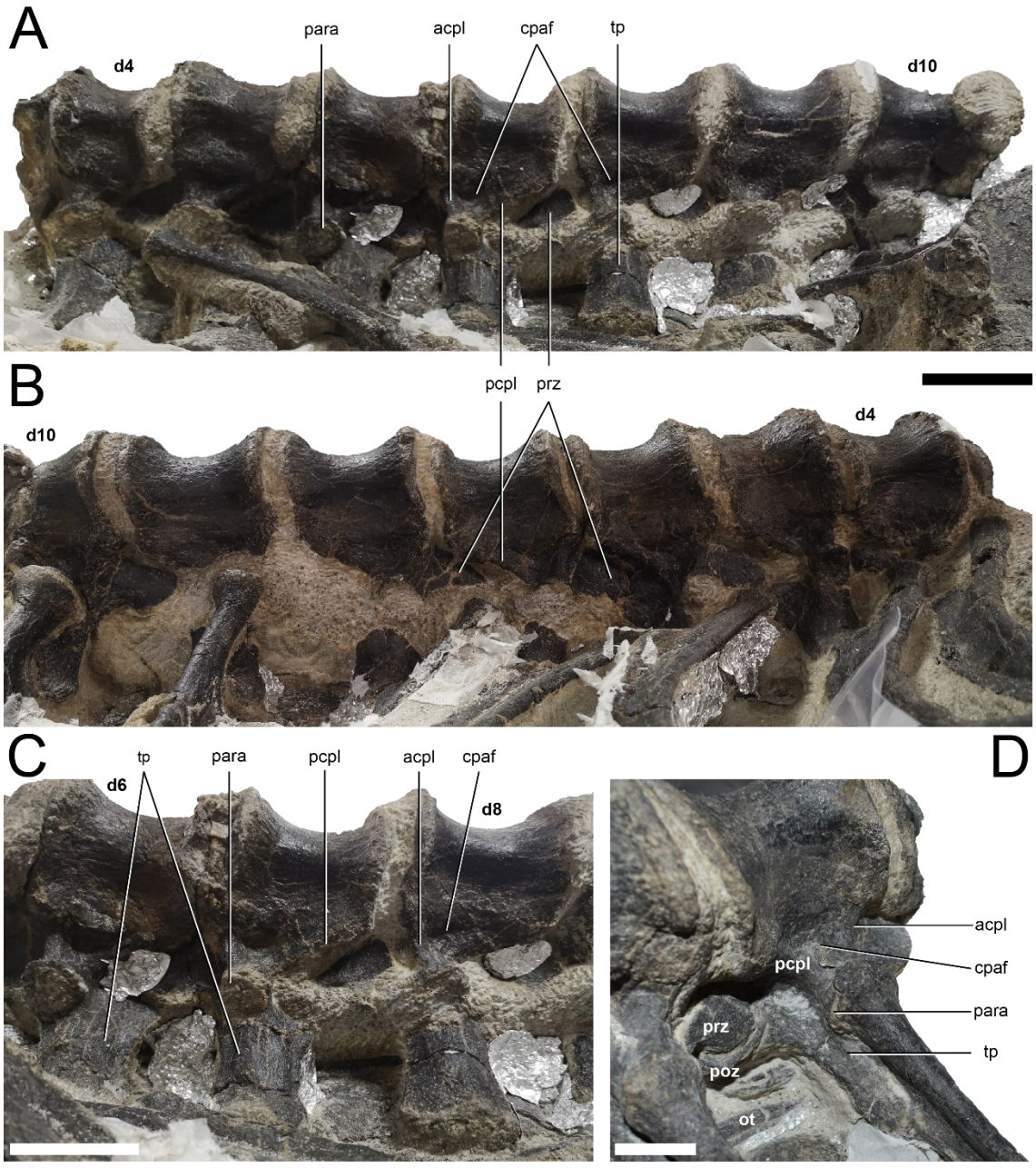

Figure 4.2.2.4. Dorsal vertebrae of *Dracopelta zbyszewskii* (NOVA-FCT-DCT-5556). Details of the dorsal vertebrae (d4-d10) of specimen NOVA-FCT-DCT-5556. A) left lateral, B) right lateral, C) detail of d6-d8 in left lateral view, D) close-up of d11, in posterolateral view, showing the coossification of the rib at the parapophysis, along the transverse process and diapophysis. Abbreviations: acpl – anterior centroparapophyseal lamina; cpaf – centroparapophyseal fossa; d1-d10 – dorsal vertebrae; ot – ossified tendon; para – parapohysis; pcpl – posterior centroparapophyseal lamina; poz – postzygapyhysis; prz – prezygapophyses; tp – transverse process. Scale bars: 5 cm in A-C, 2 cm in D.

Park *et al.*, 2021; abbreviation ds in this work, Table 4.2.2.1). Dorsal observation is unavailable due to the presence of the pelvic shield, except for the neurapophysis of d14, which is significantly smaller than in d13. D14 is broken at the posterior edge (Fig. 4.2.2.3), but it is possible to identify the coossification suture with d15 (Fig. 4.2.2.5). A similar suture is present between d15 and d16. In these vertebrae, the ribs have completely coossified with the neural arch and have moved to an even more dorsal position. Posteriorly, almost half of the centrum of d16 is coossified laterally with the enlarged first sacral rib.

Sacrum (Figs. 4.2.1-2, 2.2.5, Tables 4.2.2.1, 2). The sacral region, as is characteristic in Ankylosauria, is composed of posterior dorsal, sacral, and caudal vertebrae, fused together into a synsacrum, which functions as a solid brace for the entire pelvic girdle and pelvic shield. It is composed by three sacrodorsals, i.e., the posteriormost three dorsals fuse with each other and to the sacrum proper to form a presacral rod, four true sacrals, and one sacrocaudal, which is the first caudal that also fuses posteriorly to the fourth sacral, forming a short postsacral rod. The sacral vertebral formula is 3:4:1 (Table 4.2.2.1). The centra are spool-shaped and longer than wide (Table 4.2.2.2). Dorsally, the sacrum is obscured from view by the pelvic shield. The anteriormost sacrodorsal vertebrae is broken and only identifiable by the remaining posterior articular surface widening, which fuses to the following vertebra. The ventral surface of the centra is smooth and generally featureless, even though in the ventral surface at the contact between s2 and s3, a very shallow, short sagittal groove is present. There is a slight dorsoventral offset observed at the midline of ds1, 2, and s1, caused by taphonomic dorsoventral shearing. This is contrary to what happens, for example, in *Gargoyleosaurus*, which exhibit a midline keel (Carpenter *et al.*, 2013), or in *Mymoorapelta*, that has a longitudinal groove. In the sacrodorsal segment of the sacrum, the ribs are broken, just distal to the tubercula on the right side but still retain the proximal T-shaped cross section. The parapohyses have migrated to a more dorsal position to the centra, as it is observed along the dorsal series. This movement towards a more dorsal placement and fusion to the diapophyses is widespread in Ankylosauria. These ribs are coosified to the neural arched and partially fuse to the medioventral surface of the preacetabular process, providing support for the wide, ventrally arching ilia. The sacral ribs are short, robust, and hourglass shaped, slightly wider anteroposterior proximally than

distally, solidly fusing to the centra and the dorsomedial wall of the acetabulum. The sacral fenestrae are piriform in ventral view, particularly the first and second, while the third has more parallel anteroposterior margins.

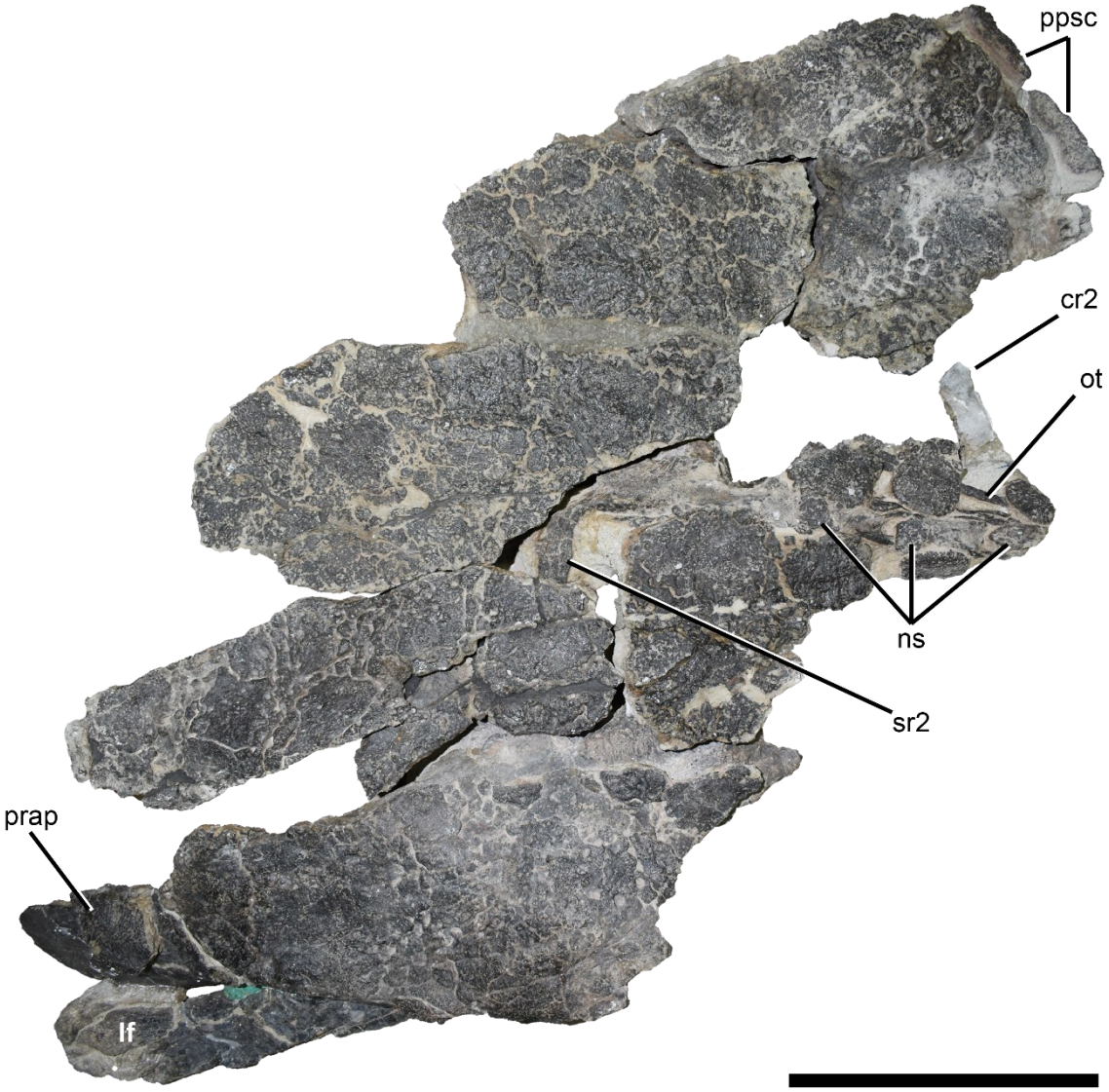

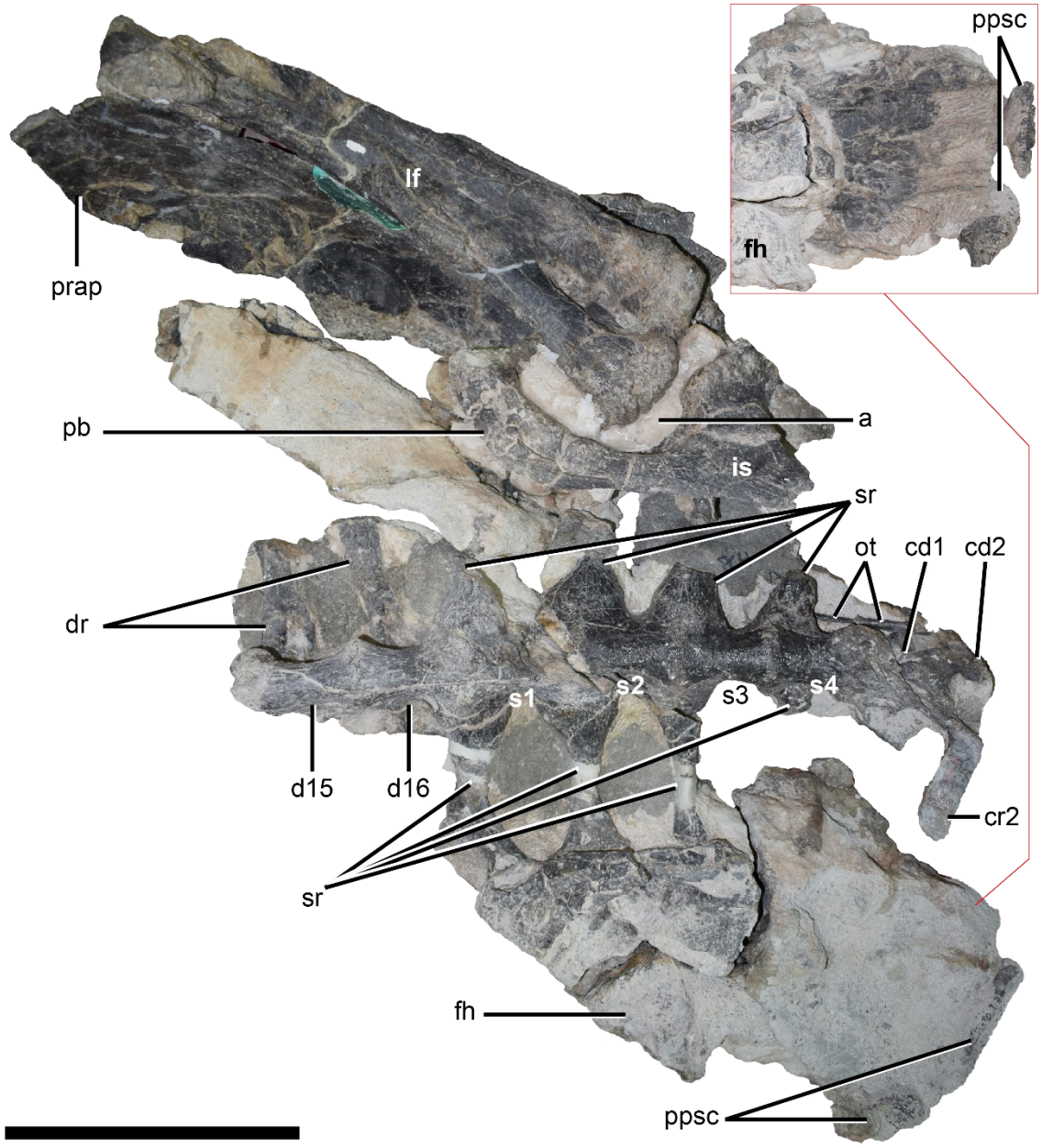

Figure 4.2.2.5. Sacrum of *Dracopelta zbyszewskii* (NOVA-FCT-DCT-5556). Dorsal (previous page) and ventral views of the sacral region of NOVA-FCT-DCT-5556. In dorsal view, the sacral shield covers most of the surface. In ventral view, in the lower right corner, the postacetabular process is obscured by sediment. Inset: ventral view of the postacetabular process after sediment removal. Abbreviations: a – acetabulum; cd1-2 – caudal vertebrae 1-2; cr2 – caudal rib 2; d15-16 – dorsal vertebrae 15-16; dr – dorsal ribs; fh – femoral head; is – ischium; lf – left femur; ns – neural spine; ot – ossified tendons; pb – pubis; ppsc – peripheral pelvic scute; prap – preacetabular process; s1-4 – sacral vertebrae 1-4; sr – sacral ribs (sr2, sacral rib 2). Scale bars: 20 cm.

Table 4.2.2.1. Vertebral formula of the ankylosaur synsacrum. Comparative non-ankylosaur taxa are represented by the early diverging ornithischian *Lesothosaurus diagnosticus*, early thyreophorans *Scutellosaurs lawleri* and *Scelidosaurus harrisonii*, and early diverging stegosaur *Huayangosaurus taibaii*. Numbers in parentheses are minimum estimates of vertebral count. Abbreviations: ds, dorsosacral; s, sacral; cs, caudosacral.

Taxa	Synacrum (ds:s:cs)	References
Lesothosaurus diagnosticus	1:3:1	Baron *et al.* (2017)
Scutellosaurus lawleri	1:(4):0	(Breeden III *et al.*, 2021)
Scelidosaurus harrisonii	1:3:1	Norman (2020a)
Huayangosaurus taibaii	1:4:0	(Maidment *et al.*, 2006)
Akainacephalus johnsoni	4:3:1	Wiersma and Irmis (2018)
Crichtonpelta benxiensis	3:3:1	Lü *et al.* (2007)
Dracopelta zbyszewskii	**3:4:1**	**This work**
Dyoplosaurus acutosquameus	?:3:1	Parks (1924); Penkalski (2001); Arbour *et al.* (2009)
Edmontonia rugosidens	4:3:2	Carpenter (1990)
Euoplocephalus tutus	3:4:1	Carpenter *et al.* (2013)
Gargoyleosaurus parkpinorum	3:4:1	Carpenter *et al.* (2013)
Gastonia burgei	4:4:1	Kinneer *et al.* (2016)
Gastonia lorriemchinneyae	(3):4:1	Kinneer *et al.* (2016)
Hungarosaurus tormai	5:4:1?	Ősi (2005)
Jinyunpelta sinensis	?:3:?	Zheng *et al.* (2018)
Mymoorapelta maysi	1:3:1	Kirkland *et al.* (1998); Kirkland (pers. comm., 2023)
Niobrarasaurus coleii	4:3:1	Mehl (1936); Carpenter *et al.* (1995)
Nodosaurus textilis	4:3:2	Lull (1921)
Panoplosaurus mirus	1?:4:1	Sternberg (1921)
Peloroplites cedrimontanus	(1):3:2	Carpenter *et al.* (2008)
Pinacosaurus grangeri	(3):4:?	Maryánska (1977); Buffetaut (1995)
Polacanthus foxii	5:4:1	Raven *et al.* (2020)
Saichania chulsanensis	3:4:1	Carpenter *et al.* (2011)

Table 4.2.2.1. Vertebral formula of the ankylosaur synsacrum. Comparative non-ankylosaur taxa are represented by the early diverging ornithischian *Lesothosaurus diagnosticus*, early thyreophorans *Scutellosaurs lawleri* and *Scelidosaurus harrisonii*, and early diverging stegosaur *Huayangosaurus taibaii*. Numbers in parentheses are minimum estimates of vertebral count. Abbreviations: ds, dorsosacral; s, sacral; cs, caudosacral.

Sauropelta edwardsorum	4:4:?	Ostrom (1970); Carpenter (1984)
Scolosaurus cutleri	4:3:2	Penkalski and Blows (2013)
Silvisaurus condrayi	(1)-5/6?:3:2	Eaton (1960); Carpenter and Kirkland (1998)
Stegouros elengassen	2:4:0	Soto-Acuña *et al.* (2021)
Struthiosaurus languedocencis	5:4:1	Garcia and Pereda-Suberbiola (2003)
Talarurus plicatospineus	4:4:1	Maleev (1952)
Tarchia tumanovae	3:4:2	Park *et al.* (2021)
Tianchisaurus nedegoapeferima	2:4:1	Zhiming (1993)
Vectipelta barretti	5:3:1	Pond *et al.* (2023)
"Zhejiangosaurus lishuiensis"	5:(3):?	Lü *et al.* (2007)

Caudal vertebrae (Figs. 4.2.1-2, 2.2.6, 7, Table 4.2.2.2). The caudal vertebral series is composed of the first eleven articulated caudals. The 12th and 13th caudal vertebrae were found disarticulated, in a more anterior position. Dorsally, the dermal armour obscures partially the vertebrae. The first caudal is fused to the sacrum (Fig. 4.2.2.5), as a sacrocaudal, a widespread feature among ankylosaurs, yet the centrum is broken off diagonally posteriorly to the anterior facet and prezygaphosyses. The first ten vertebrae are wider than long (Fig. 4.2.2.6), the anteroposterior length of the centrum tends to increase, and the width decreases posteriorly (Table 4.2.2.2). The articular facets are obscured from view by matrix, but are seemingly heart-shaped, more flattened dorsoventrally in proximal vertebrae and more rounded distally. The eleventh caudal is longer than wide, as is the posteriorly following vertebra. The 12th caudal vertebra (Fig. 4.2.2.7) was found isolated, moved from its original position in the caudal series, near the right femur, in block PC6. It is slightly distorted taphonomically through lateromedial shearing motion (Fig. 4.2.2.7A-D). The vertebra measures 54 mm anteroposteriorly and at least 70 mm dorsoventrally. Centrum is amphicoelous. Posterior articular facet is slightly offset ventrally from the

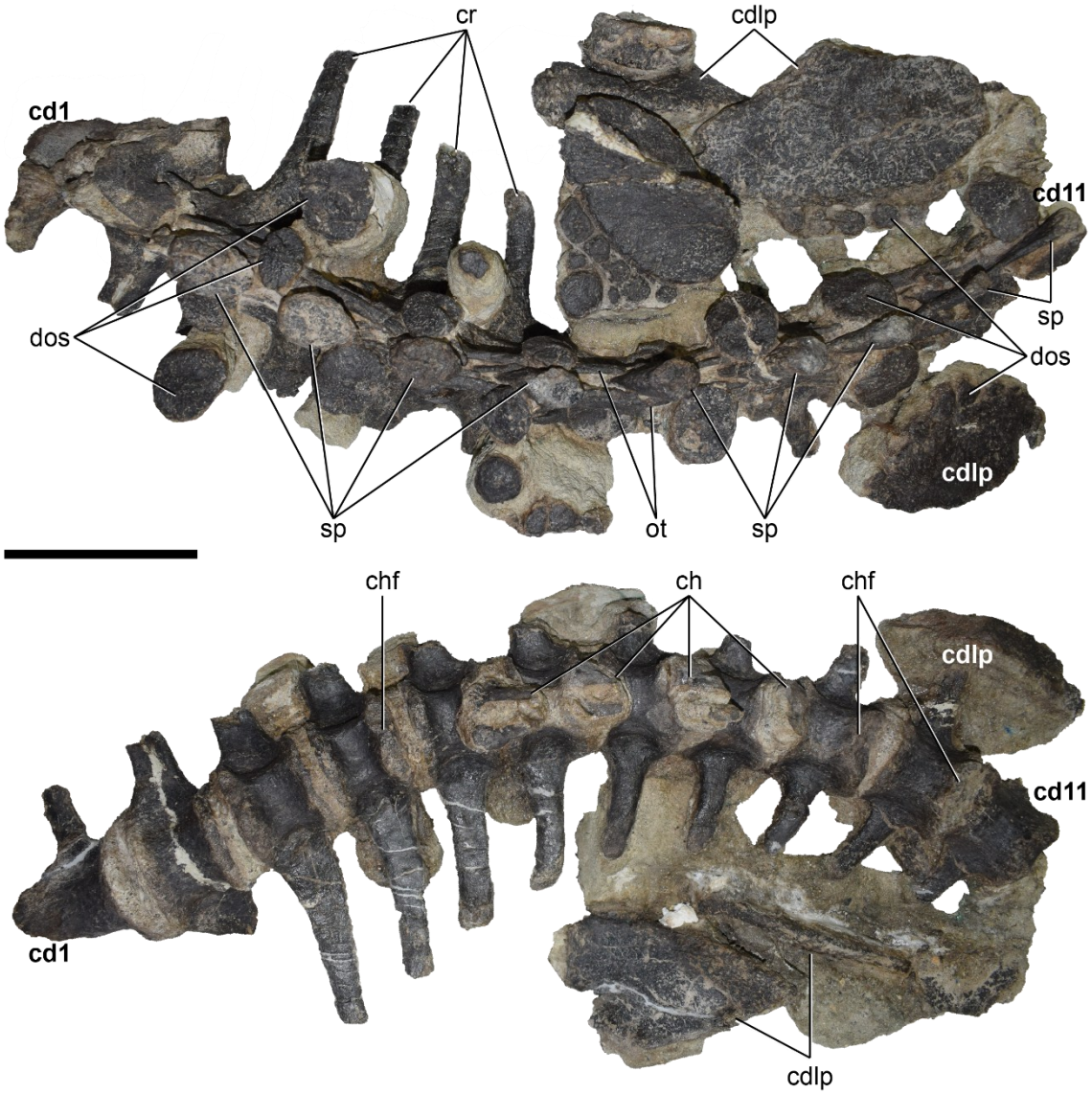

Figure 4.2.2.6. Anterior caudal vertebral series of *Dracopelta zbyszewskii* (NOVA-FCT-DCT-5556). Dorsal (top) and ventral (bottom) views of the anterior portion of the tail of NOVA-FCT-DCT-5556. Abbreviations: cd1-11 – caudal vertebra 1-11; cdlp – caudal lateral plate; ch – chevron; chevron articulation facet; cr – caudal rib; dos – dorsal ossicle; ot – ossified tendon; sp – spinous process. Scale bar: 10 cm.

anterior facet (Fig. 4.2.2.7E, F). This is in part due to the existence of the ventrally pronounced articulation facet for the chevron. Anterior centrum facet is subcircular, measuring 44 mm lateromedially and 41 mm dorsoventrally. The centre of the facet shows a small notochordal bump (Fig. 4.2.2.7A), and just dorsally to that is a second bump, halfway between the centre point of the facet and the dorsal margin of the facet. Dorsal edge of the centrum is slightly concave, composing the ventral margin

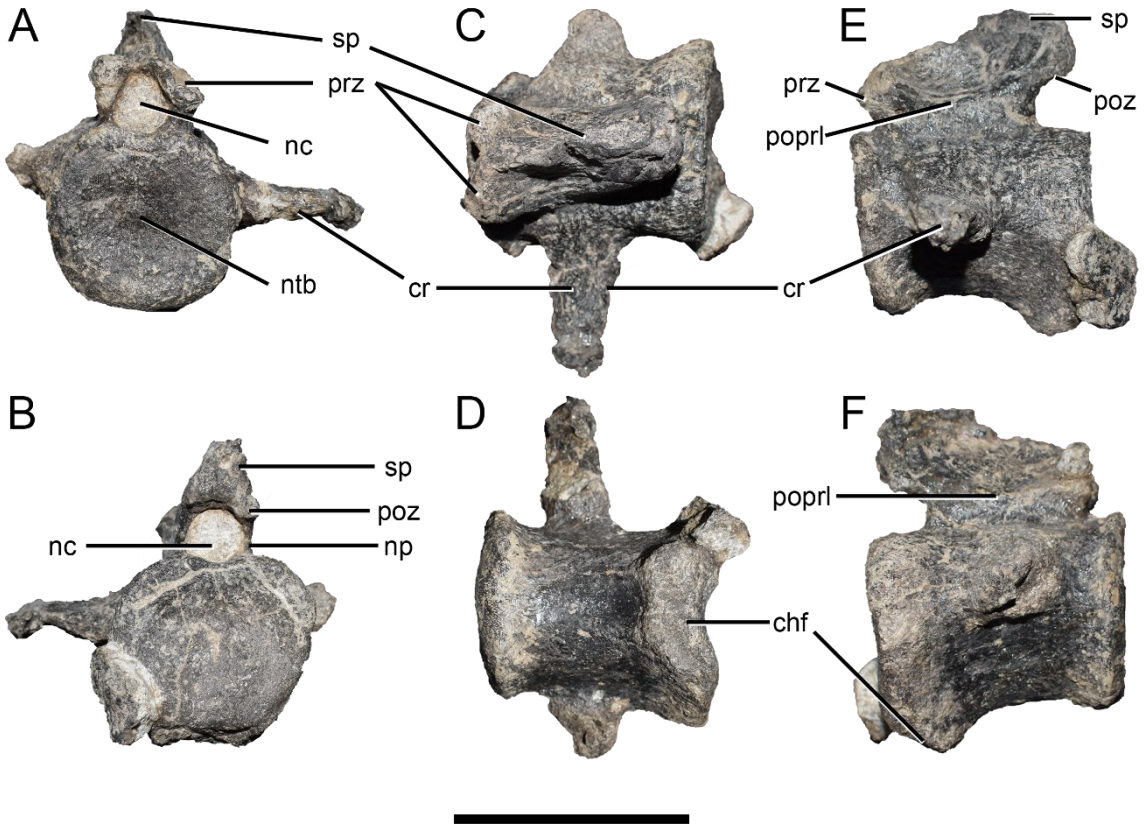

Figure 4.2.2.7. 12th caudal vertebra of *Dracopelta zbyszewskii* (NOVA-FCT-DCT-5556). Anterior (A), posterior (B), dorsal (C), ventral (D), left lateral (E), and right lateral (F) views. Abbreviations: chf – chevron facet; cr – caudal rib; nc – neural canal; np – neural pedicels; ntb – notochordal bump; poprl – postzygoprezygapophyseal lamina; poz – postzygapophysis; prz – prezygapophyses; sp – spinous process. Scale bar: 5 cm.

of the neural canal. Anteriorly, the neural canal is oval in section, wider ventrally, while posteriorly it is circular (Fig. 4.2.2.7A, B). The parapophyses are dislocated anteriorly and dorsally relative to the middle of the centrum. In the ventral surface of the centrum exists a small groove on the posterior half of the centrum that ends at the anterior margin of the chevron articulation facet (Fig. 4.2.2.7D). The posterior facet of the centrum is heart shaped (Fig. 4.2.2.7B), flattened dorsoventrally and slightly concave at the neural canal margin. The neural spine is slightly shorter than the centrum, measuring 44 mm anteroposteriorly. It is lateromedially compressed tapering out at the broken dorsal edge tip. The postzygapophyses seem poorly developed although it is hard to say conclusively in this vertebra, as they are broken. In the posterior margin of the neural spine, just above the neural canal, there is a tiny pit or foramen (Fig. 4.2.2.7B). Just dorsal to the centrum there are two low

postzygoprezygapophyseal laminae on each side which separate dorsoventrally the lateral walls of the neural canal from the neuroapophysial main body (Fig. 4.2.2.7E, F). The ribs are broken, with the right rib broken proximally, while the left rib is slightly more complete projecting laterally 26 mm. The circular neural canal is infilled by sediment. The prezygapophyses are broken, with the right one taphonomically bent posteriorly (Fig. 4.2.2.7A, C, F).

Table 4.2.2.2. Measurements (in mm) of the vertebrae of *Dracopelta zbyszewskii* (NOVA-FCT-DCT-5556). N/O) not observable; c) cervical; d) dorsal vertebrae; ds) dorsosacral vertebrae; s) sacral vertebrae; cd) caudal vertebrae; cds) caudosacral vertebrae. Numbers after vertebrae indicate position of vertebrae in the series (e.g., c3 = cervical vertebra 3).

Vertebra	Length	Width	Height
Atlas	N/O	N/O	N/O
Axis	47,88	N/O	N/O
c3	39,40	N/O	N/O
c4	N/O	N/O	N/O
c5	43,06	46,8	N/O
c6	41	59,42	N/O
c7	36,88	60,98	N/O
c8	42,60	60,90	N/O
d1	41,18	N/O	N/O
d2	43	N/O	N/O
d3	N/O	N/O	N/O
d4	51,18	58,18	41,4
d5	54,5	60	51,46
d6	53,74	56,5	54,7
d7	56,3	56,6	53,2
d8	57,38	57,48	53,92
d9	62,5	61,3	51,4
d10	56,28	56,74	53,5

Table 4.2.2.2. Measurements (in mm) of the vertebrae of *Dracopelta zbyszewskii* (NOVA-FCT-DCT-5556). N/O) not observable; c) cervical; d) dorsal vertebrae; ds) dorsosacral vertebrae; s) sacral vertebrae; cd) caudal vertebrae; cds) caudosacral vertebrae. Numbers after vertebrae indicate position of vertebrae in the series (e.g., c3 = cervical vertebra 3).

d11	61,18	63,3	58,1
d12	62,38	62,32	55
d13	65,5	72,54	61,34
d14 (ds1)	71,98	71,2	63,9
d15 (ds2)	66,08	47,41	N/O
d16 (ds3)	69,9	54,3	N/O
s1	66,4	50	N/O
s2	65,7	48	N/O
s3	62,56	48	44,34
s4	57	48	41,7
cd1 (cds1)	56	62,7	N/O
cd2	48,2	61,7	N/O
cd3	43,54	56,9	N/O
cd4	40	58,26	N/O
cd5	41,7	59	N/O
cd6	43,02	57,86	N/O
cd7	44,52	56,26	N/O
cd8	46,08	54,3	N/O
cd9	46,48	51,94	N/O
cd10	47,24	53,04	N/O
cd11	51,5	49,82	N/O
cd12	53,6	46,48	40,72
cd13	58,22	> 30	38,22

Ribs (Figs. 4.2.1-2, 4.2.2.3-5). NOVA-FCT-DCT-5556 preserves almost all its ribs, except for the left ribs 11-14. Due to the collecting conditions and the breaking and separation of the specimen in different blocks, the ribs shafts have been broken in two or three larger fragments, with consequential loss of continuity between some of them. Posteriorly, from d10 caudally, only the proximal segments are preserved, but there are ten articulated ribs (Fig. 4.2.1, 2.2.3). The left side and the anterior half of the dorsum have been more affected by *post-mortem* mobilization. The dorsal ribs have been rotated posteriorly, arching anterolaterally, contrarily to what is observed in MG 5787. Otherwise, they would project dorsolaterally from the vertebrae to form a wide arch to accommodate the enlarged gut. In the first dorsal ribs, especially the left ones, have been moved in a way as to overlap each other distally (Figs. 4.2.1, 2.2.3). The presence of cervical ribs can be attested, but sediment and anatomical articulation prevent further observations, other than, as expected, they seem to be smaller than the dorsal ribs, and subcircular in cross section (Figs. 4.2.1, 2.2.1). It is unknown if there was coossification of the cervical ribs with the vertebrae. The first dorsal rib (only the left is preserved, broken just distal to the rib head) has the largest dorsoventral section (Fig. 4.2.1, 2.2.1), and is very similar to the first dorsal ribs of MG 5787 (Fig. 4.1.1.1, 2A). The proximal cross section is T-shaped. As in MG 5787, it is impossible to know with certainty if it was coossified to the vertebra, but the rotation of the ribs relative to the vertebrae seem to suggest that it was not the case. Along the dorsal series, the ribs clearly exhibit the dorsal anteroposteriorly directed flanges (Fig. 4.2.2.3). The rib heads are short, with poorly individualized tubercula and capitula. The diapophyseal articulation facet is circular, corresponding to the diapophysis of the vertebrae (see dorsal vertebrae description above). The cross-section is T-shaped proximally, gradually becoming ellipsoidal and thinning out distally as the dorsal flanges taper into the shaft. Coossification of the ribs with the dorsal vertebrae occurs from d9 on, a condition which is observable in other ankylosaurs (e.g., Coombs, 1978; Molnar, 1980; Carpenter, 2004; Carpenter *et al.*, 2008, 2011; Kirkland *et al.*, 2013). The more posterior dorsal ribs tend to gradually become more laterally directed comparatively to the anterior ones, as the sacral ribs become completely horizontal to form the sacral yoke, eventually fusing distally to ventral surface of the preacetabular process of the ilium (Figs. 4.2.1, 2.2.5) (*sensu* Carpenter *et al.*, 2013).

The last three dorsal ribs have migrated dorsally and articulate with d14-d16 (or ds1-3, see Table 4.2.2.2), which form the presacral rod, dorsal to the centrum. These ribs are shorter, dorsoventrally flattened, and less arched than the more anterior dorsal ribs. The sacral ribs are much shorter than the dorsal ones, shaped as an hourglass and completely coossified to the sacral vertebrae. Sacral ribs 1 and 2 have the anteroposteriorly broadest ends (Figs. 4.2.2, 2.2.5). Proximally, the expansion coossifies with two contiguous sacral vertebrae, but the ribs do not coossify to each other. Distally, the expansion is not as pronounced, but it still forms a wide medial buttress for the acetabulum. Sacral rib 3 also has an expanded base but distally is comparatively much less expanded (Fig. 4.2.2.5), which is even more the case for sacral rib 4. The caudal ribs are short, slightly dorsoventrally flattened, so that the cross section is ellipsoidal, and project laterally from the middle of the centra, bending gently anteriorly (Figs. 4.2.2, 4.2.5-6). They reduce in size along the caudal series, and the bases occupy the full length of the centra until cd10, reducing onwards and eventually absent altogether.

Ossified tendons (Figs. 4.2.1-2, 4.2.2.3-6). The ossified tendons are long, thin, rod-like axial elements, subcircular in cross-section, laterally compressed at the distal ends, which follow the entirety of the vertebral column, except for the cervical region, where this is not observable due to the cervical half-rings and sediment cover (Figs. 4.2.2, 2.2.1, 3). There are two parallel bundles of dorsal tendons on each side, immediately lateral to the neural spines and another more lateral to those (Figs. 4.2.1-2, 4.2.2.3). These bundles are formed by three contiguous tendons, and the more lateral bundles seem to be restricted to the dorsum. The tendon attachment is visible in vertebrae d9-10 (Fig. 4.2.2.3), on the dorsoanterior corner of the lateral surface of the neural spines, as observed by Brown (1908) for *Ankylosaurus*. The same author also observed that tendons overlapped two consecutive vertebrae, which, even though hard to define in the dorsum, seems to be the case in *Dracopelta*. The caudal tendons (Fig. 4.2.2.5-6) however attach to the anterolateral surface of the base of the neural spines and seemingly overlap one consecutive vertebra instead of two. This could putatively be to provide higher flexibility to the tail by providing shorter anchoring distances. Immediately posterior to the sacrum, between vertebrae s3 and cd1, it is visible in dorsal view a differently oriented ossified tendon (Figs. 4.2.2, 4.2.2.4). This is slightly angled away from the

sagittal plane and likely represents a connecting tendon of the pelvic girdle to the tail.

4.2.3. Appendicular skeleton

Pectoral girdle

Scapulocoracoid (Figs. 4.2.1, 4.2.3.1). Both scapulocoracoids are preserved, with the coracoid and scapula fused together. The suture line between the scapula and coracoid is not discernible, therefore the exact contributions of each to the glenoid are unknown. The right scapulocoracoid has been displaced from its original position and is now located ventrally to the cervical region of the specimen, immediately posterior to the skull (Fig. 4.2.1). In ventral view, there are four dorsal ribs on top of the right scapula, two crossing through the middle of the glenoid fossa. Its current position allows observation only of the ventral and lateral surfaces of the coracoid, the anteriormost ventral part of the scapular blade, and partially the glenoid (Fig. 4.2.3.1C, D). The left scapulocoracoid (Fig. 4.2.3.1A, B) is more accessible, although it is more deformed and slightly less complete than the right (Fig. 4.2.3.1C, D). The scapulae are less visible due to the position in the specimen and sediment cover. The scapular blade curves very slightly medially, and has a smooth, gently convex, lateral surface. The posterior end of the left scapular is barely visible (Fig. 4.2.2.1), but the posterior margin of the scapular blade exhibits a rugosity, which, according to Coombs (1978b), likely serves as the insertion point of the *M. serratus ventralis profundus*, the muscle that connects the distal pectoral ribs and sternum to the proximal pectoral girdle. Anteriorly, and directly dorsally aligned with the ventrally projecting posterior rim of the glenoid (postglenoid process, *sensu* Carpenter 2004:978), the acromion process is well developed, and folds ventrally from the lateral surface of the scapula, so that its rugose, ridge-like enthesis points ventrally (Fig. 4.2.2.1A). It is unknown though if the acromion develops from the dorsal margin of the scapula, or if it originates lower in the lateral surface of the scapula (see Sternberg, 1921; Ostrom, 1970; Coombs Jr, 1978a; Carpenter, 2004; Vickaryous *et al.*, 2004; Ősi, 2005; Burns and Sullivan, 2011; Blows, 2015; Kinneer *et al.*, 2016; Wiersma and Irmis, 2018; Raven *et al.*, 2020). On the ventral margin of the scapulocoracoid, the glenoid is a very pronounced ventrally directed cup-like structure (Fig. 4.2.2.1A-D), defined by a thickened rugose

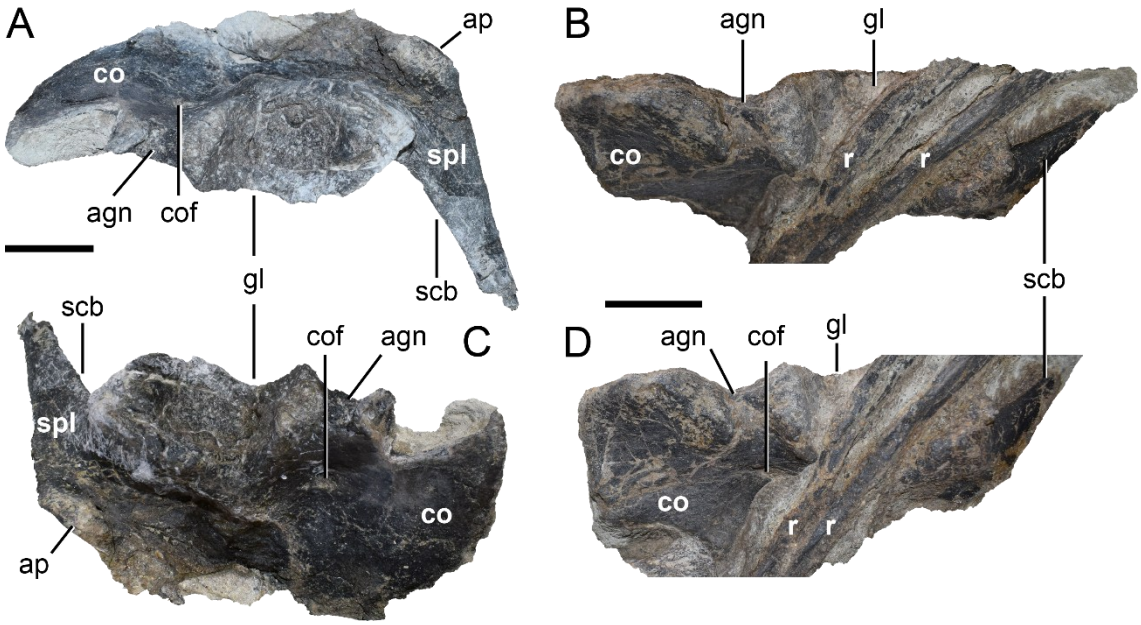

Figure 4.2.3.1. Scapulocoracoid of *Dracopelta zbyszewskii* (NOVA-FCT-DCT-5556). Left scapulocoracoid in ventral (A) and ventrolateral (B) views; right scapulocoracoid in ventral (C) and ventrolateral (D) views. In C and D, the ribs (r) are visible crossing the glenoid. Abbreviations: agn, anteglenoidal notch; ap, acromion process; co, coracoid; cof, coracoid foramen; gl, glenoid; r, rib; scb, scapular blade; spl, scapula. Scale bars: 5 cm.

rim, which projects both laterally and medially from the main body of the scapulocoracoid. The anteroposterior lengths of the right and left glenoids are 118,60 mm and 127 mm, respectively. The mediolateral widths are 71,46 mm and 68,60 mm, right and left respectively. Both the anterior and posterior rims are well developed, and project prominently ventrally, similar to what is observed for example in *Ankylosaurus* (Carpenter, 2004). The mediolateral expansion of the glenoid creates a very pronounced yet dorsoventral thin medial shelf, although, this is only observed in the left glenoid since the right is obscured from view (Fig. 4.2.3.1A, C), and could be a result of deformation. While no contact between the scapula and coracoid is identifiable on the lateral surface, there is a faint transverse line on the anterior ventral surface of the glenoid, approximately at one third of the length, at the inflection point of the curvature, which seems to be a faint scapula-coracoid suture line (Fig. 4.2.3.1A). Immediately anterior to the glenoid, there is a mediolaterally narrow notch on the ventral surface of the coracoid, which separates the thickened rugose ventral margin of the coracoid main body from the glenoid (Fig. 4.2.3.1). The rugose surface extends along the gently convex ventral rim of the

coracoid, providing a broad surface for the attachment of the *M. costacoracoideus* (Coombs Jr, 1978b). In the left scapulocoracoid, this margin is broken immediately anterior to the ventral notch (Fig. 4.2.3.1B). However, the apparent slight remodeling of bone, and comparison to the right coracoid, may indicate a healed injury or some form of pathology, although it is uncertain at this point. In the lateral surface of the coracoid, directly dorsal to anterior rim of the glenoid, at the base of the anterolateral buttress of the glenoid, there is a subcircular coracoid foramen (Figs. 4.2.3.1A B, D). The coracoid is robust and subrectangular (Fig. 4.2.3.1D). The anterior margin is slightly convex, but straight in the right coracoid (Fig. 4.2.3.1B, D). The rugosity that follows the entire anterior margin would serve as the attachment of the *M. coracobrachialis* (ventral) and *M. biceps* (dorsal) (Coombs Jr, 1978b). The left coracoid angles medially at about 60° relative to the long axis of the scapular blade, while on the right, that angle is approximately 42°. Comparatively, in *Ankylosaurus*, this angle is approximately 40° (Carpenter, 2004), while *Gastonia lorriemcwhinneyae* exhibits a higher angle (Kinneer *et al.*, 2016, Fig. 13H, I). Taphonomical deformation of the left coracoid is the most likely cause for this discrepancy.

Forelimbs

Humerus (Figs. 4.2.1, 4.2.3.2). The complete right humerus is preserved, with just the proximal margin slightly eroded, immediately lateral to the humeral head. It has been displaced from its original position to a ventral position relative to the neck (Fig. 4.2.1). Due to its position in the specimen, it is only observable in posterior and proximal views (Fig. 4.2.3.2). The humerus is short and robust, with a straight shaft and both ends mediolaterally expanded, as is typical in ankylosaurs. During extraction of the specimen, the proximal third broke off and was separated, allowing for a view of the cross-section of the proximal end (Fig. 4.2.3.2). It measures 29 cm from the top of the humeral head to the ventral edge of the intercondylary notch. Proximally, the humerus is anteroposteriorly flattened. The maximum proximal width is 15,5 cm, from the medial edge of the internal tuberosity to the lateral edge of the deltopectoral crest. The hemispherical humeral head occupies approximately half of the dorsal edge of the humerus, facing dorsoposteriorly (Fig. 4.2.3.2). It forms exclusively on the posterior (extensor) surface. Medial to the humeral head, the dorsal margin is rugose and folds anteriorly,

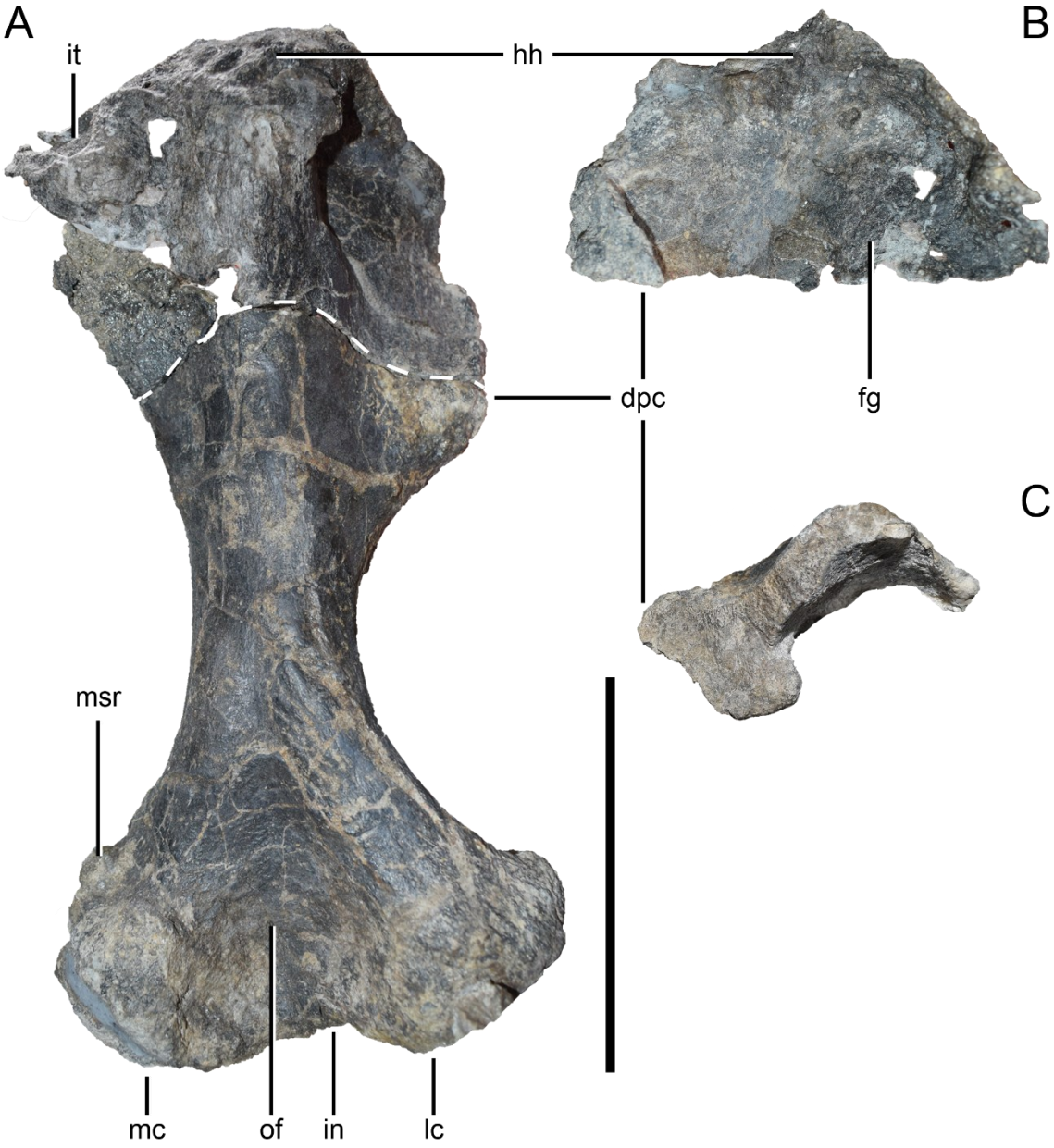

Figure 4.2.3.2. Right humerus of *Dracopelta zbyszewskii* (NOVA-FCT-DCT-5556). Right humerus of *D. zbyszewskii* in posterior (A) view; distal end in anterior (B) view; proximal (C) view of cross-section indicated by white dashed line in A. Abbreviations: dpc, deltopectoral crest; fg – flexor groove; hh – humeral head; in, intercondylary notch; it – internal tuberosity; lc, lateral condyle; mc, medial condyle; msr, medial supracondylary ridge; of, olecranon fossa; Scale bar: 10 cm.

dorsally enclosing a central shallow concave structure on the anterior proximal surface, the flexor depression (*sensu* (Coombs Jr, 1978b). This author identified this depression as the insertion point for the *M. coracobrachialis*. It should be noted the extreme thinness of the bone that forms the flexor depression, approximately 2 mm thick. This extends to the internal tuberosity, which is a small, anteroposteriorly thin,

subtriangular, medial process, which would serve as the insertion for the *M. subcoracoscapularis* (Coombs Jr, 1978b). Diametrically opposed to the internal tuberosity, on the lateral edge of the proximal end of the humerus, is a robust, anteriorly bending deltopectoral crest (Fig. 4.2.3.2). The rugose expanded lateral surface of the crest faces anterolaterally. Between the deltopectoral crest and the humeral head, the dorsal rim of the humerus is slightly thickened, providing anchorage for the scapular deltoid (Coombs Jr, 1978b). Distally, the deltopectoral crest merges with the shaft, at about mid-length of the humerus, conferring a pronouncedly concave shape to the lateral surface of the humerus compared to the medial surface (Fig. 4.2.3.2A). At its narrowest point, the diameter of the shaft is 4,8 cm, and has a perimeter of 13 cm. Distally, the humerus expands mediolaterally, to a maximum width of 15,2 cm. The hemispherical condyles are well developed, and separated by a wide, triangular olecranon fossa, which opens distally to a subtle intercondylary notch (Fig. 4.2.3.2A). Both condyles project anteriorly. The medial (ulnar) condyle is more slightly eroded. On the medial surface immediately dorsal to medial condyle, there is what seems to be a moderately pronounced supracondylary ridge. This may be an artefact of preservation, since in ankylosaurs both the medial and lateral supracondylary ridges are poorly developed, although the latter is usually more pronounced than the former (e.g., Ostrom, 1970; Carpenter, 2004; Vickaryous *et al.*, 2004; Carpenter *et al.*, 1995, 2008; Arbour and Currie, 2013). The lateral (radial) condyle is slightly larger than the medial, and the trochlear surface is more evident, defined by a faint rugose ridge (Fig. 4.2.3.2A).

Pelvic girdle

Ilium (Fig. 4.2.2.5). Both ilia are preserved, though the left ilium is the better preserved and more exposed (Figs. 4.2.1-2, 4.2.2.5). The dorsally located pelvic shield covers most of the pelvic girdle, apart from the anterolateral corner of the preacetabular process of the left ilium, thus limiting observation in dorsal view. The preacetabular process extends anterolaterally and bends ventrally from a medial horizontal position (Fig. 4.2.2.5). This ventral folding is more pronounced than in *Gargoyleosaurus* (Carpenter *et al.*, 2013) and closer to what is observed in *Mymoorapelta* (Kirkland and Carpenter, 1994; Carpenter *et al.*, 2013). The edges of the ilium are broken. As is common in Ankylosauria, the preacetabular process represents over 50% of the total length of the ilium, while the postacetabular is

reduced, albeit far from the degree seen in more late diverging ankylosaurs (e.g., Coombs Jr, 1978a; Vickaryous *et al.*, 2004; Lü *et al.*, 2009; Arbour *et al.*, 2009; Arbour and Currie, 2013; Carpenter *et al.*, 2013; Wiersma and Irmis, 2018). In fact, recent preparation of the specimen uncovered a comparatively well-developed right postacetabular process, projecting posterolaterally and oriented horizontally. In the left ilium, on the ventral surface of the preacetabular process, approximately halfway, there is a knob which corresponds to the coossified distal end of dorsal rib 15 (Fig. 4.2.2.5). Posteriorly, the first caudal rib, albeit broken distally, seems to have a continuation in the postacetabular process, indicating the articulation of the rib with the postacetabular process medially. Ventrally, even though difficult to individualize due to articulation and preservation of the pelvic elements and the femora, and considering the reduction of the pubis (see description below), the pubic peduncle of the ilium extends ventrally and seemingly contributes anteriorly and medially to the acetabulum. However, the extent of this medial contribution and of the sacral ribs is unknown. Posteriorly, the ischial peduncle of the ilium seems comparatively reduced, with the ischium having the largest contribution to the posterior acetabular wall (see description below; Fig. 4.2.3.3)

Pubis and ischium (Figs. 4.2.2.5, 3.3). The pubes and ischia are preserved in articulation, although only the proximal ends are preserved, with the right pubis and ischium heavily eroded and broken (Fig. 4.2.2.5). The left pubis and ischium are better preserved but are only visible in ventral view (Fig. 4.2.3.3). Medially, the sacral ribs brace the medial wall of the acetabulum, therefore hindering direct observation of the exact contributions of each bone to the acetabulum. Also, sediment cover and the articulation of the left femur in the acetabulum further limit observation of the acetabulum (Fig. 4.2.3.3). For this reason, it is unknown at this time if the acetabulum is fully closed or not, the latter being a condition observed in early diverging ankylosaurs, such as *Gargoyleosaurus*, *Mymoorapelta* or *Gastonia* (Kirkland and Carpenter, 1994; Carpenter *et al.*, 2013; Kinneer *et al.*, 2016). In these taxa there is a gap between the ischium and the pubis, opening the acetabulum. In *Edmontonia*, the existence of this opening is unclear (Carpenter *et al.*, 2013). Both the ischia and pubes articulate with the ilia at an angle from the sagittal plan, so that the acetabulum faces slightly lateroposteriorly (Figs. 4.2.1, 2.5, 3.3), thereby allowing the leg to move forward in an anterolateral direction to accommodate the

likely enlarged gut. The acetabulum is shallow and the posterior wall and at least partially the medial wall are formed by the ischium (Fig. 4.2.15).

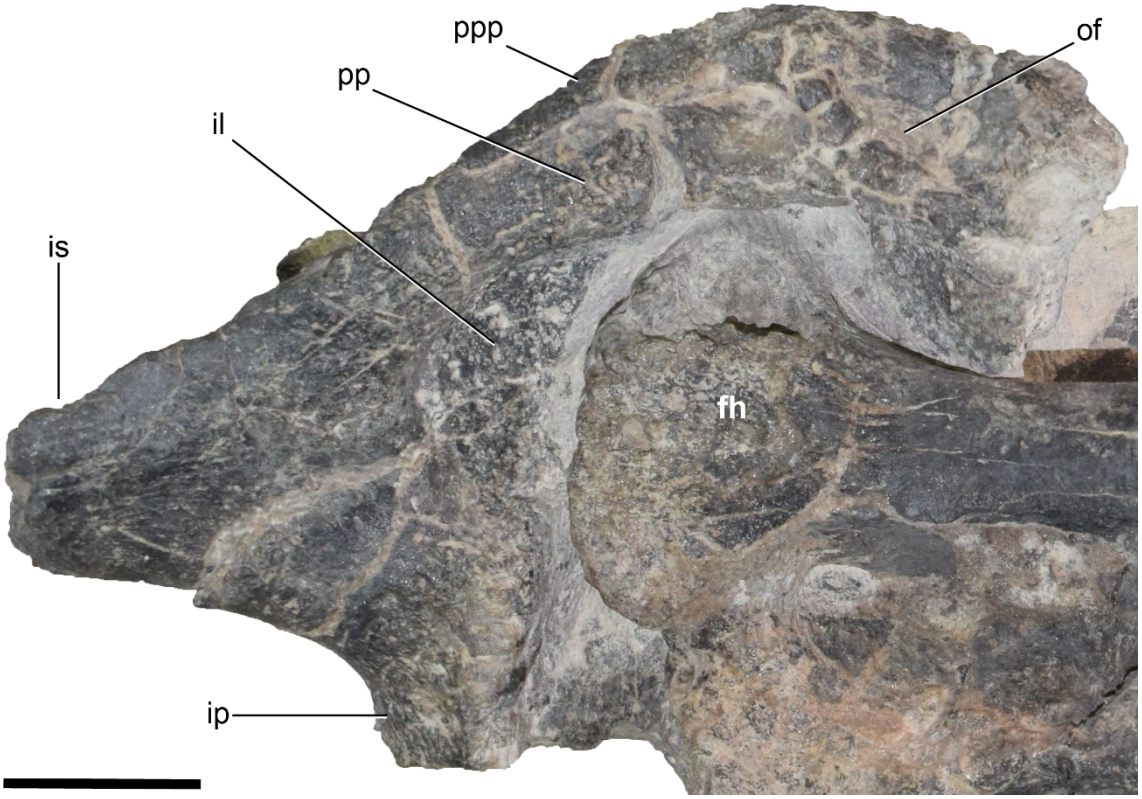

Figure 4.2.3.3. Pubis and ischium of *Dracopelta* zbyszewskii (NOVA-FCT-DCT-5556). Left pubis and ischium in ventral view. Abbreviations: fh, femoral head; il, ischial lamina; ip, iliac peduncle; is, ischial shaft; of, obturator foramen; pp, pubic peduncle; ppp, postpubic process. Scale bar: 5 cm.

The pubis is considerably smaller than the ischium, as is common in ankylosaurs, being in some cases nonexistent (e.g., Romer, 1927, 1956; Coombs, 1979; Vickaryous *et al.*, 2004; Carpenter *et al.*, 2011; Arbour and Currie, 2013; Carpenter *et al.*, 2013). Although only the posterior half of the pubic body and the proximal portion of the postpubic process are preserved, the pubis is a small, blunt bone. In Ankylosauria, the prepubic process is lost (Coombs, 1979). The pubic peduncle and pubic body are difficult to individualize due to the preservation and sediment cover, but the contribution to the acetabulum seems to be minimal or none (Fig. 4.2.3.3). The visible surfaces are rugose. The postpubic process (Fig. 4.2.3.3) projects caudoventrally and bends in a way as to follow the ventral surface of the ischium. It is a thin, slender rod, broken distally, therefore its full length is unknown. Its shape is very similar to *Gargoyleosaurus*, but thinner distally (Kilbourne and Carpenter, 2005; Carpenter *et al.*, 2013). In *Mymoorapelta*, the postpubic process extends as

far as the middle of the ischium (Carpenter *et al.*, 2013). There is a faint crest projecting ventrally from the proximal end of the process. The obturator foramen is ellipsoidal in ventral view, closed off posteriorly by the curved postpubic process (Fig. 4.2.15), like *Gargoyleosaurus*. In *Gastonia*, the obturator foramen is subcircular and opens posteriorly (Kilbourne and Carpenter, 2005; Kinneer *et al.*, 2016).

The ischium is incomplete, broken just distal to the descending process of the shaft (Fig. 4.2.3.3). The proximal end is mediolaterally expanded, and both the iliac and pubic peduncles are enlarged, specially the first, which is immediately posterior and lateral to the acetabulum, partially contributing to the posterior wall of the acetabulum (Fig. 4.2.3.3). The rim of iliac peduncle is rugose. Between the pubic and iliac peduncles, the ischial lamina (*sensu* Kinneer *et al.*, 2016) is anterolaterally concave, forming a cup-like depression that constitutes most of the posterior wall of the acetabulum, as well as contributing to the medial wall (Fig. 4.2.3.3).

Hindlimbs

Femora (Figs. 4.2.1, 4.2.2.5, 3.4). Both femora are nearly complete and articulated with the acetabula (Figs. 4.2.1, 4.2.2.5, 3.4). The distal lateral edge of the shaft and the lateral condyle of the left femur are missing (Fig. 4.2.3.4A-B). Although the right femur is practically complete, it is broken and divided among three different blocks (Figs. 4.2.3.4C-K): one with most of the femur (most of the proximal end, shaft, posterior surface of the distal end); the femoral head is separated from the shaft and articulated with the acetabulum; the anterior portion of the distal end. It is 40 cm in length from the greater trochanter to the distal end. Approximately 2/3 distally, the shaft is diagonally fractured transversely, with the distal end (about 14 cm) loose from the rest of the femoral body, but still in situ. Another fracture diagonally separates the posterior condylar region from the anterior face of distal end. The latter is mostly covered by matrix, hampering further observation. The shaft is asymmetrically tear shaped in cross section, more curved anteriorly. It is compressed anteroposteriorly and transversely expanded, in that mediolaterally it is almost twice the anteroposterior length. The minimum femoral shaft perimeter is 188 mm. There is a visible medullary cavity filled by sediment encased by an approximately 8 mm thick periosteum wall. As aforementioned, the femoral head is articulated in the acetabulum, but very eroded and covered by sediment which makes it impossible to describe further. The greater trochanter is a

rounded knob, slightly protruding laterally, separated from the femoral head by a distinct notch (visible in the left femur), with a pronounced rugose surface for muscle attachment, specifically the *M. puboischiofemoralus internus* and the *M. iliotrochantericus* (Coombs Jr, 1979). The anterior trochanter is obscured in the right femur. An intermediate, deep, erosive depression is present, extending almost to the distal margin of the fourth trochanter. This structure might possibly correspond partially to an intertrochanteric fossa, since it is present in both femora, but it is impossible to confirm to what extent. The fourth trochanter is a ridge-like structure located distally in the proximal half of the shaft, with a rugose surface and slightly offset medially. Distally, the lateral surface of the shaft is rounded and smooth, with no discernible muscle scar. The distal end expands both anteroposteriorly and lateromedially to almost more than twice the shaft. The distal end lateromedial width is 131,62 mm. The medial face of the distal end is flattened and bears longitudinal grooves indicating presence of tendon attachment. The distalmost edge is continuous without a well-defined groove between both condyles. The intercondylary fossa is deep, while also being taphonomically compressed. Distally, it is less deep and bears a shallow bridge between both condyles. The posterior condyles are taller than wider. The tibial or medial condyle is approximately twice the size of the lateral or fibular condyle. In posterior view, it has a well-defined subtriangular outline. The lateral epicondyle is very pronounced, projecting laterally. It provides both laterally and laterodistally. In medial view, the distal end is rounded. The distal edge of the lateral condyle is in a slightly more proximal position than the medial one.

Figure 4.2.3.4 (next page). Femora of *Dracopelta zbyszewskii* (NOVA-FCT-DCT-5556). Left femur in lateral (A), posterior (B) views; right femur in posterior (C) view; distal end of right femur in posterior (D), anterior (E), medial (F), lateral (G), proximal (H) and distal (I) views; complete distal end of right femur in posterior (J) and distal (K) views. Dashed red line in J and K indicate the breakage line of the two distal femur fragments. Abbreviations: at – anterior trochanter; fh – femoral head; ft – fourth trochanter; gt – greater trochanter; if – intercondylary fossa; in – intercondylary notch; itf – intertrochanteric fossa; lc – lateral condyle; lec – lateral epicondyle; lp – lateral plate; mc – medial condyle; mdc – medullary cavity; pf – popliteal fossa. Scale bars: 10 cm in A-C, 5 cm in D-K.

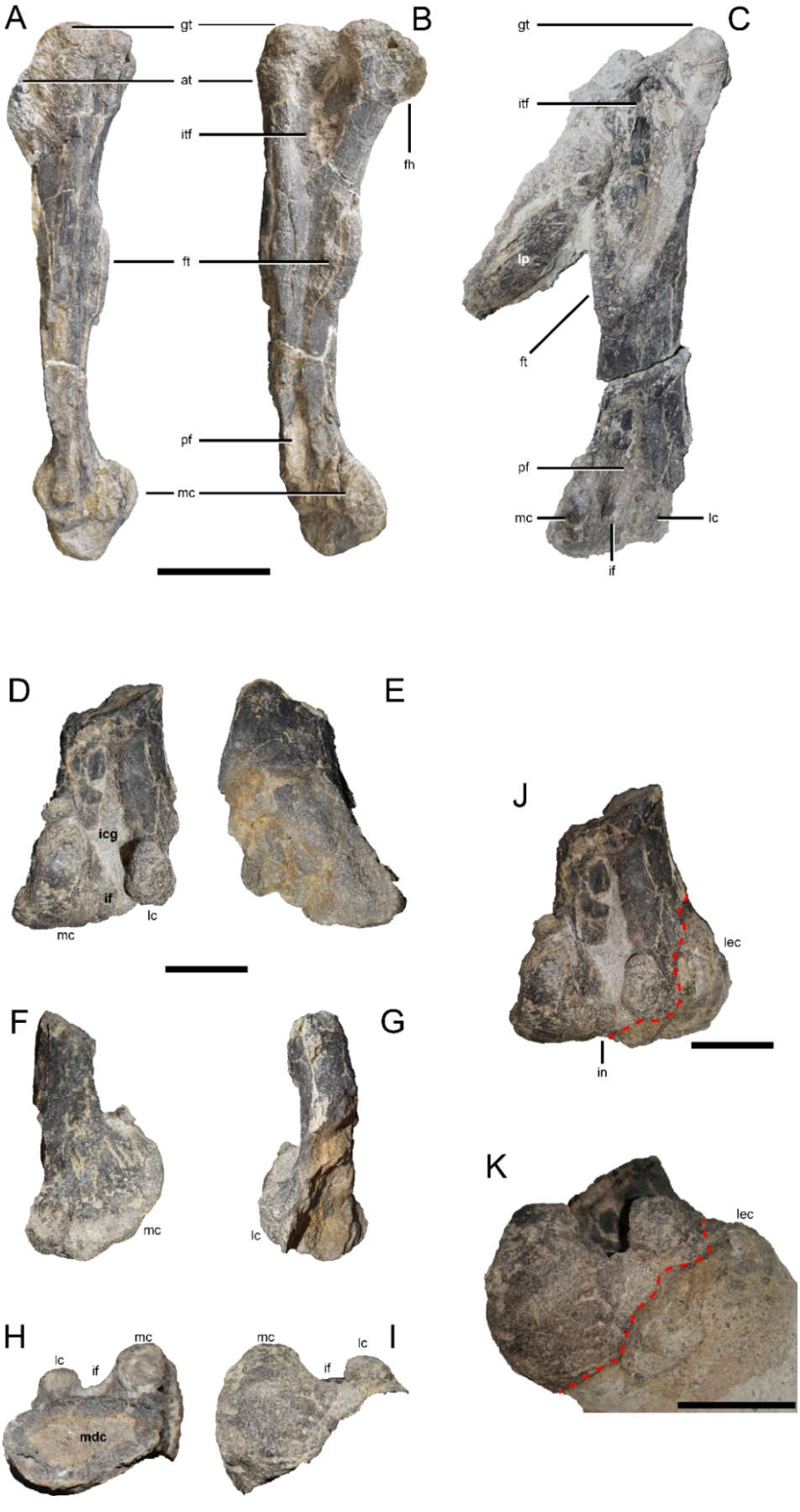
A
B
gt
at
itf
fh
ft
pf
mc
C
gt
itf
lp
ft
pf
mc
lc
if
D
E
icg
if
lc
mc
J
lec
in
F
G
mc
lc
K
lec
H
I
mc
lc
if
mdc
mc
lc
if

4.2.4. Dermal skeleton

The post-cranial dermal armour of NOVA-FCT-DCT-5556 is mostly preserved articulated (Figs. 4.2.1-2, 2.1, 3, 5, 6, 4.1). It consists of cervical, transitional, thoracic, pelvic, and anterior caudal armour elements. For the cranial ornamentation, see sub-section 4.2.1. Although the lateral areas of the specimen are not preserved, there are both isolated lateral osteoderms and a few associated with larger axial elements, which allows to infer the presence of a lateral row of plates on each side. These are the largest osteoderms in the specimen, measuring more than 15 cm mediolaterally. Some elements of the armour have been displaced. The nomenclature for the dermal armour merges and adapts from previous works on the placement and morphology (Blows, 2001, 2015; Arbour *et al.*, 2011, 2014b; Burns and Currie, 2014; Brown, 2017) and is illustrated in Figure 4.2.4.1. See sub-chapter 2.1 of Material and Methods of this work for further details on the nomenclatural system.

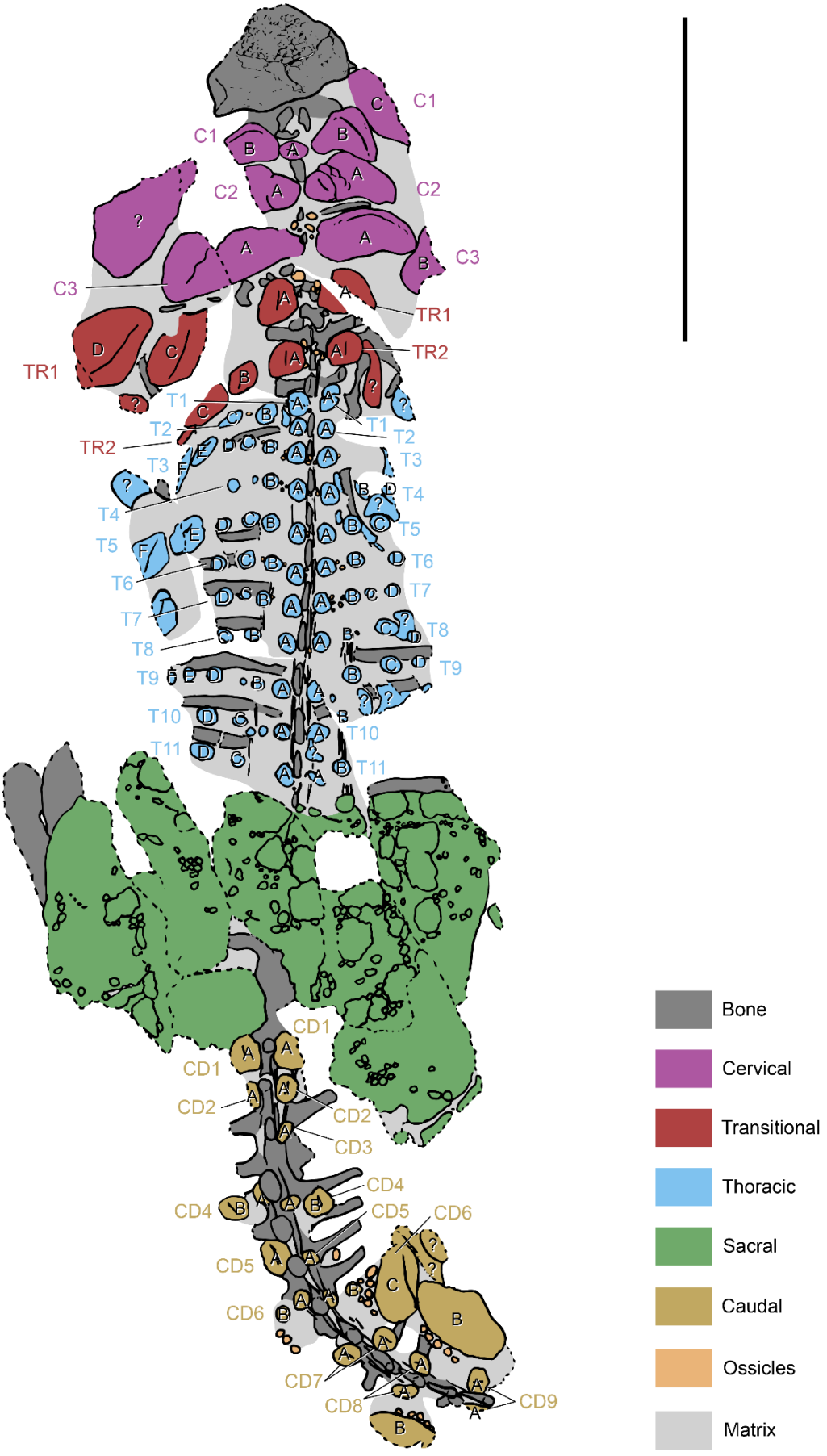
C1
C2
C3
TR1
TR2
T1
T2
T3
T4
T5
T6
T7
T8
T9
T10
T11
CD1
CD2
CD3
CD4
CD5
CD6
CD7
CD8
CD9
Bone
Cervical
Transitional
Thoracic
Sacral
Caudal
Ossicles
Matrix

Figure 4.2.4.1 (previous page). Schematic drawing of NOVA-FCT-DCT-5556 in dorsal view illustrating dermal armour classification. Colours represent dermal armour regions, numbers together with letters represent transverse bands, and letters on the osteoderms indicate position along the band. Refer to sub-section 2.1.1 on Anatomical Nomenclature for further details. Scale bar: 50 cm.

Cervical (Fig. 4.2.2-3, 4.1). The cervical armour consists of three bands of osteoderms (C1, C2, C3), covering the dorsal and lateral parts of the neck, and forming cervical half-rings (Fig. 4.2.4.1). These are formed by two quarter rings (unfused at the dorsal midline), composed of smaller, subcircular medial ossicles, and larger, laterally elongated, keeled scutes (*sensu* Blows, 2015). The anteriormost ring, C1, differs from C2 and C3 in the presence of an ellipsoidal (5 by 3 cm) medial ossicle (C1A), with a low central peak and pitted dorsal surface, dorsal to the atlas, abutting the two elements lateral to it (Fig. 4.2.4.1). A similar osteoderm is also present in the first cervical band of *Gargoyleosaurus* (Kilbourne and Carpenter, 2005). Lateral to C1A, there are two subtype II scutes. C1BL is broken laterally, while C1BR is complete. Both show a prominent anteriorly projecting midline keel. The anterior projection of the keel makes it so that, medial to the keel, the external surface is oriented dorsally, while lateral to the keel is facing anterolaterally. A second, larger dermal element, located anteroventrolaterally to the first scute, broken laterally, is only visible in dorsal view, and abuts the lateral rim of C1BR (Fig. 4.2.4.1). Based on the size (it is the largest element of the first cervical ring) and shape (the posterior edge projects posterolaterally, tapering posteriorly, and making the posterior rim slightly concave), it seems to be the first lateral plate (corresponding to position C1CR; Fig. 4.2.4.1), similar to what is observed also in *Gargoyleosaurus* (Kilbourne and Carpenter, 2005; Carpenter *et al.*, 2013). A left large dorsoventrally flat element is located laterally to the cervical rings (Fig. 4.1.4.1). It measures at least 22 cm and is broken anteriorly. Size and morphology indicate that it is a lateral plate (see details on lateral armour below). However, a comparison between this element and C1CR suggests that the former likely is not the first cervical lateral plate but may have been slightly displaced from its original position, likely at base of the neck/shoulder region. The second cervical ring (C2) has two elements, but, laterally to these, there would be a lateral plate, as in C1. C2AR-L are each formed by two fused elements: a medial, smaller sub-circular subtype II ossicle and a lateral, keeled, lateroposteriorly projecting subtype II scute

(Fig. 4.2.4.1). The ossicles are approximately 4 cm in diameter and exhibit an incipient median keel, and the scutes measure approximately 10 cm, with a well-developed keel that projects anteriorly and anterolaterally, so that half of the osteoderm faces dorsally and the other half is obscured in dorsal view (Fig. 4.2.4.1). Medially, the osteoderms abut each other at their most medial point, in a dorsal position to the intervertebral gap between the tip of the neural spines of the axis and the third cervical vertebra (Fig. 4.2.4.1). In dorsal view, and similarly to the first ring, the scutes have a sub-reniform shape, creating a pronounced anterior concavity bounded laterally by the anteriormost extension of the keel (Fig. 4.2.4.1). Distally, there is a large dorsoventrally flat element, which may correspond to the second lateral plate (C2?BL). The third cervical band (C3) is also composed of two subtype II scutes oriented mediolaterally, reniform shaped in dorsal view (Fig. 4.2.4.1). C3AR-L are the largest elements of the cervical armour (proximodistal length ≈ 20 cm), excluding possibly the lateral plates, which have either been lost or displaced from their original position. The midline keel is, as in C2, projected anteriorly proximally and gradually becoming more dorsally directed as it curves anterolaterally until it tapers into the dorsally facing external surface of the scute, which is observable in C3AL (Fig. 4.2.4.1). At the posterolateral corner of C3AR, there is a fragment of a larger osteoderm, possibly a scute, which could either be a proximal portion of C3BR or part of a slightly displaced TR1CR. Medially, the space between C3AR-L is filled by subtype III ossicles, some of which are fused to the larger scutes. Comparing with other ankylosaur cervical bands, namely *Gargoyleosaurus*, and due to the presence of the first right cervical lateral plate, the cervical region armour would be made of three bands ("quarter-rings") of two scutes each (and a medial ossicle in C1), followed laterally by plates.

Transitional (Figs. 4.2.2-3, 2.1, 4.1). Transitional osteoderms (TR) make up two bands in the cervicothoracic region and consist of subtype I ossicles, with an intermediate morphology between the large scutes of the cervical region and the smaller subtype II ossicles of the thoracic region (Figs. 4.2.2.1, 4.1). The transitional bands correspond to the fourth and fifth overall of the dermal armour (the first three are cervical). The medial osteoderms, TR1AR-L, TR2AR-L and TR2BL are *in situ* and the best preserved (see Material and Methods, sub-section 2.1, on the dermal armour nomenclature system used in this work). Lateral to these, the specimen is

broken, therefore conditioning observation. Nonetheless, there is a partial scute (TR2CL), which, considering its position and comparison with the rest of the dermal armour, belongs to subtype I, i.e., sub-rectangular with a low keel. The pairs of medial ossicles TR1-2AR-L are morphological identical, but TR1AR-L are slightly larger than TR2AR-L (7 cm and 5 cm, respectively). The ossicles are sub-circular, with a midline keel and thickened edges, located dorsal to the transverse processes of vertebrae c8 and d2. As in the holotype, in dorsal view the wing-like transverse processes of vertebrae d1. These two pairs of ossicles are an autapomorphy of *Dracopelta* (Figs. 4.1.1.1-2A, 4.2.2.1). The posterior half of TR1AR is better preserved than the anterior half, which is partially covered by sediment and more fractured (Figs. 4.2.2.1, 4.1). The characteristic midline keel and thickened rim is visible on the better-preserved half, corresponding to the posteromedial corner. Its left counterpart, TR1AL, is complete and is sagittal and transversely asymmetrical, as in the holotype (Figs. 4.1.1.2A, 4.2.2.1). Dispersed throughout the dermal armour, there are subtype III ossicles. Apart from the partial scute TR2CL, there are no preserved distal elements of the transitional region. However, it is possible to observe that transitional band 2 (dermal armour band 5 overall) merges distally (at position TR2CL) with the first band of the thoracic region (Fig. 4.2.4.1).

Thoracic (Figs. 4.2.1-3, 2.3, 4.1). The thoracic armour is composed of ten thoracic transverse bands of at least four medial subtype II ossicles each, followed laterally by an uncertain number (possibly two or three) of subtype I scutes. More distally, the specimen is broken (the right side is more incomplete than the left) and the articulated armour has been lost (Fig. 4.2.2). By comparing with the holotype (Figs. 4.1.1.1, 2D, E) there would also be at least a row of subtype II lateral scutes, medial to the lateral plate row (see lateral armour description below). Dispersed throughout between the larger elements are subtype III ossicles (≤ 1 cm) (Figs. 4.2.2-3, 2.3, 4.1). The bands arch slightly anteriorly and are separated from each other at approximately 3 cm intervals, with T1-11AR-L roughly coinciding with the spaces between dorsal neural spines, except in bands 1-3, due to the shorter length of the anterior dorsal vertebrae. It is unclear though if the bands were located dorsally and aligned to the ribs when the animal was alive, since many of the ribs have been displaced. The subtype II ossicles are sub-circular, most exhibiting a faint midline keel (Fig. 4.2.4.1-2), with a surface showing a reticular neurovascular groove

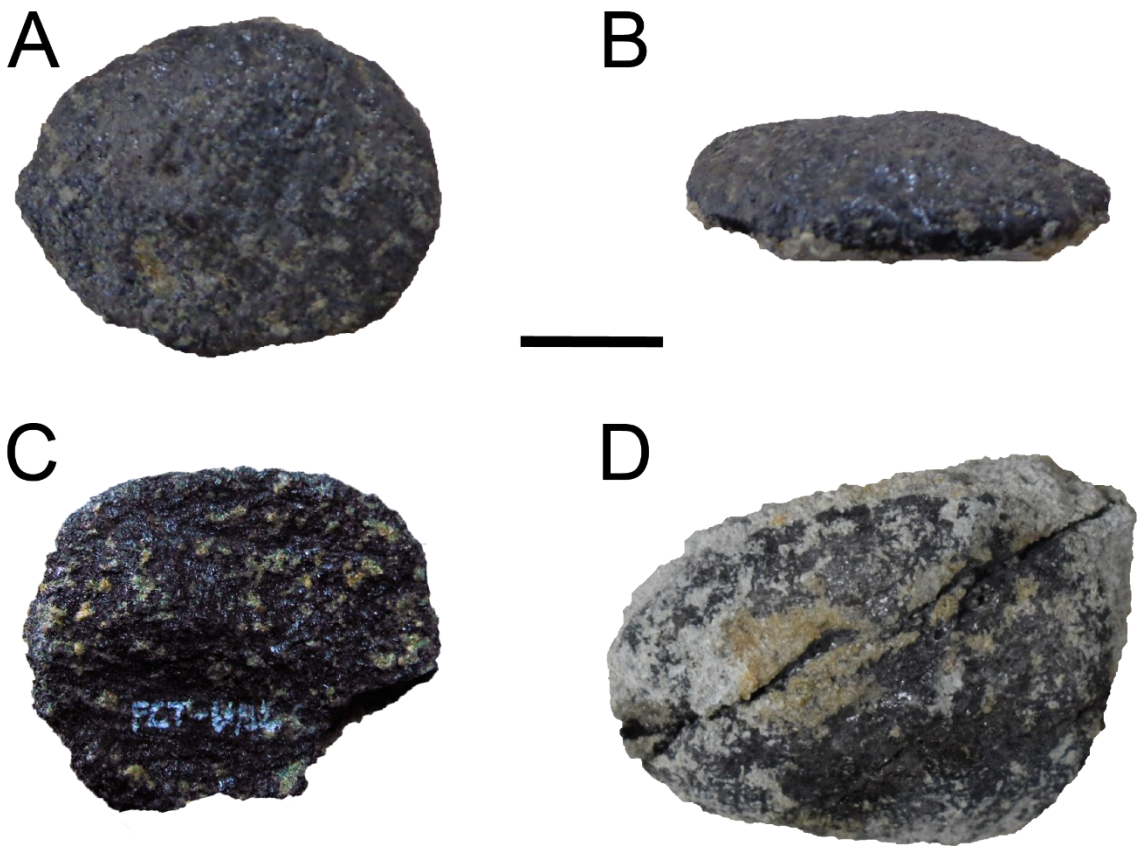

Figure 4.2.4.2. Associated thoracic osteoderms of *Dracopelta zbyszewskii* (NOVA-FCT-DCT-5556). Four thoracic subtype II ossicles from NOVA-FCT-DCT-5556 in dorsal (A, C, D), and lateral (B) views. Exact position unknown. Note the faint keel in A and C. Scale bar: 1 cm.

orientation (*sensu* Hieronymus *et al.*, 2009) and compare well with the ossicles from the holotype (Figs. 4.1.1.2C, 4). The first two bands differ from the others in the number and arrangement of the ossicles. Immediately lateral to T1-2A, the bands merge into a single band, resulting in eleven pairs of medial ossicles (T1-11A) but ten bands of osteoderms overall. In turn, this first band merges with the second transitional band, at the position of scute TR2CL (Figs. 4.2.2, 2.2.3; see also description on the transitional armour above). Thus, in the first band, the lateralmost osteoderm is T1CR-L, which is slightly more elongated than T1A-B. T1AR-L are slightly larger than T2AR-L (Fig. 4.2.2.3, 4.1). In fact, the medialmost osteoderms of each band (T1-11A) are the largest, as successively more lateral ossicles tend to decrease in size until the larger, more lateral scutes. This size difference is less marked though in the more posterior bands, e.g., band 9-11 (Fig. 4.2.2.3, 4.1). In band 2, T2ER is ellipsoidal, measuring 6 cm, and the midline keel is more pronounced than in the ossicles in more medial positions. It serves as a transition

ossicle between the medial ossicles and the lateral scutes. The subtype I scutes that are in the more lateral positions are subellipsoid, with a medially offset midline keel (Figs. 4.2.2-3, 2.2.3, 4.1; see also the armour description of MG 5787), and increase in size distally. It is unknown the exact number of elements that make up each band, but it is plausible that more posterior bands would have a higher number of osteoderms due to the increasing width of the body. This thoracic dermal armour arrangement is autapomorphic for *Dracopelta zbyszewskii*.

Pelvic (Figs. 4.2.2, 2.2.5, 2.4.1). The sacral shield lays dorsally on the pelvic girdle (Figs. 4.2.2, 2.2.5). It is mostly complete, missing its right lateral and left posterior edges, as well as some smaller more medial fragments (Fig. 4.2.2.5). It forms a sub-rectangular sheet of armour covering the sacrum and most of the ilia, with only the ventrally curving, anterior margin of the preacetabular process of the ilia visible dorsally. It narrows slightly posteriorly (Fig. 4.2.2.5), following what would be the body shape of the animal towards the tail. Posteriorly, the posterior rim of the shield curves gently medioanteriorly (Fig. 4.2.2.5), so that the anterior and posterior rims are not parallel, and the lateroposterior corners extend more posteriorly than the medial part. It is composed of coossified roughly shaped rosettes (the Category 2 of pelvic shield morphology of Arbour *et al.*, 2011), with larger ossicles (subtype II) surrounded by smaller subtype III. Various taxa exhibit a similar morphology, such as *Gargoyleosaurus*, *Mymoorapelta*, *Gastonia*, *Hylaeosaurus*, and *Polacanthus* (Mantell, 1833a; Hulke, 1887; Kirkland and Carpenter, 1994; Kirkland, 1998; Blows, 2001; Kilbourne and Carpenter, 2005; Arbour *et al.*, 2011). *Shamosaurus* is reported to have a thin pelvic armour like that of *Polacanthus* (Tumanova, 1987). Surrounding the shield are small ellipsoid, keeled scutes (Fig. 4.2.2.5). At the posterior edge of the pelvic shield, there is a pair of slightly more individualised medial rosette-like ossicles, in a transition to the caudal medial osteoderms.

Caudal (Figs. 4.2.2-3, 2.2.6, 2.4.1). The caudal armour follows the same pattern as the thoracic armour, with rows of smaller medial ossicles, lateral scutes, and a row of lateral plates (see above for definition and description of ossicles and scutes subtypes). Two subtypes of ossicles can be observed in the tail: subtype II, small (3-4 cm), subcircular dorsoventrally flat ossicles, located in rows along the medial axis of the tail, and subtype III, the smallest elements (≤1 cm), subcircular, which

permeate the dermal armour and encircle the larger tail scutes (Figs. 4.2.2-3, 2.2.6, 2.4.1). Nine bands of paired ossicles (subtype II) can be identified, exhibiting a faint midline keel and a pitted surface, composed of at least one element (CD1-9AR-L). In band 3 and 5, there is a second ossicle, CD3BR-L, and CD5BR-L, respectively (Fig. 4.2.4.1). Anteriorly, from bands 1 to 4, all the osteoderms have been lost, therefore it is unknown whether there might have been more than two ossicles in each row. However, posteriorly, the dermal armour is better preserved (Fig. 4.2.4.1) and shows subtype II scutes as the third elements of the caudal bands (specifically, CD5CR), until at least the fifth band. The scute is ellipsoidal with a very developed midline keel, and it seems to have been encircled by subtype III ossicles, although only five medial of these are preserved. In the immediately distal position to it, there is an elongated osteoderm which, due to its rugose margins, hollow base, concave dorsal and ventral surfaces, and distal placement in the row, is identified as a caudal plate, broken distally. Due to the larger dimensions of the scutes, not all medial osteoderms are accompanied laterally by a corresponding scute (e.g., CD6AR-L are the only elements in its bands) (Fig. 4.2.4.1). Posteriorly, slightly larger elements occupy position CD7BR-L, extending into band 8, similarly to scute CD5CR. Even though broken distally and mostly covered by sediment ventrally, the presence of an edge visible in ventral view in these, suggests that in fact these are plates, which, similarly to the scute CD5CR, are surrounded, at least medially by subtype III ossicles.

Lateral. (Figs. 4.2.4.3). Most of the lateral armour of NOVA-FCT-DCT-5556 has been lost. Few elements are preserved, and most are broken or have been displaced from its original location on the body, either stacked over each other or dispersed among other bones (e.g., ribs, scapula, pelvic girdle), which considerably hinders direct observation. However, even though rare, there are a couple of better-preserved elements that were possible to isolate, corresponding to large dorsoventrally flat plates (Fig. 4.2.4.3). These are the largest dermal armour elements (> 14 cm). The largest preserved plate seems to belong to the cervical region (see above for cervical armour description). Another large proximal fragment of a plate (Fig. 4.2.4.3A-C) shows a distinct basal deep groove, bordered by thickened rugose margins, for dermal insertion. This groove extends posteriorly so that its dorsal margin forms a posteriorly pointing keel on the dorsal surface of the

plate, as observable in cross-section in both *Dracopelta* specimens (Figs. 4.1.1.2E, 4.2.4.3C). Since most of the plate is broken distally, the exact extension of this keel is unknown. However, the posterior extension of the basal groove is seemingly

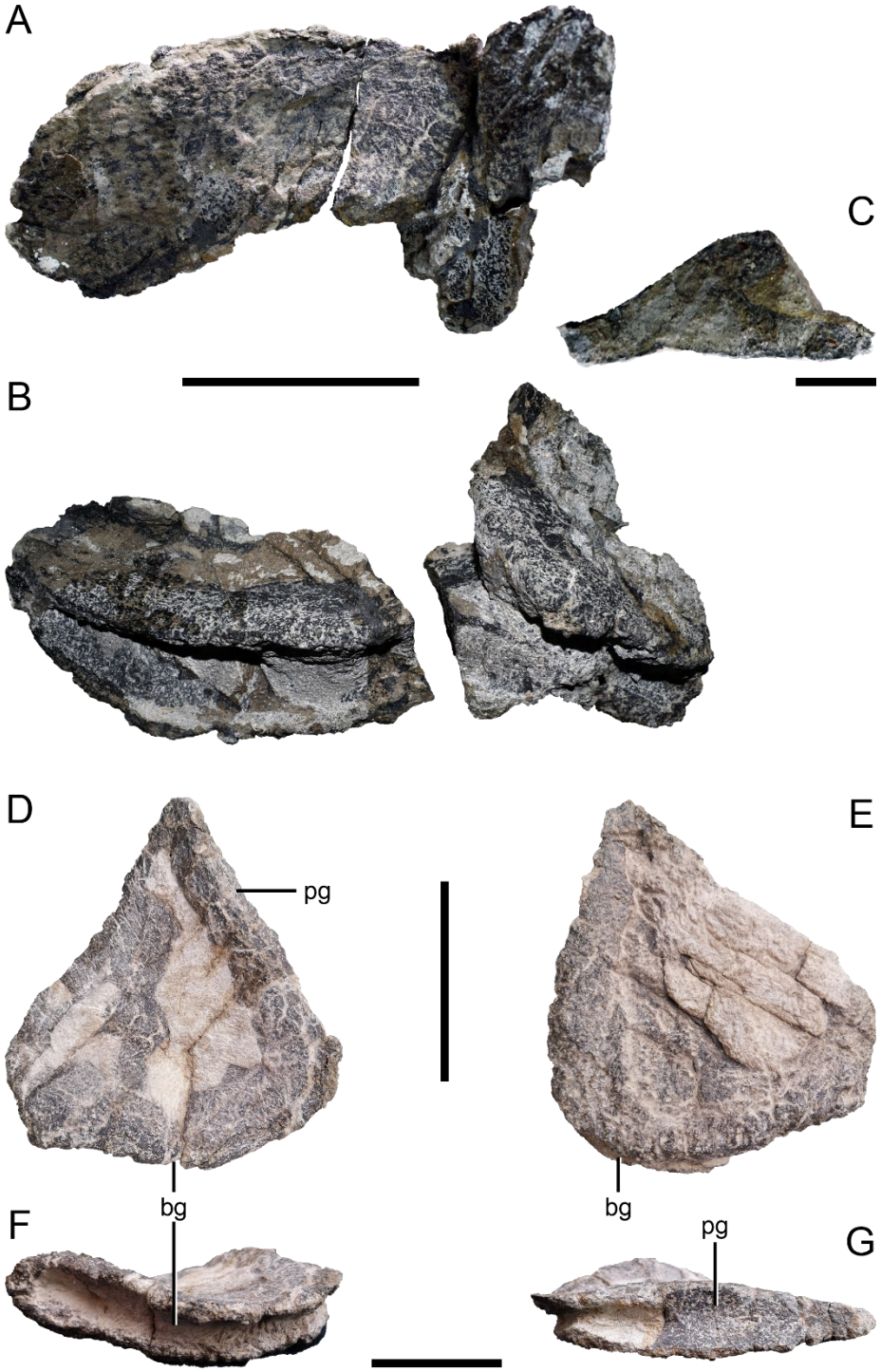

Figure 4.2.4.3. Lateral plates of *Dracopelta zbyszewskii* (NOVA-FCT-DCT-5556). Lateral plates in ventral (A, E), dorsal (B, D), proximal (F) and posterior (G) views; cross-section of plate in C, with dorsal keel prominent. Note in F the rugose margins of the basal groove. Abbreviations: bg – basal groove; pg – posterior groove. Scale bar: 10 cm in A, B, D, and E, 5 cm in F and G, 2 cm in C.

variable across the lateral plate series, as more developed keels are found in more anterior (cervical, cervicothoracic, and anterior thoracic), usually larger plates (Fig. 4.1.1.2E). The keel tapers distally into the flat dorsal surface. This is similar to what is observed to a varying degree in other polacanthids, such as *Gastonia*, *Mymoorapelta*, or *Polacanthus* (Kirkland and Carpenter, 1994; Blows, 2015; Kinneer *et al.*, 2016). Another incomplete, large, triangular plate is better-preserved (Fig. 4.2.4.3D-G). The base has a deep groove and rugose margins (Fig. 4.2.4.3E, F), which continues into the posterior margin. The posterior groove (Fig. 4.2.4.3D, G) is conspicuous, although not as deep as in other plates (Fig. 4.2.4.3B, C). The presence of a posterior groove in the lateral plates might have served as an interlocking mechanism between consecutive plates to accommodate movement. Observation of the lateral section of the holotype seem to support this assertion, at least in the cervicothoracic region (Fig. 4.1.1.2E). The plates are broken distally, not preserving the presumably posteriorly pointing apex. Also, the displacement of the lateral plates precludes an exact positioning along the body, but a comparison with the holotype of *Dracopelta* (Fig. 4.1.1.2E) seems to suggest a right, possibly cervicothoracic, plate (Fig. 4.2.4.3D-G), and a left plate (Fig. 4.2.4.3A-C). While not articulated, the plates are mostly found in more distal areas of the skeleton, which, together with its large size, morphology, and comparable material from the holotype and other ankylosaurs, supports the existence of a row of lateral plates along the sides of the animal.

5

PHYLOGENETIC RESULTS

The phylogenetic analyses performed to resolve the position of *Dracopelta* within Ankylosauria were based on a heavily modified version of the dataset of Loewen and Kirkland (2013). To assess the phylogenetic relationships and position of *Dracopelta*, five rounds of Maximum Parsimony analysis were performed, one with equal weighting and four with implied weighting. The EW round produced 50000 MPTs of 1391 steps, with a Consistency Index (CI) = 0,289, Retention Index (RI) = 0,755, and Rescaled Consistency Index (RSI) = 0,218. The IW rounds with k = 5, 10, and 12, produced, respectively, 5250 MPTs of 1419 steps, 11970 MPTs of 1406 steps, 8736 MPTs of 1401 steps. The round with k = 15 produced 624 MPTs of 1397 steps, with a CI = 0,288, RI = 0,753, and RSI = 0,217. Overall, the analyses recovered consistent, reasonably well supported (Bremer ≥1, bootstrap ≥50) results, although with expected topological variations. Both the EW (Figs. 5.1.1, 6.2.1) and IW (Figs. 5.2.1, 2, 6.2.2) recovered four major groups within Ankylosauria, together with a large polytomy, which in IW is slightly more resolved, as well as *Scelidosaurus* as the earliest diverging ankylosaur. All analyses show Ankylosauridae and Struthiosauridae as the most stable and consistent across all topologies. The Polacanthidae exhibits the highest internal topological variation (Figs. 5.1.1-3), while in "nodosaurids", the instability of the internal specifier for Nodosauridae,

Nodosaurus textilis, as it falls outside the group (in EW) or inside (in IW) has implications on the definition and validity of Nodosauridae.

5.1. Equal Weighting Analysis

The strict consensus tree of the EW analysis (Figs. 5.1.1, 6.2.1) returned a well-resolved Stegosauria while Ankylosauria shows a lower level of topological resolution. *Scelidosaurus harrisonii* is recovered as the earliest diverging member of Ankylosauria (*sensu* Madzia *et al.*, 2021). There are four more deeply nested clades (Panoplosaurini, Struthiosauridae, Ankylosauridae, Polacanthidae) forming a large polytomy alongside some unstable taxa (e.g., *Kunbarrasaurus*, *Minmi*, *Tianchisaurus*, *Chuanqilong*, *Liaoningosaurus*) (Fig. 5.1.1). Parankylosauria, a group formed by Gondwanan ankylosaurs, like *Antarctopelta*, *Kunbarrasaurus*, and *Stegouros*, recovered by Soto-Acuña *et al.* (2021) at the base of Ankylosauria as sister group to all other ankylosaurs (as Euankylosauria) is not recovered in this analysis. Also, Nodosauridae becomes invalid due to its internal specifier *Nodosaurus textilis* falling in a large polytomy and outside of the group hitherto considered as Nodosauridae (see Thompson *et al.*, 2012; Arbour and Currie, 2016; Soto-Acuña *et al.*, 2021; Raven *et al.*, 2023). Following the definition of Raven *et al.* (2023), the group composed of *Denversaurus schlessmanii*, *Edmontonia longiceps*, '*Chassternbergia*', *Edmontonia rugosidens*, *Panoplosaurus mirus*, and *Propanoplosaurus marylandicus*, corresponds to Panoplosauridae (the Panoplosaurini of Madzia *et al.*, 2021, and is here supported by the following synapomorphies: ch. 18[0] (absence of premaxillary notch at the ventral margin of the premaxilla in rostral view), ch. 20[1] (cutting surface of beak extends caudally, lateral to the maxillary tooth row), ch. 76[1] (basioccipital is the only contributor to the occipital condyle), and ch. 104[1] (absence of premaxillary teeth). Within Panoplosaurini, there is a polytomy between *D. schlessmanii*, *E. longiceps*, '*Chassternbergia*', *E. rugosidens*, and bigeneric group containing *P. mirus* and *P. marylandicus*. The latter is supported by a single synapomorphy: ch. 45[0] (supraorbital postorbital boss absent or minimal).

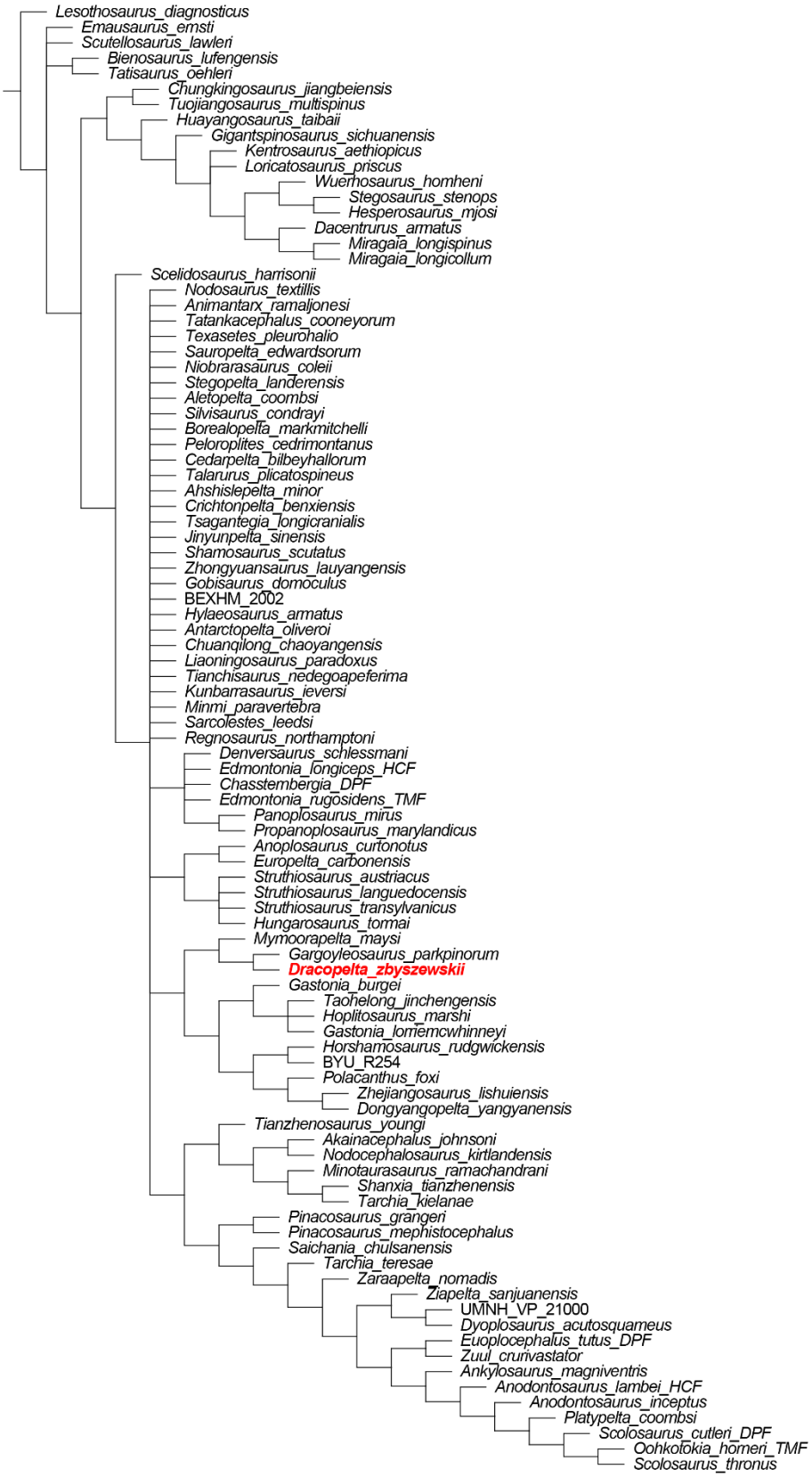

Figure 5.1.1. Strict consensus tree with equal weighting. Consensus tree from 50000 MPTs recovered from the NTS analysis followed by TBR. 1391 steps; CI = 0,289; RI = 0,755; RSI = 0,218. *Dracopelta zbyszewskii* highlighted in red.

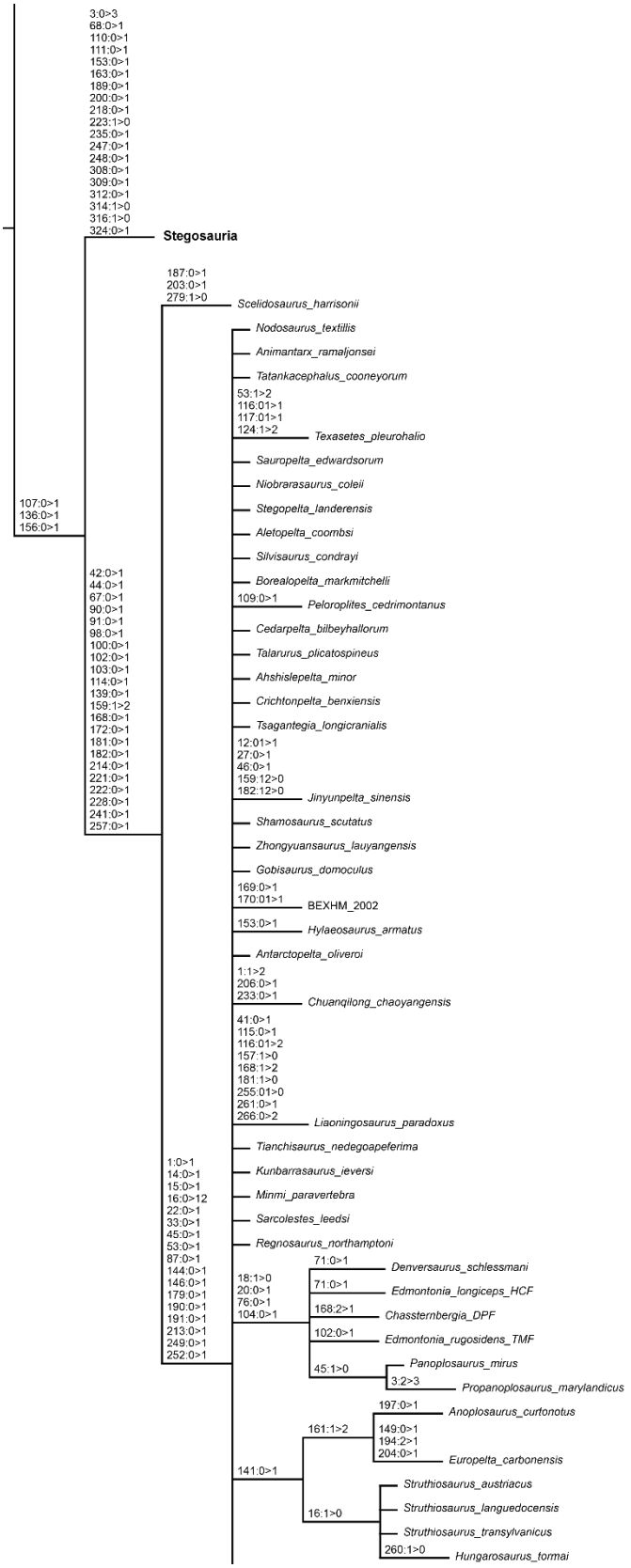

Figure 5.1.2. Map of synapomorphies of equal weighting analysis. Strict consensus tree showing the synapomorphic characters and character states of Ankylosauria, including of Panoplosauridae (four synapomorphies) and Struthiosauridae (one synapomorphy), the lowermost branches of the tree.

A second group (Fig. 5.1.1) is composed of *Anoplosaurus curtonotus*, *Europelta carbonensis*, *Struthiosaurus austriacus*, *Struthiosaurus languedocensis*, *Struthiosaurus transylvanicus*, and *Hungarosaurus tormai*. This corresponds to the Struthiosauridae of Raven *et al*. (2023), and in this analysis is supported by a single synapomorphy: ch.141[1] (mandibular ornamentation extends well below the ventral edge of the angular and dentary). Within it, two groups were recovered: *A. curtonotus* + *E. carbonensis*, supported by ch. 161[2] (strongly ventrally concave arched sacrum), and a bigeneric group supported by ch. 16[0] (completely visible laterotemporal fenestra in lateral view) and composed of the three *Struthiosaurus* species (*S. austriacus*, *S. languedocensis*, *S. transylvanicus*) and *H. tormai*.

A third ankylosaur group (Fig. 5.1.1) consists of *Mymoorapelta maysi*, *Gargoyleosaurus parkpinorum*, *Dracopelta zbyszewskii*, *Gastonia burgei*, *Taohelong jinchengensis*, *Hoplitosaurus marshi*, *Gastonia lorriemcwhinneyi*, HORSM 1988.1546 (*'Horshamosaurus rudgwickensis'*), BYU R254, *Polacanthus foxii*, *Zhejiangosaurus lishuiensis*, and *Dongyangopelta yangyanensis*. Madzia *et al*. (2021) formally defined the group containing *Polacanthus foxii* as Polacanthinae. However, the same authors also recognize that should "polacanthids" be "…*reconstructed outside the Ankylosauridae + Nodosauridae node, the name Polacanthinae becomes inapplicable and the preferred name for the grouping should probably be Polacanthidae*…". Since this is the case in this analysis, Polacanthidae is used and defined herein, even though no unambiguous synapomorphies were found. Thus, Polacanthidae is the largest clade containing *Polacanthus foxii*, but not *Ankylosaurus magniventris*, *Panoplosaurus mirus*, and *Struthiosaurus austriacus*. Two polacanthid subgroups are recovered (Fig. 5.1.1): one including *M. maysi*, *G. parkpinorum*, and *D. zbyszewskii*, and another containing all other polacanthids. The first corresponds to an early branching clade of polacanthids, supported by six synapomorphies: ch. 124[1] (flat scale impressions on the nasal region of the skull roof), ch. 151[0] (long dorsal vertebrae), ch. 154[1] (presence of ossified tendons along the neural spine), ch. 212[0] (ilium does not expand laterally), ch. 213[0] (small lateral deflection of the preacetabular process), and ch. 247[0] (claw-shaped unguals). This group is recovered for the first time in this analysis and is herein named and defined, as Jurapelta clade. nov., the largest clade containing *Dracopelta zbyszewskii* but not *Polacanthus foxii*. *Mymoorapelta* is

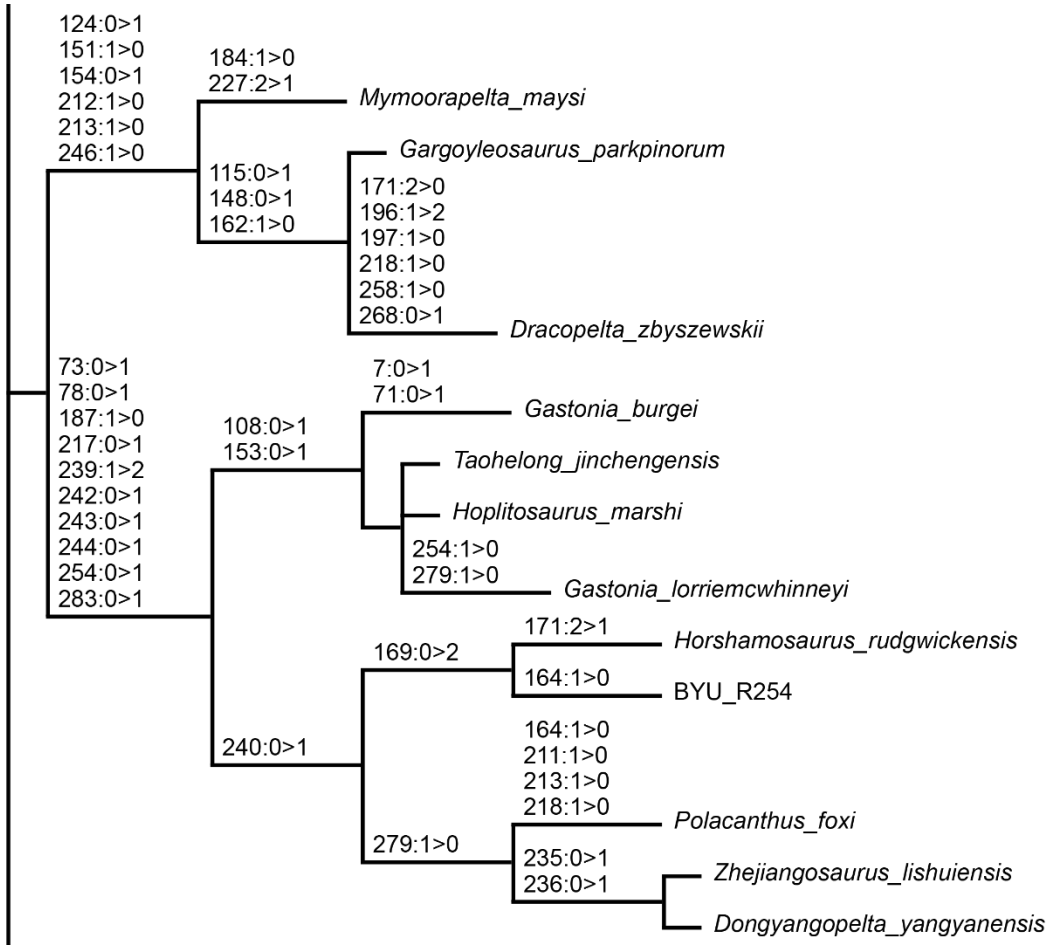

Figure 5.1.3. Map of synapomorphies of equal weighting analysis. Strict consensus tree showing the synapomorphic characters and character states for the Polacanthidae.

the earliest diverging jurapeltan, as sister taxa to a clade containing *Dracopelta* + *Gargoyleosaurus*. The latter is supported by the following synapomorphies: ch. 115[1] (presence of a distinct pattern of cranial scale polygons), ch. 148[1] (presence of sagittal keel on the ventral surface of cervical vertebrae), and ch. 162[0] (absence of longitudinal groove in the ventral surface of the sacrum). All other polacanthids are nested within a group supported by ten synapomorphies: ch. 73[1] (medial depression on the ventral surface of the basioccipital), ch. 78[1] (neck of the occipital condyle oriented caudoventrally), ch. 187[0] (presence of a ventral process of the scapula at the caudoventral margin of the glenoid), ch. 217[1] (closed acetabulum), ch. 239[2] (short lower limb relative to femoral length), ch. 242[1] (astragalus and tibia fused), ch. 243[1] (calcaneum and fibula fused), ch. 244[1] (astragalus and calcaneum fused), ch. 254[1] (presence of marginal ornamentation on dorsal scutes), and ch. 283[1] (presence of vertical dorsal spines). Non-

jurapeltine polacanthids branch into two groups: one consisting of *G. burgei*, *T. jinchengensis*, *H. marshi*, and *G. lorriemwhinneyi*, supported by ch. 108[1] (rounded tooth crown of dentary or maxillary teeth) and ch. 153[1] (elliptical neural canal in cross-section, with dorsoventral long axis), and another including HORSM 1988.1546 (*'H. rudgwickensis'*), BYU R254, *P. foxii*, *Z. lishuiensis*, and *D. yangyanensis*, supported by the single synapomorphy ch. 240[1] (distal end of the tibia wider than the proximal end). In the first, *G. burgei* is the earliest diverging member, defined by ch. 7[1] (slightly concave non-domed cranial roof between and behind the orbits, in lateral profile) and ch. 71[1] (laterally directed paroccipital process in dorsal view), and sister taxon to the group containing the other three ankylosaurs, including *G. lorriemcwhinneyi*, which is here found to be defined by ch. 254[0] (absence or smooth marginal ornamentation on rim of dorsal scutes or ridges around the periphery of the osteoderm) and ch. 279. The sister group to "gastoninins" branches into two subgroups, one including HORSM 1988.1546 (*'H. rudgwickensis'*) and BYU R254, and defined by a single synapomorphy, ch. 169[2] (laterally projecting transverse processes of the caudal vertebrae), and another defined by a single synapomorphy, ch. 279[0] (thin or hollow base of the thoracic osteoderms), which has *P. foxii* as sister taxon to the bigeneric grouping of *Z. lishuiensis* + *D. yangyanensis*.

The fourth group corresponds to the consistently stable Ankylosauridae (e.g., Sereno, 1986; Carpenter, 2001; Thompson *et al.*, 2011; Arbour and Currie, 2016; Wiersma and Irmis, 2018; Soto-Acuña *et al.*, 2021; Raven *et al.*, 2023), even though this analysis found no defining unambiguous synapomorphies. Ankylosauridae branches into two groups: one defined by ch. 72[2] (distal end of the paroccipital processes not expanded), ch. 122[2] (peaked scale impressions on frontoparietal region of skull roof), and ch. 151[0] (long dorsal vertebrae), and includes *Tianzhenosaurus youngi*, *Akainacephalus johnsoni*, *Nodocephalosaurus kirtlandensis*, *Minotaurasaurus ramachandrani*, *Shanxia tianzhenensis*, and *Tarchia kielanae*; the other ankylosaurid subgroup is defined by six synapomorphies: ch. 11[2] (external nares oriented anteriorly), ch. 61[1] (anterior surface of the shaft of the quadrate is flat in cross-section), ch. 259[0] (presence of a large keel or spine on C1A of the anteriormost cervical armour band), ch. 260[0] (presence of a large keel or spine on C1B), ch. 264[0] (presence of a large keel or spine on C2A), and

ch. 265[0] (presence of a large keel or spine on C2B). This clade is composed of an early-diverging bigeneric grouping containing *P. grangeri* and *P. mephistocephalus*,

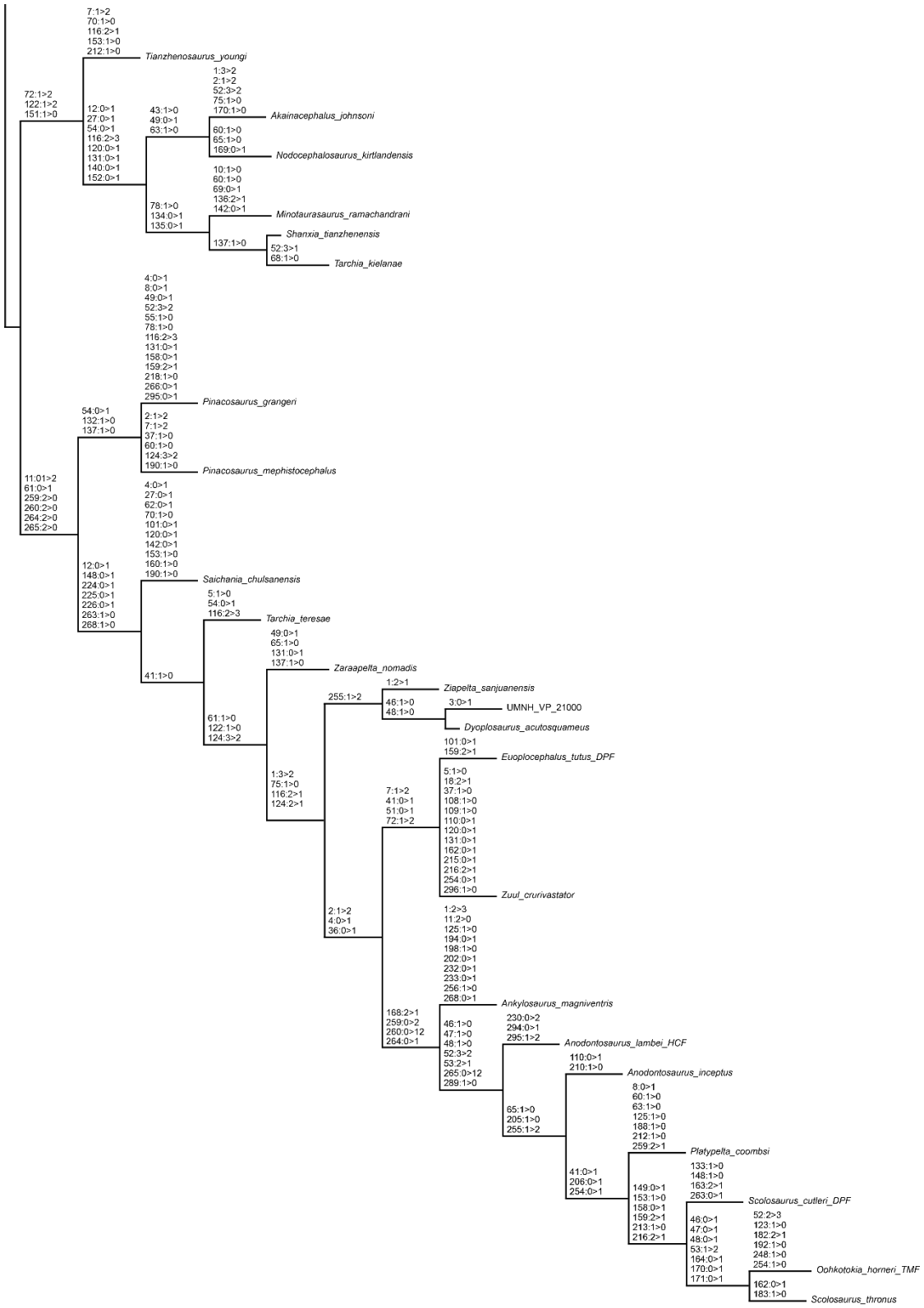

Figure 5.1.4. Map of synapomorphies of equal weighting analysis. Strict consensus tree showing the synapomorphic characters and character states for the Ankylosauridae.

which is defined by ch. 54[1] (presence of a distinct neck in the suborbital boss), ch. 132[0] (absence of a circumorbital ring scale complex), and ch. 137[0] (absence of discrete nuchal caputegulae), and is sister group to the group containing all other ankylosaurids. The latter is defined by seven unambiguous synapomorphies, such as ch. 12[1] (external nares in dorsal view is almost completely hidden), ch. 224[1] (lateral deflection of the preacetabular pubic process relative to the sagittal plane), ch. 226[1] (preacetabular pubic process integrated into the acetabulum), or ch. 268[0] (presence of abutting osteoderms on C2). Within this group, the earliest diverging member is *Saichania chulsanensis*, followed successively by *Tarchia teresae* and *Zaraapelta nomadis* (Fig. 5.1.1). *Z. nomadis* comes out as sister taxa to a larger group defined by five unambiguous synapomorphies, including ch. 1[2] (a maximum width to length ratio between 95%-110%), ch. 116[1] (flat scale impression with perpendicular bone remodelling), or ch. 137[2] (more than two discrete nuchal caputegulae). This group branches into two subgroups: an earlier diverging clade, defined by the single synapomorphy ch. 255[2] (extremely rugose surface texture of the dermal armour), containing *Ziapelta sanjuanensis* as sister taxon to *Dyoplosaurus acutosquameus* + UMNH VP 21000, and a group consisting of later diverging ankylosaurids. In the latter, there is an early diverging pairing of *Euoplocephalus tutus* + *Zuul crurivastator*, defined by four synapomorphies: ch. 7[2] (strongly concave non-domed cranial roof between and behind the orbits in lateral view), ch. 41[1] (anterolaterally oriented orbit), ch. 51[1] (presence of distinct apices of the supraorbital complex), and ch. 72[2] (non-expanded distal end of the paroccipital processes). The *E. tutus* + *Z. crurivastator* pair is sister group to a well-resolved sub-group defined by four synapomorphies, three of which on the cervical armour bands, such as ch. 259[2] (low bump or rounded swelling in C1A) or ch. 264[1] (low keel in C2A). *Ankylosaurus magniventris* is recovered as the earliest diverging member within the subgroup, followed by successively the later diverging *Anodontosaurus lambei*, *Anodontosaurus inceptus*, *Platypelta coombsi*, and *Scolosaurus cutleri*. The latter is the sister taxon to a group containing *Oohkotokia horneri* and *Scolosaurus thronus*, and defined by seven synapomorphies, namely ch. 46[1] (supraorbital boss is a longitudinal ridge or peak), ch. 48[1] (supraorbital complex forms a lateral rim), ch. 164[1] (presence of notochordal projection in

proximal caudal vertebrae, and ch. 171[1] (presence of transverse processes in posterior caudal vertebrae).

5.2. Implied Weighting Analysis

The IW analyses produced generally consistent results to the EW analyses, with the four strict consensus trees (k = 5, 10, 12, and 15) showing overall similar topologies (Figs. 5.2.1, 2, 6.2.2) to each other, but increasingly more resolved

Figure 5.2.1. Strict consensus trees with implied weighting (left, k = 5; right, k = 10). Consensus trees from 5250 MPTs (left) and 11970 (right) recovered from the NTS analysis followed by TBR. Left: 1419 steps; CI = 0,283; RI = 0,748; RSI = 0,212. Right: 1406 steps; CI = 0, 286; RI = 0, 751; RSI = 0,215. *Dracopelta zbyszewskii* highlighted in red.

within the major ankylosaur clades with higher k values. The Parankylosauria recovered by Soto-Acuña *et al.* (2021) at the base of Ankylosauria as sister group to all other ankylosaurs is not recovered here. However, the analyses show there is a trend for the clustering of early diverging Gondwanan ankylosaurs (Figs. 5.2.1, 2; see text below). *Scelidosaurus harrisonii* is recovered as the earliest diverging ankylosaur, as sister taxon to a group containing all other ankylosaurs. As the next earliest diverging group, only the analysis with k = 5 (Fig. 5.2.1) finds the *Chuanqilong chaoyangensis* + *Liaoningosaurus paradoxus* dichotomy, defined by three unambiguous synapomorphies (ch. 111[1], teeth small relative to skull size,

Figure 5.2.2. Strict consensus trees with implied weighting (left, k=12; right, k=15). Consensus trees from 8736 MPTs (left) and 624 (right) recovered from the NTS analysis followed by TBR. Left: 1401 steps; CI = 0,287; RI = 0,752; RSI = 0,216. Right: 1397 steps; CI = 0,288; RI = 0,753; RSI = 0,217. *Dracopelta zbyszewskii* highlighted in red.

ch. 174 [1], pre and postzygapohyses extend over more than 45% the length of

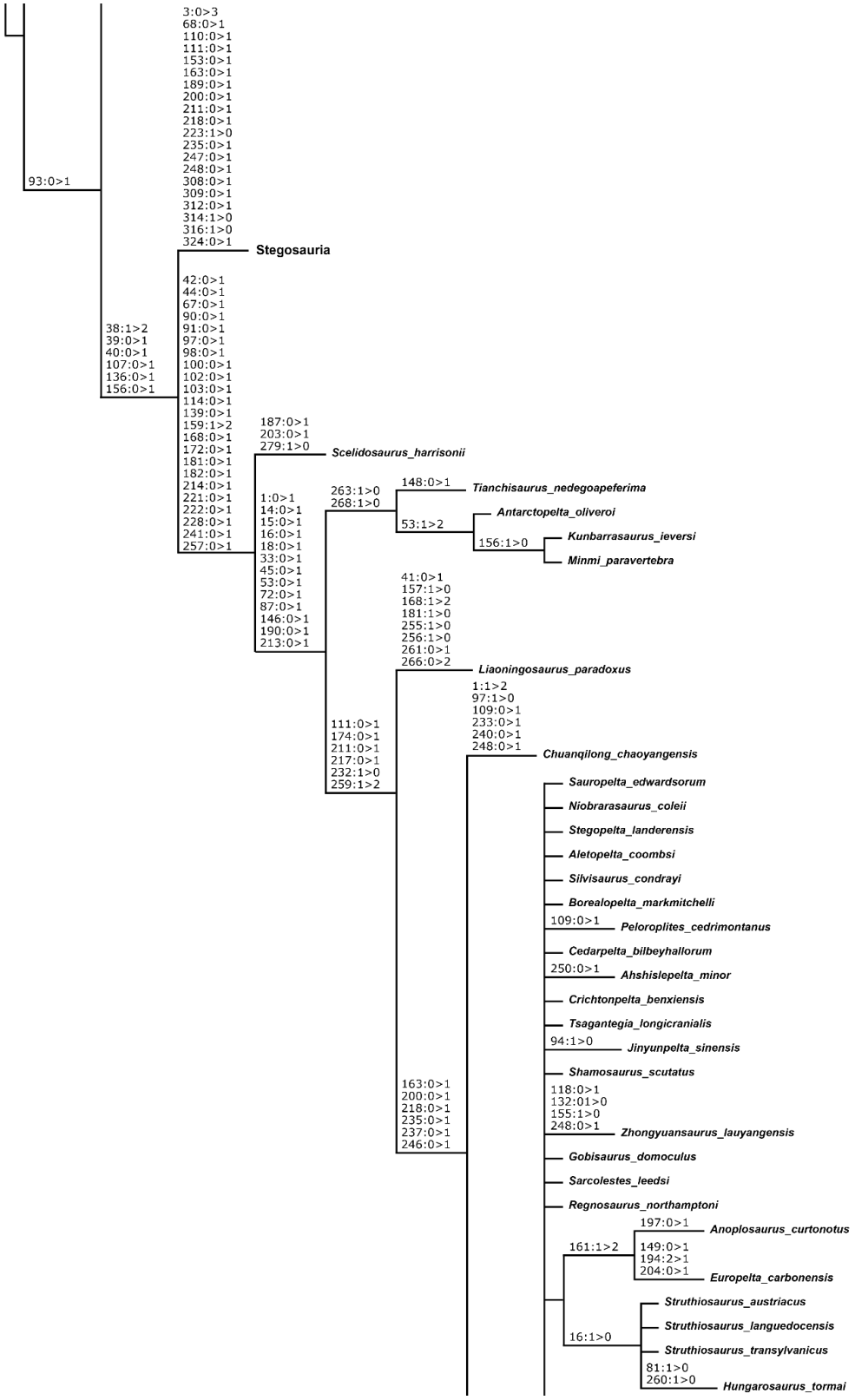

Figure 5.2.3 (previous page). Map of synapomorphies of implied weighting analysis (k = 15). Strict consensus tree showing the synapomorphic characters and character states of Ankylosauria, including Struthiosauridae, the lowermost branch of the tree shown.

the adjacent centrum, ch. 217[1], closed acetabulum), whereas k = 10, 12, and 15 recover a second earliest diverging group composed of *Tianchisaurus*, as the earliest branching taxon, and the pairing of *Kunbarrasaurus* + *Minmi* (Figs. 5.2.1, 2). The k = 12, 15 analyses, add *Antarctopelta* to this group, placed between *Tianchisaurus* and *Kunbarrasaurus* + *Minmi* (Fig. 5.2.2). This group is defined by two synapomorphies: ch. 263[0] (absence of osteoderms capping anteriormost cervical armour ring), and ch. 268[0] (absence of osteoderms capping second cervical armour ring). The positions of *Liaoningosaurus* and *Chuanqilong* are consecutively later divergent (Figs. 5.2.1, 2) in the analyses with k = 10, 12, and 15, contrarily to k = 5, as pointed out above. Immediately later diverging to these early diverging taxa, the main group of ankylosaurs is subdivided into a large polytomy, where four major clades stand out, consistent across all topologies: Struthiosauridae, Panoplosauridae, Polacanthidae, and Ankylosauridae. Struthiosauridae (*sensu* Raven *et al*., 2023) is stable across all analyses, including EW, and comprises two bigeneric subgroups: one of *Anoplosaurus curtonotus* + *Europelta carbonensis*, defined by a single synapomorphy (ch. 161[2], strongly ventrally concave arched sacrum), and the other formed by *Struthiosaurus austriacus*, *Struthiosaurus languedocensis*, *Struthiosaurus transylvanicus*, and *Hungarosaurus tormai*, also defined by a single synapomorphy (ch. 16[0], completely visible laterotemporal fenestra in lateral view).

A second clade corresponds to Panoplosauridae, considering an approximation to the definition provided by Raven *et al*. (2023) which uses *Panoplosaurus mirus* as the internal specifier and *Ankylosaurus magniventris* as the external specifier (see sub-chapter 6.2 for discussion on the problematic of clade definition). The clade is supported by a single synapomorphy, ch. 95 [1] (laterally concave alveolar margin in dorsal view), and divides in two subgroups (Figs. 5.2.1, 2). One group is composed by *Texasetes pleurohalio*, *Nodosaurus textilis*, *Animantarx ramaljonesi*, and *Tatankacephalus cooneyorum*, and is supported by at least six synapomorphies, such as ch. 50[1] (apex of supraorbital boss placed ventrally to the dorsal margin of the orbit), ch. 147[0] (articulation facets of anterior cervical vertebrae centra are parallel and aligned), or ch. 205[1] (deltopectoral crest extending at least 50% of total length of humerus). Analyses with k = 5, 15, and k = 10, 12 differ in the arrangement (Figs. 5.2.1, 2), the first two recovering *Texasetes* as sister taxa to the trichotomy *Nodosaurus* + *Animantarx* + *Tatankacephalus*, whereas the latter two

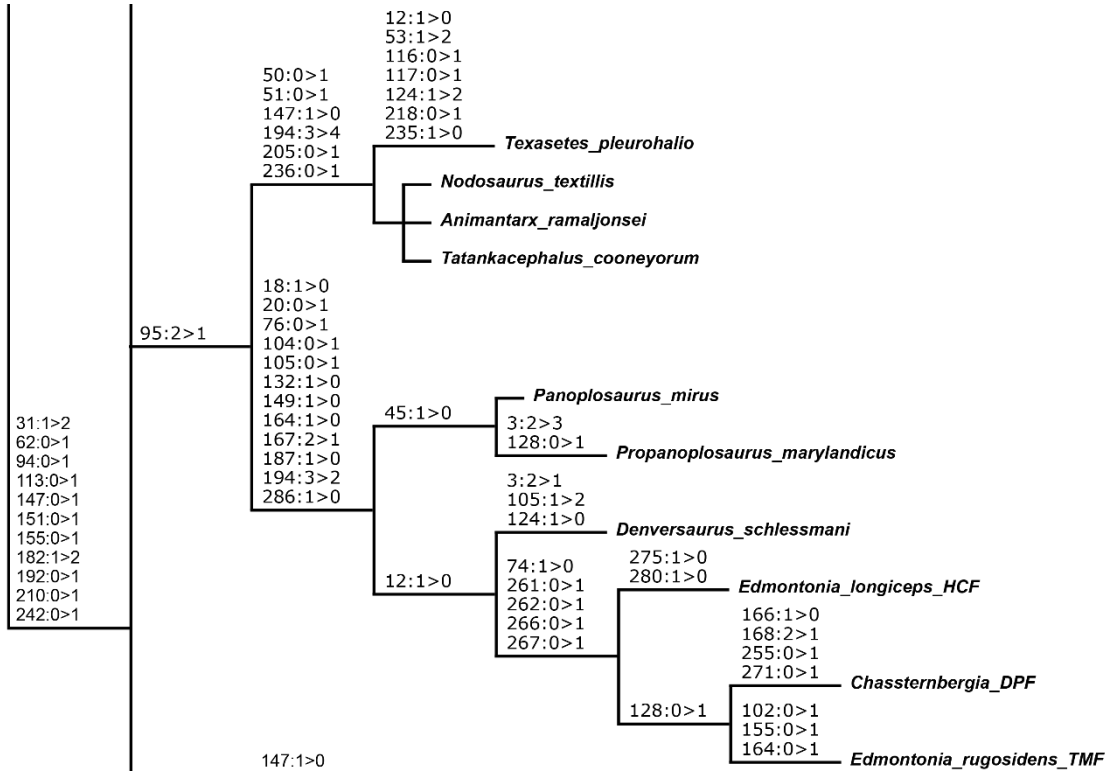

Figure 5.2.4. Map of synapomorphies of implied weighting analysis (k = 15). Strict consensus tree showing the synapomorphic characters and character states for the Panoplosauridae (one synapomorphy).

place *Animantarx* as the earliest diverging taxa, followed by *Texasetes*, as sister taxa to the latest diverging pairing *Nodosaurus* + *Tatankacephalus*. Characters 3[2] (width at the orbits is 130-145% of the width at the squamosals) and 132[1] (presence of a distinct ring of scales around the orbit) support the latter placement of *Texasetes* as sister taxa to *Nodosaurus* + *Tatankacephalus*, itself supported by a single synapomorphy, ch. 204[0] (proximal end of the deltopectoral crest positioned near the humeral head). The other subgroup within Panoplosauridae is taxonomically equivalent to a similar one in the EW analysis (Figs. 5.1.1, 5.2.1, 2), composed of *Denversaurus schlessmani*, *Edmontonia longiceps*, *Panoplosaurus mirus*, *Propanoplosaurus marylandicus*, '*Chassternbergia*', and *Edmontonia rugosidens*. It is supported by at least five synapomorphies, such as ch. 18[0] (absence of mediolateral constriction in the lacrimal region anterior to the orbits), ch. 76[1] (basioccipital is the only contributor to the occipital condyle excluding the suture), or ch. 286[0] (true sacral osteoderms excluding skin impressions adjacent to each other). The earliest diverging 'panoplosaurinin' is *Denversaurus*, immediately

followed by two subgroups: *E. longiceps* + *Panoplosaurus*, supported by ch. 275[0] (absence of true cervical spines on the cervical armour bands) and ch. 280[0] (absence of lateral parascapular shoulder spines), and a group containing *Propanoplosaurus* as sister taxa to '*Chassternbergia*' + *E. rugosidens*. The grouping of *Propanoplosaurus* with '*Chassternbergia*' + *E. rugosidens* is supported by the presence of a large midline frontal scale (ch. 128[1]), as is the later diverging pairing, ch. 200[1] (robust forelimb). In the analysis with k = 15, the topology is slightly different though, with the earliest diverging branch composed of *Panoplosaurus* + *Propanoplosaurus*, here supported by the single synapomorphy ch. 45[0] (absence or minimal supraorbital postorbital boss), as sister group to a clade, also supported by a single synapomorphy, ch. 12[0] (most of the external naris visible in dorsal view), which includes *Denversaurus* as the earliest diverging and sister taxon to a group consisting of *E. longiceps* and its sister group '*Chassternbergia*' + *E. rugosidens*. The latter is supported by the single synapomorphy ch. 128[1] (presence of a large midline frontal scale). Five synapomorphies support *E. longiceps* as sister taxa to '*Chassternbergia*' + *E. rugosidens*, including ch. 74[0] (absence of a distinct medial longitudinal ridge on ventral surface of basioccipital), ch. 262[1] (abutting osteoderms capping first cervical armour ring), and ch. 267[1] (presence of a large keel or spine in osteoderm C2D).

A third clade, corresponding to the Polacanthidae, was found in all analyses (Figs. 5.2.1-2), although supported by four unambiguous synapomorphies only in k = 12, 15 (Fig. 5.2.2), which are a deltaic suborbital boss (ch. 53[2]), the length of the base of the jugal/quadratojugal horn is ≤ the length of the orbit (ch. 56[0]), quadratojugal not visible in lateral view as the quadratojugal is medial to the jugal (ch. 58[1]), and the presence of splates (ch. 253[1]). However, the internal relationships within the clade vary slightly across the four analyses. In all, BEXHM 2002 is the earliest diverging polacanthid and sister taxa to a group containing all other polacanthids. When k = 5 (Fig. 5.2.1), that group is supported by a single synapomorphy, ch. 168[2] (proximal caudal transverse processes approximately twice the length of neural spine height), whereas in all other IW analyses, it is supported by at least two additional synapomorphies: ch. 57[1] (presence of a large medially facing pocket on the medial surface of the jugal) and ch. 210[0] (claw-shaped manual unguals). Also, in k = 5, BYU R254 is the second earliest diverging

polacanthid, while in every other analysis, that position is occupied by *Gastonia lorriemcwhinneyi* (Figs. 5.2.1-2) and BYU R254 is either found within a polytomy with other taxa (k = 10, 12, Figs. 5.2.1-2) or falls as a deeply nested polacanthid sister taxa to '*Horshamosaurus rudgiwckensis*' (k = 15, Fig. 5.2.2). Immediately deeper into Polacanthidae, the trees diverge in topology. In k = 5 (Fig. 5.2.2), Polacanthidae branch into two groups. One, herein referred as Jurapelta and supported by eight synapomorphies, is composed of *Mymoorapelta maysi* as the earliest-diverging jurapeltine and as sister taxa to *Gargoyleosaurus* + *Dracopelta*. Another group, supported by at least ten synapomorphies, includes all other later diverging polacanthids, with *G. lorriemcwhinneyi* as the earliest-diverging member, and a polytomy formed by *Taohelong jinchengensis*, '*H. rudgwickensis*', *Hoplitosaurus marshi*, *Gastonia burgei*, and a small group including *Polacanthus*

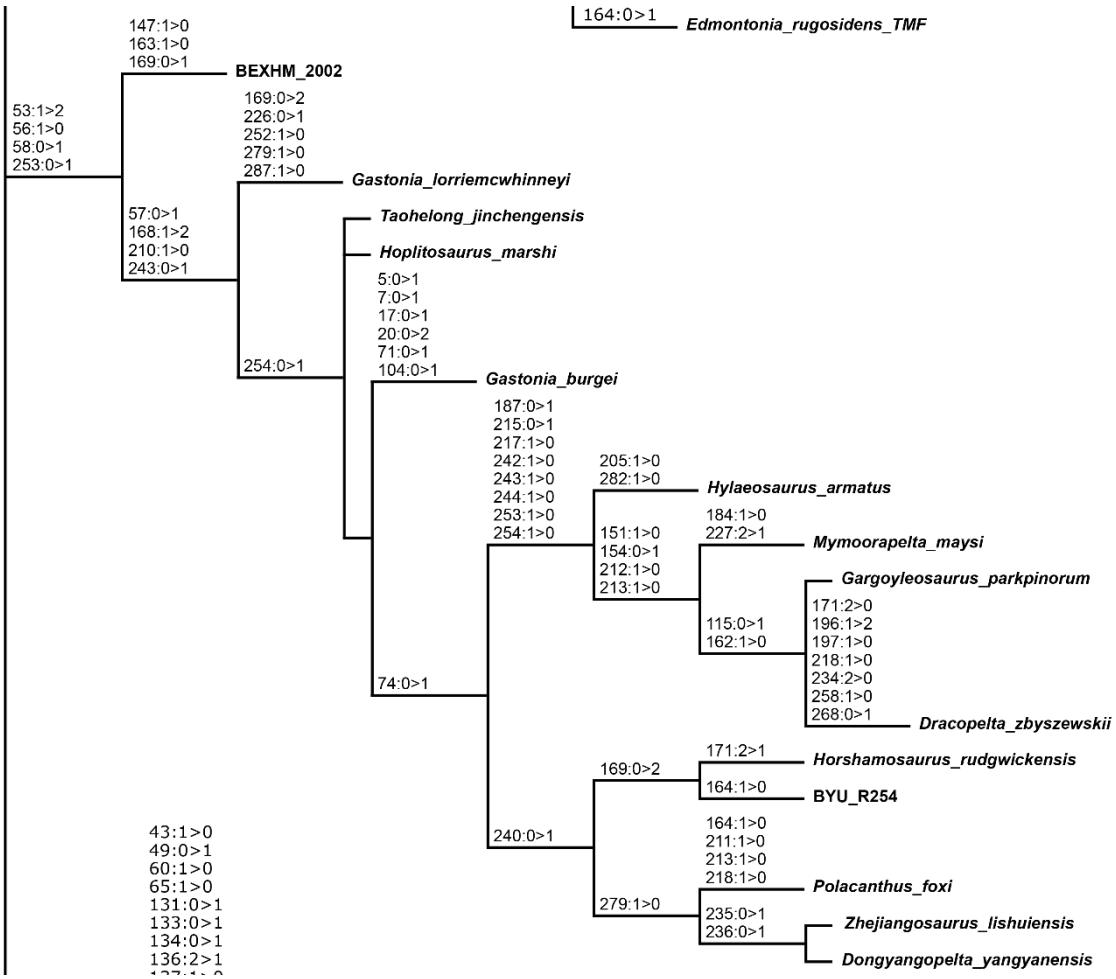

Figure 5.2.5. Map of synapomorphies of implied weighting analysis (k = 15). Strict consensus tree showing the synapomorphic characters and character states for the Polacanthidae (four synapomorphies).

foxii and *Zhejiangosaurus lishueinsis* + *Dongyangopelta yangyanensis*. The analyses with k = 10, 12 (Figs. 5.2.1-2), also recover two subgroups of later-diverging polacanthids, but places *Hylaeosaurus armatus* as sister taxa to Jurapelta, in a clade that is supported by five synapomorphies, such as ch. 62[0] (dorsal end of the quadrate unfused to the paroccipital), ch. 215[1] (pronounced ventral curvature of the preacetabular process of the ilium), and ch. 217[0] (open acetabulum). The other subgroup consists of the remaining polacanthids, which is supported by the single synapomorphy ch. 254[1] (presence of marginal ornamentation as a rim around the dorsal scutes), and places *P. foxii* within the previously referred polytomy, while keeping the *Zhejiangosaurus lishueinsis* + *Dongyangopelta yangyanensis* dichotomy (Figs. 5.2.1-2). As for the analysis with k = 15 (Fig. 5.2.2), the topology immediately deeper to *G. lorriemcwhinneyi* changes the most from the others, with *T. jinchengensis* forming a polytomy with *H. marshi* and a large grouping containing all other polacanthids. No synapomorphies were found supporting this group. Within it, *G. burgei* comes out as sister taxa to a dual branched subgroup, supported by a single synapomorphy (ch. 74[1], presence of a distinct medial longitudinal ridge on the ventral surface of the basipterygoid). One of the branches corresponds to the group found in the other analyses (k = 10, 12) containing *H. armatus* and the Jurapeltans (Fig. 5.2.2; see also text above). The other group is supported by ch. 240[1] (wider distal end of tibia relative to the proximal end), and subdivides into two groups, one consisting of the pairing of '*H. rudgwickensis*' and BYU R254 and the other consisting of the previously found *P. foxii* and *Z. lishuiensis* + *D. yangyanensis*, the latter as the latest-diverging polacanthids.

The fourth major clade in the IW analysis corresponds to the Ankylosauridae, similar to the group as defined by Raven *et al.* (2023). No unambiguous synapomorphies were found to support this group but is the one consistently with the least amount of polytomy in all analyses and the most stable topologically and taxonomically (Figs. 5.2.1-2). It branches into two subgroups: one mostly composed of Asian ankylosaurids, supported by a single synapomorphy, ch. 124[2] (rounded scale impressions on the nasal region of the skull), and another almost exclusively including North American forms, the only exception being *Talarurus plicatospineus*, its earliest diverging member. This group is supported by at least five synapomorphies, such as ch. 116[1] (cranial bone remodeling perpendicular to scale

but flat scale impression), ch. 224[1] (preacetabular pubic process laterally deflected), and ch. 226[1] (preacetabular pubic process integrated into the acetabulum). The group containing mostly Asian taxa has as its earliest diverging member *Zaraapelta nomadis*, which is sister taxa to a dual branching group that includes all other ankylosaurs of this clade and is supported by three unambiguous

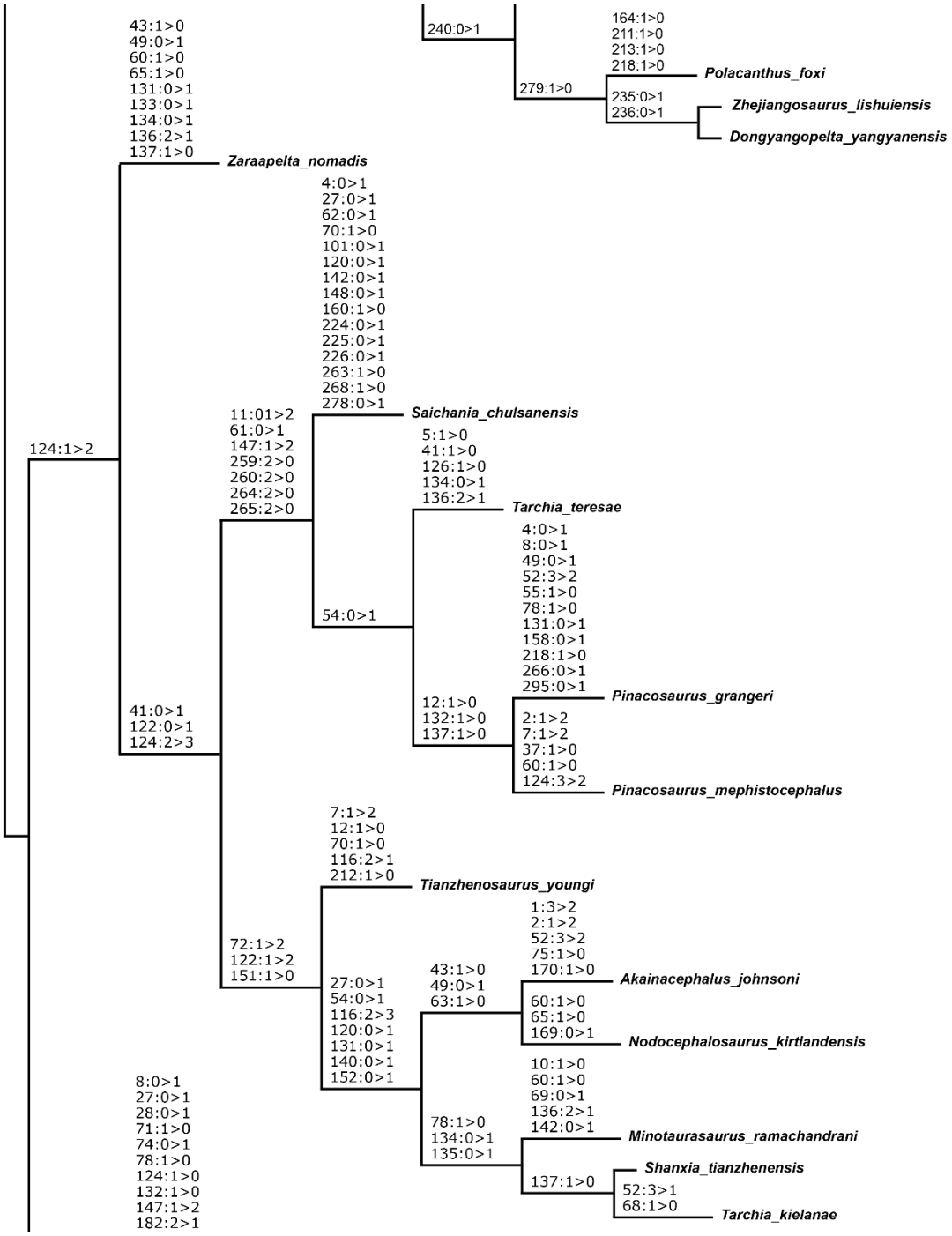

Figure 5.2.6. Map of synapomorphies of implied weighting analysis (k = 15). Strict consensus tree showing the synapomorphic characters and character states for the "Asian" group (one synapomorphy) of ankylosaurids.

synapomorphies: ch. 41[1] (anterolaterally oriented orbits), ch. 122[1] (rounded scale impressions on frontoparietal region of skull), and ch. 124[3] (peaked scale impressions on nasal region of skull). One of the branches is supported by at least five synapomorphies, such as ch. 61[1] (flat anterior surface of the quadrate shaft in cross-section), ch. 260[0] (presence of a large keel or spike on C1B), and ch. 265[0] (presence of a large keel or spike on C2B), and has *Saichania chulsanensis* as the earliest diverging taxa. At this point, the topologies diverge between k = 5 and k = 10, 12, 15 (Figs. 5.2.1-2) with *Pinacosaurus mephistocephalus* as sister taxa to *Tarchia teresae* + *Pinacosaurus grangeri* in k = 5, whereas in all others *Tarchia* is the sister taxa to both *Pinacosaurus* species. The latter topology is supported by three synapomorphies (ch. 12[0], external nares mostly visible in dorsal view; ch. 132[0], absence of a distinct circumorbital ring scale complex; ch. 151[0], dorsal vertebrae longer than tall) instead of one as in k = 5. The other earlier diverging branch is supported by at least three synapomorphies, such as ch. 72[2], unexpanded distal paroccipital processes relative to its neck, ch. 122[2], peaked scale impressions on frontoparietal region of skull, ch. 151[0], dorsal vertebrae longer than tall) and consists of *Tianzhenosaurus youngi* as sister taxa to a subgroup supported by seven synapomorphies, such as ch. 27[1] (presence of premaxillary sinuses), ch. 116[3] (extensive cranial bone remodeling with peaked bulbous scale impressions), and ch. 131[1] (pointed and pyramidal polygons covering the prefrontal). The latter subgroup subdivides into two groups, each supported by three unambiguous synapomorphies: one formed by *Akainacephalus johnsoni* + *Nodocephalosaurus kirtlandensis* and another consisting of *Minotaurasaurus ramachandrani* and *Shanxia tianzhenensis* + *Tarchia kielanae*.

The “North American” branch of ankylosaurids (see text above), which would correspond by definition to the Ankylosaurini of Madzia *et al.* (2021), is supported by at least five synapomorphies, such as ch. 116[1] (cranial bone remodeling perpendicular to scale but flat scale impression), ch. 224[1] (preacetabular pubic process laterally deflected), and ch. 226[1] (preacetabular pubic process integrated into the acetabulum). *T. plicatospineus* is sister taxa to all other ankylosaurids (Figs. 5.2.1-2), which form a clade supported by ten unambiguous synapomorphies, such as ch. 2[2] (maximum dorsoventral height of skull is >60% of maximum length), ch. 126[2] (presence of a large trapezoidal mid-nasal scale impression between the

external nares), ch. 163[2] (length of first caudal vertebrae, cd1, is < 50% of centrum height), ch. 188[1] (glenoid oriented ventrally), and ch. 263[0] (C1A osteoderms do not abut each other). The earliest diverging taxa in this clade is *A. magniventris*, which is sister taxa to yet another clade, supported by at least four synapomorphies: ch. 1[2] (maximum width of skull is between 95% to 110% of length), ch. 11[2] (anterior orientation of the external nares orientation), ch. 260[1] (presence of a low keel in C1B), and 268[0] (C2 osteoderms abut each other). The trees differ slightly at this point, as one of the branches may be a polytomy (k = 5, 15; Figs. 5.2.1-2) that places *Dyoplosaurus acutosquameus* together with *Ziapelta sanjuanensis* and *Euoplocephalus tutus*, or the dichotomy *Z. sanjuanensis* + *E. tutus* (k = 10, 12; Figs. 5.2.1-2). In fact, *D. acutosquameus* consistently falls in a polytomy, either in an earlier-diverging position as referred immediately before, or in a later diverging position, together with UMNH VP 21000 and the clade containing *Anodontosaurus lambei*, *Anodontosaurus inceptus*, *Platypelta coombsi*, *Scolosaurus cutleri*, *Scolosaurus thronus*, and *Zuul crurivastator*. However, the earlier polytomy is not supported by any unambiguous synapomorphies, whereas the pairing *Z. sanjuanensis* + *E. tutus* is supported by three synapomorphies (ch. 259[0], ch. 260[0], and ch. 264[0], presence of large keeled or spines in C1A-B, C2A) in the analyses with k = 10, 12. Regardless of the position of *D. acutosquameus*, the sister clade to *Z. sanjuanensis* + *E. tutus* is supported by at least one synapomorphy (ch. 133[1], presence of small scale impressions between squamosal horn and quadratojugal horn) and its earliest diverging member is *Oohkotokia horneri*. Its sister group is supported by at least two synapomorphies (ch. 46[0], supraorbital boss is a rounded protuberance, ch. 48[0], rounded supraorbital complex) and comprises UMNH VP 21000 as the earliest diverging taxa (or in an unsupported polytomy with *D. acutosquameus* with k = 10, 12, as aforementioned), and all other later diverging ankylosaurids in a group (k = 5, 15; Figs. 5.2.1-2) supported by ch. 47[0] (laterally oriented supraorbital boss) and ch. 53[1] (suborbital boss is a rounded protuberance). In all analyses (Figs. 5.2.1-2), *A. lambei* is immediately earlier diverging to *A. inceptus*, which constitutes one of the two branches of a clade supported by two synapomorphies (ch. 65[0], large medial condyle of the quadrate so that in ventral view the anteroposterior thickest point is located medially, ch. 123[1], nasal ornamentation more pronounced than premaxillary ornamentation). In

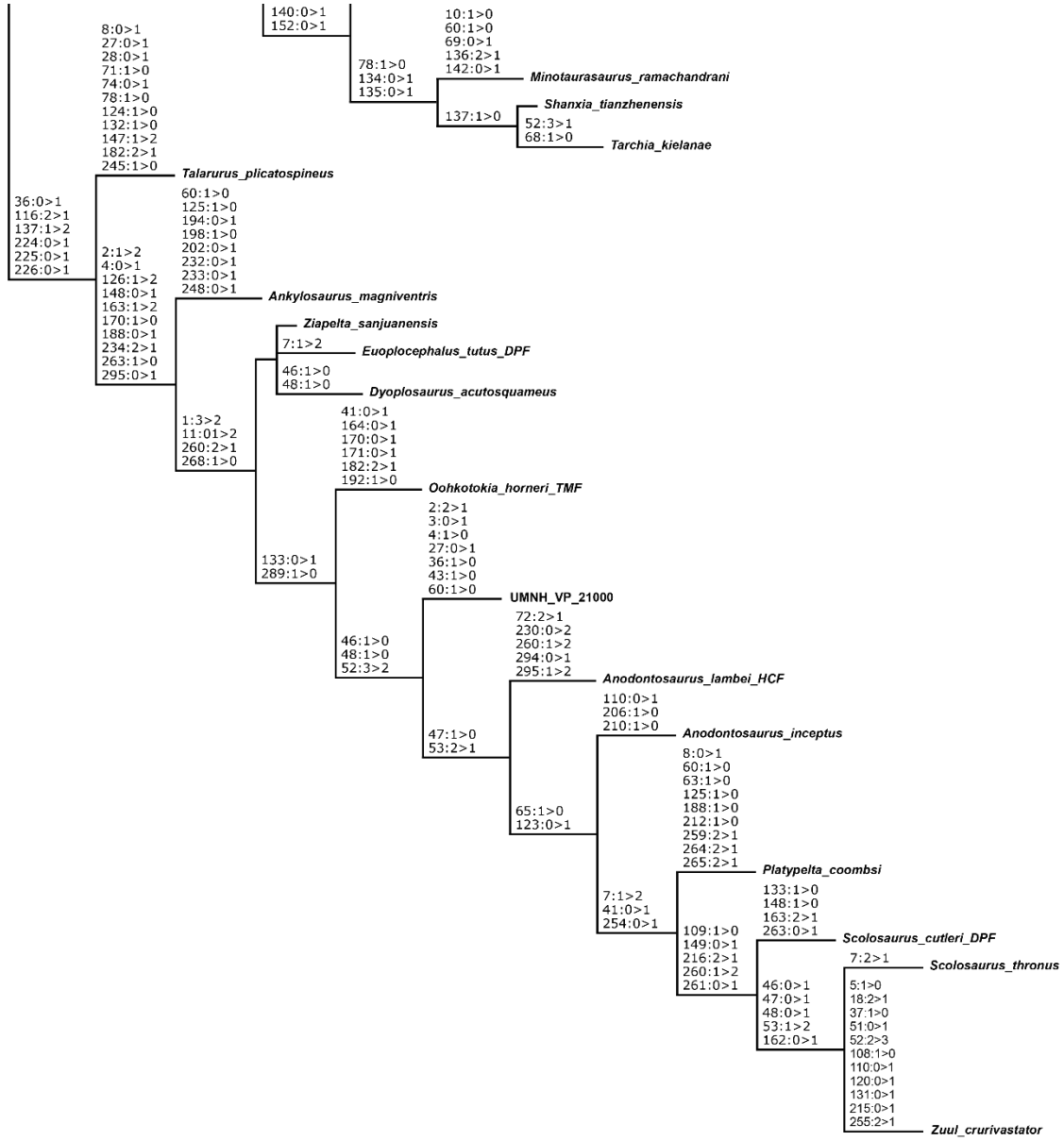

Figure 5.2.7. Map of synapomorphies of implied weighting analysis (k = 15). Strict consensus tree showing the synapomorphic characters and character states for the "North American" group (six synapomorphies) of ankylosaurids.

turn, the sister group of *A. inceptus* is supported by three synapomorphies: ch. 7[2] (non-domed cranial roof is strongly concave in lateral profile between and behind the orbits), ch. 41[1] (anterolaterally oriented orbits), and ch. 254[1] (presence of marginal ornamentation as a rim around the dorsal scutes). It includes *P. coombsi* and the subgroup of *S. cutleri* and *S. thronus* + *Z. crurivastator*. The clade containing *S. cutleri* and *S. thronus* + *Z. crurivastator* is supported by five synapomorphies, such as ch. 109[0} (less than 13 denticles in dentary or maxillary teeth), ch. 149[1]

(presence of fossa on the ventral surface of the cervical vertebrae), and ch. 260[2] (presence of a low raised bump or swelling on C1B). The *S. thronus* + *Z. crurivastator* pairing is also supported by five synapomorphies, such as ch. 46[1] (supraorbital boss is a longitudinal ridge or peak), ch. 48[1] (supraorbital complex forms a lateral rim), and ch. 162[1] (presence of a longitudinal groove in the ventral surface of the sacrum).

6

Discussion

The analysis of *Dracopelta zbyszewskii*, both the holotype MG 5787 (also including MG 3 and unnumbered holotype material) and NOVA-FCT-DCT-5556, allows a deeper understanding of a hitherto poorly known ankylosaur taxon and the evolution of Ankylosauria. The classification of *D. zbyszewskii* has been problematic since its description (see also Galton, 1980b; Carpenter, 2001; Vickaryous *et al.*, 2004; Pereda-Suberbiola *et al.*, 2005). While on the original description (Galton, 1980) the holotype was successfully identified as an ankylosaur, tentatively ascribed to the Nodosauridae, based on the different armour elements, the diagnosis was lacking and, in fact, could be considered invalid, since the presence of different types of dermal armour as the sole diagnostic character is insufficient on its own. As discussed further ahead, this is because osteoderm morphology varies within every taxon across Ankylosauria, with anatomical location, function, or ontogenetic origin, which warranted a proposed differential definition for the distinct dermal elements (Blows, 2001, 2015; Arbour *et al.*, 2011). However, the dermal armour is such a unique and defining feature for ankylosaurs that it stands out as a privileged diagnostic character, as long as the variability in osteoderm morphology is expressed in as many characters as phylogenetically significant (e.g., Ford, 2000; Burns *et al.*, 2013; Arbour and Currie, 2013, 2016; Arbour *et al.*, 2014; Penkalski and Tumanova, 2017; Penkalski, 2013, 2018). This is especially relevant when

considered that the dermal armour can reasonably be thought of as the most evident external feature used for interspecific distinction by the animals (putatively even intraspecific, i.e., sexual dimorphism). Therefore, articulating skeletal and armour characters whenever possible is invaluable to help increase the resolution of the phylogenetic results.

6.1. Anatomical remarks

The unique combination of characters and autapomorphies observed in *Dracopelta zbyszewskii* illustrate the complex evolution of ankylosaur anatomy, reflected for example in the high degrees of homoplasy. The presence of plesiomorphic characters for Ankylosauria (e.g., presence of dermal armour across the dorsal and lateral surface of the body, or simple, unornamented teeth), and character states observed in more late-diverging ankylosaurs (e.g., lateral expansion of the skull to form a trapezoidal shape in dorsal view, or pronouncedly medially concave tooth rows) across the skeleton is expected from an early-diverging taxon that possesses anatomical affinities with distinct taxa across Ankylosauria. Furthermore, while showing that characters observed in deeply nested ankylosaurs appear earlier than previously known, and therefore, that ankylosaurs developed a successful body plan early in their evolution, *Dracopelta* could also help in understanding the relationship between some of the ankylosaur anatomical innovations and its paleobioecology.

The cranium of *Dracopelta* assumes special relevance because of the scarcity of ankylosaur cranial material from earlier than the Late Jurassic and the presence of early and late diverging features, such as the flat cranial roof or the wide, trapezoidal (in dorsal view) skull. A flat cranial roof is plesiomorphic for Ankylosauria, such as the Early Jurassic *Scelidosaurus*, and the early diverging thyreophoran *Emausaurus* and stegosaurs also have a flat dorsal surface of the skull (Haubold, 1990; Vickaryous *et al.*, 2004; Norman, 2020a). The flat cranial roof (evident in lateral view) in *Dracopelta* (Figs. 4.2.3.C-D) and *Gargoyleosaurus* is covered by the mosaic of small, raised bumps of the caputegulae. It contrasts with the domed, heavily ornamented frontoparietal region of the skull in more late diverging ankylosaurs, e.g., *Gastonia*, *Tsagantegia*, *Talarurus*, *Panoplosaurus*, or *Ankylosaurus* (Lambe,

1919; Maleev, 1952; Tumanova, 1993; Kirkland, 1998; Carpenter, 2004; Vickaryous *et al.*, 2004; Arbour and Currie, 2017; Arbour and Mallon, 2017; Parks *et al.*, 2020), and the dorsal raising of nasal region in Ankylosauridae (observed also in *Kunbarrasaurus*). Despite its dorsal premaxillary/nasal expansion, the skull of *Kunbarrasaurus* (QM F18101), an early diverging ankylosaur (or a member of Parankylosauria, *sensu* Soto-Acuña *et al.*, 2021) from the Albian-Cenomanian of Australia, also has a flat skull roof (Leahey *et al.*, 2015). However, the skull of *Dracopelta* (NOVA-FCT-DCT-5556) is laterally expanded, so that in dorsal view it has a trapezoidal shape (Fig. 4.2.3.A). This lateral expansion of the skull from the narrower early diverging condition is observed at its extreme in ankylosaurids. It is relevant to point out that the general different cranial architecture (broad, trapezoidal skulls, dorsoventrally taller nasal region, in ankylosaurids vs pyriform, subtriangular skulls, in non-ankylosaurid ankylosaurs) houses nasal vestibules of distinct complexities and seems to be related at least partially to differential heat exchange and body size (Bourke *et al.*, 2018). These authors demonstrated that the nasal passages were more convoluted in *Euoplocephalus* (AMNH 5405) than in *Panoplosaurus* (ROM 1215), a deeply nested ankylosaurid and panoplosaurid respectively, both from the Late Cretaceous (Campanian) of North America. According to the authors, *Euoplocephalus* evolved these more complex, more efficient nasal passages as a response to higher heat loads resulting from the larger body mass than *Panoplosaurus*. Paulina-Carabajal *et al.* (2016) observed a similar morphology to *Panoplosaurus* for the airways of *Pawpawsaurus* (SMU73203, now FWMSH93B.00026), indicating also a possible functional relationship with the inner ear morphology, and production and perception of different ranges of sounds among different groups of ankylosaurs. This potential acoustic functionality is worth noting when correlated with recent studies describing fossilized hyolaryngeal apparatus elements (the exact function and evolutionary origin of such elements remains debatable) in *Edmontonia*, *Saichania*, and *Pinacosaurus* (Maryańska, 1977; Hill *et al.*, 2015; Yoshida *et al.*, 2023). Further evidence came from the skull of *Kunbarrasaurus*, a small, early diverging ankylosaur, which had short, possibly simpler airways, with a lateromedial narrow rostrum (Leahey *et al.*, 2015), albeit it existed millions of years before and in a different environment than *Euoplocephalus* and *Panoplosaurus*. *Pawpawsaurus* is also younger (late Albian) and slightly smaller

than *Panoplosaurus* and *Euoplocephalus* (Lee, 1996). Although more sampling is needed to corroborate this hypothesis, the evidence seems to suggest that ankylosaur airways became increasingly more complex due to increasing body sizes, evolving from a more simplistic architecture towards more complexity in derived forms. That being the case, and considering the laterally expanded skull, *Dracopelta* may have more complex airways than known in other early ankylosaurs, but more evidence is needed, namely a detailed CT analysis of the skull of *Dracopelta*, to help clarify the possible correlation with skull morphology. A caveat of such an assumption is that the external nares and premaxilla of *Dracopelta* are unknown. Nonetheless, the skull of *Dracopelta* (NOVA-FCT-DCT-5556) is dorsoventrally low (Fig. 4.2.1.C); in fact, the ratio between dorsoventral height and anteroposterior length is approximately 0,21, compared to the 0,28 for *Gargoyleosaurus* (DMNH 27726), 0,57 for *Panoplosaurus*. (CMN 2759), or 0,55 for *P. grangeri* (ZPAL MgD-II/I) (Lambe, 1919; Maryańska, 1977; Kilbourne and Carpenter, 2005). Therefore, the available space to accommodate extensive convoluted nasal passageways would be limited, at least with the morphology known so far. It is plausible to assume a component of potential taphonomical vertical compression to explain the low dorsoventral height of the skull, of which the abnormally elliptical orbit could be the most evident expression. However, no other visible skull structures seem heavily affected by deformation (Figs. 4.2.3, 4.2.4), meaning that, even considering potential taphonomical alterations to the original shape (e.g., deformation, fracturing, bone erosion), the dorsoventral height of the skull of *Dracopelta* would still be comparatively low. For example, the skull of *Gargoyleosaurus* (DMNH 27726), sister taxa of *Dracopelta*, has the ventral margin of the orbit aligning with the ventral margin of the maxillary shelf, so that the orbit is located dorsally to the palatal plane, whereas in *Dracopelta*, the midline of the orbit aligns with the ventral surface of the maxillary shelf, resulting in a uniquely lower orbit relatively to the palatal plane (Fig. 4.2.3.C). Moreover, the nasal chamber of *Gargoyleosaurus* does not seem to be divided by an osseous nasal septum (Kilbourne and Carpenter, 2005). It is unknown at this time if this is the case in *Dracopelta* or if the vomer extends dorsally to fully divide the respiratory passages, as variably observed in most ankylosaurs (Vickaryous and Russell, 2003). Finally, Miyashita *et al.* (2011) points out that an enlarged olfactory cavity and the convoluted airways may have

resulted in an increased olfactory acuity, but that it would be a functional byproduct of an evolutionary adaptation to thermoregulation, in a similar way to potential vocal resonance functions. The same authors state that the exact evolutionary drivers of the distinct morphologies of the nasal airways are unclear, but a mix of environmental and intrinsic factors is the most likely scenario. This could be especially relevant, when considering that Late Jurassic ankylosaurs were relatively small sized (≈3 m, ≈600-700 kg) comparatively to later, more derived forms, such as *Panoplosaurus* and *Euoplocephalus* (see Bourke *et al.*, 2018, and references therein for size estimates for these taxa; see also sub-chapter 5.5 of this dissertation for the size estimation of *Dracopelta*), and therefore heat exchange might have played a smaller role in Late Jurassic taxa, which might, in turn, have been reflected in a more simplistic nasal airway architecture in these earlier forms.

The presence of plesiomorphic and derived characters can be observed also in the palatal region of the skull of *Dracopelta*. One such example is the tomial crest, a ventral process of the maxillae and premaxillae, which constitutes the bony anterior and lateral cutting edges of the beak. The beak itself would be covered by a rhamphotheca (Miles and Miles, 2009; Ősi *et al.*, 2014; Leahey *et al.*, 2015; Nabavizadeh and Weishampel, 2016). In ankylosaurids, the tomial crest extends caudally as a ventrally folding process of the lateral surface of the maxillary, paralleling the alveolar ridge, partially or even totally obscuring the tooth rows in lateral view (e.g., *Ankylosaurus*, *Euoplocephalus*, *Saichania*, *Shamosaurus*, *Talarurus*). In *Dracopelta*, the maxillary extends laterally and overhangs the tomial crest, forming a horizontal shelf, so that it is visible in ventral view (Fig. 4.2.3.F), a feature shared only with *Ankylosaurus* (AMNH 5214), and which contributes to the wide skull of *Dracopelta*, when compared to the slightly more narrow skull of *Gargoyleosaurus* or earlier thyreophorans like *Scutellosaurus* or *Emausaurus*, and the earliest ankylosaur *Scelidosaurus* (Haubold, 1990; Carpenter *et al.*, 1998; Carpenter, 2004; Norman *et al.*, 2004a; Norman, 2020b). In non-ankylosaurid ankylosaurs (also in *Tarchia*, an Asian Late Cretaceous ankylosaurine), the tomia are restricted to the premaxillae and, to a varying extent, the anterior end of the maxillary (approximately the premaxillae-maxillae contact). This occurs both in deeply nested ankylosaurs, such as *Panoplosaurus*, *Edmontonia*, *Silvisaurus*, or *Pawpawsaurus* (e.g., Bakker 1988; Eaton Jr., 1960; Lee, 1996) as well as in more

early diverging ankylosaurs, such as *Gargoyleosaurus* and *Dracopelta*. This condition is even more pronounced in its extension (or absence) throughout Stegosauria and early diverging thyreophorans and ankylosaurs, like *Emausaurus* and *Scelidosaurus* (e.g., Haubold, 1990; Galton and Upchurch, 2004; Norman *et al.*, 2004; Norman, 2020a; see also Supplementary Data of Thompson *et al.*, 2012; Arbour and Currie, 2016; Raven *et al.*, 2023, for the coding of characters 21, 13, and 16, respectively). The plesiomorphic condition is the absence of premaxillary tomium, which in Ankylosauria tends to extend posteriorly during the evolution of the group, albeit, as stated, remains anteriorly restricted in non-ankylosaurid ankylosaurs. The fact that the derived state is limited to most ankylosaurids could be related to the more extensive remodeling of the skull observed in that group. Furthermore, autapomorphic for *Dracopelta*, the maxillary tomial crest curves medially joining the alveolar ridges at the premaxillae/maxillae contact, and completely separates the buccal emargination from the premaxillary palate. This separation is observed in some panoplosaurids, such as *Edmontonia*, *Panoplosaurus*, or *Texasetes*, and also in *Pawpawsaurus*, and results from the maxillary tooth rows converging with the premaxillary tomium through a ridge that connects the anterior end of the tooth row to the posterior end of the premaxillary tomium, giving an hourglass shape to the palate in those taxa. In ankylosaurids, this partition is absent, because the anterior ends of the tooth rows are aligned medially relative to the posterior end of the premaxillary tomium, resulting in the anterior opening of the buccal emargination to the premaxillary palate. This happens due to two main reasons: the generally wider skull and the less medially deflected tooth rows. Unique to *Dracopelta* is that it is the maxillary tomium bending medially at the anterior end which closes off the buccal emargination, instead of a ridge as described above. *Gargoyleosaurus* shows a similar condition, however the buccal emargination is not fully enclosed by the maxillary tomium, rather it is connected to the premaxilla by a narrow anterior opening. In fact, in *Gargoyleosaurus* the maxillary tooth rows align with the premaxillary tooth rows and the tomia form a continuous seamless edge, both in ventral and lateral views. The premaxillaries are missing in *Dracopelta*, therefore the articulation of these structures is unknown. Nonetheless, considering the affinities between *Dracopelta* and *Gargoyleosaurus*, it is plausible to assume similar morphologies. An additional unique character observed in *Dracopelta* is the degree

to which the tooth rows narrow anteriorly in relation to its posteriormost width. Comparatively, in *Gargoyleosaurus*, the tooth rows are lightly arched, or almost straight in *Gastonia* (Carpenter *et al.*, 1998; Kilbourne and Carpenter, 2005; Kinneer *et al.*, 2016). In several deeply nested ankylosaurids, such as *Ankylosaurus*, *Euoplocephalus*, *Minotaurasaurus*, *Talarurus* or *Tarchia*, the tooth rows are curved anteromedially (Vickaryous and Russell, 2002; Carpenter, 2004; Miles and Miles, 2009; Park *et al.*, 2020, 2021), but less pronouncedly than in *Dracopelta*, where the width between the anteriormost teeth is 34 mm and the posteriormost teeth reaches 111 mm. Ankylosaurids have generally wider skulls, including the rostrum, which results in a wider palate (Coombs Jr, 1971, 1978a; Sereno, 1986; Vickaryous *et al.*, 2004; Thompson *et al.*, 2012; Arbour and Currie, 2016). Non-ankylosaurids ankylosaurs on the other hand generally have a narrower pyriform skull in dorsal view, resulting in a narrower anterior palate. In *Dracopelta* the skull is wide, but the palate itself is comparatively narrow. The implications on feeding are unclear, and further studies on the dentition, mandible biomechanics, and even Late Jurassic herbivore paleoecology of the Lourinhã formation are needed.

The dorsal vertebrae of *Dracopelta* are unique in the extreme anterior placement of the diapophyses and parapophyses (Fig. 4.2.8) and in the low neural arch in general, but more specifically in the low position of the prezygapophyses relative to the neural, so that they are aligned with parapophyses. Although the anteroposterior position of the diapophyses and parapophyses can vary throughout Ankylosauria, it is mostly placed near or at the midline of the centrum, migrating from a more anterior position in the cervical vertebrae (e.g., Ostrom, 1970; Dong, 1993; Kirkland and Carpenter, 1994; Kirkland *et al.*, 2013; Wiersma and Irmis, 2018; Norman, 2020a; Park *et al.*, 2021; Soto-Acuña *et al.*, 2021; Pond *et al.*, 2023). A pronounced anterior placement in dorsal vertebrae is uncommon, but it is observed in both earlier and later diverging taxa like *Peloroplites cedrimontanus* (CEUM 26283, 36701), *Crichtonpelta benxiensis* (BXGMV0012-1), *Jinyunpelta sinensis* (ZMNH M8960), *Gastonia burgei* (CEUM 5411), and *Ankylosaurus magniventris* (AMNH 5895). In the latter, the position of the parapophyses and lateral processes is the most similar to *Dracopelta*, which further reinforces the high anatomical plasticity in ankylosaurs. The exact reason for such an anteriormost placement of the rib articulation surfaces is currently unknown. However, it could be

related to the low position of the prezygapophyses (Fig. 4.2.8), forming an extra structural buttress between the transverse processes and the base of the prezygapophyseal peduncle. The lower position of the prezygapophyses in *Dracopelta* comparatively to other ankylosaurs is seemingly correlated to the short neural arches, which accommodates the dorsolaterally projecting transverse processes. This condition in *Dracopelta* would likely contribute to a robust cervical and thoracic vertebral bracing system, a hypothesis reinforced by the existence of two ossified bundles of overlapping tendons (Figs. 4.2.2, 8), one located medially and another more lateral, parallel to the former. While ossified tendons are widespread in ornithischians (e.g., Romer, 1956; Molnar and Frey, 1987; Sereno, 1999; Norman *et al*., 2004a; Organ, 2006; Holmes and Organ, 2007; Arbour and Currie, 2016), placed axially as attachment connections for the epaxial musculature, the existence of a second, lateral bundle is so far unique to *Dracopelta*. The rare ankylosaur specimens that preserve large articulated sections of the dorsum, such as *Sauropelta* (AMNH 3032), *Borealopelta* (TMP 2011.033.0001), or *Kunbarrasaurus* (QM F18101), do not have a secondary bundle of epaxial tendons. The reason for this absence is unknown and requires further research to determine if it is a result of a sampling or preservation bias of specimens, or a unique adaptation of *Dracopelta*. The presence of a second tendinous system in *Dracopelta* may have increased the strength to tensile stresses of the dorsal axial skeleton, in a similar way to that of crocodiles (Molnar and Frey, 1987; Salisbury and Frey, 2001; Organ, 2006; Grigg and Kirshner, 2015). Also, ankylosaurs are the only archosaurs besides crocodilians with extensive osteodermal cover, which, in the latter, is used as anchorage for the epaxial musculature. Ankylosaurs had a uniquely wide ribcage, which would have been reflected in a uniquely differentiated epaxial musculature, namely the *M. longissimus dorsi* and the *M. iliocostalis*, respectively inserting on the transverse processes dorsally and on the fascia of the *M. longissimus dorsi* medially (Molnar and Frey, 1987; Organ, 2006). These positions correspond well with the position of the secondary bundle of tendons (Fig. 4.2.2, 8). Overall, short neural spines, and consequent smaller attachment area for epaxial musculature when compared to other ornithischians with higher neural spines, together with the additional weight of the dermal armour itself, broad dorsal surface, and quadrupedality/graviportality, likely would produce high strains on the dorsal region

(Molnar and Frey, 1987; Salisbury and Frey, 2001; Organ, 2006; Grigg and Kirshner, 2015). Therefore, a robust bracing system formed by various elements (strong epaxial muscles, larger dorsal surface of the ribs, multiple ossified tendons, dermal armour) would be needed to properly accommodate the stresses generated during gait and stance of the animal. Still, this unique condition in *Dracopelta* prompts future studies on the poorly known ankylosaur biomechanics and the relationship with dermal armour and axial osteology.

The development of dermal armour likely had implications on the biomechanics of ankylosaurs, as discussed above, and understanding its evolution could be crucial to clarify aspects of ankylosaur biology, such as the role in inter- and intraspecific relationships, ontogenetic developmental implications, or potential coevolutionary response to predators. However, occurrences of skeletons with articulated armour are rare, e.g., *Kunbarrasaurus* (QM F18101), *Scolosaurus cutleri* (NHMUK 5161), *Sauropelta* (AMNH 3035, 3036), *Borealopelta* (TMP 2011.033.0001), *Edmontonia* (AMNH 5665), *Scelidosaurus* (BRSMG LEGL 0004), *Dracopelta* (this study). *Scelidosaurus* and *Dracopelta* are the only aforementioned examples from the Jurassic, although separated by approximately 45 million years. *Borealopelta*, the oldest example from the Cretaceous, dated from the early Albian (~112 Ma), is approximately 35 million years younger than *Dracopelta*. Therefore, *Dracopelta* offers additional insight into the evolution of dermal armour between the earliest and later diverging forms, a time interval of 80 million years. The dermal armour arrangement of *Dracopelta* is distinctive but shares similarities with other ankylosaurs. The reconstructions of *Scelidosaurus* and *Yuxisaurus* (Norman, 2020c:46; Yao *et al.*, 2022:31) show a putative armour arrangement and suggests that as early as the Early Jurassic dermal armour had already differentiated into multiple elements, namely scutes and ossicles, although comparatively incipient to later derived ankylosaurs. *Scelidosaurus* already exhibits some degree of cranial ornamentation, namely occipital horns, although not as extensive as in later diverging ankylosaurs (Norman, 2020). The cervical dermal armour consisted of as much as five pairs of quarter-rings composed of varyingly keeled scutes growing outwards from juxtaposing base-plates and successively larger from the midline to the side (Norman, 2020). *Dracopelta*, on the other hand, had three pairs of quarter rings formed by large keeled coossified scutes abutting at the midline and lateral

dorsoventrally flat plates to form three cervical bands of armour (Figs. 4.2.2, 4.2.17). This is closer to what is observed in the North American Aptian-aged *Sauropelta* and *Borealopelta*, although *Sauropelta* (AMNH 3035) had splates (*sensu* Blows, 2015) rather than plates on each side of the neck (Carpenter, 1984; Brown *et al*., 2017). *Edmontonia* (AMNH 5665), from the Campanian (~75-71 Ma) of North America also had three cervical bands, but the scutes are coossified to form continuous half-rings (Sternberg, 1928; Brown *et al*., 2017). *Gargoyleosaurus*, sister taxon of *Dracopelta*, had a similar cervical arrangement, including a medial ellipsoidal osteoderm in the first cervical band and likely a third cervical band (Figs. 4.2.2, 4.2.2.12; Kilbourne, 2005; Kirkland, pers. comm). Early Cretaceous ankylosaurs, such as *Silvisaurus* and *Gastonia*, from the Albian and Barremian respectively, also had cervical quarter rings instead of half-rings (Carpenter and Kirkland, 1998; Kirkland, 1998; Kinneer *et al*., 2016). This condition is distinct from what is observed in ankylosaurids, which have cervical half-rings composed of osteoderms coossified to an underlying band of bone (e.g., Ford, 2000; Arbour and Currie, 2016; Brown, 2017). This means that *Dracopelta* (and likely closely related taxa, and other polacanthids) already had developed a cervical dermal armour pattern closer to other later-diverging ankylosaurs than to earlier ankylosaurs.

The development of highly differentiated dermal armour elements seemed to be fully established by the Late Jurassic, as can be attested also by the presence in *Dracopelta*, but also in *Gargoyleosaurus* and *Mymoorapelta*, of distinct osteoderm morphologies and arrangement. Like the cervical armour, dorsal armour of *Dracopelta* (Figs. 4.2.2, 4.2.2.3, 12) shared more similarities with later ankylosaurs. Large, sub-rectangular, keeled scutes, smaller, sub-circular or elliptical, low keeled scutes, small, circular or elliptical, faintly keeled or flat ossicles, and large plates or spines forming a lateral row were ubiquitous in all late-diverging ankylosaurs, namely in non-ankylosaurid ankylosaurs (e.g., *Borealopelta*, *Edmontonia*, *Europelta*, *Gastonia*, *Hoplitosaurus*, *Panoplosaurus*, *Sauropelta*).

6.2. Phylogenetic results

The phylogenetic analyses performed to resolve the position of *Dracopelta* within Ankylosauria were based on a heavily modified version of the dataset of

Loewen and Kirkland (2013), and both the EW and IW converge on similar topologies (Figs. 5.2.1-2), reasonably well-supported (Figs. 6.2.1-2), indicating that the relationships within Ankylosauria are more complex than previous studies have shown (e.g., Coombs, 1978; Sereno, 1986, 1999; Thompson *et al.*, 2012; Arbour and Currie, 2016). Rather these results agree with more recent studies, namely by Raven *et al.* (2023), in recognizing four major monophyletic lineages, previously defined by those authors: Ankylosauridae, Polacanthidae, Struthiosauridae, and Panoplosauridae. However, this study reaches a different arrangement within these major clades (Figs. 5.2.1-2, 6.2.1-2) while at the same time revealing the uncertain placement of some taxa, illustrated by the large polytomy observed outside the more well-supported groups (Figs. 6.2.1-2), which indicates more work is needed in terms of anatomical description of some taxa (e.g., *Nodosaurus*, *Borealopelta*, *Cedarpelta*), character scoring and increasingly refined datasets. Still, even considering the low CI, revealing a high degree of homoplasy, the analysis resolves the position of hitherto phylogenetically problematic taxa, namely those of Late Jurassic ankylosaurs *Dracopelta*, *Gargoyleosaurus*, and *Mymoorapelta*. It should be pointed out also that the analyses included as successive outgroups *Lesothosaurus*, early diverging thyreophorans like *Scutellosaurus* and *Emausaurus*, and Stegosauria. The latter, even though it comes out as well-resolved (Figs. 5.2.1-2) and its phylogenetic relationships are strongly supported, falls out of the scope of this work and therefore will not be discussed.

The analyses show a strong support for Ankylosauria as sister group to Stegosauria within Eurypoda (Figs. 5.2.1-5), which was expected and in agreement with previous phylogenetic works (e.g., Sereno, 1986, 1999; Thompson *et al.*, 2012; Arbour and Currie, 2016; Norman, 2021; Raven *et al.*, 2023). Ankylosauria is supported by 23 synapomorphies, such as ch. 67[1] (depth of the pterygoid process of the quadrate), ch. 137[1] (ornamentation on lateral surface of mandible), ch. 222[1] (rotation of the pubic body), and ch. 257[1,2] (fusion of cervical osteoderms into armour bands or "rings"), which are unambiguous synapomorphies, including in *Scelidosaurus*. Most previous phylogenetic analyses have placed *Scelidosaurus* as sister taxa of Eurypoda (e.g., Sereno, 1986, 1999; Thompson *et al.*, 2012; Arbour and Currie, 2016; Brown *et al.*, 2017; Zheng *et al.*, 2018; Soto-Acuña *et al.*, 2021; Raven *et al.*, 2023). Other authors have argued for a sister taxa

relationship between *Scelidosaurus* and Ankylosauria (e.g., Carpenter, 2001; Norman, 2021). Carpenter (2001) proposed the name Ankylosauromorpha for the clade including *Scelidosaurus* + Ankylosauria. However, the definition of Ankylosauromorpha, provided by Norman (2021) as "*all taxa more closely related to* Euoplocephalus *and* Edmontonia *than to* Stegosaurus", coincide with the definitions of Ankylosauria by Carpenter (1997) and Sereno (1998), respectively: "*all thyreophoran ornithischians closer to* Ankylosaurus *than to* Stegosaurus" and "*all eurypods closer to* Ankylosaurus *than* Stegosaurus". As such, Ankylosauria takes precedence and Ankylosauromorpha is redundant and unnecessary. Yao *et al*. (2022) suggest that a formal redefinition of Ankylosauromorpha that includes *Scelidosaurus*, *Ankylosaurus*, their common ancestor and all its descendants would be necessary to further support it. The results presented herein seem to support this hypothesis, although the discussion on the validity or synonymy of Ankylosauromorpha is beyond the aim of this work. The position of *Scelidosaurus* at the base of the ankylosaur lineage, even though statistically and character supported, has the caveat that it would imply the existence of a ghost lineage of approximately 25 Ma between *Scelidosaurus* (from the Sinemurian-Pliensbachian) to the Bathonian-Callovian-aged *Spicomellus afer*, considered the oldest ankylosaur by Maidment *et al*. (2021) and not included in this dataset. However, this could also be a result of sampling and preservation bias, since not only is the fossil record for this time interval very scarce and what exists is very fragmentary, but also by the Late Jurassic, forms exhibiting features found in later-diverging ankylosaurs are already present (e.g., *Dracopelta*).

Within Ankylosauria, the analyses converge on a topology with a higher number of reasonably well-supported clades (Figs. 5.2.1-2, 6.2.1-2) rather than the previously accepted Ankylosauridae + Nodosauridae dichotomy. The IW trees tend to become more resolved as the value of *k* is increased (Figs. 5.2.1-2), which is to be expected since IW downweighs homoplasy, although the number of necessary steps increase from 1391 with EW to between 1397 with k = 15 to 1419 with k = 5. Still, the analyses consistently produce a topology with four major clades alongside a large polytomy, formed by taxa for which, for example, character scoring is problematic, either because of the fragmentary nature (e.g., *Aletopelta*, *Silvisaurus*, *Nodosaurus*) or difficulties in observing and scoring characters (e.g.,

Borealopelta, *Sauropelta*). A group of early diverging ankylosaurs emerges from the IW analyses with higher k values (10, 12, and 15), which includes *Tianchisaurus*, as

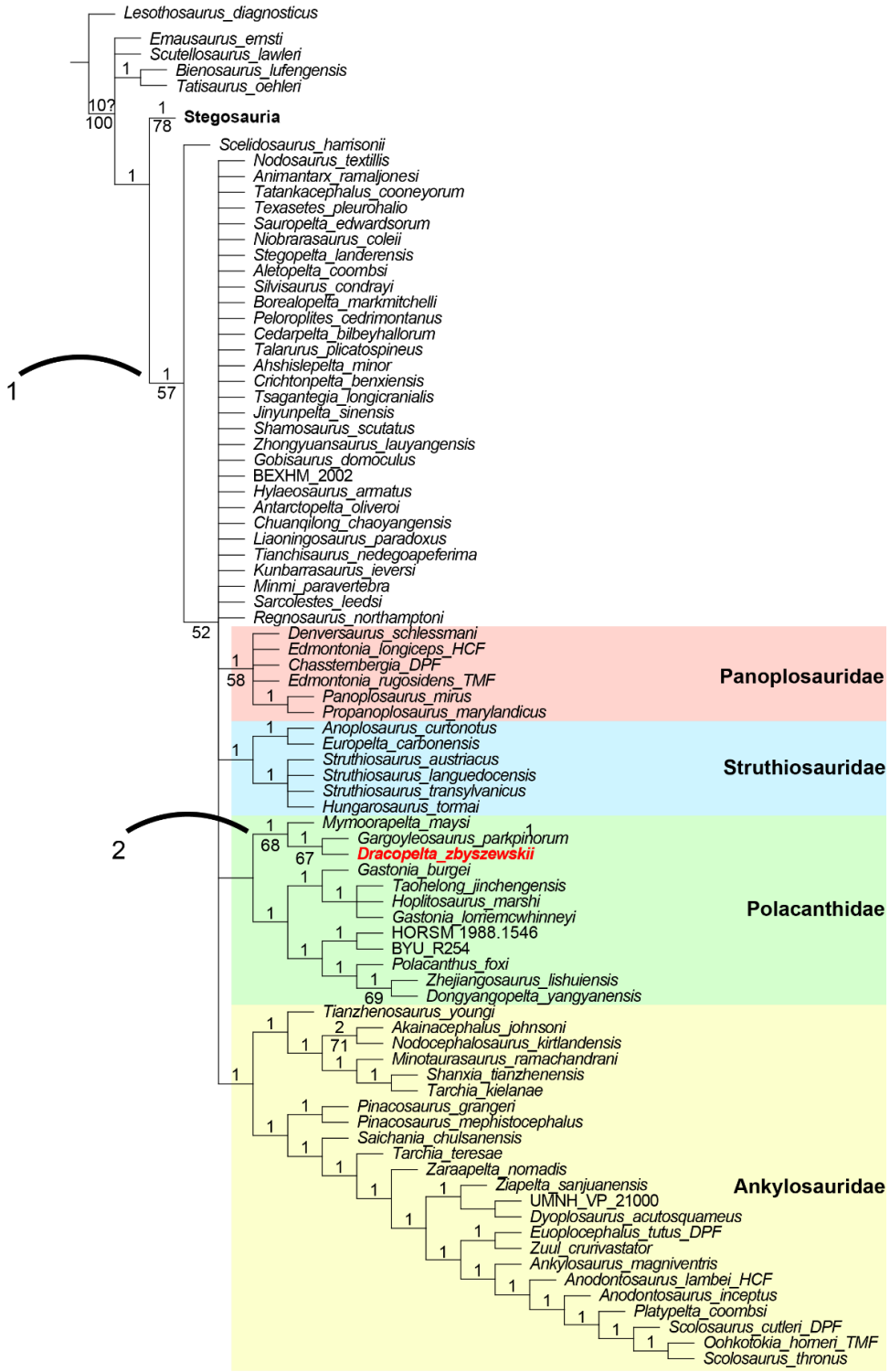

Figure 6.2.1. Strict consensus tree of the parsimony analysis, with equal weighting. Phylogenetic relationships of Ankylosauria, with *Dracopelta zbyszewskii* highlighted in red. Numbers over branches indicate bootstrap values, while numbers below branches indicate Bremer support (only values above 50% are shown). 1) Ankylosauria; 2) Jurapelta.

sister taxa to *Minmi* and *Kunbarrasaurus* (Figs. 5.2.1-2, 5). This grouping is supported by just two synapomorphies: ch. 263[0] and ch. 268[0], respectively scoring the first and second cervical band osteoderms abutting each other. In two analyses (k=12, k=15), *Antarctopelta* is placed in an intermediate position (Fig. 5.2.2, 5). When all characters are equal weighted against homoplasy, these taxa fall together in a large polytomy outside the four main ankylosaur groups, which can be accounted by the fact that, excluding *Kunbarrasaurus* (QM F18101, formerly *Minmi* sp.), all other taxa are known from very fragmentary material (Molnar, 1980; Zhimming, 1993; Gasparini *et al*., 1987, 1996; Salgado *et al*., 2006), thus reflected in the uncertain placement of some of them in this study as well as in previous analyses (Kirkland, 1998; Carpenter, 2001; Thompson *et al*., 2012; Arbour and Currie, 2016). The recent work of Soto-Acuña *et al*. (2021) on *Stegouros elengassen* grouped all Gondwanan taxa known at the time in the proposed Parankylosauria, the earliest diverging group of ankylosaurs and sister group to Euankylosauria. More recently, the revision of *Antarctopelta* by Soto-Acuña *et al*. (2024) has indicated a close affinity with *Stegouros* as well as other Gondwanan taxa, further supporting the existence of an early diverging group of ankylosaurs in the Late Cretaceous of Southern Gondwana. Future iterations of the dataset used herein should account for these taxa to assess its influence on the current phylogeny, but the IW analyses in this work (Figs. 5.2.1-2, 6.2.2) seem to suggest indeed the existence of an early-diverging group of ankylosaurs from Gondwana. In all but one IW analyses (k = 5), *Tianchisaurus* is recovered as sister taxon to the branch containing *Minmi* and *Kunbarrasaurus* instead of in a large polytomy with other unstable ankylosaurs, but this topology is the one that takes the most steps (1419), 28 more steps than the EW analysis (1391). *Tianchisaurus* is a problematic taxon because, even though it is known from a partial skeleton from the early Upper Jurassic of China, the holotype specimen IVPP V 10614 is poorly preserved, has not been reviewed since Zhimming (1993) described it, and, according to Arbour and Currie (2016), its whereabouts are unknown, hindering an updated reassessment. However, some of the results found here coupled with its age seem to support its position as one of the earliest diverging ankylosaurs.

Other labile taxa are *Chuanqilong* and *Liaoningosaurus*, which in the IW analyses are placed as earlier diverging taxa, outside the main grouping of ankylosaurs,

instead as part of the large polytomy that characterizes all topologies (Figs. 5.1.1, 2.1-2). Only in one analysis (k = 5) are these taxa placed as sister taxa (Fig. 5.2.1), supported by three synapomorphies: ch. 111[1] (relative size of maxillary and

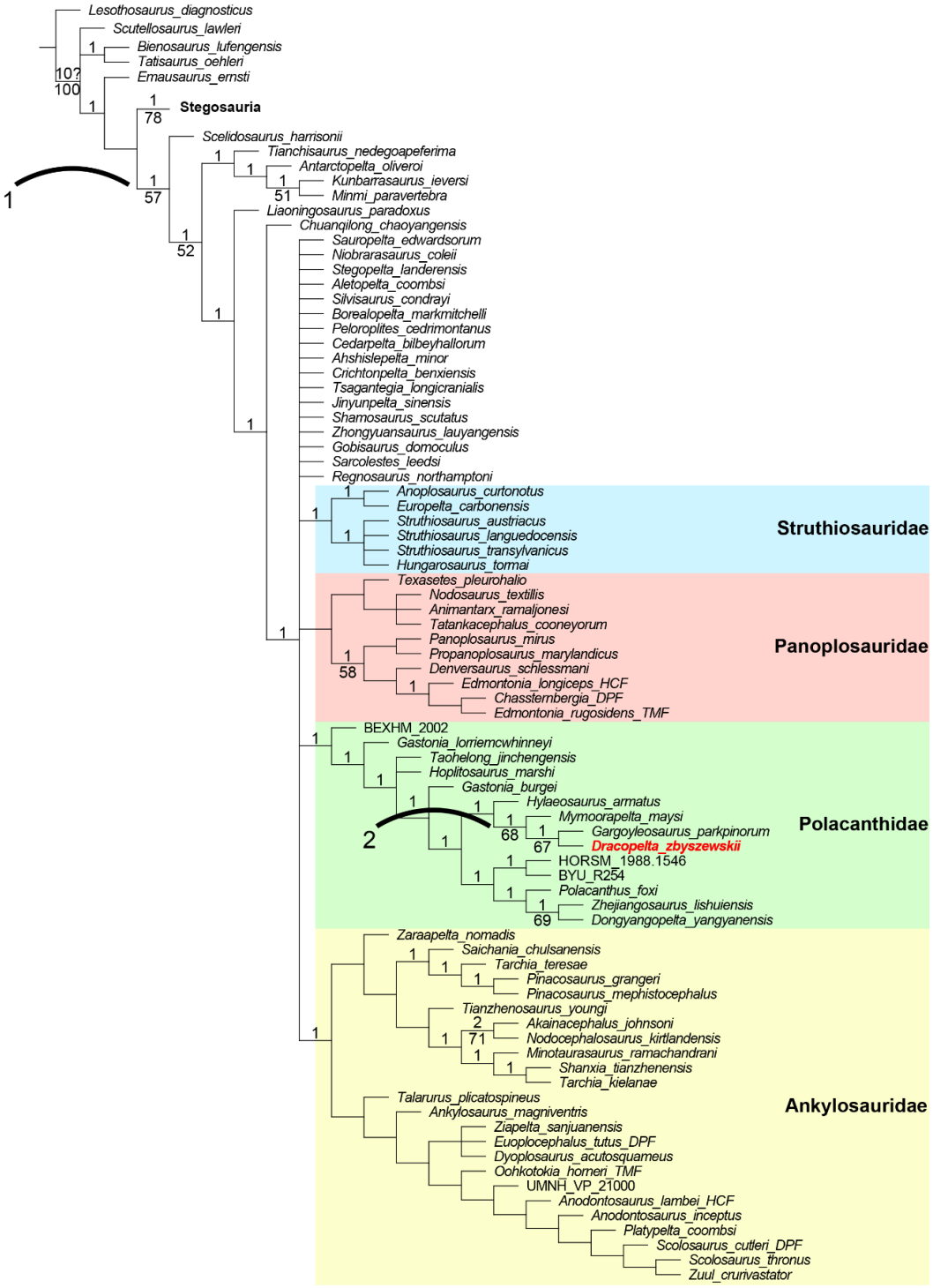

Figure 6.2.2. Strict consensus tree of the parsimony analysis, with implied weighting (k=15). Phylogenetic relationships of Ankylosauria, with Dracopelta zbyszewskii highlighted in red. Numbers over branches indicate bootstrap values, while numbers below branches indicate Bremer support (only values above 50% are shown). 1) Ankylosauria; 2) Jurapelta.

dentary teeth), ch. 174[1] (extension of the distal caudal zygapophyses over adjacent centra to form a "handle"), and ch. 217[1] (closure of the acetabulum). In the other three IW analyses, *Liaoningosaurus* is placed as immediately early diverging to *Chuanqilong*, which becomes sister-taxa to the main grouping of ankylosaurs (Figs. 5.2.1-2). However, recent evidence seems to suggest that *Liaoningosaurus* and *Chuanqilong* might be the same taxon at different ontogenetic stages (Zheng, 2018; Xiaobo and Reisz, 2019). This being the case will help understand the ontogeny of many ankylosaur characters and therefore ultimately contribute to clarify its phylogenetic position. Lack of early-stage ontogenetic specimens is just one of several factors contributing to the phylogenetic instability of these and other taxa. The fragmentary nature of the remains can severely affect character scoring, eschewing the phylogenetic signal of a taxa towards an unexpected placement (e.g, suffering from long-branch attraction, for example, as seems to be the case with *Sarcolestes*, a taxon from the Callovian of the UK known from a partial mandible, falling together with Cretaceous ankylosaurs), while, on the other end, abundant, well-preserved material may not necessarily imply a more meaningful result if character observation is hindered, such as is the case for exceptionally preserved specimens, the best example being *Borealopelta*, which also falls within a large polytomy, together with ankylosaurs based on highly incomplete or poorly preserved specimens, like *Stegopelta*, *Silvisaurus*, *Tsagantegia*, or *Ahshislepelta*. Furthermore, observation of cranial characters in ankylosaurs is often difficulted by the presence of the cranial ornamentation, bone remodelling and obliteration of cranial bone sutures. Another factor influencing the phylogenetic result is character definition and sampling. Some previous analyses for example have focused on cranial characters comparatively to postcranial and dermal armour characters (e.g., Lee, 1996; Vickaryous, 2001; Arbour and Currie, 2016; Penkalski and Tumanova, 2017; Penkalski, 2018). To counter these effects, more work is needed in reassessing specimens, accounting for incompleteness, potentially relevant characters, and scoring.

The four main clades recovered in this study, Panoplosauridae, Struthiosauridae, Polacanthidae, and Ankylosauridae, although recovered in all analyses in the large resulting polytomy, show some topological inconsistencies, stemming from the reasons discussed above. The Panoplosauridae (*sensu* Raven *et al.*, 2023) is

supported by four synapomorphies in the EW analysis: ch. 19[0] (cutting edge of premaxilla extends laterally to the maxillary teeth), ch. 21[1] (maximum anteroposterior length of premaxillary rostrum is less than premaxillary palate width), ch. 77[1] (ovoid/round morphology of the occipital condyle in posterior view), and ch. 105[1] (tooth row extends to rostral end of maxilla diastema at least two alveoli length). However, in the IW (k = 15) analysis, a single synapomorphy supports it (ch. 95[1], laterally concave alveolar margin in dorsal view). Moreover, the composition of the Panoplosauridae in the EW analysis overlaps with the Panoplosaurini of Madzia *et al.* (2021), excluding *Animantarx* and *Texasetes*, both of which fall outside, within the large polytomy found (Fig. 6.2.1). On the other hand, in the IW analysis (k = 15), a similar composition constitutes a deeper branch within Panoplosauridae, with *Nodosaurus*, *Animantarx*, *Texasetes*, and *Tatankacephalus* forming its sister group (Figs. 5.2.3, 6.2.2), approximately similar to the Nodosaurinae of Madzia *et al.* (2021). The consistent presence of *Panoplosaurus mirus* within the clade, contrary to *Nodosaurus*, another labile taxon, agrees with the definition of Raven *et al.* (2023) for Panoplosauridae (all ankylosaurs more closely related to *Panoplosaurus* than to *Ankylosaurus*, *Struthiosaurus austriacus* or *Gastonia burgei*), thus justifying its use herein instead of Nodosauridae. Deeper into Panoplosauridae, only the pairing *Panoplosaurus* + *Propanoplosaurus* is recovered in all analyses (Figs. 5.1.1, 2.2-3, 6.2.1-2). The topological instability within Panoplosauridae, the potential dubious nature of the holotype of *Propanoplosaurus* (USNM 540686, Stanford *et al.*, 2011), and the additional work needed on *Edmontonia* and its closest relatives *Denversaurus* and *Chassternbergia*, require a more in-depth study of these ankylosaurs, also to clarify the validity of names previously used to refer to specific clades with approximate compositions, such as Nodosaurinae, Panoplosaurinae, Edmontoniinae, or Panoplosaurini (Nopcsa, 1929; Russell, 1940; Bakker, 1988; Rivera-Sylva *et al.*, 2018; Madzia *et al.*, 2021; Raven *et al.*, 2023). Nonetheless, Panoplosauridae is a North American clade mostly composed of Late Cretaceous forms (Fig. 6.2.3).

The clade Struthiosauridae (*sensu* Raven *et al.*, 2023) is the most topological and taxonomical stable across all analyses (Figs. 5.1.1, 2.1-2). Even though a single synapomorphy supports it in the EW analysis (ch.141[1], distinct boss on lateral surface extends well below the ventral edge of the angular and dentary), whereas

no synapomorphies support this group in the IW analyses (Fig. 5.2.3), the composition and arrangement within Struthiosauridae remains consistent. *Europelta* and *Anoplosaurus* are united by the presence of strongly ventrally concave arched sacrum (ch. 161[2]). *Struthiosaurus* and *Hungarosaurus* are united in a sister clade by having a completely visible laterotemporal fenestra in lateral view (ch. 16[0]). Cranial material from both *Struthiosaurus* and *Hungarosaurus* is fragmentary, therefore the status of this character in these taxa will need future revision. Still, the topology holds in all analyses, indicating a strong support for the relationships recovered in this study. Recent works (e.g., Rivera-Sylva *et al.*, 2018, Raven *et al.*, 2023; Soto-Acuña *et al.*, 2024) had also pointed to close relationships between *Struthiosaurus*, *Hungarosaurs*, and *Europelta*, albeit with slightly different topologies. Based on the results obtained herein, not only does Struthiosauridae agree with the definition provided by Raven *et al.* (2023) for a clade with an approximate composition as "*all ankylosaurs more closely related to* Struthiosaurus austriacus *than to* Ankylosaurus, Panoplosaurus *or* Gastonia burgei", but it is possible to propose two clades within Struthiosauridae: the Europeltinae, formed by *Anoplosaurus curtonotus* and *Europelta carbonensis*, and defined as all struthiosaurid ankylosaurs more closely related to *Europelta* than to *Struthiosaurus austriacus*, and the Struthiosaurinae, composed of *Struthiosaurus austriacus*, *S. transylvanicus*, *S. languedocensis*, and *Hungarosaurus tormai*, and defined as all struthiosaurid ankylosaurs more closely related to *S. austriacus* than to *Europelta*. Struthiosaurinae had been previously proposed by Kirkland *et al.* (2013) based on a combination of characters, such as a narrow predentary, a nearly horizontal, unfused quadrate that is oriented less than 30° from the skull roof, relatively long slender limbs, or a sacral shield. However, this character-based definition is problematic, either because they are widespread in ankylosaurs or not visible and ambiguous in struthiosaurines (Ősi, 2015). Madzia *et al.* (2021) provide a maximum-clade definition for a group similar to Struthiosaurinae, as "*the largest clade containing* Struthiosaurus austriacus, *but not* Nodosaurus textilis *and* Panoplosaurus mirus", but name it Struthiosaurini, since in the reference phylogeny used (Rivera-Sylva *et al.*, 2018), the clade is nested within Nodosaurinae and, as to avoid confusion, the lesser inclusive suffix -ini is preferred. In this work, this problem disappears with the recovery of Struthiosauridae and of a struthiosaurine clade

within it. Struthiosauridae is then an exclusively European group, composed of the late Early Cretaceous europeltines and the Late Cretaceous struthiosaurines (Fig. 6.2.3).

Polacanthidae is recovered in all analyses, strongly supporting its validity, and conforming to the definition provided by Raven *et al*. (2023) as "*all ankylosaurs more closely related to* Gastonia burgei *than to* Ankylosaurus, Panoplosaurus *or* Struthiosaurus austriacus." The topology and composition vary slightly across the analyses, but overall sister taxa relationships remain stable (Figs. 5.1.1, 2.2-3). Some placements are particularly noteworthy, namely the position of both species of *Gastonia*, *G. burgei* and *G. lorriemcwhinneyi*. Across all topologies, both species are not recovered as sister taxa and are further apart than initially thought (Kinneer *et al*., 2016), suggesting that *G. lorriemchwhinneyi* could likely be a distinct genus (Kirkland, pers. comm). Future work on these taxa could help elucidate this relationship. Another problematic taxon is *Hylaeosaurus armatus*, which falls either in a large polytomy outside the four major clades (EW analysis, Figs. 5.1.1, 6.2.1) or as a polacanthid, sister taxa to the group composed of *Mymoorapelta*, *Gargoyleosaurus*, and *Dracopelta* (Figs. 5.2.1-2). The lability of *Hylaeosaurs*, as well as other uncertain taxa, may be explained by the incompleteness of the material and lack of sufficiently robust diagnostic characters that could help account for the high levels of homoplasy observed in ankylosaurs. Recently, though, Raven *et al*. (2020) reviewed the Wealden ankylosaurs, such as *Hylaeosaurus* and *Polacanthus*, and observed four autapomorphies. In the comprehensive analysis of Thyreophora, Raven *et al*. (2023) recovered *Hylaeosaurus* in an early diverging position in a group corresponding to the Polacanthidae, which, together with the results from this analysis, seem to support *Hylaeosaurus* as a polacanthid.

Other polacanthids are more stable. An example is the sister taxa relationship between *Zhejiangosaurus* and *Dongyangopelta* which is consistently recovered (Figs. 5.1.1, 2.1-2). Both taxa come from the Chaochuan Formation (Albian-Cenomanian) and the lack of diagnostic features in *Zhejiangosaurus* has raised questions about its validity, leading some authors to postulate that both ankylosaurs may represent one taxon (Arbour and Currie, 2016). This analysis and the same result obtained by Raven *et al*. (2023) reinforces that hypothesis. On the other hand,

the consistent placement of *Polacanthus* as sister taxon to those is supported by a single synapomorphy, ch. 279[0] (thin and/or hollow base of the thoracic armour).

All trees recovered *Dracopelta* and *Gargoyleosaurus* as sister taxa, and both as sister group to *Mymoorapelta*, forming either an early branching clade of polacanthids (Figs. 5.2.3-4), or a more derived group within Polacanthidae (Figs. 5.2.1-2,5). The pairing of *Dracopelta* and *Gargoyleosaurus* as sister-taxa is supported by at least two synapomorphies: ch. 115[1] (distinct pattern of scale polygons in the cranial ornamentation) and ch. 162[0] (longitudinal groove in the ventral surface of the sacrum). *Dracopelta* itself is diagnosed by four autapomorphies (see Chapter 4 of this dissertation for further details), most of which are not expressed in the analyses though. This discrepancy is explained by the fact that these autapomorphic characters resulted from first-hand identification and observation in *Dracopelta* specimens (MG 5787, NOVA-FCT-DCT-5556) and comparison with other ankylosaurs either through literature or photographs, but not their inclusion or exact matching of the characters in the dataset used. An example of this is the presence of two pairs of cervicothoracic, medial, suboval, keeled ossicles, with thickened rims, which is an autapomorphy of *Dracopelta*, but is a character not coded in the dataset. Nonetheless, the coupling of *Dracopelta* and *Gargoyleosaurus* is consistent across all analyses (Figs. 5.2.1-3) and is one of the more well-supported nodes both by the Bremer support (1) and the bootstrap value (67) (Figs. 5.2.4-5). The *Dracopelta* + *Gargoyleosaurus* group comes out across all trees, and jurapeltans are supported by at least four unambiguous synapomorphies in the implied weight analysis (k=15) and six unambiguous synapomorphies in the equal weight analysis, as for example ch. 151[0] (ratio of anteroposterior length of dorsal centrum to posterior centrum height) or ch. 212[0] (lateral expansion of ilium). Within Polacanthidae, regardless of the position of Jurapelta, there is a stable group of polacanthids, including *Polacanthus*, which either fall as sister clade to Jurapelta (Fig. 6.2.2) or within the group containing all non-jurapeltan polacanthids (Fig. 6.2.1). In this manner, and following the reasoning presented by Madzia *et al.* (2021) for clade nomenclature, the former would correspond to the Polacanthinae, as a group with the internal specifier being *Polacanthus foxii* and the external specifier *Dracopelta zbyszewskii*. On the other hand, in the IW analysis (Fig. 6.2.2), by falling deeper in the tree, the largest clade including *P. foxii* but not *D.*

zbyszewskii would be less inclusive than Polacanthinae, and instead be a polacanthine branch, together with Jurapelta. In this case, following nomenclatural convention, this group could be named Polacanthini, resulting thus in, for example, *Dracopelta* being a jurapeltan polacanthinin.

Regardless of the internal nomenclatural status of Polacanthidae, it is clear the clustering of Late Jurassic ankylosaurs to form Jurapelta, and that Polacanthidae represent one of the earliest groups of ankylosaurs, appearing at least in the Late Jurassic of Laurasia and lasting to the late Early Cretaceous (Fig. 6.2.3).

The Ankylosauridae remains generally stable, with some minor changes of positioning of its members (Figs. 6.2.1-2), even though no unambiguous synapomorphies recovered for Ankylosauridae. This is likely due to ankylosaurids being the most extensively studied of all ankylosaurs (e.g., Arbour and Currie, 2013a, 2013b, 2016; Arbour *et al.*, 2014a, 2014c; Arbour and Evans, 2017; Penkalski and Tumanova, 2017; Penkalski, 2018; Zheng *et al.*, 2018), and therefore its phylogeny more thoroughly scrutinized and tested, which these results seem to corroborate. Taxonomically, it conforms to the Ankylosauridae of Raven *et al.* (2023). However, there a couple of noteworthy discrepancies, namely the fact that in this study, *Jinyunpelta* and *Shamosaurus* fall outside Ankylosauridae, and, following the work of Madzia *et al.* (2021) and the clade definitions provided therein, only the less inclusive ankylosaurid clade Ankylosaurini holds. This is because other clade definitions, such as Ankylosaurinae, are anchored externally to *Shamosaurus scutatus*, which falls consistently outside Ankylosauridae (Figs. 6.2.1-2). The implication is that, even though there is consistent support for two clades within Ankylosauridae, the formal definitions would need to be revised. Still, the presence of two branches, one largely composed of North American taxa and another with mostly Asian ankylosaurids, indicates that ankylosaurids were restricted to North America and Asia during the latest Cretaceous (Fig. 6.2.3).

The instability and discrepancies due to analytical settings in this study is consistent with other datasets, which have encountered difficulties in resolving, for example, non-ankylosaurid relationships with a strong support (Thompson *et al.*, 2012; Arbour and Currie, 2016; Brown *et al.*, 2017; Wiersma and Irmis, 2018; Raven *et al.*, 2023). These difficulties can be attributed to various factors, of which the high levels of homoplasy paired with an often-incomplete fossil record seem to

be main contributors. A solution for this is a clade-specific character revision. However, such a study would require a much broader approach to Ankylosauria as a whole and falls beyond the scope of this work.

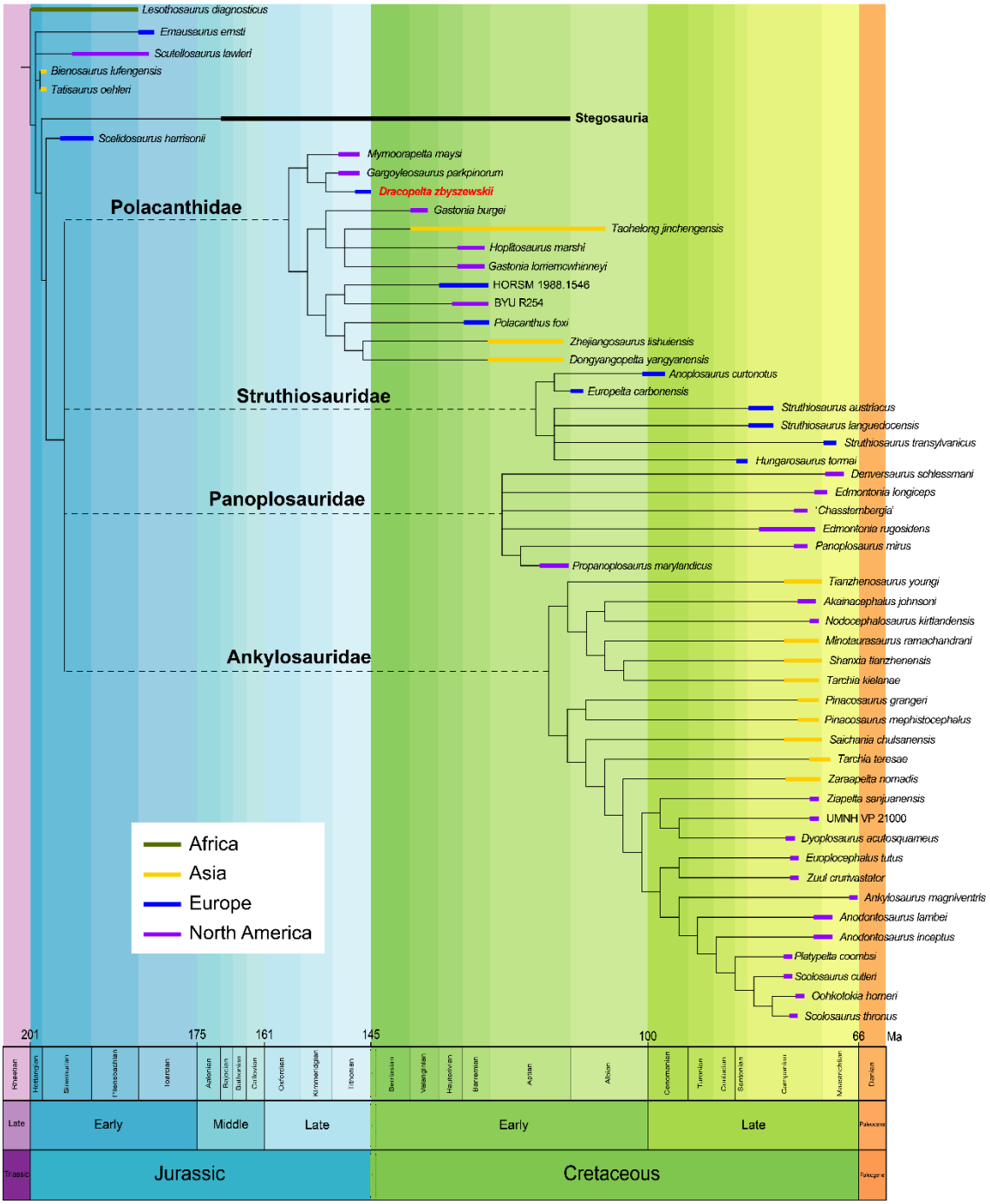

Figure 6.2.3. Distribution of taxa from the main clades of Ankylosauria over time. Phylogeny (EW, Fig. 6.2.1 of this dissertation) of Ankylosauria showing the time range of the taxa of the four main clades. Taxa falling outside the main ankylosaur clades were removed as to highlight the members of each group. Dashed lines represent uncertainty of lineage origin in time. Duration of taxa was taken from the literature.

6.3. Paleobiogeographical implications

Dracopelta is restricted to the uppermost Tithonian of the Assenta Member of Lourinhã formation, and to a small geographic area (less than one km^2) between the municipalities of Mafra and Torres Vedras, in Western Portugal (refer to Figs. 1.4.1-2 for stratigraphic and geographic correlation of the occurrences). Despite the abundance of dinosaur remains, particularly from the Kimmeridgian and lower Tithonian strata of the Lourinhã formation, ankylosaur material is limited to the two occurrences studied in this work, meaning there is no evidence of the presence of *Dracopelta* in Iberia before the latest Tithonian. However, and even though ankylosaurs were poorly represented during the Late Jurassic, the recovery of *Dracopelta* as sister taxon of *Gargoyleosaurus* and the grouping of both with *Mymoorapelta* to form a Late Jurassic branch of polacanthids, the Jurapelta, has implications on the understanding of dinosaur biogeographical patterns during the Late Jurassic.

Mateus (2006) detailed the general similarities between the Upper Jurassic dinosaur fauna recovered from the Lourinhã Formation and the overall coeval Morrison and Tendaguru Beds formations. In particular, the close relationship between North American and Iberian faunas during the Late Jurassic has been extensively documented, and illustrated by the occurrence of shared genera of dinosaurs, such as *Supersaurus*, *Stegosaurus*, *Torvosaurus*, *Allosaurus*, *Ceratosaurus*, and *Miragaia* (Antunes and Mateus, 2003; Mateus *et al.*, 2006; Escaso *et al.*, 2007; Hendrickx and Mateus, 2014a; Malafaia *et al.*, 2015; Tschopp *et al.*, 2015; Costa and Mateus, 2019). The inclusion of North American and Iberian Late Jurassic ankylosaurs into the same clade further supports this affinity. However, it should be noted that the discovery of new dinosaur taxa in Iberia in recent years has complicated this scenario. The faunal composition of the Late Jurassic of Portugal shows a strong mixture of typically European (Hendrickx and Mateus, 2014a), Gondwanan (Malafaia *et al.*, 2020) and cosmopolitan clades (Costa and Mateus, 2019; Mocho *et al.*, 2019; Bonaparte and Mateus, 1999). Cosmopolitan faunas are expected to be the standard for the Late Jurassic (Ezcurra and Agnolin, 2012), however some evidence of slight regionalism has been shown at least for sauropod taxa (Mannion *et al.*, 2019). Recent work carried out on iguanodontian

dinosaurs (Escaso *et al.*, 2014; Sanchéz-Fenollosa *et al.*, 2023; Rotatori *et al.*, 2020, 2022, 2024) indicates this clade diversified in Laurasia and most probably Europe. Megalosauridae and Allosauridae seem to be another clear Laurasian faunal component, respectively of European and North American origin (Mateus *et al.*, 2006; Malafaia *et al.*, 2010; Rauhut *et al.*, 2016). In this context, jurapeltine polacanthids are another Laurasian component of the faunal assemblage of the Lourinhã Formation. Furthermore, the occurrence of the two North American taxa, *Mymoorapelta maysi* and *Gargoyleosaurus parkpinorum*, in strata slightly older than *Dracopelta* (Carpenter *et al.* 1998; Kirkland and Carpenter, 1998) suggests that Jurapeltans, and consequently Polacanthidae, originated in North America and subsequently dispersed to Iberia, achieving a Laurasian distribution by the Early Cretaceous. These findings support the pivotal role of the Iberian plate in dispersal and vicariance events of megafauna during the Late Jurassic, namely of the ancestor of *Gargoyleosaurus* and *Dracopelta*, which had to occur prior to the Tithonian and may tentatively indicate a latest Kimmeridgian - earliest Tithonian land connection between North America and Iberia, although more precise dating of both taxa coupled with broader, more comprehensive paleobiogeographical analyses are needed to test this hypothesis.

6.4. Paleoecology

The Lourinhã Formation has an abundant and important fossil record from the Upper Jurassic, which has been extensively documented and attests to the rich paleobiodiversity of fauna and flora (e.g., (Saporta and Choffat, 1894; Sauvage, 1898; Lapparent and Zbyszewski, 1957; Galton, 1981, 1996; Antunes *et al.*, 1998; Pais, 1998; Schwarz, 2002; Antunes and Mateus, 2003; Mateus, 2006; Mateus *et al.*, 2006; Pérez-García and Ortega, 2011; Escaso *et al.*, 2014; Hendrickx and Mateus, 2014a; Ribeiro *et al.*, 2014; Russo *et al.*, 2017; Costa and Mateus, 2019; Mocho *et al.*, 2019; Guillaume *et al.*, 2020; Malafaia *et al.*, 2020; Rotatori *et al.*, 2022). This richness is consistent with paleoclimatic models for the Lourinhã Formation and Western Iberia during the Late Jurassic. Studies indicate a strong seasonality in precipitation (i.e., monsoonal climatic pattern), with dry and warm summers and wet winters, averaging estimated surface temperatures of 31°C

(Martinius and Gowland, 2011; Myers *et al.*, 2012a, 2014). Therefore, water supply and food availability would have been alternatingly more or less available. Myers *et al.* (2012b) estimated that the high faunal richness of the Lourinhã Formation was linked to the high primary productivity, based on the measured soil pCO_2. It is then clear that the paleoclimatic conditions were favourable to the presence and development of a diverse biome.

The fossil plant record consists mostly of conifers, cycads, and ferns (Saporta and Choffat, 1894; Pais, 1998; Mateus *et al.*, 2017, Gowland *et al.*, 2018), suggesting forested areas with low lying plant cover, which provided a high diversity of low, mid-height, and high food sources. While both coalified and silicified remains are common throughout the Lourinhã Formation, evidencing the ubiquitous presence of a diverse flora in time and space, detailed paleobotanical studies are lacking. On the other hand, the fauna was highly diverse, with every major Late Jurassic vertebrate group represented across the timespan and length of the formation (e.g., (Sauvage, 1898; Lapparent and Zbyszewski, 1957; Galton, 1981; Schwarz, 2002; Antunes and Mateus, 2003; Balbino, 2003; Mateus *et al.*, 2006; Pérez-García and Ortega, 2011; Mocho *et al.*, 2017; Guillaume *et al.*, 2020; Rotatori *et al.*, 2020; Russo and Mateus, 2021; Fernandes *et al.*, 2023). However, the rarity of *Dracopelta* reinforces that ankylosaurs were minor components of Late Jurassic ecosystems, further corroborated by what is observed for example in the Morrison Formation, where even though more abundant, occurrences are still scarce when compared to other dinosaur groups (Kirkland and Carpenter, 1994; Kirkland *et al.*, 1998; Kilbourne and Carpenter, 2005; (Maidment, 2023). In other coeval deposits, such as Tendaguru, in Tanzania, and Villar del Arzobispo, in Spain, ankylosaurs are so far absent. At around 3-3,5 meters long and weighing approximately 625 kg, *Dracopelta* was a small to medium sized herbivore that lived alongside other low-browsing taxa, like stegosaurs (Escaso *et al.*, 2007; Mateus and Antunes, 2003, Mateus *et al.*, 2009) and at least three species of iguanodontian dinosaurs (Escaso *et al.*, 2014; Mateus and Antunes, 2001; Rotatori *et al.*, 2020, 2022, 2024), which potentially had overlapping (at least partially) ecological niches. Future ecological niche modelling studies of these taxa would clarify niche partitioning of herbivores in the Lourinhã formation and in the Late Jurassic in general.

The lithostratigraphic and taphonomical evidence suggest that *Dracopelta* may have preferred distal deltaic-fluvial floodplain environments, such as marshlands subjected to seasonal high-low energy waterflows intervals, established on a paralic plain, with episodic short-lived, marine influence, in agreement with previous works on the stratigraphy of the Lourinhã formation (Hill, 1988, 1989; Martinius and Gowland, 2011; Taylor *et al.*, 2014; Mateus *et al.*, 2017; Gowland *et al.*, 2018). Nonetheless, additional specimens would help clarify if this habitat preference assertion is indeed valid or an artifact of geographical and stratigraphical bias.

7

CONCLUSIONS

This work provides for the first time a detailed description of *Dracopelta zbyszewskii*, based on a new, partially complete, articulated specimen, and a full reassessment of the holotype material, thus prompting a re-diagnosis of the taxon, defined by a unique combination of characters, ten of which are autapomorphic. The redescription of *D. zbyszewskii* allowed its inclusion in a comprehensive dataset used to ascertain its phylogenetic relationships, as well as reassess the evolutionary relationships within Ankylosauria as a whole. In sum, this work allowed to conclude that:

i) a new ankylosaur skeleton (NOVA-FCT-DCT-5556), composed of articulated cranial and postcranial elements, shows a unique combination of characters, including the four autapomorphic characters observed in the holotype of *D. zbyszewskii*. This allows to confidently assign the new specimen to *D. zbyszewskii*, making *Dracopelta* the most complete dinosaur from Portugal, and the most complete from the Jurassic. At least six new and unique characters were observed in the new specimen, further supporting the validity of *D. zbyszewskii*.

ii) *D. zbyszewskii* is thus a valid taxon, diagnosed by a unique combination of characters, identified across the cranial, axial, appendicular, and dermal skeleton. Furthermore, the presence of features found in later

diverging taxa, such as a wide skull, short and robust forelimbs, fusion of posterior dorsal ribs to the ventral surface of the preacetabular process of the ilium, reduction of the pubis, and multiple osteoderm morphologies, including large lateral plates, indicate that the general bauplan of Ankylosauria appeared at least as early as the Late Jurassic.

iii) Ankylosauria includes four major clades: the Ankylosauridae, the Panoplosauridae, the Struthiosauridae, and the Polacanthidae. Polacanthids are the earliest diverging group of ankylosaurs and include closely related Late Jurassic forms from North America and Iberia. *D. zbyszewskii* is recovered as the sister taxa of the Morrison Formation *Gargoyleosaurus parkpinorum*, and both as sister group to *Mymoorapelta maysi*, also from Morrison. These three taxa form an early diverging polacanthid group, the Jurapelta clade nov., supported by at least four synapomorphies.

iv) Jurapeltans further reinforce the Late Jurassic North American-Iberian paleobiogeographical connections and paleoecological relationships. Moreover, the occurrence of Morrison taxa stratigraphically lower than the Portuguese taxa seems to point to a North American origin for Jurapeltans and, more broadly, for polacanthids, first appearing in the Kimmeridgian, having spread to Europe by the latest Tithonian, and achieving a Laurasian distribution by the late Early Cretaceous.

The first thorough description and phylogenetic analysis of *D. zbyszewskii* was crucial to better understand this hitherto poorly known ankylosaur. Altogether, it was possible to produce a detailed look of the anatomy of *D. zbyszewskii*, including a reconstruction of its aspect (Fig. 7.1), and at the same time increase the knowledge of the early evolution of ankylosaurs, as well as clarify its phylogenetic position. Furthermore, by having an additional key data point from early in the evolution of the group, it was possible to increase the resolution of the evolutionary history of Ankylosauria, confirming a more complex history than previously thought. Nevertheless, this study highlights that more work is needed to further shed light on the factors affecting the phylogenetic signal, particularly at the base of the tree. Improved fossil sampling, whether through fossil collection, preparation, or both,

updated revision of existing specimens, and better character scoring, which needs to include often overlooked characters, namely postcranial and dermal armour, will certainly help. Moreover, future approaches should include, for example, ecological niche modelling, finite element analysis, and biomechanical analysis, as to further increase the knowledge on the paleobiology and paleoecology of ankylosaurs.

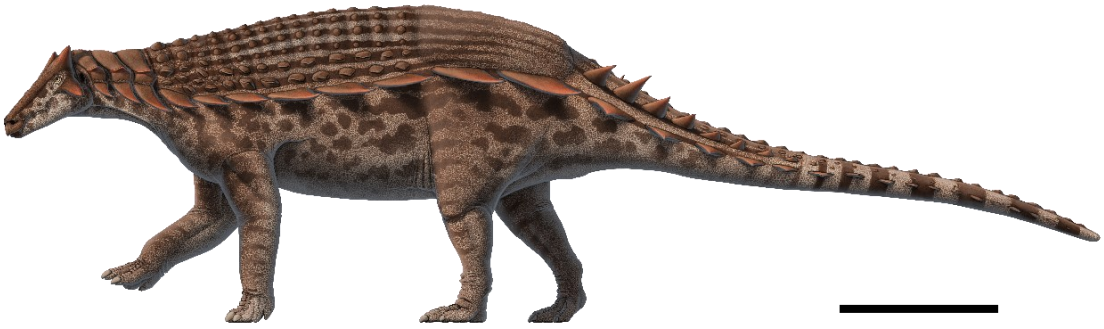

Figure 7.1. Life reconstruction of *Dracopelta zbyszewskii*. Artistic rendering of *D. zbyszewskii* showing its distinct armour pattern and flat head. Coloring is based on *Borealopelta markmitchelli* (Brown *et al.*, 2017). Scale bar: 50 cm. Illustration by Pedro Andrade.

BIBLIOGRAPHY

Agnolin, F. L., M. D. Ezcurra, D. F. Pais, and S. W. Salisbury. 2010. A reappraisal of the Cretaceous non-avian dinosaur faunas from Australia and New Zealand: evidence for their Gondwanan affinities. Journal of Systematic Palaeontology 8:257–300.

Alves, T. M., G. Manuppella, R. L. Gawthorpe, D. W. Hunt, and J. H. Monteiro. 2003. The depositional evolution of diapir- and fault-bounded rift basins: examples from the Lusitanian Basin of West Iberia. Sedimentary Geology 162:273–303.

Antunes, M. T., and D. Sigogneau-Russell. 1991. Nouvelles données sur les Dinosaures du Crétacé supérieur du Portugal. Comptes Rendus de l'Académie Des Sciences. Série 2, Mécanique, Physique, Chimie, Sciences de l'Univers, Sciences de La Terre 313:113–119.

Antunes, M. T., and O. Mateus. 2003. Dinosaurs of Portugal. Comptes Rendus Palevol 2:77–95.

Antunes, M. T., P. Taquet, and V. Ribeiro. 1998. Upper Jurassic dinosaur and crocodile eggs from Paimogo nesting site (Lourinha-Portugal). Memórias Da Academia de Ciências de Lisboa 37:83–100.

Apesteguía, S., and P. A. Gallina. 2011. Tunasniyoj, a dinosaur tracksite from the Jurassic-Cretaceous boundary of Bolivia. Anais Da Academia Brasileira de Ciências 83:267–277.

Araújo, R., R. Castanhinha, R. M. Martins, O. Mateus, C. Hendrickx, F. Beckmann, N. Schell, and L. C. Alves. 2013. Filling the gaps of dinosaur eggshell phylogeny: Late Jurassic theropod clutch with embryos from Portugal. Scientific Reports 3.

Arbour, V. M., and P. J. Currie. 2013a. *Euoplocephalus tutus* and the diversity of ankylosaurid dinosaurs in the Late Cretaceous of Alberta, Canada, and Montana, USA. PloS One 8:e62421–e62421.

Arbour, V. M., and P. J. Currie. 2013b. The taxonomic identity of a nearly complete ankylosaurid dinosaur skeleton from the Gobi Desert of Mongolia. Cretaceous Research 46:24–30.

Arbour, V. M., and P. J. Currie. 2016. Systematics, phylogeny and palaeobiogeography of the ankylosaurid dinosaurs. Journal of Systematic Palaeontology 14:385–444.

Arbour, V. M., and D. C. Evans. 2017. A new ankylosaurine dinosaur from the Judith River Formation of Montana, USA, based on an exceptional skeleton with soft tissue preservation. Royal Society Open Science 4:161086.

Arbour, V. M., and J. C. Mallon. 2017. Unusual cranial and postcranial anatomy in the archetypal ankylosaur Ankylosaurus magniventris. Facets 2:764–794.

Arbour, V. M., and L. E. Zanno. 2019. Tail Weaponry in Ankylosaurs and Glyptodonts: An Example of a Rare but Strongly Convergent Phenotype. The Anatomical Record.

Arbour, V. M., M. E. Burns, and R. L. Sissons. 2009. A redescription of the ankylosaurid dinosaur Dyoplosaurus acutosquameus Parks, 1924 (Ornithischia: Ankylosauria) and a revision of the genus. Journal of Vertebrate Paleontology 29:1117–1135.

Arbour, V. M., M. E. Burns, and P. J. Currie. 2011. A review of pelvic shield morphology in ankylosaurs (Dinosauria: Ornithischia). Journal of Paleontology 85:298–302.

Arbour, V. M., P. J. Currie, and D. Badamgarav. 2014a. The ankylosaurid dinosaurs of the Upper Cretaceous Baruungoyot and Nemegt formations of Mongolia. Zoological Journal of the Linnean Society 172:631–652.

Arbour, V. M., M. E. Burns, P. R. Bell, and P. J. Currie. 2014b. Epidermal and dermal integumentary structures of ankylosaurian dinosaurs. Journal of Morphology 275:39–50.

Arbour, V. M., N. L. Lech-Hernes, T. E. Guldberg, J. H. Hurum, and P. J. Currie. 2013. An ankylosaurid dinosaur from Mongolia with *in situ* armour and keratinous scale impressions. Acta Palaeontologica Polonica 58:55–64.

Arbour, V. M., D. Larson, M. Vavrek, L. Buckley, and D. Evans. 2020. An ankylosaurian dinosaur from the Cenomanian Dunvegan Formation of northeastern British Columbia, Canada. Fossil Record 23:179–189.

Arbour, V. M., M. E. Burns, R. M. Sullivan, S. G. Lucas, A. K. Cantrell, J. Fry, and T. L. Suazo. 2014c. A new ankylosaurid dinosaur from the Upper Cretaceous (Kirtlandian) of New Mexico with implications for ankylosaurid diversity in the Upper Cretaceous of western North America. PloS One 9:e108804.

Augustin, F. J., A. T. Matzke, M. W. Maisch, and H.-U. Pfretzschner. 2020. First evidence of an ankylosaur (Dinosauria, Ornithischia) from the Jurassic Qigu Formation (Junggar Basin, NW China) and the early fossil record of Ankylosauria. Geobios 61:1–10.

Averianov, A. O. 2002. An ankylosaurid (Ornithischia: Ankylosauria) braincase from the Upper Cretaceous Bissekty Formation of Uzbekistan. Bulletin de l'Institut Royal Des Sciences Naturelles de Belgique, Sciences de La Terre 72:97–110.

Bakker, R. 1988. Review of the Late Cretaceous nodosauroid Dinosauria. Hunteria 1:1–23.

Balbino, A. C. 2003. Upper Jurassic Hybodontidae (Selachii) from Lourinhã, Portugal. Ciências Da Terra/Earth Sciences Journal 45–52.

Baron, M. G., D. B. Norman, and P. M. Barrett. 2017. Postcranial anatomy of *Lesothosaurus diagnosticus* (Dinosauria: Ornithischia) from the Lower

Jurassic of southern Africa: implications for basal ornithischian taxonomy and systematics. Zoological Journal of the Linnean Society 179:125–168.

Barrett, P. M., Y. Hailu, P. Upchurch, and A. C. Burton. 1998. A new ankylosaurian dinosaur (Ornithischia: Ankylosauria) from the Upper Cretaceous of Shanxi Province, People's Republic of China. Journal of Vertebrate Paleontology 18:376–384.

Barrett, P. M., T. H. Rich, P. Vickers-Rich, T. A. Tumanova, M. Inglis, D. Pickering, L. Kool, and B. P. Kear. 2010. Ankylosaurian dinosaur remains from the Lower Cretaceous of southeastern Australia. Alcheringa 34:205–217.

Bell, P. R., M. E. Burns, and E. T. Smith. 2018. A probable ankylosaurian (Dinosauria, Thyreophora) from the Early Cretaceous of New South Wales, Australia. Alcheringa: An Australasian Journal of Palaeontology 42:120–124.

Bertozzo, F., B. C. Da Silva, D. Martill, E. Marlene, T. A. Vorderwuelbecke, R. Schouten, and P. Aquino. 2021. A large pterosaur femur from the Kimmeridgian, Upper Jurassic of Lusitanian Basin, Portugal. Acta Palaeontologica Polonica 66:815–825.

Blows, W. 2001. Dermal Armor of the Polacanthine Dinosaurs; pp. 363–385 in The Armored Dinosaurs, Kenneth Carpenter. Indiana University Press, Bloomington and Indianapolis, Indiana, USA.

Blows, W. T. 1987. The armoured dinosaur *Polacanthus foxi* from the Lower Cretaceous of the Isle of Wight. Palaeontology 30:557–580.

Blows, W. T. 1996. A new species of *Polacanthus* (Ornithischia; Ankylosauria) from the Lower Cretaceous of Sussex, England. Geological Magazine 133:671–682.

Blows, W. T. 2015. British Polacanthid Dinosaurs. Siri Scientific Press, 224 pp.

Blows, W. T., and K. Honeysett. 2013. New teeth of nodosaurid ankylosaurs from the Lower Cretaceous of Southern England. Acta Palaeontologica Polonica 59:835–842.

Blows, W. T., and K. Honeysett. 2014. First Valanginian *Polacanthus foxii* (Dinosauria, Ankylosauria) from England, from the Lower Cretaceous of Bexhill, Sussex. Proceedings of the Geologists' Association 125:233–251.

Bohlin, B. 1953. Fossil Reptiles from Mongolia and Kansu. Statens Etnografiska Museum, Stockholm, 113 pp.

Bonaparte, J., and O. Mateus. 1999. A new diplodocid, *Dinheirosaurus lourinhanensis* gen. et sp. nov., from the Late Jurassic beds of Portugal. Revista del Museo Argentino de Ciencias Naturales Bernardino Rivadavia e Instituto Nacional de Investigación de las Ciencias Naturales 5:13-29.

Botfalvai, G., E. Prondvai, and A. Ősi. 2020. Living alone or moving in herds? A holistic approach highlights complexity in the social lifestyle of Cretaceous ankylosaurs. Cretaceous Research 104633.

Bourke, J. M., W. R. Porter, and L. M. Witmer. 2018. Convoluted nasal passages function as efficient heat exchangers in ankylosaurs (Dinosauria: Ornithischia: Thyreophora). PLoS One 13:e0207381.

Breeden III, B. T., T. J. Raven, R. J. Butler, T. B. Rowe, and S. C. Maidment. 2021. The anatomy and palaeobiology of the early armoured dinosaur *Scutellosaurus lawleri* (Ornithischia: Thyreophora) from the Kayenta Formation (Lower Jurassic) of Arizona. Royal Society Open Science 8:201676.

Brown, B. 1908. The Ankylosauridae, a new family of armored dinosaurs from the Upper Cretaceous. Bulletin of the American Museum of Natural History 12:187–201.

Brown, C. M. 2017. An exceptionally preserved armored dinosaur reveals the morphology and allometry of osteoderms and their horny epidermal coverings. PeerJ 5:e4066.

Brown, C. M., D. M. Henderson, J. Vinther, I. Fletcher, A. Sistiaga, J. Herrera, and R. E. Summons. 2017. An exceptionally preserved three-dimensional armored dinosaur reveals insights into coloration and Cretaceous predator-prey dynamics. Current Biology 27:2514–2521.

Brown, C. M., D. R. Greenwood, J. E. Kalyniuk, D. R. Braman, D. M. Henderson, C. L. Greenwood, and J. F. Basinger. 2020. Dietary palaeoecology of an Early Cretaceous armoured dinosaur (Ornithischia; Nodosauridae) based on floral analysis of stomach contents. Royal Society Open Science 7:200305.

Buffetaut, E. 1995. An ankylosaurid dinosaur from the Upper Cretaceous of Shandong (China). Geological magazine 131:683-692.

Bunzel, E. 1871. Die Reptilfauna Der Gosau-Formation in Der" Neuen Welt" Bei Wiener-Neustadt. Brockhaus, pp.

Burns, M. E., and R. M. Sullivan. 2011. A new ankylosaurid from the Upper Cretaceous Kirtland Formation, San Juan Basin, with comments on the diversity of ankylosaurids in New Mexico. Fossil Record 3: Bulletin 53 53:169.

Burns, M. E., and P. J. Currie. 2014. External and internal structure of ankylosaur (Dinosauria, Ornithischia) osteoderms and their systematic relevance. Journal of Vertebrate Paleontology 34:835–851.

Burns, M. E., and S. G. Lucas. 2015. Biostratigraphy of ankylosaur (Dinosauria: Ornitischia) osteoderms from New Mexico. Fossil Record 4:9-14.

Butler, R. J., P. Upchurch, and D. B. Norman. 2008. The phylogeny of the ornithischian dinosaurs. Journal of Systematic Palaeontology 6:1-40.

Campione, N. E., and D. C. Evans. 2012. A universal scaling relationship between body mass and proximal limb bone dimensions in quadrupedal terrestrial tetrapods. BMC Biology 10:1-22.

Canudo, J. I., J. I. Ruiz-Omeñaca, and G. Cuenca-Bescós. 2004. Los primeros dientes de anquilosaurio (Ornithischia: Thyreophora) descritos en el Cretácico Inferior de España. Revista Española de Paleontología 19:33–46.

Canudo, J. I., O. Amo, G. Cuenca-Bescós, A. Meléndez, J. Ruiz-Omeñaca, and A. Soria. 1997. Los vertebrados del Tithónico-Barremiense de Galve (Teruel, España). Cuadernos de Geología Ibérica 23:209–241.

Carpenter, K. 1984. Skeletal reconstruction and life restoration of *Sauropelta* (Ankylosauria: Nodosauridae) from the Cretaceous of North America. Canadian Journal of Earth Sciences 21:1491–1498.

Carpenter, K. 1990. Ankylosaur systematics: example using *Panoplosaurus* and *Edmontonia* (Ankylosauria: Nodosauridae); pp. 281–298 in Dinosaur Systematics: Approaches and Perspectives, Kenneth Carpenter&Phil J. Currie. Cambridge University Press.

Carpenter, K. 2001. Phylogenetic Analysis of the Ankylosauria; pp. 455–483 in The Armored Dinosaurs, Kenneth Carpenter. Indiana University Press, Bloomington and Indianapolis, Indiana, USA.

Carpenter, K. 2004. Redescription of *Ankylosaurus magniventris* Brown 1908 (Ankylosauridae) from the Upper Cretaceous of the Western Interior of North America. Canadian Journal of Earth Sciences 41:961–986.

Carpenter, K., and J. I. Kirkland. 1998. Review of Lower and middle Cretaceous ankylosaurs from North America. New Mexico Museum of Natural History and Science Bulletin 14:249–270.

Carpenter, K., D. Dilkes, and D. B. Weishampel. 1995. The dinosaurs of the Niobrara Chalk Formation (Upper Cretaceous, Kansas). Journal of Vertebrate Paleontology 15:275–297.

Carpenter, K., C. Miles, and K. Cloward. 1998. Skull of a Jurassic ankylosaur (Dinosauria). Nature 393:782–783.

Carpenter, K., J. I. Kirkland, D. Burge, and J. Bird. 1999. Ankylosaurs (Dinosauria: Ornithischia) of the Cedar Mountain Formation, Utah, and their stratigraphic distribution. Vertebrate Paleontology in Utah 9:243–251.

Carpenter, K., J. I. Kirkland, D. Burge, and J. Bird. 2001. Disarticulated skull of a new primitive ankylosaurid from the Lower Cretaceous of eastern Utah; pp. 211–238 in The Armored Dinosaurs, Kenneth Carpenter. Indiana University Press Bloomington.

Carpenter, K., J. Bartlett, J. Bird, and R. Barrick. 2008. Ankylosaurs from the Price River Quarries, Cedar Mountain Formation (Lower Cretaceous), east-central Utah. Journal of Vertebrate Paleontology 28:1089–1101.

Carpenter, K., T. DiCroce, B. Kinneer, and R. Simon. 2013. Pelvis of *Gargoyleosaurus* (Dinosauria: Ankylosauria) and the origin and evolution of the ankylosaur pelvis. PloS One 8:e79887.

Carpenter, K., S. Hayashi, Y. Kobayashi, T. Maryańska, R. Barsbold, K. Sato, and I. Obata. 2011. *Saichania chulsanensis* (Ornithischia, Ankylosauridae) from the upper cretaceous of Mongolia. Palaeontographica Abteilung A 294:1–61.

Cerda, I. A., Z. Gasparini, R. A. Coria, L. Salgado, M. Reguero, D. Ponce, R. Gonzalez, J. M. Jannello, and J. Moly. 2019. Paleobiological inferences for the Antarctic dinosaur *Antarctopelta oliveroi* (Ornithischia: Ankylosauria) based on bone histology of the holotype. Cretaceous Research 103:104171.

Chatterjee, S. 2020. The age of dinosaurs in the land of Gonds; pp. 181–226 in Biological Consequences of Plate Tectonics. Springer.

Chatterjee, S., and D. K. Rudra. 1996. KT events in India: impact, rifting, volcanism and dinosaur extinction. Memoirs of the Queensland Museum 39:489–532.

Chen, R., W. Zheng, Y. Azuma, M. Shibata, T. Lou, Q. Jin, and X. Jin. 2013. A new nodosaurid ankylosaur from the Chaochuan Formation of Dongyang, Zhejiang Province, China. Acta Geologica Sinica-English Edition 87:658–671.

Clark, N. 2001. A thyreophoran dinosaur from the Early Bajocian (Middle Jurassic) of the Isle of Skye, Scotland. Scottish Journal of Geology 37:19–26.

Coombs Jr, W. P. 1971. The Ankylosauria. Ph.D. dissertation, Columbia University, 487 pp.

Coombs Jr, W. P. 1972. The bony eyelid of *Euoplocephalus* (Reptilia, Ornithischia). Journal of Paleontology 46:637–650.

Coombs Jr, W. P. 1978a. The families of the ornithischian dinosaur order Ankylosauria. Palaeontology 21:143–170.

Coombs Jr, W. P. 1978b. Forelimb muscles of the Ankylosauria (Reptilia, Ornithischia). Journal of Paleontology 642–657.

Coombs Jr, W. P. 1979. Osteology and myology of the hindlimb in the Ankylosauria (Reptillia, Ornithischia). Journal of Paleontology 666–684.

Coombs Jr, W. P. 1986. A juvenile ankylosaur referable to the genus *Euoplocephalus* (Reptilia, Ornithischia). Journal of Vertebrate Paleontology 6:162–173.

Coombs Jr, W. P. 1990. Teeth and taxonomy in ankylosaurs; pp. 269–279 in Dinosaur Systematics: Approaches and Perspectives. Cambridge University Press.

Coombs Jr, W. P. 1995a. A nodosaurid ankylosaur (Dinosauria: Ornithischia) from the Lower Cretaceous of Texas. Journal of Vertebrate Paleontology 15:298–312.

Coombs Jr, W. P. 1995b. Ankylosaurian tail clubs of middle Campanian to early Maastrichtian age from western North America, with description of a tiny club from Alberta and discussion of tail orientation and tail club function. Canadian Journal of Earth Sciences 32:902–912.

Coombs Jr, W. P., and T. A. Deméré. 1996. A Late Cretaceous nodosaurid ankylosaur (Dinosauria: Ornithischia) from marine sediments of coastal California. Journal of Paleontology 70:311–326.

Coria, R. A., and L. Salgado. 2001. South American ankylosaurs; pp. 159–168 in The Armored Dinosaurs. Indiana University Press Bloomington.

Costa, F., and O. Mateus. 2019. Dacentrurine stegosaurs (Dinosauria): a new specimen of *Miragaia longicollum* from the Late Jurassic of Portugal resolves taxonomical validity and shows the occurrence of the clade in North America. PloS One 14:e0224263.

Currie, P. J., D. Badamgarav, E. B. Koppelhus, R. Sissons, and M. K. Vickaryous. 2011. Hands, feet, and behaviour in *Pinacosaurus* (Dinosauria: Ankylosauridae). Acta Palaeontologica Polonica 56:489–504.

De Valais, S., S. Apesteguía, and D. U. Sauthier. 2003. Nuevas evidencias de dinosaurios de la formacion Puerto Yerua (Cretacico), provincia de Entre Rios, Argentina. Ameghiniana 40:631–635.

Delsate, D., X. Pereda-Suberbiola, R. Felten, and G. Felten. 2018. First thyreophoran dinosaur from the Middle Jurassic (Bajocian) of Luxembourg. Geologica Belgica 21:19–26.

Eaton Jr, T. H. 1960. A new armored dinosaur from the Cretaceous of Kansas. The University of Kansas Paleontological Contributions 8:1–24.

Escaso, F., F. Ortega, P. Dantas, E. Malafaia, B. Silva, and J. L. Sanz. 2007. Elementos postcraneales de *Dacentrurus* (Dinosauria: Stegosauria) del Jurásico Superior de Moçafaneira (Torres Vedras, Portugal). Cantera Paleontológica 157:172.

Escaso, F., F. Ortega, P. Dantas, E. Malafaia, B. Silva, J. M. Gasulla, P. Mocho, I. Narváez, and J. L. Sanz. 2014. A new dryosaurid ornithopod (Dinosauria, Ornithischia) from the Late Jurassic of Portugal. Journal of Vertebrate Paleontology 34:1102–1112.

Escaso, F., F. Ortega, P. Dantas, E. Malafaia, N. L. Pimentel, X. Pereda-Suberbiola, J. L. Sanz, J. C. Kullberg, M. C. Kullberg, and F. Barriga. 2007. New evidence of shared dinosaur across Upper Jurassic proto-North Atlantic: *Stegosaurus* from Portugal. Naturwissenschaften 94:367–374.

Ezcurra, M. D., and F. L. Agnolín. 2012. A new global palaeobiogeographical model for the late Mesozoic and early Tertiary. Systematic Biology 61:553-566.

Fernandes, A. E., V. Beccari, A. W. Kellner, and O. Mateus. 2023. A new gnathosaurine (Pterosauria, Archaeopterodactyloidea) from the Late Jurassic of Portugal. PeerJ 11:e16048.

Ford, T. 2000. A review of ankylosaur osteoderms from New Mexico and a preliminary review of ankylosaur armor. New Mexico Museum of Natural History and Science Bulletin 17:157-176.

Ford, T. L., and J. I. Kirkland. 2001. Carlsbad Ankylosaur (Ornithischia, Ankylosauria): An Ankylosaurid and Not a Nodosaurid; pp. 239–260 in The Armored Dinosaurs, Kenneth Carpenter. Indiana University Press Bloomington.

Foster, J. 2020. Jurassic West: the dinosaurs of the Morrison Formation and their world. Indiana University Press, 560 pp.

Fox, W. 1866. On a new Wealden saurian named *Polacanthus*. Reports of the British Association for the Advancement of Science 35:56.

Francischini, H., M. A. Sales, P. Dentzien–Dias, and C. L. Schultz. 2018. The presence of ankylosaur tracks in the Guará Formation (Brazil) and remarks on the spatial and temporal distribution of Late Jurassic dinosaurs. Ichnos 25:177–191.

Fujita, M., Y. Azuma, M. Goto, Y. Tomida, S. Hayashi, and Y. Arakawa. 2003. First ankylosaur footprints in Japan and their significance. 23:52A-52A.

Galton, P., and P. Upchurch. 2004. Stegosauria; pp. 343–362 in The Dinosauria: Second Edition. Univ of California Press.

Galton, P. M. 1980a. Armored dinosaurs (Ornithischia: Ankylosauria) from the Middle and Upper Jurassic of England. Geobios 13:825–837.

Galton, P. M. 1980b. Partial skeleton of *Dracopelta zbyszewskii* n. gen. and n. sp., an ankylosaurian dinosaur from the Upper Jurassic of Portugal. Géobios 13:451–457.

Galton, P. M. 1981. A juvenile stegosaurian dinosaur, "*Astrodon pusillus*", from the Upper Jurassic of Portugal, with comments on Upper Jurassic and Lower Cretaceous biogeography. Journal of Vertebrate Paleontology 1:245–256.

Galton, P. M. 1983a. Armored Dinosaurs (Ornithischia: Ankylosauria) from the Middle and Upper Jurassic of Europe. Palaeontographica Abteilung A A182:1–25.

Galton, P. M. 1983b. *Sarcolestes leedsi* Lydekker, an ankylosaurian dinosaur from the Middle Jurassic of England. Neues Jahrbuch Für Geologie Und Paläontologie-Monatshefte 141–155.

Galton, P. M. 1991. Postcranial remains of stegosaurian dinosaur Dacentrurus from Upper Jurassic of France and Portugal. Geologica et Palaeontologica 25:299–327.

Galton, P. M. 1994a. Dermal scutes of *Sarcolestes*, an ankylosaurian dinosaur from the Middle Jurassic of England. Neues Jahrbuch Für Geologie Und Paläontologie-Monatshefte 726–732.

Galton, P. M. 1994b. Notes on Dinosauria and Pterodactylia from the Cretaceous of Portugal. Neues Jahrbuch Für Geologie Und Paläontologie, Abhandlungen 194:253–267.

Galton, P. M. 1996. Notes on Dinosauria from the Upper Cretaceous of Portugal. Neues Jahrbuch Für Geologie Und Paläontologie-Monatshefte 83–90.

Galton, P. M. 2019. Earliest record of an ankylosaurian dinosaur (Ornithischia: Thyreophora): dermal armor from Lower Kota Formation (Lower Jurassic) of India. Neues Jahrbuch Für Geologie Und Paläontologie-Abhandlungen 291:205–219.

Garcia, G., and X. Pereda-Suberbiola. 2003. A new species of *Struthiosaurus* (Dinosauria: Ankylosauria) from the Upper Cretaceous of Villeveyrac (southern France). Journal of Vertebrate Paleontology 23:156–165.

Gasparini, Z., X. Pereda-Suberbiola, and R. E. Molnar. 1996. New data on the ankylosaurian dinosaur from the Late Cretaceous of the Antarctic Peninsula. Memoirs of the Queensland Museum 39:583-594.

Gasparini, Z., E. Olivero, R. Scasso, and C. Rinaldi. 1987. Un ankylosaurio campaniano en el continente antarctico. Ciencia Hoy 1:9–10.

Gasulla, J. M., F. Ortega, X. Pereda-Suberbiola, F. Escaso, and J. L. Sanz. 2011. Elementos de la armadura dérmica del dinosaurio anquilosaurio *Polacanthus* Owen, 1865, en el Cretácico Inferior de Morella (Castellón, España). Ameghiniana 48:508–519.

Gilmore, C. W. 1930. On dinosaurian reptiles from the Two Medicine formaton of Montana. Proceedings of the United States National Museum 77:1–39.

Gilmore, C. W. 1933. On the dinosaurian fauna of the Iren Dabasu Formation. Bulletin of the American Museum of Natural History 67:23–78.

Godefroit, P., X. Pereda-Suberbiola, H. Li, and Z.-M. Dong. 1999. A new species of the ankylosaurid dinosaur *Pinacosaurus* from the Late Cretaceous of Inner Mongolia (PR China). Bulletin de l'Institut Royal Des Sciences Naturelles de Belgique, Sciences de La Terre 69:17–36.

Godefroit, P., L. Golovneva, S. Shchepetov, G. Garcia, and P. Alekseev. 2009. The last polar dinosaurs: high diversity of latest Cretaceous arctic dinosaurs in Russia. Naturwissenschaften 96:495–501.

Goloboff, P. A., and S. A. Catalano. 2016. TNT version 1.5, including a full implementation of phylogenetic morphometrics. Cladistics 32:221–238.

Gowland, S., A. M. Taylor, and A. W. Martinius. 2018. Integrated sedimentology and ichnology of Late Jurassic fluvial point-bars–Facies architecture and colonization styles (Lourinha Formation, Lusitanian Basin, western Portugal). Sedimentology 65:400–430.

Grigg, G., and D. Kirshner. 2015. Biology and Evolution of Crocodylians. CSIRO and Cornell University Press, 672 pp.

Grigorescu, D. 2003. Dinosaurs of Romania. Comptes Rendus Palevol 2:97–101.

Guillaume, A. R., M. Moreno-Azanza, E. Puértolas-Pascual, and O. Mateus. 2020. Palaeobiodiversity of crocodylomorphs from the Lourinhã Formation based on the tooth record: insights into the palaeoecology of the Late Jurassic of Portugal. Zoological Journal of the Linnean Society 189:549–583.

Han, F., W. Zheng, D. Hu, X. Xu, and P. M. Barrett. 2014. A new basal ankylosaurid (Dinosauria: Ornithischia) from the Lower Cretaceous Jiufotang Formation of Liaoning Province, China. PloS One 9:e104551.

Haubold, H. 1990. Ein neuer Dinosaurier (Ornithischia, Thyreophora) aus dem unetren Jura des Nördlichen Mitteleuropa. Revue de Paleobiologie 9:149–177.

Hawakaya, H., M. Manabe, and K. Carpenter. 2005. Nodosaurid ankylosaur from the Cenomanian of Japan. Journal of Vertebrate Paleontology 25:240–245.

Hendrickx, C., and O. Mateus. 2014a. *Torvosaurus gurneyi* n. sp., the largest terrestrial predator from Europe, and a proposed terminology of the maxilla anatomy in nonavian theropods. PloS One 9:e88905.

Hendrickx, C., and O. Mateus. 2014b. Abelisauridae (Dinosauria: Theropoda) from the Late Jurassic of Portugal and dentition-based phylogeny as a contribution for the identification of isolated theropod teeth. Zootaxa 3759:1-74.

Hennig, E. 1915. Fossilium Catalogus I: Animalia - Pars 9: Stegosauria. W. Junk, Berlin, 15 pp.

Hieronymus, T. L., L. M. Witmer, D. H. Tanke, and P. J. Currie. 2009. The facial integument of centrosaurine ceratopsids: morphological and histological correlates of novel skin structures. The Anatomical Record: Advances in Integrative Anatomy and Evolutionary Biology: Advances in Integrative Anatomy and Evolutionary Biology 292:1370–1396.

Hill, G. 1988. The sedimentology and lithostratigraphy of the Upper Jurassic Lourinha formation, Lusitanian Basin, Portugal. Open University, 407 pp.

Hill, G. 1989. Distal alluvial fan sediments from the Upper Jurassic of Portugal: controls on their cyclicity and channel formation. Journal of the Geological Society 146:539–555.

Hill, R. V., L. M. Witmer, and M. A. Norell. 2003. A new specimen of *Pinacosaurus grangeri* (Dinosauria, Ornithischia) from the late Cretaceous of Mongolia: ontogeny and phylogeny of ankylosaurs. American Museum Novitates 3395:1-29.

Hill, R. V., M. D. D'Emic, G. Bever, and M. A. Norell. 2015. A complex hyobranchial apparatus in a Cretaceous dinosaur and the antiquity of avian paraglossalia. Zoological Journal of the Linnean Society 175:892–909.

Hornung, J. J., and M. Reich. 2014. *Metatetrapous valdensis* Nopcsa, 1923 and the presence of ankylosaur tracks (Dinosauria: Thyreophora) in the Berriasian (Early Cretaceous) of Northwestern Germany. Ichnos 21:1–18.

Huang, D. 2019. Jurassic integrative stratigraphy and timescale of China. Science China Earth Sciences 62:223–255.

Huene, F. von. 1909. Skizze zu einer Systematik und Stammesgeschichte der Dinosaurier. Zbl. Miner., Geol. u. Palaont 12–22.

Hulke, J. W. 1881. *Polacanthus foxii*, a large undescribed dinosaur from the Wealden formation in the Isle of Wight. Philosophical Transactions of the Royal Society of London 653–662.

Hulke, J. W. 1887. VII. Supplemental note on *Polacanthus foxii*, describing the dorsal shield and some parts of the endoskeleton, imperfectly known in 1881. Philosophical Transactions of the Royal Society of London (B.) 178:169-172.

Huxley, T. H. 1867. On *Acanthopholis horridus*, a New Reptile from the Chalk-marl. Geological Magazine 4:65–67.

Huxley, T. H. 1869. On the classification of the Dinosauria, with observations on the Dinosauria of the Trias. Quarterly Journal of the Geological Society 26:32–51.

Ishigaki, S., M. Watabe, K. Tsogtbaatar, and M. Saneyoshi. 2009. Dinosaur footprints from the Upper Cretaceous of Mongolia. Geological Quarterly 53:449–460.

Jaekel, O. 1910. Über das System der Reptillen. Zeitschrift Für Induktive Abstammungs-Und Vererbungslehre 4:300–301.

Jerzykiewicz, T., P. Currie, D. Eberth, P. Johnston, E. Koster, and J.-J. Zheng. 1993. Djadokhta Formation correlative strata in Chinese Inner Mongolia: an overview of the stratigraphy, sedimentary geology, and paleontology and comparisons with the type locality in the pre-Altai Gobi. Canadian Journal of Earth Sciences 30:2180–2195.

Ji, S., L. Zhang, S. Zhang, L. Zhang, and S. Hang. 2014. Large-Sized Ankylosaur (Dinosauria) from the Lower Cretaceous Jiufotang Formation of Western Liaoning, China. Acta Geologica Sinica-English Edition 88:1060–1065.

Jia, S., J. Lü, L. Xu, W. Hu, J. Li, and J. Zhang. 2010. Discovery and significance of ankylosaur specimens from the Late Cretaceous Qiupa Formation in Luanchuan, Henan, China. Geological Bulletin of China 29:483–487.

Jurcsák, T., and E. Kessler. 1991. The Lower Cretaceous paleofauna from Cornet, Bihor County, Romania. Nymphaea 21:5–32.

Kappus, E. J., S. G. Lucas, and R. Langford. 2011. The Cerro de Cristo Rey Cretaceous dinosaur tracksites, Sunland Park, New Mexico, USA, and Chihuahua, Mexico. Fossil Record 3:272–288.

Kilbourne, B., and K. Carpenter. 2005. Redescription of *Gargoyleosaurus parkpinorum*, a polacanthid ankylosaur from the Upper Jurassic of Albany County, Wyoming. Neues Jahrbuch Für Geologie Und Paläontologie, Abhandlungen 237:111–160.

Kinneer, B., K. Carpenter, and A. Shaw. 2016. Redescription of *Gastonia burgei* (Dinosauria: Ankylosauria, Polacanthidae), and description of a new species. Neues Jahrbuch Für Geologie Und Paläontologie-Abhandlungen 282:37–80.

Kirkland, J. 1998. A polacanthine ankylosaur (Ornithischia: Dinosauria) from the Early Cretaceous (Barremian) of eastern Utah. New Mexico Museum of Natural History and Science Bulletin 14:271–281.

Kirkland, J., M. Suarez, C. Suarez, and R. Hunt-Foster. 2016. The Lower Cretaceous in east-central Utah - the Cedar Mountain Formation and its bounding strata. Geology of the Intermountain West 3:101–228.

Kirkland, J. I., and K. Carpenter. 1994. North America's first pre-Cretaceous ankylosaur (Dinosauria) from the Upper Jurassic Morrison Formation of western Colorado. Brigham Young University Geology Studies 40:25–42.

Kirkland, J. I., K. Carpenter, A. Hunt, and R. D. Scheetz. 1998. Ankylosaur (Dinosauria) specimens from the Upper Jurassic Morrison Formation. Modern Geology 23:145–177.

Kirkland, J. I., L. Alcala, M. A. Loewen, E. Espilez, L. Mampel, and J. P. Wiersma. 2013. The basal nodosaurid ankylosaur *Europelta carbonensis* n. gen., n. sp. from the Lower Cretaceous (Lower Albian) Escucha Formation of Northeastern Spain. PLoS One 8:e80405.

Knoll, F., É. Buffetaut, and B. Dubus. 1998. Un ostéoderme d'ankylosaure (Ornithischia) dans l'Albien de l'Aube (France). Bull. Ann. Assoc. Géol. Auboise 19:61–65.

Kubo, T., W. Zheng, M. O. Kubo, and X. Jin. 2021. Dental microwear of a basal ankylosaurine dinosaur, *Jinyunpelta* and its implication on evolution of chewing mechanism in ankylosaurs. Plos One 16:e0247969.

Kullberg, J. C., R. B. Rocha, A. F. Soares, J. Rey, P. Terrinha, A. C. Azerêdo, P. Callapez, L. V. Duarte, M. C. Kullberg, L. Martins, R. M. Miranda, C. Alves, J. Mata, J. Madeira, O. Mateus, M. Moreira, and C. R. Nogueira. 2013. A Bacia Lusitaniana : estratigrafia, paleogeografia e tectónica; pp. 195–347 in Geologia de Portugal, Vol. II: Geologia Meso-cenozóica de Portugal. Escolar, Lisboa.

Kuzmin, I., I. Petrov, A. Averianov, E. Boitsova, P. Skutschas, and H.-D. Sues. 2020. The braincase of *Bissektipelta archibaldi* - new insights into endocranial osteology, vasculature, and paleoneurobiology of ankylosaurian dinosaurs. Biological Communications 65.

Lambe, L. 1910. Note on the parietal crest of *Centrosaurus apertus* and a proposed new generic name for *Stereocephalus tutus*. Ottawa Naturalist 14:149–151.

Lambe, L. M. 1902. New genera and species from the Belly River Series (mid-Cretaceous). Contributions to Canadian Palaeontology 3:25–81.

Lambe, L. M. 1919. Description of a new genus and species (*Panoplosaurus mirus*) of armored dinosaur from the Belly River Beds of Alberta. Transactions of the Royal Society of Canada 3:39–50.

Lapparent, A. F. de, and G. Zbyszewski. 1951. Un Stégosaurien nouveau dans le Lias du Portugal. Bol. Mus. Lab. Mineral. Geol., Faculdade de Ciências da Universidade de Lisboa:107-108.

Lapparent, A. F., and R. Lavocat. 1955. Dinosauriens; pp. 785–962 in Traité de Paléontologie, Jean Piveteau. vol. 5.

Lapparent, A. F. de, and G. Zbyszewski. 1957. Les dinosauriens du Portugal. Memoires Des Services Géologiques Du Portugal 2:1–63.

Leahey, L. G., and S. W. Salisbury. 2013. First evidence of ankylosaurian dinosaurs (Ornithischia: Thyreophora) from the mid-Cretaceous (late Albian–Cenomanian) Winton Formation of Queensland, Australia. Alcheringa: An Australasian Journal of Palaeontology 37:249–257.

Leahey, L. G., R. E. Molnar, and S. W. Salisbury. 2019. More than *Minmi*: a new Australian ankylosaurian from the Lower Cretaceous (Albian) of Queensland, with implications for understanding global thyreophoran diversity. Journal of Vertebrate Paleontology, Program and Abstracts 139.

Leahey, L. G., R. E. Molnar, K. Carpenter, L. M. Witmer, and S. W. Salisbury. 2015. Cranial osteology of the ankylosaurian dinosaur formerly known as *Minmi* sp. (Ornithischia: Thyreophora) from the Lower Cretaceous Allaru Mudstone of Richmond, Queensland, Australia. PeerJ 3:e1475.

Lee, J. E. 1843. Notice of Saurian Dermal Plates from the Wealden of the Isle of Wight. Annals and Magazine of Natural History 11:5–7.

Lee, Y.-N. 1996. A new nodosaurid ankylosaur (Dinosauria: Ornithischia) from the Paw Paw Formation (late Albian) of Texas. Journal of Vertebrate Paleontology 16:232–245.

Lefeld, J. 1971. Geology of the Djadokhta Formation at Bayn Dzak (Mongolia). Palaeontologia Polonica 25:101–127.

Leidy, J. 1856. Notice of remains of extinct reptiles and fishes, discovered by Dr. FV Hayden in the badlands of the Judith River, Nebraska Territory. Proceedings of the Academy of Natural Sciences of Philadelphia 8:72–73.

Leinfelder, R. R. 1993. A sequence stratigraphic approach to the Upper Jurassic mixed carbonate-siliciclastic succession of the central Lusitanian Basin, Portugal. Profil 119–140.

Leinfelder, R. R., and R. C. L. Wilson. 1999. Third-Order Sequences in an Upper Jurassic Rift-Related Second-Order Sequence, Central Lusitanian Basin, Portugal; pp. 507–525 in P.-C. de Graciansky, J. Hardenbol, T. Jacquin, and P. R. Vail (eds.), Mesozoic and Cenozoic Sequence Stratigraphy of European Basins. vol. 60. SEPM Society for Sedimentary Geology.

Lockley, M. G. 2006. An ankylosaur-dominated dinosaur tracksite in the Cretaceous Dakota Group of Colorado: paleoenvironmental and sequence stratigraphic context. New Mexico Museum of Natural History & Science Bulletin 1.

Lockley, M. G., and G. D. Gierlinski. 2014. Notes on a new ankylosaur track from the Dakota Group (Cretaceous) of northern Colorado. Fossil Footprints of Western North America. New Mexico Museum of Natural History and Science Bulletin 62:301–306.

Loewen, M. A., and J. I. Kirkland. 2013. The evolution and biogeographic distribution of Ankylosauria: new insights from a comprehensive phylogenetic analysis. Journal of Vertebrate Paleontology, Program and Abstracts:163-164.

Loewen, M. A., M. E. Burns, M. A. Getty, J. I. Kirkland, and M. K. Vickaryous. 2013. Review of Late Cretaceous ankylosaurian dinosaurs from the Grand Staircase region, southern Utah. At the Top of the Grand Staircase: The Late Cretaceous of Southern Utah 445–462.

López-Rojas, V., S. Mateus, J. Marinheiro, O. Mateus, and E. Puértolas-Pascual. 2024. A new goniopholidid crocodylomorph from the Late Jurassic of Portugal. Palaeontologia Electronica 27:1–33.

Lü, J., X. Jin, Y. Sheng, Y. Li, G. Wang, and A. Yoichi. 2007. New nodosaurid dinosaur from the Late Cretaceous of Lishui, Zhejiang Province, China. Acta Geologica Sinica-English Edition 81:344–350.

Lucas, F. 1901. A new dinosaur, *Stegosaurus marshi*, from the Lower Cretaceous of South Dakota. Proceedings of the United States National Museum 23:591-592.

Lucas, F. 1902. Paleontological notes. Science 16:435–435.

Lydekker, R. 1889. On the remains and affinities of five genera of Mesozoic reptiles. Quarterly Journal of the Geological Society 45:41–59.

Lydekker, R. 1893. On the jaw of a new carnivorous dinosaur from the Oxford Clay of Peterborough. Quarterly Journal of the Geological Society 49:284–287.

Maidment, S. C. 2010. Stegosauria: a historical review of the body fossil record and phylogenetic relationships. Swiss Journal of Geosciences 103:199–210.

Maidment, S. C. 2023. Diversity through time and space in the Upper Jurassic Morrison Formation, western USA. Journal of Vertebrate Paleontology 43:e2326027.

Maidment, S. C., and L. B. Porro. 2010. Homology of the palpebral and origin of supraorbital ossifications in ornithischian dinosaurs. Lethaia 43:95–111.

Maidment, S. C., G. Wei, and D. B. Norman. 2006. Re-description of the postcranial skeleton of the Middle Jurassic stegosaur *Huayangosaurus taibaii*. Journal of Vertebrate Paleontology 26:944–956.

Maidment, S. C., S. J. Strachan, D. Ouarhache, T. M. Scheyer, E. E. Brown, V. Fernandez, Z. Johanson, T. J. Raven, and P. M. Barrett. 2021. Bizarre dermal armour suggests the first African ankylosaur. Nature Ecology & Evolution 5:1576–1581.

Malafaia, E., F. Ortega, F. Escaso, and B. Silva. 2015. New evidence of *Ceratosaurus* (Dinosauria: Theropoda) from the Late Jurassic of the Lusitanian Basin, Portugal. Historical Biology 27:938–946.

Malafaia, E., P. Mocho, F. Escaso, and F. Ortega. 2020. A new carcharodontosaurian theropod from the Lusitanian Basin: evidence of allosauroid sympatry in the European Late Jurassic. Journal of Vertebrate Paleontology 40:e1768106.

Maleev, E. 1952. [A new ankylosaur from the Upper Cretaceous of Mongolia]. Doklady Akademia Nauk SSSR 87:273–278.

Maleev, E. 1954. [The armored dinosaurs of the Cretaceous Period in Mongolia (family Syrmosauridae)]. Works of the Paleontological Institute of the Academy of Sciences of the USSR 48:142–170.

Maleev, E. 1956. [Armored dinosaurs of the Upper Cretaceous of Mongolia, Family Ankylosauridae]. Works of the Paleontological Institute of the Academy of Sciences of the USSR 62:51–91.

Mallon, J. C., and J. S. Anderson. 2014. The functional and palaeoecological implications of tooth morphology and wear for the megaherbivorous dinosaurs from the Dinosaur Park Formation (upper Campanian) of Alberta, Canada. PloS One 9:e98605.

Mallon, J. C., D. M. Henderson, C. M. McDonough, and W. Loughry. 2018. A "bloat-and-float" taphonomic model best explains the upside-down preservation of ankylosaurs. Palaeogeography, Palaeoclimatology, Palaeoecology 497:117–127.

Mannion, P. D., P. Upchurch, R. N. Barnes, and O. Mateus. 2013. Osteology of the Late Jurassic Portuguese sauropod dinosaur *Lusotitan atalaiensis* (Macronaria) and the evolutionary history of basal titanosauriforms. Zoological Journal of the Linnean Society 168:98–206.

Mannion, P. D., P. Upchurch, D. Schwarz, and O. Wings. 2019. Taxonomic affinities of the putative titanosaurs from the Late Jurassic Tendaguru Formation of Tanzania: phylogenetic and biogeographic implications for eusauropod dinosaur evolution. Zoological Journal of the Linnean Society 185:784-909.

Mantell, G. 1833a. Observations of the remains of the Iguanodon, and other fossil reptiles, of the strata of Tilgate Forest in Sussex. Proceedings of the Geological Society of London 1:410–411.

Mantell, G. A. 1833b. The Geology of the South-East of England. Longman, Rees, Orme, Brown, Green, & Longman, London :, 415 pp.

Mantell, G. A. 1841. Memoir on a portion of the lower jaw of the Iguanodon, and on the remains of the *Hylæosaurus* and other saurians, discovered in the strata of Tilgate Forest, in Sussex. Philosophical Transactions of the Royal Society of London 131–151.

Mantell, G. A. 1849. Additional observations on the osteology of the *Iguanodon* and *Hylæosaurus*. Philosophical Transactions of the Royal Society of London 271–305.

Manuppella, G., M. T. Antunes, J. Pais, M. M. Ramalho, and J. Rey. 1999. Notícia Explicativa da Folha 30-A Lourinhã. Instituto Geológico e Mineiro 1–83.

Marsh, O. C. 1877. A new order of extinct Reptilia (Stegosauria) from the Jurassic of the Rocky Mountains. American Journal of Science 3:513–514.

Marsh, O. C. 1888. Notice of a new genus of Sauropoda and other new dinosaurs from the Potomac Formation. American Journal of Science 3:89–94.

Marsh, O. C. 1889. Notice of gigantic horned Dinosauria from the Cretaceous. American Journal of Science Series 3-38:173–176.

Marsh, O. C. 1890a. Description of new dinosaurian reptiles. American Journal of Science (Series 3) 39:81–86.

Marsh, O. C. 1890b. Additional characters of the Ceratopsidae, with notice of new Cretaceous dinosaurs. American Journal of Science Series 3-39:418–426.

Marsh, O. C. 1895. On the affinities and classification of the dinosaurian reptiles. American Journal of Science Series 3-50:483–498.

Martinius, A. W., and S. Gowland. 2011. Tide-influenced fluvial bedforms and tidal bore deposits (late Jurassic Lourinhã Formation, Lusitanian Basin, Western Portugal). Sedimentology 58:285–324.

Maryańska, T. 1969. Remains of armoured dinosaurs from the uppermost Cretaceous in Nemegt Basin, Gobi Desert. Paleontologica Polonica 21:23-32.

Maryańska, T. 1971. New data on the skull of *Pinacosaurus grangeri* (Ankylosauria). Palaeontologia Polonica 25:45–53.

Maryańska, T. 1977. Ankylosauridae (Dinosauria) from Mongolia. Paleontologica Polonica 37:85–151.

Mateus, I., H. Mateus, M. T. Antunes, O. Mateus, P. Taquet, V. Ribeiro, and G. Manuppella. 1997. Couvée, oeufs et embryons d'un dinosaure théropode du Jurassique supérieur de Lourinhã (Portugal). Comptes Rendus de l'Académie Des Sciences-Series IIA-Earth and Planetary Science 325:71–78.

Mateus, O. 1998. *Lourinhanosaurus antunesi*, a new upper Jurassic allosauroid (Dinosauria: Theropoda) from Lourinhã, Portugal. Memórias Da Academia de Ciências de Lisboa 37:111–124.

Mateus, O. 2006. Late Jurassic dinosaurs from the Morrison Formation (USA), the Lourinha and Alcobaça formations (Portugal), and the Tendaguru Beds (Tanzania): a comparison. New Mexico Museum of Natural History and Science Bulletin 36:223–231.

Mateus, O., and M. T. Antunes. 2001. *Draconyx loureiroi*, a new camptosauridae (Dinosauria, Ornithopoda) from the Late Jurassic of Lourinhã, Portugal. 87:61–73.

Mateus, O., A. Walen, and M. T. Antunes. 2006. The large theropod fauna of the Lourinhã Formation (Portugal) and its similarity to that of the Morrison Formation, with a description of a new species of Allosaurus. Paleontology and Geology of the Upper Jurassic Morrison Formation: Bulletin 36 36:123.

Mateus, O., S. C. Maidment, and N. A. Christiansen. 2009. A new long-necked 'sauropod-mimic'stegosaur and the evolution of the plated dinosaurs. Proceedings of the Royal Society B: Biological Sciences 276:1815–1821.

Mateus, O., P. D. Mannion, and P. Upchurch. 2014. *Zby atlanticus*, a new turiasaurian sauropod (Dinosauria, Eusauropoda) from the Late Jurassic of Portugal. Journal of Vertebrate Paleontology 34:618–634.

Mateus, O., J. Dinis, and P. P. Cunha. 2017. The Lourinhã Formation: the Upper Jurassic to lower most Cretaceous of the Lusitanian Basin, Portugal–landscapes where dinosaurs walked. Ciências Da Terra/Earth Sciences Journal 19:75–97.

McCrea, R. F., M. G. Lockley, and C. A. Meyer. 2001. Global Distribution of Purported Ankylosaur Track Occurrences; pp. 413–454 in The Armored Dinosaurs, Kenneth Carpenter. Indiana University Press.

McDonald, A. T., and D. G. Wolfe. 2018. A new nodosaurid ankylosaur (Dinosauria: Thyreophora) from the Upper Cretaceous Menefee Formation of New Mexico. PeerJ 6:e5435.

Mehl, M. 1936. *Hierosaurus coleii*: a new aquatic dinosaur from the Niobrara Cretaceous of Kansas. Denison University Bulletin Journal of the Scientific Laboratory 31:1–20.

Miles, C. A., and C. J. Miles. 2009. Skull of *Minotaurasaurus ramachandrani*, a new Cretaceous ankylosaur from the Gobi Desert. Current Science (00113891) 96.

Miyashita, T., V. M. Arbour, L. M. Witmer, and P. J. Currie. 2011. The internal cranial morphology of an armoured dinosaur *Euoplocephalus* corroborated by X-ray computed tomographic reconstruction. Journal of Anatomy 219:661–675.

Mocho, P., R. Royo-Torres, and F. Ortega. 2014. Phylogenetic reassessment of *Lourinhasaurus alenquerensis*, a basal Macronaria (Sauropoda) from the Upper Jurassic of Portugal. Zoological Journal of the Linnean Society 170:875–916.

Mocho, P., R. Royo-Torres, and F. Ortega. 2019. A new macronarian sauropod from the Upper Jurassic of Portugal. Journal of Vertebrate Paleontology 39:e1578782.

Mocho, P., R. Royo-Torres, F. Escaso, E. Malafaia, C. de Miguel Chaves, I. Narvaez, A. Perez-Garcia, N. Pimentel, B. C. Silva, and F. Ortega. 2017. Upper Jurassic sauropod record in the Lusitanian Basin (Portugal): geographical and lithostratigraphical distribution. Palaeontologia Electronica 20:27A.

Molnar, R. E. 1980. An ankylosaur (Ornithischia: Reptilia) from the Lower Cretaceous of southern Queensland. Memoirs of the Queensland Museum 20:65–75.

Molnar, R. E. 1996. Preliminary report on a new ankylosaur from the Early Cretaceous, Australia. Memoirs of the Queensland Museum 39:653–668.

Molnar, R. E., and E. Frey. 1987. The paravertebral elements of the Australian ankylosaur *Minmi* (Reptilia: Ornithischia, Cretaceous). Neues Jahrbuch für Geologie und Paläontologie Abhandlungen 175:19-37.

Molnar, R. E., and J. Wiffen. 1994. A Late Cretaceous polar dinosaur fauna from New Zealand. Cretaceous Research 15:689–706.

Molnar, R. E., and H. T. Clifford. 2000. Gut contents of a small ankylosaur. Journal of Vertebrate Paleontology 20:194–196.

Moodie, R. L. 1910. An armored dinosaur from the Cretaceous of Wyoming. Kansas University Science Bulletin 5:257–273.

Mouterde, R., R. Rocha, C. Ruget, and H. Tintant. 1979. Faciès, biostratigraphie et paléogéographie du Jurassic portugais. Ciências Da Terra/Earth Sciences Journal 5:29–52.

Mouterde, R., M. Ramalho, R. Rocha, C. Ruget, and H. Tintant. 1972. Le Jurassique du Portugal. Esquisse stratigraphique et zonale. .

Murray, A., F. Riguetti, and S. Rozadilla. 2019. New ankylosaur (Thyreophora, Ornithischia) remains from the Upper Cretaceous of Patagonia. Journal of South American Earth Sciences 96:102320.

Myers, T. S., N. J. Tabor, and N. A. Rosenau. 2014. Multiproxy approach reveals evidence of highly variable paleoprecipitation in the Upper Jurassic Morrison Formation (western United States). Bulletin 126:1105–1116.

Myers, T. S., N. J. Tabor, L. L. Jacobs, and O. Mateus. 2012a. Palaeoclimate of the Late Jurassic of Portugal: comparison with the western United States. Sedimentology 59:1695–1717.

Myers, T. S., N. J. Tabor, L. L. Jacobs, and O. Mateus. 2012b. Estimating soil pCO2 using paleosol carbonates: implications for the relationship between primary productivity and faunal richness in ancient terrestrial ecosystems. Paleobiology 38:585–604.

Nabavizadeh, A., and D. B. Weishampel. 2016. The predentary bone and its significance in the evolution of feeding mechanisms in ornithischian dinosaurs. The Anatomical Record 299:1358–1388.

Naish, D., and D. M. Martill. 2008. Dinosaurs of Great Britain and the role of the Geological Society of London in their discovery: Ornithischia. Journal of the Geological Society 165:613.

Nessov, L. 1995. Dinozavri severnoj Yevrasii: Novye dannye o sostave kompleksov, ekologii i paleobiogeografii. Institute for Scientific Research on the Earth's Crust, St Petersburg State University, St Petersburg 156.

Nopcsa, F. 1915. Die Dinosaurier der Siebenbürgischen Landesteile Ungarns. Mitteilungen Aus Dem Jahrbuche Der Königlichen Ungarischen Geologischen Reichsanstalt 23:1–26.

Nopcsa, F. 1923a. Die Familien der Reptilien. Fortschritte Der Geologie Und Paläontologie 2:1–210.

Nopcsa, F. 1923b. Notes on British Dinosaurs. Part VI: *Acanthopholis*. Geological Magazine 60:193-199.

Nopcsa, F. 1929. Dinosaurierreste aus Siebenbürgen V. Geologica Hungarica Series Paleontologica 4:1–76.

Nopcsa, F. B. 1902. Notizen über cretacische Dinosaurier. Sitzungsberichte Der Mathematisch-Naturwissenschaftlichen Classe Der Kaiserlichen Akademie Der Wissenschaften 111:93–114.

Nopcsa, F. B. 1905. I.—Notes on British Dinosaurs. Part II: *Polacanthus*. Geological Magazine 2:241–250.

Nopcsa, F. B. 1918. *Leipsanosaurus* n. gen, in neuer thyreophore aus der Gosau. Földtani Közlöny 48:324–328.

Nopcsa, F. B. 1928. Paleontological notes on reptiles. Geologica Hungarica Series Paleontologica 1:1–84.

Norman, D. B. 1984. A systematic reappraisal of the reptile order Ornithischia. Short Papers 1:157–162.

Norman, D. B. 2020a. *Scelidosaurus harrisonii* from the Early Jurassic of Dorset, England: postcranial skeleton. Zoological Journal of the Linnean Society 189:47–157.

Norman, D. B. 2020b. *Scelidosaurus harrisonii* from the Early Jurassic of Dorset, England: cranial anatomy. Zoological Journal of the Linnean Society 188:1–81.

Norman, D. B. 2020c. *Scelidosaurus harrisonii* from the Early Jurassic of Dorset, England: the dermal skeleton. Zoological Journal of the Linnean Society 190:1–53.

Norman, D. B. 2021. *Scelidosaurus harrisonii* (Dinosauria: Ornithischia) from the Early Jurassic of Dorset, England: biology and phylogenetic relationships. Zoological Journal of the Linnean Society 191:1-86.

Norman, D. B., L. M. Witmer, and D. B. Weishampel. 2004a. Basal Thyreophora; pp. 335–342 in The Dinosauria. vol. 2. Univ of California Press.

Norman, D. B., L. M. Witmer, and D. B. Weishampel. 2004b. Basal Ornithischia; pp. 325–334 in The Dinosauria. vol. 2. Univ of California Press.

Olivero, E. B., Z. Gasparini, C. A. Rinaldi, and R. Scasso. 1991. First record of dinosaurs in Antarctica (Upper Cretaceous, James Ross Island): paleogeographical implications. Geological Evolution of Antarctica. Cambridge University Press, Cambridge 617–622.

Organ, C. L. 2006. Biomechanics of ossified tendons in ornithopod dinosaurs. Paleobiology 32(4):652-665.

Osborn, H. F. 1923. Two Lower Cretaceous dinosaurs from Mongolia. American Museum Novitates 95:1–10.

Ősi, A. 2005. *Hungarosaurus tormai*, a new ankylosaur (Dinosauria) from the Upper Cretaceous of Hungary. Journal of Vertebrate Paleontology 25:370–383.

Ősi, A. 2015. The European ankylosaur record: a review. Hantkeniana 10:89–106.

Ősi, A., and L. Makádi. 2009. New remains of *Hungarosaurus tormai* (Ankylosauria, Dinosauria) from the Upper Cretaceous of Hungary: skeletal reconstruction and body mass estimation. Paläontologische Zeitschrift 83:227–245.

Ősi, A., and E. Prondvai. 2013. Sympatry of two ankylosaurs (*Hungarosaurus* and cf. *Struthiosaurus*) in the Santonian of Hungary. Cretaceous Research 44:58–63.

Ősi, A., P. M. Barrett, T. Földes, and R. Tokai. 2014. Wear pattern, dental function, and jaw mechanism in the Late Cretaceous ankylosaur *Hungarosaurus*. The Anatomical Record 297:1165–1180.

Ostrom, J. H. 1970. Stratigraphy and Paleontology of the Cloverly Formation (Lower Cretaceous) of the Bighorn Basin Area, Wyoming and Montana. Yale University Press, New Haven, 234 pp.

Owen, R. 1842. Report on British Fossil Reptiles Pt. II. Report of the British Association for the Advancement of Science 1841:60–204.

Owen, R. 1858. Monograph on the fossil Reptilia of the Wealden and Purbeck formations—part IV. Dinosauria (*Hylaeosaurus*). Paleontographical Society Monograph 10:1–26.

Owen, R. 1861. A monograph of a fossil dinosaur (*Scelidosaurus harrisonii*, Owen) of the Lower Lias. Part II. Monographs on the British Fossil Reptilia from the Oolitic Formations, Part II 1–26.

Pais, J. 1998. Jurassic plant macroremains from Portugal. Mem. Acad. Ciências de Lisboa 37:25–47.

Pang, Q., and Z. Cheng. 1998. A new ankylosaur of Late Cretaceous from Tianzhen, Shanxi. Progress in Natural Science 8:326–334.

Parish, J. C. 2005. The Evolution and Palaeobiology of the Armoured Dinosaurs (Ornithischia: Ankylosauria). Ph.D. dissertation, University of Oxford, 478 pp.

Parish, J. C., and P. M. Barrett. 2004. A reappraisal of the ornithischian dinosaur *Amtosaurus magnus* Kurzanov and Tumanova 1978, with comments on the status of *A. archibaldi* Averianov 2002. Canadian Journal of Earth Sciences 41:299–306.

Park, J.-Y., Y.-N. Lee, P. J. Currie, Y. Kobayashi, E. Koppelhus, R. Barsbold, O. Mateus, S. Lee, and S.-H. Kim. 2020. Additional skulls of *Talarurus plicatospineus* (Dinosauria: Ankylosauridae) and implications for paleobiogeography and paleoecology of armored dinosaurs. Cretaceous Research 108:104340.

Park, J.-Y., Y.-N. Lee, Y. Kobayashi, L. L. Jacobs, R. Barsbold, H.-J. Lee, N. Kim, K.-Y. Song, and M. J. Polcyn. 2021. A new ankylosaurid from the Upper Cretaceous Nemegt Formation of Mongolia and implications for paleoecology of armoured dinosaurs. Scientific Reports 11:1–14.

Parks, W. A. 1924. *Dyoplosaurus acutosquameus*: a new genus and species of armoured dinosaur; and notes on a skeleton of *Prosaurolophus maximus*. Univ. Library, Toronto, 35 pp.

Parsons, W. L., and K. M. Parsons. 2009. A new ankylosaur (Dinosauria: Ankylosauria) from the Lower Cretaceous Cloverly Formation of central Montana. Canadian Journal of Earth Sciences 46:721–738.

Paulina-Carabajal, A., Y.-N. Lee, and L. J. Jacobs. 2016. Endocranial morphology of the primitive nodosaurid dinosaur *Pawpawsaurus campbelli* from the Early Cretaceous of North America. PLoS One 11(3): e0150845.

Paulina-Carabajal, A., Y.-N. Lee, Y. Kobayashi, H.-J. Lee, and P. J. Currie. 2018. Neuroanatomy of the ankylosaurid dinosaurs *Tarchia teresae* and *Talarurus plicatospineus* from the Upper Cretaceous of Mongolia, with comments on endocranial variability among ankylosaurs. Palaeogeography, Palaeoclimatology, Palaeoecology 494:135–146.

Penkalski, P. 2001. Variation in specimens referred to *Euoplocephalus tutus*; pp. 363–385 in The Armored Dinosaurs, Kenneth Carpenter. Indiana University Press, Bloomington and Indianapolis, Indiana, USA.

Penkalski, P. 2013. A new ankylosaurid from the Late Cretaceous Two Medicine Formation of Montana, USA. Acta Palaeontologica Polonica 59:617–634.

Penkalski, P. 2018. Revised systematics of the armoured dinosaur *Euoplocephalus* and its allies. Neues Jahrbuch für Geologie und Paläontologie, Abhandlungen 261–306.

Penkalski, P., and T. Tumanova. 2017. The cranial morphology and taxonomic status of *Tarchia* (Dinosauria: Ankylosauridae) from the Upper Cretaceous of Mongolia. Cretaceous Research 70:117–127.

Perales-Gogenola, L., J. Elorza, J. I. Canudo, and X. Pereda-Suberbiola. 2019. Taphonomy and palaeohistology of ornithischian dinosaur remains from the Lower Cretaceous bonebed of La Cantalera (Teruel, Spain). Cretaceous Research 98:316–334.

Pereda-Suberbiola, X. 1993. *Hylaeosaurus*, *Polacanthus*, and the systematics and stratigraphy of Wealden armoured dinosaurs. Geological Magazine 130:767–781.

Pereda-Suberbiola, X. 1999. Ankylosaurian dinosaur remains from the Upper Cretaceous of Laño (Iberian Peninsula). Estudios Del Museo de Ciencias Naturales de Alava 14:273–288.

Pereda-Suberbiola, X., and P. M. Barrett. 1999. A systematic review of ankylosaurian dinosaur remains from the Albian-Cenomanian of England. Special Papers in Palaeontology 60:177–208.

Pereda-Suberbiola, X., and P. M. Galton. 1999. Thyreophoran ornithischian dinosaurs from the Iberian Peninsula. 147–162.

Pereda-Suberbiola, X., and J. I. Ruiz-Omeñaca. 2005. Los primeros descubrimientos de dinosaurios en España. Spanish Journal of Palaeontology 20:15–28.

Pereda-Suberbiola, X. P., P. Dantas, P. M. Galton, and J. L. Sanz. 2005. Autopodium of the holotype of *Dracopelta zbyszewskii* (Dinosauria, Ankylosauria) and its type horizon and locality (Upper Jurassic: Tithonian, western Portugal). Neues Jahrbuch Für Geologie Und Paläontologie-Abhandlungen 175–196.

Pereda-Suberbiola, X., C. Fuentes, M. Meijide, F. Meijide-Fuentes, and M. Meijide-Fuentes Jr. 2007. New remains of the ankylosaurian dinosaur *Polacanthus* from the Lower Cretaceous of Soria, Spain. Cretaceous Research 28:583–596.

Pereda-Suberbiola, X., J. I. Ruiz-Omeñaca, J. I. Canudo, F. Torcida, and J. L. Sanz. 2012. Dinosaur faunas from the Early Cretaceous (Valanginian-Albian) of Spain; pp. 379–407 in Bernissart Dinosaurs and Early Cretaceous Terrestrial Ecosystem. Indiana University Press Bloomington.

Pereda-Suberbiola, X., M. Meijide, F. Torcida, J. Welle, C. Fuentes, L. Izquierdo, D. Montero, G. Pérez, and V. Urién. 1999. Espinas dérmicas del dinosaurio anquilosaurio *Polacanthus* en las facies Weald de Salas de los Infantes (Burgos, España). Estudios Geológicos 55:267–272.

Pérez-García, A., and F. Ortega. 2011. *Selenemys lusitanica*, gen. et sp. nov., a new pleurosternid turtle (Testudines: Paracryptodira) from the Upper Jurassic of Portugal. Journal of Vertebrate Paleontology 31:60–69.

Petti, F. M., S. D. Porchetti, E. Sacchi, and U. Nicosia. 2010. A new purported ankylosaur trackway in the Lower Cretaceous (lower Aptian) shallow-marine carbonate deposits of Puglia, southern Italy. Cretaceous Research 31:546–552.

Pond, S., S.-J. Strachan, T. J. Raven, M. I. Simpson, K. Morgan, and S. C. Maidment. 2023. *Vectipelta barretti*, a new ankylosaurian dinosaur from the Lower Cretaceous Wessex Formation of the Isle of Wight, UK. Journal of Systematic Palaeontology 21:2210577.

Puértolas-Pascual, E., and O. Mateus. 2020. A three-dimensional skeleton of Goniopholididae from the Late Jurassic of Portugal: implications for the Crocodylomorpha bracing system. Zoological Journal of the Linnean Society 189:521–548.

Rasmussen, E. S., S. Lomholt, C. Andersen, and O. V. Vejbæk. 1998. Aspects of the structural evolution of the Lusitanian Basin in Portugal and the shelf and slope area offshore Portugal. Tectonophysics 300:199–225.

Rauhut, O. W. M., T. Hübner, and K.-P. Lanser. 2016. A new megalosaurid theropod dinosaur from the late Middle Jurassic (Callovian) of north-western Germany: implications for theropod evolution and faunal turnover in the Jurassic. Palaeontologia Electronica 19.2.26A:1-65

Raven, T. J. 2021. The Taxonomic, Phylogenetic, Biogeographic and Macroevolutionary History of the Armoured Dinosaurs (Ornithischia: Thyreophora). University of Brighton, 658 pp.

Raven, T. J., P. M. Barrett, S. B. Pond, and S. C. Maidment. 2020. Osteology and Taxonomy of British Wealden Supergroup (Berriasian–Aptian) Ankylosaurs (Ornithischia, Ankylosauria). Journal of Vertebrate Paleontology 40:e1826956.

Raven, T. J., P. M. Barrett, C. B. Joyce, and S. C. R. Maidment. 2023. The phylogenetic relationships and evolutionary history of the armoured dinosaurs (Ornithischia: Thyreophora). Journal of Systematic Palaeontology 21:2205433.

Ravnås, R., J. Windelstad, D. Mellere, A. Nøttvedt, T. Stuhr Sjøblom, R. J. Steel, and R. C. L. Wilson. 1997. A marine Late Jurassic syn-rift succession in the Lusitanian Basin, western Portugal — tectonic significance of stratigraphic signature. Sedimentary Geology 114:237–266.

Riabinin, A. 1939. The Upper Cretaceous vertebrate fauna of South Kazakhstan. I. Reptilia. Part. 1. Ornithischia. Trudy Tsentral'nogo Nauchno-Issledovatel'skogo Geologo-Razvedochnogo Instituta 118:3–39.

Ribeiro, V., O. Mateus, F. Holwerda, R. Araújo, and R. Castanhinha. 2014. Two new theropod egg sites from the Late Jurassic Lourinhã Formation, Portugal. Historical Biology 26:206–217.

Ricqlès, A. de, X. P. Suberbiola, Z. Gasparini, and E. Olivero. 2001. Histology of dermal ossifications in an ankylosaurian dinosaur from the Late Cretaceous of Antarctica. Publicación Electrónica de La Asociación Paleontológica Argentina 7.

Riguetti, F., X. Pereda-Suberbiola, D. Ponce, L. Salgado, S. Apesteguía, S. Rozadilla, and V. Arbour. 2022. A new small-bodied ankylosaurian dinosaur from the Upper Cretaceous of North Patagonia (Río Negro Province, Argentina). Journal of Systematic Palaeontology 20:2137441.

Rivera-Sylva, H. E., and B. Espinosa-Chávez. 2006. Ankylosaurid (Dinosauria: Thyreophora) osteoderms from the Upper Cretaceous Cerro del Pueblo Formation of Coahuila, Mexico. Carnets de Géologie.

Rivera-Sylva, H. E., K. Carpenter, and F. J. Aranda-Manteca. 2011. Late Cretaceous nodosaurids (Ankylosauria: Ornithischia) from Mexico. Revista Mexicana de Ciencias Geológicas 28:371–378.

Rivera-Sylva, H. E., E. Frey, W. Stinnesbeck, G. Carbot-Chanona, I. E. Sanchez-Uribe, and J. R. Guzmán-Gutiérrez. 2018. Paleodiversity of Late Cretaceous Ankylosauria from Mexico and their phylogenetic significance. Swiss Journal of Palaeontology 137:83–93.

Rodríguez-de la Rosa, R. A., M. P. Velasco-de León, J. Arellano-Gil, and D. E. Lozano-Carmona. 2018. Middle Jurassic ankylosaur tracks from Mexico. Boletín de La Sociedad Geológica Mexicana 70:379–395.

Romer, A. 1956. Osteology of the Reptiles. University of Chicago Press, Chicago, 772 pp.

Romer, A. S. 1927. The pelvic musculature of ornitischian dinosaurs. Acta Zoologica 8:225–275.

Rotatori, F. M., M. Moreno-Azanza, and O. Mateus. 2020. New information on ornithopod dinosaurs from the Late Jurassic of Portugal. Acta Palaeontologica Polonica 65.

Rotatori, F. M., M. Moreno-Azanza, and O. Mateus. 2022. Reappraisal and new material of the holotype of *Draconyx loureiroi* (Ornithischia: Iguanodontia) provide insights on the tempo and modo of evolution of thumb-spiked dinosaurs. Zoological Journal of the Linnean Society 195:125–156.

Rotatori, F. M., L. Ferrari, C. Sequero, B. Camilo, O. Mateus, and M. Moreno-Azanza. 2024. An unexpected early-diverging iguanodontian dinosaur (Ornithischia, Ornithopoda) from the Upper Jurassic of Portugal. Journal of Vertebrate Paleontology:e2310066.

Russell, D., D. Russell, P. Taquet, and H. Thomas. 1976. New collections of vertebrates in the Upper Cretaceous continental terrains of the Majunga region (Madagascar). Comptes Rendus de La Société Geologique de France 5:205–208.

Russell, L. S. 1940. *Edmontonia rugosidens* (Gilmore): An Armoured Dinosaur from the Belly River Series of Alberta. University of Toronto Studies, Geology Series 43:3-28.

Russo, J., and O. Mateus. 2019. A new ankylosaur dinosaur skeleton from the Upper Jurassic of Portugal. Journal of Vertebrate Paleontology, Program and Abstracts 184.

Russo, J., and O. Mateus. 2021. History of the discovery of the ankylosaur *Dracopelta zbyszewskii* (Upper Jurassic), with new data about the type specimen and its locality. Comunicações Geológicas 108:27–34.

Russo, J., O. Mateus, M. Marzola, and A. Balbino. 2017. Two new ootaxa from the Late Jurassic: The oldest record of crocodylomorph eggs, from the Lourinhã Formation, Portugal. PloS One 12:e0171919.

Sacchi, E., M. A. Conti, S. D. Porchetti, A. Logoluso, U. Nicosia, G. Perugini, and F. M. Petti. 2009. Aptian dinosaur footprints from the Apulian platform (Bisceglie, Southern Italy) in the framework of periadriatic ichnosites. Palaeogeography, Palaeoclimatology, Palaeoecology 271:104–116.

Sachs, S., and J. J. Hornung. 2013. Ankylosaur remains from the Early Cretaceous (Valanginian) of northwestern Germany. PloS One 8:e60571.

Salgado, L., and R. A. Coria. 1996. First evidence of an ankylosaur (Dinosauria, Ornithischia) in South America. Ameghiniana 33:367–371.

Salgado, L., and Z. Gasparini. 2006. Reappraisal of an ankylosaurian dinosaur from the Upper Cretaceous of James Ross Island (Antarctica). Geodiversitas 28:119–135.

Salisbury, S. W., and E. Frey. 2001. A biomechanical transformation model for the evolution of semi-spheroidal articulations between adjoining vertebral bodies in crocodilians; pp. 85–134 in Crocodilian Biology and Evolution. Surrey Beatty & Sons, Chipping Norton, NSW.

Saporta, G. de, and P. Choffat. 1894. Flore Fossile Du Portugal: Nouvelles Contributions à La Flore Mésozoïque. Direction des Travaux Géologiques du Portugal, 288 pp.

Sauvage, H. É. 1898. Vertébrés Fossiles Du Portugal: Contributions à l'étude Des Poissons et Des Reptiles Du Jurassique et Du Crétacique. Direction des Travaux Géologiques du Portugal, 103 pp.

Scheyer, T. M., and P. M. Sander. 2004. Histology of ankylosaur osteoderms: implications for systematics and function. Journal of Vertebrate Paleontology 24:874–893.

Schneider, S., F. T. Fürsich, and W. Werner. 2009. Sr-isotope stratigraphy of the Upper Jurassic of central Portugal (Lusitanian Basin) based on oyster shells. International Journal of Earth Sciences 98:1949–1970.

Schneider, S., F. T. Fürsich, and W. Werner. 2010. Marking the Kimmeridgian-Tithonian transition with a bivalve - *Protocardia gigantea* sp. nov. (Bivalvia: Cardiidae) and its relatives from the Lusitanian Basin (Portugal). Neues Jahrbuch Fur Geologie Und Palaontologie-Abhandlungen 258:167.

Schwarz, D. 2002. A new species of *Goniopholis* from the Upper Jurassic of Portugal. Palaeontology 45:185–208.

Seeley, H.G. 1869. Index to the Fossil Remains of Aves, Ornithosauria, and Reptilia, from the Secondary System of Strata Arranged in the Woodwardian Museum of the University of Cambridge. Deighton, Bell, and Company, Cambridge, 143 pp.

Seeley, H. 1879. On the dinosauria of the Cambridge Greensand. Quarterly Journal of the Geological Society 35:591–636.

Seeley, H. G. 1875. On the maxillary bone of a new dinosaur (*Priodontognathus phillipsii*), contained in the Woodwardian Museum of the University of Cambridge. Quarterly Journal of the Geological Society 31:439–443.

Seeley, H. G. 1881. The Reptile Fauna of the Gosau Formation preserved in the Geological Museum of the University of Vienna: With a Note on the Geological Horizon of the Fossils at Neue Welt, west of Wiener Neustadt, by Edw. Suess, Ph. D., FMGS, &c., Professor of Geology in the University of Vienna, &c. Quarterly Journal of the Geological Society 37:620–706.

Sereno, P. C. 1984. The phylogeny of the Ornithischia: a reappraisal. Third Symposium on Mesozoic Terrestrial Ecosystems, Short Papers 1:219–226.

Sereno, P. C. 1986. Phylogeny of the bird-hipped dinosaurs (Order Ornithischia). National Geographic Research 2:234–256.

Sereno, P. C. 1991. *Lesothosaurus*, "Fabrosaurids," and the early evolution of Ornithischia. Journal of Vertebrate Paleontology 11:168–197.

Sereno, P. C. 1998. A rationale for phylogenetic definitions, with application to the higher-level taxonomy of Dinosauria. Neues Jahrbuch Für Geologie Und Paläontologie-Abhandlungen 41–83.

Sereno, P. C. 1999. The evolution of dinosaurs. Science 284:2137-2147.

Shuvalov, V. 1974. On geology and age of Khobur and Khuren-Dukh localities in Mongolia. Mesozoic and cenozoic faunas and biostratigraphy of Mongolia. M., Nauk 296:3–4.

Soto Acuña, S., A. O. Vargas, and J. E. Kaluza. 2024. A new look at the first dinosaur discovered in Antarctica: reappraisal of *Antarctopelta oliveroi* (Ankylosauria: Parankylosauria). Advances in Polar Science 35:78–107.

Soto-Acuña, S., A. O. Vargas, J. Kaluza, M. A. Leppe, J. F. Botelho, J. Palma-Liberona, C. Simon-Gutstein, R. A. Fernández, H. Ortiz, and V. Milla. 2021. Bizarre tail

weaponry in a transitional ankylosaur from subantarctic Chile. Nature 600:259–263.

Stanford, R., D. B. Weishampel, and V. B. Deleon. 2011. The first hatchling dinosaur reported from the eastern United States: Propanoplosaurus marylandicus (Dinosauria: Ankylosauria) from the Early Cretaceous of Maryland, USA. Journal of Paleontology 85:916–924.

Stein, M., S. Hayashi, and P. M. Sander. 2013. Long bone histology and growth patterns in ankylosaurs: implications for life history and evolution. PLoS One 8:e68590.

Sternberg, C. M. 1921. A supplementary study of *Panoplosaurus mirus*. Transactions of the Royal Society of Canada 3:93-102.

Sternberg, C. M. 1928. A new armored dinosaur from the Edmonton Formation of Alberta. Royal Society of Canada Transactions 22:93–106.

Sternberg, C. M. 1929. A toothless armored dinosaur from the Upper Cretaceous of Alberta. Bulletin of the National Museum of Canada 54:28–33.

Sternberg, C. M. 1933. XXIX.—Relationships and habitat of *Troodon* and the Nodosaurs. Annals and Magazine of Natural History 11:231–235.

Sternberg, C. M. 1932. Dinosaur tracks from Peace River, British Columbia; pp. 59–85 in Annual Report of the National Museum of Canada.

Sternberg, C. M. 1970. Comments on Dinosaurian Preservation in the Cretaceous of Alberta and Wyoming. National Museums of Canada, National Museum of Natural Sciences, Ottawa, 1–9 pp.

Sullivan, R. M. 1999. *Nodocephalosaurus kirtlandensis*, gen. et sp. nov., a new ankylosaurid dinosaur (Ornithischia: Ankylosauria) from the Upper Cretaceous Kirtland Formation (Upper Campanian), San Juan Basin, New Mexico. Journal of Vertebrate Paleontology 19:126–139.

Tang, F., Z.-X. Luo, Z.-H. Zhou, H.-L. You, J. Georgi, Z.-L. Tang, and X.-Z. Wang. 2001. Biostratigraphy and palaeoenvironment of the dinosaur-bearing

sediments in Lower Cretaceous of Mazongshan area, Gansu Province, China. Cretaceous Research 22:115–129.

Taylor, A. M., S. Gowland, S. Leary, K. J. Keogh, and A. W. Martinius. 2014. Stratigraphical correlation of the Late Jurassic Lourinhã Formation in the Consolação Sub-basin (Lusitanian Basin), Portugal. Geological Journal 49:143–162.

Thompson, R. S., J. C. Parish, S. C. Maidment, and P. M. Barrett. 2012. Phylogeny of the ankylosaurian dinosaurs (Ornithischia: Thyreophora). Journal of Systematic Palaeontology 10:301–312.

Tremaine, K., M. D. D'Emic, S. Williams., R. K. Hunt-Foster, J. Foster, and J. Mathews. 2015. Paleoecological implications of a new specimen of the ankylosaur *Mymoorapelta maysi* from the Hanksville-Burpee Quarry, latest Jurassic (Tithonian) Morrison Formation (Brushy Basin Member). Journal of Vertebrate Paleontology, Program and Abstracts 226.

Tschopp, E., O. Mateus, and R. B. Benson. 2015. A specimen-level phylogenetic analysis and taxonomic revision of Diplodocidae (Dinosauria, Sauropoda). PeerJ 3:e857.

Tumanova, T. 1977. New data on the ankylosaur Tarchia gigantea. Paleontological Zhurnal 4:92–100.

Tumanova, T. 1983. [The first ankylosaur from the Lower Cretaceous of Mongolia]. The Joint Soviet-Mongolian Palaeontological Expedition Transaction 24:110–120.

Tumanova, T. 1986. Skull morphology of the ankylosaur *Shamosaurus scutatus* from the Lower Cretaceous of Mongolia. 73–79.

Tumanova, T. 1987. [The armored dinosaurs of Mongolia]. The Joint Soviet-Mongolian Palaeontological Expedition Transaction 32:1–76.

Tumanova, T. 1993. [On A New Armored Dinosaur from Southeastern Gobi]. Paleontologicheskii Zhurnal 92.

Vickaryous, M. K. 2001. Skull morphology of the Ankylosauria. Ph.D. dissertation, University of Calgary, 287 pp.

Vickaryous, M. K., and A. P. Russell. 2002. A redescription of the skull of Euoplocephalus tutus (Archosauria: Ornithischia): a foundation for comparative and systematic studies of ankylosaurian dinosaurs. Zoological Journal of the Linnean Society 137:157–186.

Vickaryous, M. K., T. Maryańska, and D. B. Weishampel. 2004. Ankylosauria; pp. 363–392 in The Dinosauria: Second Edition. University of California Press.

Vickaryous, M. K., A. P. Russell, P. J. Currie, and X.-J. Zhao. 2001. A new ankylosaurid (Dinosauria: Ankylosauria) from the Lower Cretaceous of China, with comments on ankylosaurian relationships. Canadian Journal of Earth Sciences 38:1767–1780.

Vila, B., A. Sellés, M. Moreno-Azanza, N. L. Razzolini, A. Gil-Delgado, J. I. Canudo, and À. Galobart. 2022. A titanosaurian sauropod with Gondwanan affinities in the latest Cretaceous of Europe. Nature Ecology & Evolution 6:288–296.

Vullo, R., D. Neraudeau, and T. Lenglet. 2007. Dinosaur teeth from the Cenomanian of Charentes, western France: evidence for a mixed Laurasian-Gondwanan assemblage. Journal of Vertebrate Paleontology 27:931–943.

Wang, K., Y. Zhang, J. Chen, S. Chen, and P. Wang. 2020. A new ankylosaurian from the Late Cretaceous strata of Zhucheng, Shandong Province. Geological Bulletin of China 39:958–962.

Ward, L. F. 1985. The Mesozoic flora of Portugal compared with that of the United States. Science 1:337-346.

Wieland, G. R. 1909. A new armored saurian from the Niobrara. American Journal of Science (1880-1910) 27:250.

Wieland, G. R. 1911. Notes on the armored Dinosauria. American Journal of Science 112–124.

Wiersma, J. P. 2016. The evolution and biogeography of ankylosaurid dinosaurs from the Late Cretaceous of Western North America. Master Thesis, The University of Utah, 419 pp.

Wiersma, J. P., and R. B. Irmis. 2018. A new southern Laramidian ankylosaurid, *Akainacephalus johnsoni* gen. et sp. nov., from the upper Campanian Kaiparowits Formation of southern Utah, USA. PeerJ 6:e5016.

Williston, S. 1905. A new armored dinosaur from the Upper Cretaceous of Wyoming. Science 22:503–504.

Wilson, R. C. 1979. A reconnaissance study of Upper Jurassic sediments of the Lusitanian Basin. Ciências Da Terra/Earth Sciences Journal 5:53–84.

Wilson, R. C. 1988. Mesozoic development of the Lusitanian Basin, Portugal. Revista de La Sociedad Geológica de España 1:393–407.

Wilson, J. A., M. D. D'Emic, T. Ikejiri, E. M. Moacdieh, and J. A. Whitlock. 2011. A nomenclature for vertebral fossae in sauropods and other saurischian dinosaurs. PLoS One 6: e17114

Xiaobo, L., and R. Reisz. 2019. The Early Cretaceous ankylosaur *Liaoningosaurus* from Western Liaoning, China: progress and problems. 7th Annual Meeting of the Canadian Society of Vertebrate Palaeontology Abstracts 31.

Xu, X., X.-L. Wang, and H.-L. You. 2001. A juvenile ankylosaur from China. Naturwissenschaften 88:297–300.

Xu, X., J. Lü, Z. Xingliao, S. Jia, W. Hu, Z. Jiming, W. Yanhua, and J. Qiang. 2007. New nodosaurid ankylosaur from the Cretaceous of Ruyang, Henan Province. Acta Geologica Sinica 81:433–440.

Yang, J., H. You, D. Li, and D. Kong. 2013. First discovery of polacanthine ankylosaur dinosaur in Asia. Vertebrata PalAsiatica 51:265–277.

Yao, X., P. M. Barrett, L. Yang, X. Xu, and S. Bi. 2022. A new early branching armored dinosaur from the Lower Jurassic of southwestern China. eLife 11:e75248.

Yoshida, J., Y. Kobayashi, and M. A. Norell. 2023. An ankylosaur larynx provides insights for bird-like vocalization in non-avian dinosaurs. Communications Biology 6:152.

Young, C. C. 1935. On a new nodosaurid from Ninghsia. Palaeontologia Sinica 11:1–34.

Zheng, W. 2018. New ankylosaurid from the Cretaceous of China and the early evolution of Ankylosauridae. Ph.D. dissertation, University of Chinese Academy of Sciences, 290 pp

Zheng, W., X. Jin, Y. Azuma, Q. Wang, K. Miyata, and X. Xu. 2018. The most basal ankylosaurine dinosaur from the Albian–Cenomanian of China, with implications for the evolution of the tail club. Scientific Reports 8:3711.

Zhiming, D. 1993. An ankylosaur (ornithischian dinosaur) from the Middle Jurassic of the Junggar Basin, China. Vertebrata PalAsiatica 257–266.

Zhiming, D. 2002. A new armored dinosaur (Ankylosauria) from Beipiao Basin, Liaoning Province, northeastern China. Vertebrata Pal Asiatica 40:276–285.

Appendixes

Appendix 1. Assorted fragmentary material from NOVA-FCT-DCT-5556. Scale bars: 2 cm.

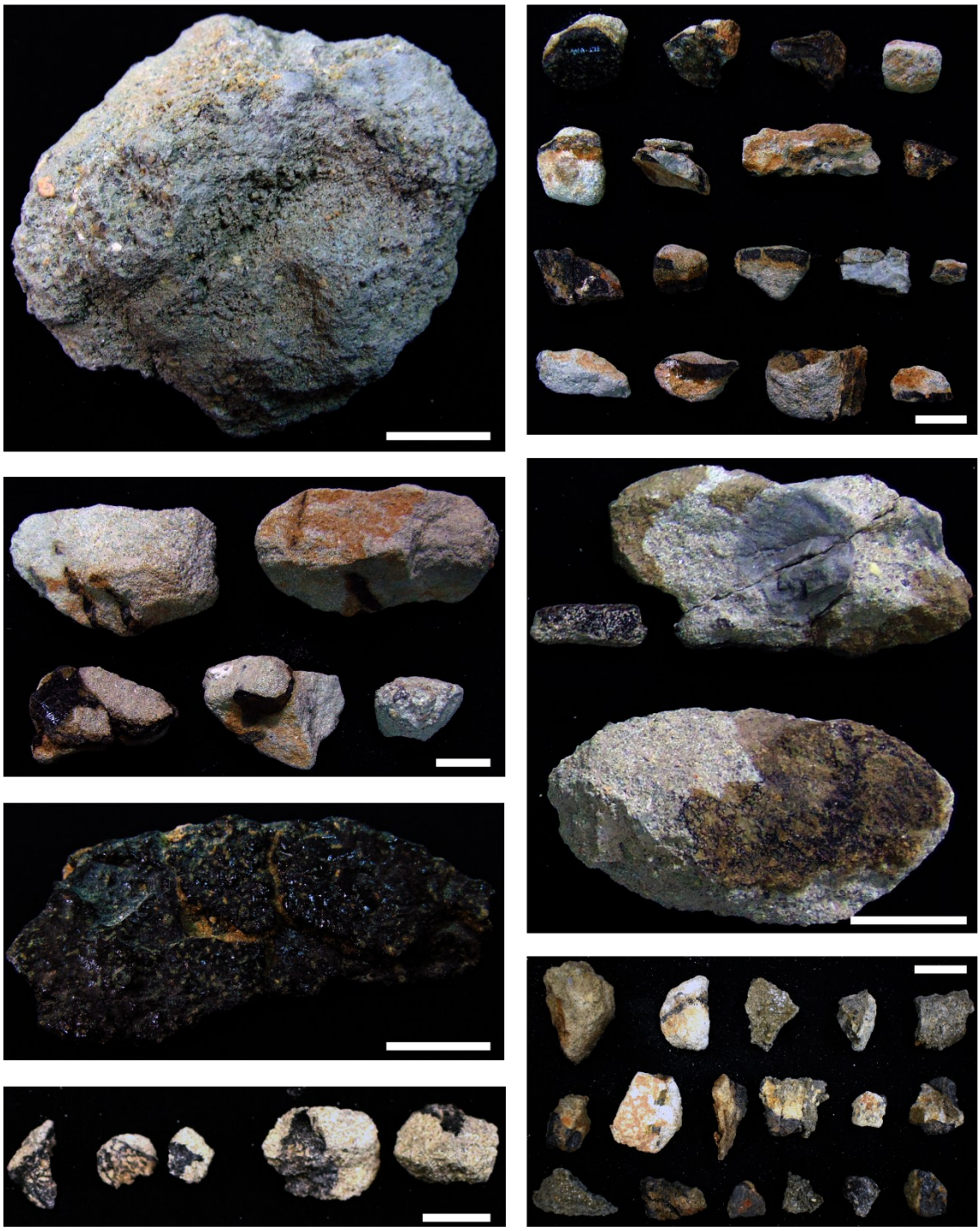

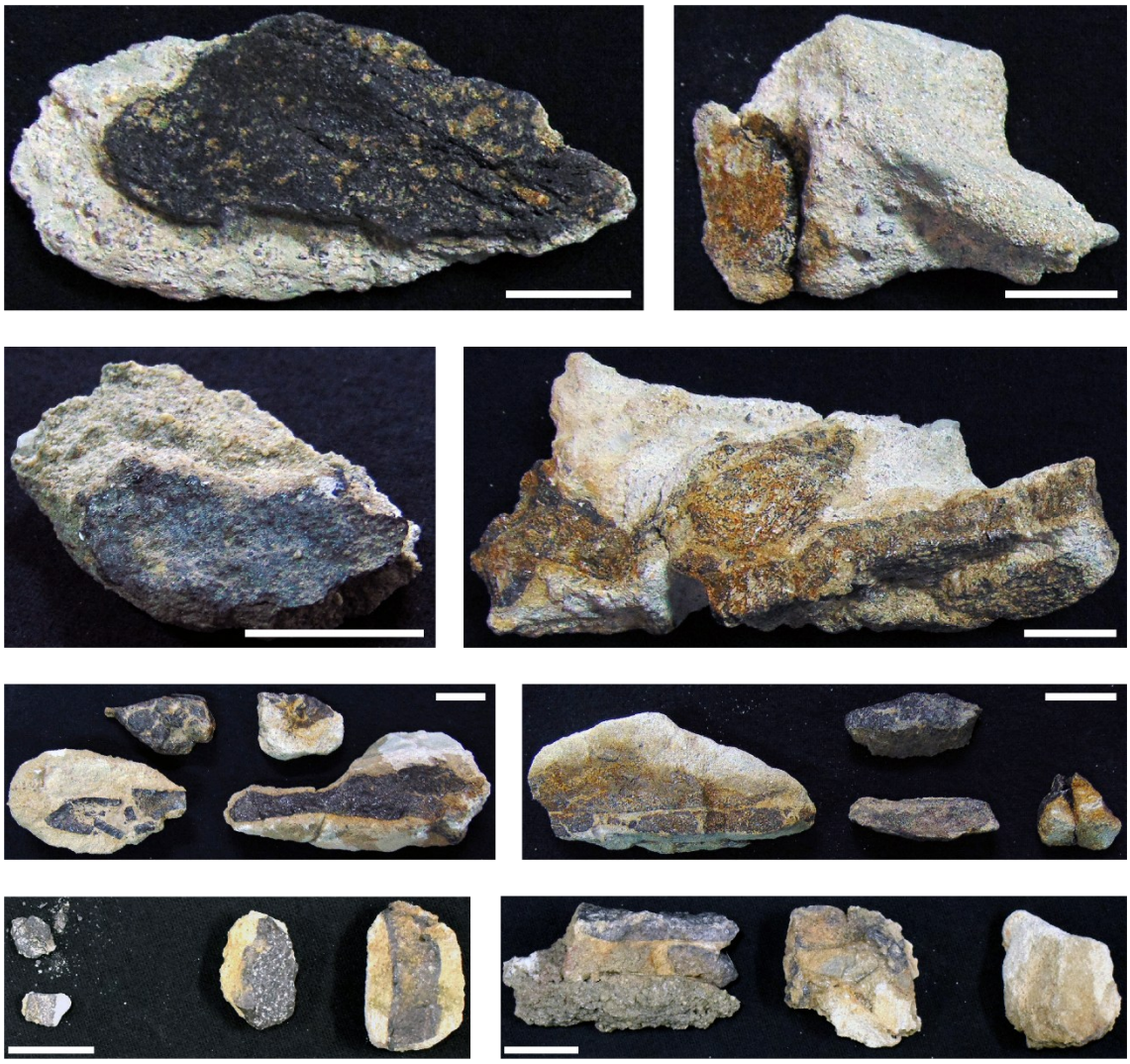

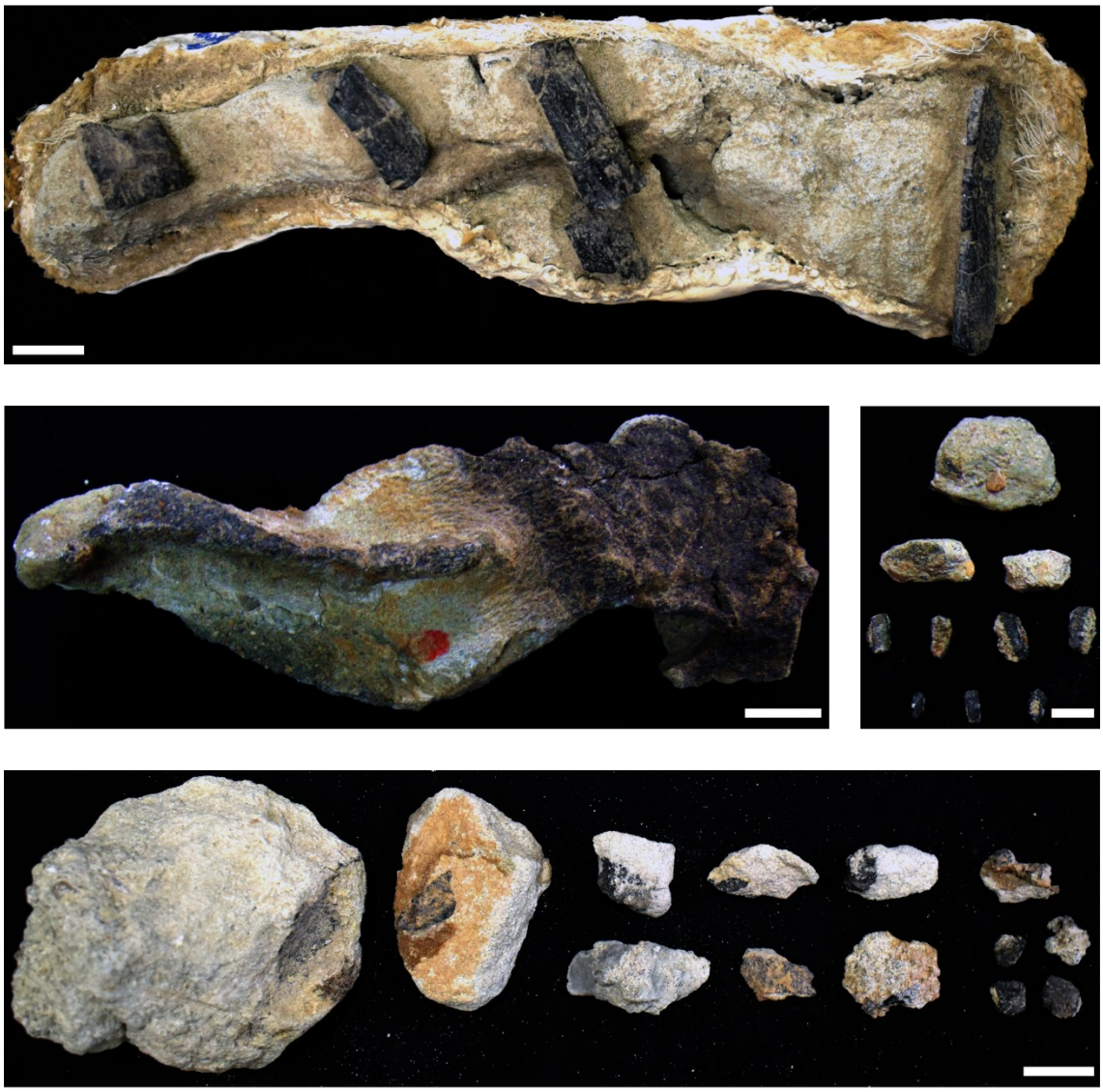

Appendix 2. NEXUS file of the data matrix used in this work. DPF, HCF, and TMF next to some taxa (e.g., *Edmontonia_longiceps*_TMF) stand for Dinosaur Park Formation, Horseshoe Canyon Formation, and Two Medicine Formation, respectively.

BEGIN TAXA;

TITLE Taxa;

DIMENSIONS NTAX=95;

TAXLABELS

Lesothosaurus_diagnosticus

Scutellosaurus_lawleri

Emausaurus_ernsti

Tatisaurus_oehleri

Tuojiangosaurus_multispinus

Chungkingosaurus_jiangbeiensis

Huayangosaurus_taibaii

Gigantspinosaurus_sichuanensis

Regnosaurus_northamptoni

Loricatosaurus_priscus

Kentrosaurus_aethiopicus

Dacentrurus_armatus

Miragaia_longicollum

Miragaia_longispinus

Wuerhosaurus_homheni

Hesperosaurus_mjosi

Stegosaurus_stenops

Scelidosaurus_harrisonii

Bienosaurus_lufengensis

Sarcolestes_leedsi

Minmi_paravertebra

Kunbarrasaurus_ieversi

Tianchisaurus_nedegoapeferima

Liaoningosaurus_paradoxus

Chuanqilong_chaoyangensis

Antarctopelta_oliveroi

Dracopelta_zbyszewskii

Gargoyleosaurus_parkpinorum

Mymoorapelta_maysi

Hylaeosaurus_armatus

BEXHM_2002

Gastonia_burgei

Gastonia_lorriemcwhinneyi

BYU_R254

Hoplitosaurus_marshi

Polacanthus_foxii

Horshamosaurus_rudgwickensis

Taohelong_jinchengensis

Dongyangopelta_yangyanensis

Zhejiangosaurus_lishuiensis

Gobisaurus_domoculus

Zhongyuansaurus_lauyangensis

Shamosaurus_scutatus

Jinyunpelta_sinensis

Tsagantegia_longicranialis

Crichtonpelta_benxiensis

Pinacosaurus_mephistocephalus

Pinacosaurus_grangeri

Ahshislepelta_minor

Talarurus_plicatospineus

Tianzhenosaurus_youngi

Saichania_chulsanensis

Tarchia_kielanae

Tarchia_teresae

Minotaurasaurus_ramachandrani

Zaraapelta_nomadis

Shanxia_tianzhenensis

Nodocephalosaurus_kirtlandensis

Akainacephalus_johnsoni

Zuul_crurivastator

Dyoplosaurus_acutosquameus

Platypelta_coombsi

*Scolosaurus_cutleri*_DPF

*Euoplocephalus_tutus*_DPF

Anodontosaurus_inceptus

Scolosaurus_thronus

*Oohkotokia_horneri*_TMF

UMNH_VP_21000

*Anodontosaurus_lambei*_HCF

Ziapelta_sanjuanensis

Ankylosaurus_magniventris

Cedarpelta_bilbeyhallorum

Europelta_carbonensis

Anoplosaurus_curtonotus

Hungarosaurus_tormai

Struthiosaurus_transylvanicus

Struthiosaurus_languedocensis

Struthiosaurus_austriacus

Peloroplites_cedrimontanus

Borealopelta_markmitchelli

Silvisaurus_condrayi

Aletopelta_coombsi

Stegopelta_landerensis

Niobrarasaurus_coleii

Sauropelta_edwardsorum

Texasetes_pleurohalio

Tatankacephalus_cooneyorum

Animantarx_ramaljonsei

Nodosaurus_textillis

Propanoplosaurus_marylandicus

Panoplosaurus_mirus

*Edmontonia_rugosidens*_TMF

*"Chassternbergia"*_DPF

*Edmontonia_longiceps*_HCF

Denversaurus_schlessmani

;

END;

BEGIN CHARACTERS;

TITLE Ankylosauria;

DIMENSIONS NCHAR=330;

FORMAT DATATYPE = STANDARD RESPECTCASE GAP = - MISSING = ? SYMBOLS = " 0 1 2 3 4";

MATRIX

Lesothosaurus_diagnosticus

-0000000000000000000000000000-000000000000000------00---
000000000000??0????0000000000000000000000010-0000000000000---0000----------
000???00000100-0100000000000000010000000000000000-
0000100000??000?0000001000000000000000010000?1100010?00000000?0----------
----------000000000000000--1-----0---------

Scutellosaurus_lawleri

-0??????????????0??0000????00-1??????????????????????0---
???????0000???0?01?0000?????????00?00000?0???????000000000---????----------0000--
00000010-0000000000000000102000000000000000-
000000000010000?000000100?0000000000000100000000000000000100000000000000110----
----------00--000000----0---0000000000000000-101---0--00-0000

Emausaurus_ernsti

-11000000000??0000??0000???000-100000010000000------00---
0000??0?????????00?00000??????????0111010010-0000000000000---0000----------0000--
?00??????????00?????????????000000000000?????????????????????????0????????????
?????????????????????????000000000100----------
1?????????????????000??????0?????????????0?????????

Tatisaurus_oehleri

-
??
??????0110?0000-????010000?????????????????????????????????0--
??

??0000?????????
?????????????????????

Tuojiangosaurus_multispinus

-003000000000000000???????000-1????0?21?00000------00---

0000???????1000?000?011100?????????01000?0???????010011000---0000-------------1000--

000110???1?1?0?1010002001100000????0????0-

002111000020110001?010000?1?111011010000000000????01?010100000??11????00100-----

----------------10--1--00-????????011?1110000111010000(0 1)000?????????

Chungkingosaurus_jiangbeiensis

-01?00?????0000??0000????00000-

10000?0???11000?0?????11010??1

000---0000--------------?000--

?????????0?1?0?101000100020012000000000??????????????????1????????1?11001101??

????????0001011010100000??11????00100---------------------10--1--00-0---0---

0?0??110010????10?00(0 1)00?0?01010-0

Huayangosaurus_taibaii

-003001-0000000000000000000000-100000021200000------00---

0000?001110100001000001100?10002000011020000-0000010011000---0000-------------

1000--01010000-0011011010002000201???0000000000-

001011000010110010000100?1110011010000000000????0110001000000111????00100-----

----------------12001--00-0---0---100100000?0110010000(0 1)001(0 1)101010-0

Gigantspinosaurus_sichuanensis

-?23001-000000??0000?????00??0-1?0????21?00000------00---

000???0???01?0?0???0011???????????0011020000-000?01???1000---????--------------?000--

???10????0?0101101000100010110000000000100-

001011000010000010000000000111101000000000?112110?101?100000?111????00100----

-----------------12001--00-0---0---101?0000100110010000(0 1)001(0 1)?01010-0

Regnosaurus_northamptoni

-

??

????????1112??????????1?????????????????????????????????0--

??

??00?????????

?????????????????????

Loricatosaurus_priscus

-

??

??0??001000101?01??????100

0110120????00?????????????????????10100110????????0?0000?000010211011010100111

??11????00100---------------------12001??????????????????110111????????0(0 1)001?????????

Kentrosaurus_aethiopicus

-

0????000?????000??????????0??????????????????????????????????????101000?0000?1100

00???????001102?0???????0?10??000---0000--------------1000--01010000-

001?01101100100120111000000000000-

0020100100000000100000100111110010100000100011211011010?00000?111????00100----

-----------------12001--00-0---0---110?0110111110110000000001000101110

Dacentrurus_armatus

-

??

??1110-

110?011011001001?0?11??11001010000?????000

10011010??????111????00100---------------------10--0?????????0---

????01001?1????101000?0???11??0-0

Miragaia_longicollum

-00??0??0?00000?00000000000000-1000000???00000------

???011?????1000---0000--------------

?000--???01110-110?011011001001?0?11??????????0-

002010??0010000010000001001?11101101000000000??????????????????11????00100-------

--------------10--0?????????0---????1100?11111110100 1000?01111111

Miragaia_longispinus

-

??

???011???1?000?101100???

120???000000??00???????????????????????????????1110110100000000001000011010??????

??1?????00????????????????????????10--0--00-0---0---

????11001?0????100?01??0??0111??1

Wuerhosaurus_homheni

-

??

??10????1?00011010??100
100110?????0????????????????????????????????????1110110100000000000?????????????????
11????001?0----------10--0?????????????????0111010????11110110??????????

Hesperosaurus_mjosi

-002001-000000000??????????000-100000021200000------00---
0000000111010?01???0?11??00?????????11??0000-00?1?11011000---0000----------?000--
00010010-1110011010002001001110000000000-0020111-
0000000?1000?0100111110110100000000001210011010100000?111????00110----------
----10--0--00-0---0---?1111111120110011110111011010 10-0

Stegosaurus_stenops

-002001-000000000000000000000-100000021200000------00---
0000?00111010011110001100000000200001002000 0-0011011111000---0000----------
?000--01010010-1?000110100020010011100000000000-
00211001000000001001001001111001101000001000012200110101000000111????00110----
----------10--0--00-0---0---1111111112011011111011101101010-0

Scelidosaurus_harrisonii

-000000000000000000000000000-100000021101010------00---
0000000001100??00000000000?0000001101001111101100010000001---0000-0000-000-
000010010000000000-0000011?20??0000110001000?000011-
0001000000???000001100000100101010000111000010001000000101000000000000011100
000100001000000100101001000001 0000---0000000000000000-101------00--0--

Bienosaurus_lufengensis

-
??
???????010?00???????0100000?????-
????????00?????????????100??
??
??

Sarcolestes_leedsi

-
??
?????????1120?1????1??0?0000?????????????????????????????100????????????????????
??
??

Minmi_paravertebra -
??
??00?100?????????
??00
??1------???????

Kunbarrasaurus_ieversi
-100100000000011212000?1010000-
2010??0210010111010000200100100010011011010000000100000011????01??011110?11?01
1000011--00010-?000-001-00001001000??1?????00010010??00?????????1?0??0??011-
0000?01-0?????000010000001?0111010000111000010011000???0?000?000????00111110-
00?1?00------100110--00000010000---?000?000??000000-101------00--0--

Tianchisaurus_nedegoapeferima
-
???1???????????????????00000?????
????????????????11011???1??10-
0?0?01102000000????????????0??
00??00????????00????00111?110?0????0??????????1????00??0?????????????000?????????
??1------???????

Liaoningosaurus_paradoxus
-1?0?00000?10111?010001000?000-
1?1??0?21?1???100000?0??????0???????????????????????????????10?0?0?1???11000110?
1101120000010000-000-?000100100???11000-000001002000000012000101010110001-
0000001-
00????000000000001011110110001110000100000?000001010001000????000011221012220 1
------0--0?100?0000?????0---000?000000000000-101------00--0--

Chuanqilong_chaoyangensis
-
2?0??????????11?0???????????0??1??????21?01?????????1??????1?00?1011??????????????
??????????010??01?101????111?1?0???????????????????????????????11000-
00?001?????010???????1010?????1110000101-
00??????1000001001011110111??????????0000101010111000?1101????001?11????????????
????????1?????????????????000?????0?000000-101------???????

Antarctopelta_oliveroi
-
???1000000?2???0?????????????????????????

??????????1?????????????100?0111---????-????????????????0????11000-
?????1102?00110???1001????0???1????????????????????????????0????????????????????
??????????????000????0011?????????????????????1????00000?????????0??0????0??????
???1------???????

Dracopelta_zbyszewskii

-

100?000010???11????????????0102?????0???01011101000?2000?1????????????0?????????
???????????11????????1?1?100?1112110????1?1??000100000100l0?0?111?10-
0001111011?01?01120001????0????211??11???101?200?1?10111????100111?00011????2?
????100?101?1????000????001110210?011??111??1????11???0001201??0????????0??00??
????0???1------00-????

Gargoyleosaurus_parkpinorum

-

1001000?10000110010000101000102011000212010111010000200011020???11110000100
0011000000???1101120111101101010011112110001010101000100000100101001111l0-
?????1101100110?1?002100??0?10???????1?01?0??11??1????110??0100111010011100021
????120010???????000110100111121000110l0------
10011101000120100?????000?0???00?????0-?01------00--0--

Mymoorapelta_maysi

-

?????00010?????????????????????????????????1?1110?0000200011020O?001111?0?0100001
1000?????????????????????0??100?1112010????1?1?????10????100???00?11100-
000101101001110112002100010010?2100??1????01??1??111111101?010011101001110001
11221????????1000?0001001001111-100011000------1001110100012010000---
????0000000000?0-101------00--0--

Hylaeosaurus_armatus

-

??00?????????0???????????
??0??11?10-
10100?????????????00?100010010121111111O??0101100?????0??????1111?0????????????
??????????01000??00????00111???00???00???????100?1100?????????00---
????0000?000000????1------00--0--

BEXHM_2002

-

??200001?????????????????????

????????????????????????100?1?????????????????????????????????????110???100??1?????100
01111111?????????????????????????????????1?????1?????????????????????????????????0??1
00100110111???0????0?????????????1??????1101??0?????????????????????????1------???????

Gastonia_burgei

-

1000101010001110110201101000102011000212110111000000200011120100011110101000
01110000001101?????????????11?110?1112010000000000-001-
0000100??????11????1010011?1101110112002?000?0010?21111011011012?10?1?1111101
??11110111?????????1221120010201111?1001001111111--000??000------
100?1101100120100000---???0000000000000-101------00--0--

Gastonia_lorriemcwhinneyi

-

1?00?00?10????10????????????0????1??0?21?1101110000002000111201?101111001100001
11000?????????????????????????110?1112010????0?0???001-0000100???01111100-
101?1111110111011221 21?00100???21111011111010?10?1100111012011110111011121?12
11211010010201111??00??00101111--000??0--------100?0101100?0?10000---
???0000000000000-101------00--0--

BYU_R254

-

??
??1001
1220210???0??00
????1?????????????????????100?1?????????1000???????????00?????????1------???????

Hoplitosaurus_marshi

-

??
??
??????????????21111011??1010110?1??????0?????????????????????????110010????????0
010011111?????????????????????1101100??01?00?????????????00000????1------???????

Polacanthus_foxii

-

??0???0110001110?
??????????????????????100?1?????????????????????????10000011000-
10000112200110011200 2?00010??01?????????????????1?11?110??0010101100011100021

1221120010211111?100100111111?????0????0??????????010110012010000---
?????00000?????0-101------00--0--

‘*Horshamosaurus_rudgwickensis*’

-
??
???????????????????????000???????????????????????????????????????100001??????110
11?201?????0????2111?01???10?0??1?111??
001001??11??????????????????????1???1?????????????????000000000?????1------???????

Taohelong_jinchengensis

-
??
???1
12010?????0????????????????????????????????11110110???????????????????????????0
0?????111??????????????????????1????0012010?00---????????00?????0-101------???????

Dongyangopelta_yangyanensis

-
??
???1????11???0?????
???11110111??????????????121110????????0
0????1111??????????????????????0????0012010?00---????????00?????0-101------???????

Zhejiangosaurus_lishuiensis

-
??
???1?????12200?110
???00?00?0?0010??????????????????????????????111101110011100021????121110211111
1100??????????????????????????????0????00??0????????????????00?????0-101------
???????

Gobisaurus_domoculus

-
1010001001001?1200020110000010211111?0212011100000001101100100101111110100010?
001110000011????????????????11?010?011200-010000000-000-
1000201??
??
???????????????????1------???????

Zhongyuansaurus_lauyangensis

-

101?001001101?120002011000001021111?0212011100000001100100???????110010101000
01110100???????1??????????11?????01120001100000010001-
0000201?????????????110?01????????????????1112?1111??????????????????1?000010??1?
?????????????????0000?????????????101????0010?????????????????????0??????????????
????????000????????????1------???????

Shamosaurus_scutatus

-

1010001001101?120002011000001021111?02120111000000011011001001011110010100 0?
0011101000?1??1111?011110111111????11200-0100000010001-
1000201101?????????1?101??????????????????????????11-
000100011001121????????????????????????????????????1011????????00????00102122001
22001------0--0?0--0?????????????0000?000??00000????1------???????

Jinyunpelta_sinensis

-

1?0?0??00111111?????0??01?1?10??11???2120?1?110100011001?0?????????????????????
???????????11?0?????????????????001000010010000-0---1??????100???11100-
00???11?0?????????????01112111110--001101-
00????1?1?00010??1?1111011???????????0000???011?01100??0????????????????????????
?????????????????101?100100??0000??100000-101------00--0--

Tsagantegia_longicranialis

-

10011020011011121212111010001021111?021201110001000110010011110??11001010100
00110010001001??????????????11?1??01112121100000101000001000221?????????????????
???
??0????????????????------
???????

Crichtonpelta_benxiensis

-

110000100100?11212121??01000??21111?0212111111110032001001?001??1101110001?0
111101000?001??????????????11????0?1121201000101010000-1000211??????11000-
1010111011001001110111????0????210001001-
1001121?1?11?1101??11110211??????????????021011211111??01????0010212200122001--
----0--000--00000010111000????000000100000-101------00--0--

Pinacosaurus_mephistocephalus

-

3200102001201?1212121110100?112111??021211111111000321110 0?0??11111?????????

11????000?001??111?010100111?11101112121100011211000000000201101?1????????????

?1021??10001????011121?111?????100001????????11??010?01?111102?1??????????????

????????????00????0010210000100001------0--000--00000?????100??00?????0?1????0-101-

----00--0--

Pinacosaurus_grangeri

-

31011011?1201?1212121110100011211 11?12121111111100221010011101111100111000

0011101000100111111001010011111110111213110001131100001000020110 10??1?200-

1010111111001000120??0111211111210001001-

1001121111000100011111102101 1??2000210000021011?1?1111100????001021001010010

1------0--000--00000?10111011000000000100000-101------00--0--

Ahshislepelta_minor

-

??????????????????????0???

??

??????????????210001101-

101111??100000000?????????????????????????????????????00110?0011?????????????????

??????0?????????????????????????????0000????????????????????

Talarurus_plicatospineus

-

3100101101???1121212111?1011102111110212 01?1111100032011 00?1?0???????101010?0

011101?????????????????????????????0?11211110?00?011000000000221 1??????1200-

1?0011112100100011011011121111 11-0001001-

100?1211110001000111111021111??2111210000021011211111010 0????001121220012200

1------0--000--000000????1001????000000100000-101------00--0--

Tianzhenosaurus_youngi

-

3100102001001?1212121110100011211 1??121211?1111100032011001100111111001200?0

011110?0001001??11??010100?11?????1112111100021311000001000211101011 11?00-

0000111021001000 12???011?2111112100010 01-

100112111?000110?1110110?1?111120002100000?1?11?1?1110100??????10212200122001

------0--000--00000?????100??00000000?10000????1------00--0--

Saichania_chulsanensis

-

3101101001211?12121211101010112111?12121111111100032011001111111111001100100111101000100111111001011011111111011121211010113110000010002111011111121 0-1?00111020001000120100 11?211111210001000110011211110001000111111021111112111 2100000210112111111100????0011210010000000------0--100--

0000001011100100000000000100000-101------00--0--

Tarchia_kielanae

-

??0??01?01????1?????????????????????????1?1111?0??1???????1???????00112???0001?? ??????????????????????????????1?213?????2??????00???11201?????????????????????????? ?? ??

Tarchia_teresae

-

3100001?01211?121212111010?01121111?12120111111100032111001110111111011 1?0?0 0111101000?00111111001010011111???11121311?00113100000010101111 01?????????? ?? ??????????1??????????????????????????????0????????????????????????????????1---- --???????

Minotaurasaurus_ramachandrani

-

3101101100211?12121211101010112111?12121111111100032111001000111111111200100 0111101000100111111001011011111111011121311010213110000111111111111111????????? ?? ??????????????????00??2?22001?????????????????0?????????????????0000??????????????????1---- ---???????

Zaraapelta_nomadis

-

3100101001????12???????????0??21111??212010111111003201100100011011101110011?0 111101????0?????????????????????????1112121????0?2??000011110101?????????????????? ?? ??0??????????????????????? ??????

Shanxia_tianzhenensis

-

?????01001????12?????????????????????????1?1111?00032??1???????????1?11200100011
1?????????????????????????????1121?1???????????00?????201???0??11110-
011???0
21011??????????????00?????????????????????0?????????????????????0000???????????
1------???????

Nodocephalosaurus_kirtlandensis

-

3100101101011?121??2111??0?0112?11?0?21211011111110032111001000010??1????00100
1111?????????????????????1?????11121311?10213110000110002 11?????????????????
????????11110???
???????00????0022?????????????????????0?????????????????????0????00?????????1------
???????

Akainacephalus_johnsoni

-

2200101101011?121212111010101121111012121101111110022111001100011111101120000
01111010001?011111100101001111????11121311010213110000110002111 11????????011
011101110100111000011121111021000110011021111?111001100??11110210???????????00
0?01101110??????00100100212122101222 01------0--000--0?????0---
10110000000000100000-101------00--0--

Zuul_crurivastator

-

2201002001211112111211101000112?11??02121111111100132011?011??11?11101120000
01111010001001?111100101001111100111211110100111200001110022111 1????????????
???1?2101???11111111?????????????????
???????????01????0111?????????????????????00--000??0101110000000000000100000-
101------00--0--

Dyoplosaurus_acutosquameus

-

??0??01?01????1?????????????????????????????1?1?0?00?????????????????????????????????
?????????????????????????????????112111????0??????00??????21?????????????????1?11??2
00112000011121111 1?????????????????????1??????0?1011110211?????????????1110112111
111000????0021?????????????????????????0????0000010111000????????001????0-101------00-
-0--

Platypelta_coombsi

-

220110210121111212121111010?0112?11??121211111000000021011?010??0101110?1?00000
1111010001001?111100101001111111011121111000011020000011002211111???11110-
101011102100?????????????????????2100010011100?????110000100111011021 1????????????
??????????????????01????0122211100011100------0--000--
00000??????011000000000000100000-101------00--0--

*Scolosaurus_cutleri*_DPF

-

220110200121111212121111010?1112??????212111110000002 1011?0??????????????????
??????????????????????????11?110?111211110000111200000100022 1??????111011100??11
11100100?110000????1?1???????110111001111?11000010011110101111111211121000001
10112111111101????0121212210122100------0--000--0000000---????????0???001????0-101--
----???????

*Euoplocephalus_tutus*_DPF

-

220110200121111212121110100011211111121211111111001320110011001111110112000 0
011110100010011111100101101111111011121111000011120000010002211110??11110-
??????111100200112000011121111121000110111001111111000110011111102111111211 1
210000011011211111?100100100112100000000000------0--000--
00000??????011000000000000100000-101------00--0--

Anodontosaurus_inceptus

-

220110100121111212121111010?0112?111?121201111000000021011?011001101110 11?0000
0111101000100 1?111100101001111111111121111000011120000011002211 11????????????
?1?1???11000000010?????????????????????
??????????01????00222121?0??????????????100--000000????????0000?00000100000-
101------00--0--

Scolosaurus_thronus

-

220110100121111212121111010?1112?11??121211111111000220110011??1??11101120000
0111101000100 1?????????????11?110011121111000011120000011002 21?????111111100
011111101210111011 0????1????2000011011100?????????????????11010111?????????????
??????????????01????012?212210022100------0--000--000000???????????0?00000100000-
101------00--0--

*Oohkotokia_horneri*_TMF

-

2201101001211?121212111010?011211111121211111111000320110011O?11???10112000?
01111010?0??????????????????1???11011121111???00112000001100221??????11?????????
?1?1100210011011?????1????1100011011000?????11000010?11?????????????????????01
1011????????00????0021212100022100------0--000--0000000---1011???00???001????????1--
----00--0--

UMNH_VP_21000

-

2110101001211?121?121110101?11211110?212010110100002201100100011111101120000
011??01000?????????????????1???????112111?000001120000011002221?????????????????
??
??0??????????????????????
???????

*Anodontosaurus_lambei*_HCF

-

2201101001211112121211101O?01?211111121201111000000210l1?011001111110111000?
0111101000?001111?1?010100111?111?11121111000001120000011002211l1???????????
?1?102100200011000?1112111?1?????????????????1?0001???1?11110?1???????????0200
011011????????01????00112122?0022?00------0--100--0000000---11210000????001????0-
101------00--0--

Ziapelta_sanjuanensis

-

110?101001211?121212111010001121l1??12120101111110003???100?????????1011100000
11110?000??????????????????11?????111211100000011200000100022l?????????????????
??
????????????0021210010000200------0--100--??????????????????0????00?????????1------
???????

Ankylosaurus_magniventris

-

32011010010111121212111010?011211111121201111111000320110010001111110111000001
1111010001001111110010100l????????112111100000102000001000221111???11110-
101011??????2001110000111211111210001101-
101???0?1?100100??1????0?????????????0001111011???1???101????00102122?0010001---
---0--000--0000001011101100000000010000????1------00--0--

Cedarpelta_bilbeyhallorum

-1010?0-
00?000?120??001001000??2??????21201010000000110010000000111101???000000011110
001101??????01110110??100?011200?10100?000-0?0-00001-01?????11000-
1000??1111?11110220001??0?0?????????????????????111101000???1?????????????????00
00011010101 1??00000000????
????1------???????

Europelta_carbonensis

-103001-
000????11????????????01020100?021201010000000010110002101111111110000000011111?
?0????101120?1????1?00100?0112000????0?000-010-10001-
010101011101110101112212111102121110001011100??????0?1-
111?000?1?111?0???11101011111112111210011111010101100010 0????00111?1???0????0
????0?????110001011111000---00000000000????0-101------00--0--

Anoplosaurus_curtonotus

-
??
???????101120?1???????0???????????????????????????????????????11100-
1?????1?2121111?2????1??0?0????2001110????12?010?1?110?0?????????????????????????
???000?????0000000?
???1------???????

Hungarosaurus_tormai

-
?0????????000??0?1000?101000102?1????21201010000000?1001000?10?1111????????00?
??0??00????11011201101011000100?0112100?010?0?0????0?0000??0101???111???101111
1221111110212111?0000010?200111011-
1120200?001100000111101011111112111210001111 0101???00?100????00111?10000????0
????00100?1???01111?1??00---0000000000000000-101------00--0--

Struthiosaurus_transylvanicus

-1030?1-
?00????10??????????????????????21201?100000000?????0?2?00111111000000000111?1???
?????????????????????????112100???????????10?00001-0???011?1000-
????11??????????????101?????0????200111011-
11???0??????0??00????00111?11000?1000????
001001?????11???????????????00????0?0000????1------???????

Struthiosaurus_languedocensis

-

??

????????????????????????100???1110111221111???

???????00?000000?????????????????????????????11010111111211121000 1?????????????

???????0011???000???????0-101------???????

Struthiosaurus_austriacus

-?????1-

?00????10??????????????????????212?1?10000000?????0???????111100?000000111??????

????01120?1???????0100?0112100???????????10?00001-

0????????????111011??????????????????????????200111011-

11??????00???00?0?11101011?1111?111210001111010??1????100????00111?11000????0?

???0010011???0?????11000---000??000???00000-?01------00--0--

Peloroplites_cedrimontanus

-1010?1-

000010?11?10????1200??????????21201110000000100100?1?10001111001000?1111?111

000001??????11112011???01?0112100?0000??????10?10001-01000??1?100-

110011??1111111121221000000??0?100111011-

1130000000????1111111?10111??????????????01111010110??100???????????????????????

????????????????????????????0000000000000-101------???????

Borealopelta_markmitchelli

-101001-

00?01011??1?????120??102?11???2120?1?110000001011?0?????????????????????????????

??????1??????????????????1121000000000030010010001-

0100???????????????11???

???????????????????????????00????00111010001100011000101001110000 0100????????00

0??????????????????1------???????

Silvisaurus_condrayi

-101011-

0000101110100012120001 02?101?021201?1000001101001 0001?10001101001?0001011011

1000111111120110???1000100101121000000000000-010-00001-

0??????1110101010011211101??1?2?1??????0??

??????????????????????????100????0002101000120101101010000011 00000???????????0

0000000?0??????????1------???????

Aletopelta_coombsi

-

??

???????????????????????00???

????????????????????????????????00???0?10??11010???????????????????10110111??0

0????0001??????????????????????0???000110??????????????????????????1------???????

Stegopelta_landerensis

-

??

??0??00001010000?????????

????????????????20011??11-

????????0??????10??1101????????????????????????10111??00????00011?111?1????1????

0????01???000111?????????????000???0000????1------???????

Niobrarasaurus_coleii

-101??1-

0?0????11????????????102110???2??????000000?010010??????????00???000?101101?????

?????????????????0?1???0112100????0?0?0-

?10?0?????????????1???????0?1?1111?11111221??000000??0?2001?1?11-

?1?????00000?0110??1101011?11????????????011010110100??00????00011?11101????1??

??1????00?????????0---0---?????000000000?0-?01------00--0--

Sauropelta_edwardsorum

-102001-

010????10???????????????2?10???2120111110000001001000110?0110100100001011 0?1??

?????1111200111011??010010112100????0?0??-010?10001-

0100011111010100001111111111122010000000010020021101 1-

11302000001110111111101011011112000211211111010101111010010120000101000010 00

0100000100001000001001100 0---0000000000000000-101------00--0--

Texasetes_pleurohalio

-102001-

0100001100100012121011 02?111?0212011111000110200100011100011110011100111 1011

1011111?????????????00?1???0112111?001002030010010001-

0??????110010??????????01111?2??1??????0????200211011-

1140200000111110?1110101111?????????????1101???0?111?100?????????????????????

????????0???????????????????00???00000000-101------???????

Tatankacephalus_cooneyorum

-102011-

010010?10???0???????0??211????21201111000011010010 0?1110????11001?????1?1011??

??????????????????00?10??0112100????0?1031010-10001-

0???0???????????????

?????????????????????????00???0???

?????????????1------???????

Animantarx_ramaljonesi

-??1011-

?10????10?????????????????1????21201?1100001101001000111000110100111001 1110?1??

?????1111101101201??110000112100????0?1????10-00001-

0100???110011101011????01???????????????????200211011-

114020??0?11?101??????1?110?1??2????11211?11110????????00???????????????????????

???????1?????????????????00000000???00000-101------???????

Nodosaurus_textillis

-

???

??1?1?01111101???

???????00000??00??????????????????0???0???0??11010110??????????????011110101111?

?00????0001???????????????????????1????00111??????????????000???????0-101------???????

Propanoplosaurus_marylandicus

-

1?3????0???10?1?0????1?12???????1????2120???00???000?????????????????????????????

??????????????????????????????112100????0?1031110-

??00???????1?????

??????????????????????????????11??

????????????????????????????????

Panoplosaurus_mirus

-102001-

0000101100001012121011?211111021201110000000010010001110001111001110111 11011

1010111111110?101201111100?01121000001001031010-00001-010011111?00-

1???01111101?01?12????????0???0200110011-

1120200000111011011?????????????200021????????10?0?111?100????0012101???01???01?

??010??000--00000?0---0---00000???0?00000????1------00--0--

*Edmontonia_rugosidens*_TMF

-102001-
0000001100001012121011021?11102120111110000001001000111000111100110011111011
1010111111110110121111110000112100000100103111 0-00001-010011111100-
10?011111101111112210000?00??0?????????????????????1????0?1????101011011112000 21?
??????????????????00????000110111101111011010110100110000000?0---0---
00000???000????0-101------00--0--
'*Chassternbergia*'_DPF
-102001-
0000001100001012121?11021111?021201111000000010010001110001111001100111110 11
1010111111110110120111110 0?01121000??1001031110-00001-010011111?00-
1?1001??????101011100?00?00??0?200210011-
1120000010 11?0111111?????????????????????????????????????100????001010111101111011
1101111001000?????0---0---000000000000000????1------00--0--
*Edmontonia_longiceps*_HCF
-102001-
0000001100001012121011021?111?021201111100000010010001110001111011100111110 11
1010111111110110120111110000112100000100103101 0-00001-0100???11?00-
1?100111?1??1011120000????0?????????????????????1???1?1?????????????????0002112
111?1010????????00????000010111101111 01???010?1000--00000?0---0---
00000000000????????1------00--0--
Denversaurus_schlessmani
-101001-
000000110?001012121011021?1????21201111000000010010001110001111011110111110 11
1010111111110110120112 11???011210000010000310 10-00001-
0100???1????????????????
????????????????????????????00????000110110001100011010111100110000000?0---0---
0000?????????????????1------00--0--

;

END;

BEGIN ASSUMPTIONS;

TYPESET * UNTITLED = unord: 1- 330;

END;

```
BEGIN MESQUITECHARMODELS;
	ProbModelSet * UNTITLED   =  'Mk1 (est.)':  1- 330;
END;

Begin MESQUITE;
		MESQUITESCRIPTVERSION 2;
		TITLE AUTO;
		tell ProjectCoordinator;
		timeSaved 1702400783437;
		getEmployee #mesquite.minimal.ManageTaxa.ManageTaxa;
		tell It;
			setID 0 3041669230535901279;
		endTell;
		getEmployee #mesquite.charMatrices.ManageCharacters.ManageCharacters;
		tell It;
			setID 0 9104090815695633972;
			mqVersion 361;
			checksumv 0 3 703879908 null  getNumChars 330 numChars 330 getNumTaxa 95 numTaxa 95  short true  bits 31  states 31  sumSquaresStatesOnly 48058.0 sumSquares 48058.0 longCompressibleToShort false usingShortMatrix true  NumFiles 1 NumMatrices 1;
			mqVersion;
		endTell;
		getWindow;
		tell It;
			suppress;
			setResourcesState false false 100;
			setPopoutState 300;
			setExplanationSize 0;
			setAnnotationSize 0;
			setFontIncAnnot 0;
			setFontIncExp 0;
			setSize 1920 953;
			setLocation -8 -8;
```

```
                setFont SanSerif;
                setFontSize 10;
                getToolPalette;
                tell It;
                endTell;
                desuppress;
        endTell;
        getEmployee
#mesquite.charMatrices.BasicDataWindowCoord.BasicDataWindowCoord;
        tell It;
                showDataWindow                          #9104090815695633972
#mesquite.charMatrices.BasicDataWindowMaker.BasicDataWindowMaker;
                tell It;
                        getWindow;
                        tell It;
                                setExplanationSize 30;
                                setAnnotationSize 20;
                                setFontIncAnnot 0;
                                setFontIncExp 0;
                                setSize 1820 881;
                                setLocation -8 -8;
                                setFont SanSerif;
                                setFontSize 10;
                                getToolPalette;
                                tell It;
                                endTell;
                                setActive;
                                setTool
mesquite.charMatrices.BasicDataWindowMaker.BasicDataWindow.arrow;
                                colorCells  #mesquite.charMatrices.NoColor.NoColor;
                                colorRowNames
#mesquite.charMatrices.TaxonGroupColor.TaxonGroupColor;
                                colorColumnNames
#mesquite.charMatrices.CharGroupColor.CharGroupColor;
                                colorText  #mesquite.charMatrices.NoColor.NoColor;
```

```
		setBackground White;
		toggleShowNames on;
		toggleShowTaxonNames on;
		toggleTight off;
		toggleThinRows off;
		toggleShowChanges on;
		toggleSeparateLines off;
		toggleShowStates on;
		toggleReduceCellBorders off;
		toggleAutoWCharNames on;
		toggleAutoTaxonNames off;
		toggleShowDefaultCharNames off;
		toggleConstrainCW on;
		toggleBirdsEye off;
		toggleShowPaleGrid off;
		toggleShowPaleCellColors off;
		toggleShowPaleExcluded off;
		togglePaleInapplicable on;
		togglePaleMissing off;
		toggleShowBoldCellText off;
		toggleAllowAutosize on;
		toggleColorsPanel off;
		toggleDiagonal on;
		setDiagonalHeight 80;
		toggleLinkedScrolling on;
		toggleScrollLinkedTables off;
endTell;
showWindow;
getWindow;
tell It;
		forceAutosize;
endTell;
getEmployee #mesquite.charMatrices.AlterData.AlterData;
tell It;
		toggleBySubmenus off;
```

```
endTell;
getEmployee
#mesquite.charMatrices.ColorByState.ColorByState;
tell It;
	setStateLimit 9;
	toggleUniformMaximum on;
endTell;
getEmployee #mesquite.charMatrices.ColorCells.ColorCells;
tell It;
	setColor Red;
	removeColor off;
endTell;
getEmployee
#mesquite.categ.StateNamesStrip.StateNamesStrip;
tell It;
	showStrip off;
endTell;
getEmployee
#mesquite.charMatrices.AnnotPanel.AnnotPanel;
tell It;
	togglePanel off;
endTell;
getEmployee
#mesquite.charMatrices.CharReferenceStrip.CharReferenceStrip;
tell It;
	showStrip off;
endTell;
getEmployee
#mesquite.charMatrices.QuickKeySelector.QuickKeySelector;
tell It;
	autotabOff;
endTell;
getEmployee
#mesquite.charMatrices.SelSummaryStrip.SelSummaryStrip;
tell It;
```

```
                                        showStrip off;
                                endTell;
                                getEmployee
#mesquite.categ.SmallStateNamesEditor.SmallStateNamesEditor;
                                tell It;
                                        panelOpen true;
                                endTell;
                        endTell;
                endTell;
                endTell;
end;
```

2024

JOÃO PAULO VASCONCELOS MENDES RUSSO

EVOLUTION OF POLACANTHID DINOSAURS AND DESCRIPTION OF A NEW SKELETON FROM THE UPPER JURASSIC OF PORTUGAL